**M-Pos226**

EFFECT OF HORMONE FRAGMENTS ON THE MEASUREMENT OF PARATHYROID HORMONE BY RADIOIMMUNOASSAY. ((Alafuele Mbuyi-Kalala and Gerald Ehrenstein)) Biophysics Section, Clinical Neuroscience Branch, NINDS, NIH, Bethesda, MD 20892)

One of the basic assumptions underlying the use of radioimmunoassay and other competitive protein-binding assays is the homogeneity of the antigen or ligand. The existence of circulating parathyroid hormone fragments violates this assumption and hence has the potential for causing errors and high variability in the radioimmunoassay of parathyroid hormone (PTH). Even though region-specific radioimmunological and immunoradiometric assays for PTH measurement have been successful in recognizing limited regions of the hormone, (non-immunological) heteromolecular interactions between the hormone and its fragments (or other co-secreted protein) may still cause significant measurement errors. We therefore undertook to carefully examine experimentally and by modelling the impact of fragments on the estimation of a highly purified intact bovine PTH by radioimmunoassay. Our experimental results show that the impact of fragments could not be attributed only to the simple binding of fragments to the antibody. Indeed we found that the mere presence of the fragments can result in a pronounced underestimation of the amount of the intact hormone. We account for this "fragment's screen effect" by interactions between the hormone and its fragments.

**M-Pos227**

ANALYSIS OF X-RAY IN-PLANE SCATTERING: DISTRIBUTIONS OF PROTEINS IN MEMBRANES.
((Ke He, S.J.Ludtke, Y.Wu and H.W.Huang)) Physics Department, Rice University,Houston, TX 77251.

We have developed a technique for measuring X-ray (or neutron) scattering with the momentum transfer parallel to the plane of the membrane to study the lateral organization of proteins and peptides in membranes (He et al. Biophys. J. 64 (1993), He et al. J. Phys. (Paris) to be publ., He et al. Biophys Chem. to be publ.). Since there is no analytical solution for X-ray scattering in a two dimensional system, we used Monte-Carlo methods to simulate the scattering pattern of protein particles freely diffusing in the membrane. We found that:
1). The scattering peak position is mainly determined by the size of protein, relatively independent of the concentration of protein.
2). The peak intensity is mainly determined by the area ratio of the protein to the lipid.
We will show three examples of in-plane scattering: distribution of gramicidin in a membrane, distribution of gramicidin monomers in a membrane and distribution of inserted alamethicin in a membrane.

**M-Pos228**

IMPLICATIONS OF SEQUENCE ANALYSIS FOR THE P5C DEHYDROGENASE ACTIVITY OF PUTA, A MULTIFUNCTIONAL *ESCHERICHIA COLI* PROTEIN
((Mingfu Ling and Janet M. Wood)) Department of Microbiology, University of Guelph, Guelph, Ontario, Canada N1G 2W1)

Membrane-associated *E. coli* PutA has two enzymatic activities: proline dehydrogenase (DH) and δ'-pyrroline-5-carboxylate (P5C) DH. This protein also represses expression of its corresponding gene *putA*. Previous studies of PutA from *E. coli* and *Salmonella typhimurium* have demonstrated correlations among reduction of the PutA flavin by proline, PutA conformation and association of PutA with membranes (Brown and Wood (1993), J. Biol. Chem. 268, 8972) or with *put* intergenic DNA (Ostrovsky de Spicer and Maloy (1993) Proc. Natl. Acad. Sci. USA, 90, 4295). We would like to correlate structure with function for PutA. The objectives of this study were to sequence *E. coli putA*, to survey the deduced PutA amino acid sequence for DNA, membrane, proline, P5C, FAD and NAD binding sites and to enhance the expression of *E. coli putA*. The 4 kb *E. coli putA* sequence revealed both similarities to and differences from the *S. typhimurium putA* sequence reported by Allen *et al.*, (1993) Nucleic Acids Res. 21, 1676. A region of sequence similarity with several aldehyde DHs from both prokaryotes and eukaryotes and with *Saccharomyces cerevisiae* P5C DH extends from residue 700 through residue 1100 of *E. coli* PutA. These sequence analyses suggest that γ-glutamic semialdehyde, which is believed to equilibrate spontaneously with P5C, is the substrate for P5C DHs. We can test this hypothesis by using aldehyde analogs and affinity-labelling techniques. Limited and intriguing similarities were also found between a portion of the PutA sequence and a sequence near a consensus FAD-binding region shared by succinate DH and fumarate reductase from several organisms. As well, partly for supplying sufficient amounts of protein for X-ray crystallographic structural studies, we have achieved overexpression of the *putA* gene under the promoter of phage T7 RNA polymerase.
(Supported by the Natural Sciences and Engineering Research Council of Canada)

**M-Pos229**

**FLUORESCENCE PREDICTS LOCAL SECONDARY STRUCTURE: Time-Resolved Fluorescence and Circular Dichroism Studies of Highly Purified Neurotoxins**
((T.E.S. Dahms[1,2] and A.G. Szabo[1,2])) [1]Institute for Biological Sciences, National Research Council, Ottawa, Ont., Canada, K1A 0R6. [2]University of Ottawa.

The relationship between ß-sheet secondary structure and intrinsic tryptophan fluorescence parameters of Erabutoxin b, α-cobratoxin and α-bungarotoxin were examined. NMR and X-ray crystallography have shown that these neurotoxins have comparable ß-sheet, ß-turn and random coil secondary structure. Each toxin contains a single tryptophan (Trp) residue (on ß-sheet) and no more than two tyrosine (Tyr) residues. The identity and purity of the HPLC purified toxins and toxin-derivatives were verified by electro-spray ionization mass spectrometry. The time-resolved fluorescence properties of native erabutoxin b and α-cobratoxin are best described by triple exponential decay kinetics, whereas native α-bungarotoxin exhibits a distribution of lifetimes.

Each neurotoxin, treated with 2M, 4M and 6M GuHCl, was studied both by circular dichroism (CD) and time-resolved fluorescence spectroscopy (TRFS). Disappearance of the ß-sheet secondary structural features with increasing concentrations of GuHCl was accompanied by a shift in the relative contribution ('c' value) of each fluorescence decay time (TRFS). At 6M GuHCl the native toxins were completely denatured as evidenced by CD (random coil) and the 'c' values of the three fluorescence decay times (TRFS) were identical to those found for single Trp α-helical peptides in 6M GuHCl (random coil) and were dramatically different than those of the native toxins.

The disulphide bonds of each toxin were reduced to facilitate carboxymethylation and amidocarboxymethylation. The two different toxin derivatives displayed triple exponential decay kinetics for all three neurotoxins. The relative contributions of the fluorescence decay times (TRFS) were similar to those observed for the native toxin in 6M GuHCl. The data suggests that the 'c' values observed for the native toxins are indicative of ß-sheet secondary structure.

## MOLECULAR RECOGNITION I: PROTEINS

**M-Pos230**

A THEORETICAL MODEL OF ANTIGEN RECOGNITION BY A T CELL RECEPTOR AND ITS POSSIBLE IMPLICATIONS FOR SIGNAL TRANSDUCTION. ((A.E. Kister,*† J. Malinsky,‡ A. Smolyar‡ and E.L. Reinherz*§)) *Laboratory of Immunobiology, Dana-Farber Cancer Institute, Departments of †Pathology and §Medicine, Harvard Medical School, Boston, MA 02115 and ‡Mt. Sinai School of Medicine, New York, NY 10029.

A computer model of the trimolecular complex of the murine B10 T cell receptor (TCR), its peptide antigen derived from the C-terminal fragment of pigeon cytochrome c and the α1 and β1 domains of the MHC class II I-Ek molecule was created. This model takes into consideration the effect of hydrophobic interactions during the long distance attraction of molecules and short range specific recognition mediated by hydrogen bond formation between molecules. Ab initio quantum mechanical calculations of putative binding residues predict the effect of electronic redistribution. The model suggests that electrostatic interactions are crucial for receptor binding to antigen. They may also trigger an initial step of signal transduction via charge transfer. Possible mechanisms for this process are proposed based on recent work on conductivity in disordered systems. Phase transitions which may occur in the trimolecular complex and drastically change its electronic properties are considered.

**M-Pos231**

CRYSTALLOGRAPHIC AND SPECTROSCOPIC SOLUTION STUDIES OF THE INTERACTION OF RAT ANNEXIN V WITH LIGANDS. ((M.A. Swairjo*, N.O. Concha*, J.F. Head*, M.-B. Campos**, J.R. Dedman**, M.F. Roberts***, B.A. Seaton*)) *Department of Physiology, Boston University School of Medicine, Boston, MA 02118. **Department of Physiology and Biophysics, University of Cincinnati, College of Medicine, Cincinnati, OH 45267. *** Department of Chemistry, Boston College, Chestnut Hill, MA 02167.

Annexins are a family of twelve homologous calcium-binding proteins, distinct from the "E-F hand" calcium-binding proteins, that bind to acidic-phospholipid (PL) membranes in a calcium-dependent manner. Despite their unknown physiological functions, they are implicated in membrane processes in cells, such as exocytosis and membrane trafficking. Their primary structures exhibits a highly conserved four/eight-domain core, consisting of approximately 70 amino acids and a highly variable $NH_2$-terminal region.

In an attempt to understand the effect of annexin binding on the membrane we conducted $^{31}P$- and $^{1}H$-NMR spectroscopic experiments on the interaction of annexin V (35 kDa) with small unilamellar vesicles containing phosphatidylcholine (PC) and phosphatidic acid (PA). The $^{1}H$-NMR data show no significant insertion of annexin V into the bilayer hydrophobic core. Instead, a peripheral interaction, in which the PA headgroups on the outer vesicular surface are prefered, is indicated from the $^{31}P$-NMR data. CD data, together with the crystal structure of annexin V are consistent with an insertion-free mechanism of interaction. Further, the NMR data reveal that annexin binding to the vesicle outer-leaflet PL affects inner-leaflet phospohlipids as well. The effects ovserved are consistent with a protein-induced reduction in membrane curvature. In parallel, we investigated the effect of ligand binding on the structure of rat annexin V, both in the presence and absence of phospholipids, using X-ray crystallographic and solution methods. In light of the observed ligand-induced conformational changes and the NMR results, a model of the calcium-mediated annexin-membrane interaction is presented.

**M-Pos232**

MODELING OF IMMUNOGLOBULIN-LIKE DOMAINS OF A YEAST CELL ADHESION PROTEIN. ((P.N. Lipke[1,2], D.J. Mallows[1], M.-H. Chen[2], and P. C. Kahn[1])) [1]Dep't of Biochemistry & Microbiology, Rutgers Univ., New Brunswick, NJ 08903, and [2]Dep't of Biology, Hunter College, CUNY, New York, NY 10021. (Spon. by P.C. Kahn)

α-agglutinin of yeast is a cell adhesion protein mediating cel-cell contact during mating of haploid cells of Saccharomyces cerevisiae. The N-terminal 350 residues have a CD spectrum characteristic of β sheet and include three possible immunoglobulin-like domains. The sequence containing residues 200 through 320 has significant similarity to a consensus sequence for immunoglobulin V-like domains. Segments containing residues 20-105, 105-185, and 200-320 each has sequence similarity and a Chou-Fasman profile consistent with the presence of an immunoglobulin-like domain. Tertiary and secondary structural models will be presented based on disulfide mapping and on comparisons with crystallographically determined structures of immunoglobulins, CD4, and CD8.

**M-Pos233**

REGULATION OF BAND 3 ROTATIONAL MOBILITY BY ANKYRIN IN INTACT HUMAN RED CELLS. ((M.R. Cho, S.W. Eber, S.E. Lux, and D.E. Golan)) Departments of Biological Chemistry and Molecular Pharmacology, Medicine, and Pediatrics, Harvard Medical School; Divisions of Hematology/Oncology, Brigham and Women's and Children's Hospitals, Boston, MA 02115.

Spectrin deficiency and ankyrin defects are prominent features of red cells in patients with hereditary spherocytosis (HS). We have used fluorescence photobleaching recovery (FPR) and polarized fluorescence depletion (PFD) to study the lateral and rotational mobilities of band 3 and glycophorins in intact red cells from 5 HS patients with characterized ankyrin defects and combined spectrin/ankyrin deficiency. As predicted by the steric hindrance ("fence") model, the lateral diffusion coefficients of band 3 and glycophorins were greater in HS red cells than those in control cells; the magnitudes of increase correlated with the degree of spectrin deficiency. Unlike red cells from patients with severe autosomal recessive HS with selective spectrin deficiency, which manifest normal band 3 rotational mobility, HS red cells with significant ankyrin defects exhibited a marked increase in band 3 rotation. At least 90% of band 3 molecules in cells with ~40% ankyrin deficiency had rotational correlation times (τ) of 260 to 350 μs. In contrast, control cells had ~25% rapidly rotating band 3 molecules (τ< 200 μs), ~60% slowly rotating molecules (τ= 1-3 ms), and ~15% rotationally immobile molecules. These data suggest that ankyrin deficiency significantly relaxes rotational constraints on the major (slowly rotating) population of band 3 molecules. Increases in band 3 rotation may be due to release of band 3 oligomers (primarily tetramers) from low affinity binding sites (such as immobilized ankyrin-band 3 complexes) on the membrane skeleton.

**M-Pos234**

A *XENOPUS LAEVIS* DISINTEGRIN PROTEIN WITH A POTENTIAL ROLE IN FERTILIZATION
((Urte Gayko & Carl P. Blobel)) Cellular Biochemistry and Biophysics Program, Memorial Sloan-Kettering Cancer Center, 1275 York Ave., New York, NY, 10021

Disintegrins are a large family of short soluble integrin ligands found in snake venom. They bind with high affinity to the platelet integrin gpIIb/IIIa and thereby inhibit platelet aggregation. The first recognized cellular protein with a disintegrin domain was the guinea pig sperm protein PH-30, a potential sperm-egg membrane fusion protein. PH-30 is thought to bind to an integrin type receptor on the egg plasma membrane. In order to establish a better system to study sperm-egg membrane interactions, we have searched for a PH-30 homologue in the frog *Xenopus laevis*, where large numbers of eggs can be isolated for biochemical and biophysical studies. Using degenerate oligonucleotide primers and the polymerase chain reaction, followed by 3' and 5' rapid amplification of cDNA ends (RACE) we identified a PH-30 homologue in Xenopus testis. High stringency northern blot analysis revealed an expression pattern that is restricted to the testis. Cyclic and linear peptides representing the predicted binding site of Xenopus PH-30 inhibit Xenopus fertilization in vitro, whereas control peptides do not. We conclude that Xenopus PH-30 is likely to play an important role in Xenopus fertilization.

**M-Pos235**

MECHANISM OF PHOSPHORYL TRANSFER AND PROTEIN-PROTEIN INTERACTION IN THE PTS SYSTEM--AN NMR STUDY.
((Ponni Rajagopal and Rachel E. Klevit)) Department of Biochemistry, University of Washington, Seattle, WA 98195.

HPr and Enzyme IIA$^{Glc}$ are two of the components of the bacterial PTS (phophoenolpyruvate: sugar phosphotransferase system) and are involved in the phosphorylation and the concomitant translocation of sugars across the membrane. These PTS protein complexes are also found to regulate sugar transport. HPr is phosphorylated at a histidine N-1 site by Enzyme I and phosphoenol pyruvate and transfers the phosphoryl group to a histidine N-3 position in Enzyme IIA$^{Glc}$. P-His15- HPr from the Gram-positive bacterium, *Bacillus subtilis*, was investigated by both homonuclear and heteronuclear 2D and 3D NMR experiments and the results are presented in this poster. The results show that phosphorylation causes localized changes, viz., in the conformation of the His15 ring and in the interaction of the conserved residues Arg17 and Pro18 with His15. HPr-Enzyme IIA$^{Glc}$ complexes from both *Bacillus subtilis* and Gram-negative *Escherichia coli* were also studied by a variety of $^{15}$N-edited 2D NMR experiments. The experiments were performed on uniformly $^{15}$N-labeled HPr complexed to unlabeled Enzyme IIA$^{Glc}$. The binding site of HPr in complex with Enzyme IIA$^{Glc}$ was mapped by monitoring chemical shift changes of the amide protons in HPr. The binding site was found to be the same in both the HPrs. To further characterize the changes undergone by HPr on binding, $^{15}$N-linewidths and amide exchange rates were measured for both free and bound HPr.

**M-Pos236**

CONFORMATIONAL CHANGES IN CAT AND CPT-II INDUCED BY SUBSTRATE BINDING

Bing Yan* and William R. Mann#, Departments of Central Technology* and Diabetes#, Preclinical Research, Sandoz Research Institute, Sandoz Pharmaceuticals Corporation, East Hanover, NJ 07936

The carnitine palmitoyltransferase (CPT) system, containing CPT-I and CPT-II, and the carnitine acetyltransferase (CAT) system, catalyze the transfer of acyl-CoA esters into the mitochondrial matrix for β-oxidation. CPT-II, unlike CPT-I, remains active when solubilized and is considered an appropriate model for CPT-I since it catalyzes essentially the same reaction as CPT-I does, except in reverse. L-carnitine/CAT and L-carnitine/recombinant CPT-II (rCPT-II) were studied by circular dichroism (CD) and fluorescence spectroscopy using a wide range of carnitine concentrations. CD spectra of CAT and rCPT-II were analyzed for their secondary structure content by SELCON program (kindly provided by Dr. R. Woody). From the CD spectra, CAT is predicted to contain 33% α-helices, 17% β-sheets, 28% turns and 20% unstructured coils and rCPT-II is predicted to contain 47% α-helices, 12% β-sheets, 23% turns and 18% unstructured coils. Decreased intensity of the positive band at 190 nm and the double negative bands at 208-220 nm were observed in both proteins upon carnitine binding indicating the unfolding of α-helices. Significant loss of α-helix content was observed for in both proteins when the carnitine concentration was in large excess. These conformational changes were corroborated by fluorescence studies, where both intrinsic emission and excitation intensities of CAT and rCPT-II decreased as carnitine bound to the enzymes. Analysis of data revealed an apparent negative cooperativity for carnitine binding in CPT-II. On-going studies on interactions of palmitoyl-CoA, acetyl-CoA and inhibitors with rCPT-II and CAT will also be presented.

**M-Pos237**

**Characterization of Interactions between Human IgE, Anti-Human IgE Monoclonal Antibody and High Affinity IgE Receptor.**
**((J. Liu, S. Shire, P. Lester, S. Builder)) Genentech, Inc., S. San Francisco, CA 94080.**

The interaction of human IgE with high affinity IgE receptors on cells of the immune system plays an essential role in type one hypersensitivity reaction. An anti-human IgE monoclonal antibody(E25, by Presta, et al., 1993) has been shown to be a potential inhibitor of IgE-mediated response by competitively blocking the binding of IgE to its high affinity receptor since the E25 and receptors share the similar binding sites on IgE. In pursuit of better understanding the molecular basis and physiological roles of these molecules, sedimentation analyses were applied to characterize the thermodynamic and hydrodynamic behaviors of these interactions. In this study, we demonstrate that both E25 and the high affinity chimeric receptor, which contains two extracellular portions of the binding domain (a chain) are able to form a variety of larger complexes with IgE. The sizes of the dominant species depend on the molar ratio of molecules involved. The interaction of human IgE with E25 appears to be the thermodynamic favorable process.

**M-Pos238**

PHOTOINDUCED STRUCTURAL CHANGES IN THE FIBRONECTIN COLLAGEN-GELATIN BINDING DOMAIN.

((A.M. Miles and R.L Smith)) Dept. of Biochemistry and Mol. Biol., LSU Medical Center, Shreveport, LA 71130 (Spon by E. Aamodt)

Prolonged 280nm irradiation of human plasma fibronectin (pFn), its 40 kDa collagen-gelating binding domain (CGB), or a 21 kDa gelatin-binding fragment (GBF) caused decreased binding affinity for gelatin and for TR-CB7, a fluorescently labeled CNBr fragment from the Fn-binding region of the α-1 chain of type I collagen. Fluorescence polarization binding (FPB) assays of TR-CB7 with pFn and the 40 kDa CGB domain yielded progressively higher Kds with increased time of exposure to 280nm light in a model 500C SLM-Aminco spectophotoflourimeter at room temperature. Comparison of urea elution profiles of affinity chromatography on gelatin-agarose with non-irradiated and irradiated pFn and fragments correlated with FPB data, revealing diminished gelatin binding following 280nm light exposure. Emission spectra of intrinsic tryptophans in the 40 kDa CGB domain and the 21 kDa GBF exhibited spectral perturbations indicative of conformational changes. Maximum emission wavelength red-shifted from between 340 and 350nm to 360nm, with concomitant increases in fluorescence intensity. We have also determined that extended exposure to 280nm light of pFn, the CGB domain, or the 21 kDa GBF results in the generation of approximately 6, 4, and 2 free sulfhydryls per molecule respectively. No sulfhydryl release was observed in other Trp- and disulfide-containing proteins under the same conditions. We propose that the observed changes in the binding affinity for gelatin or the collagen fragment, and in the intrinsic tryptophan fluorescence spectra result from structural changes secondary to disulfide reduction, the consequence of tryptophan fluorescence quenching by nearby disulfides within one or more of the fibronectin type I repeats in the collagen-gelatin binding domain.

**M-Pos239**

**MAPPING PROTEIN DOMAINS INVOLVED IN MACROMOLECULAR INTERACTIONS: A SIMPLE PROTEIN FOOTPRINTING APPROACH**

((Ewa Heyduk and Tomasz Heyduk)) St.Louis University, Medical School, Dep. of Biochem. and Molec. Biology. 1402 S.Grand Blvd., St.Louis, MO 63104.

A great number of biological functions of proteins are expressed via interactions with other macromolecules. One of the essential steps in understanding these functions is to identify the regions of a protein molecule which participate in protein- macromolecule complex formation. When a three-dimensional structure of a complex is unknown, this task could be quite difficult. We present here a simple, direct approach, analogous to DNA footprinting, which allows mapping protein domains involved in macromolecular interactions. In this approach a protein-macromolecule complex is subjected to a nonspecific cleavage by a chemical protease. The cleavage products are resolved by SDS-PAGE electrophoresis, transferred to PVDF membrane and detected with antibodies to the N-terminal peptide of the protein. The mobility of the peptides visualized in such a way is directly proportional to a distance of the cleavage site form the N-terminus of the protein. Thus, the by comparing with the mobility of appropriate standards the positions of the cleavage sites in protein primary structure can be determined as well as the positions of sites which are protected by protein-macromolecule formation. We have tested this approach using cAMP receptor protein (CRP)-DNA interaction as a model system. The cleavage conditions have been established which result in on average less then one cleavage event/protein molecule and which preserve satisfactory levels of protein and DNA activity. Our approach correctly identified domains in CRP sequence which were known to be involved in recognition of specific DNA. Also, cAMP induced change of CRP conformation could be detected and the sites in protein primary structure affected by this change were identified. In conclusion, we believe that this approach will be a very valuable tool to study protein-macromolecule interactions and protein conformational changes. It should be applicable to any protein-macromolecule interaction, since the experimental techniques used are not specific for any particular protein, and the nature of the macromolecule is not limited only to DNA.

**M-Pos240**

EFFECTS OF MACROMOLECULAR CROWDING ON MOLECULAR RECOGNITION. ((A. P. Minton)) NIDDK, NIH, Bethesda, MD 20892

Investigations of molecular recognition are concerned with factors underlying the observed specificity of chemical reactions. When analyzing the difference in affinity of an acceptor (X) for two ligands (A and B), emphasis has traditionally been placed on factors responsible for the relative stability (i.e., the difference between the chemical potentials) of the two product species AX and BX. However, under certain conditions, thermodynamically nonideal behavior in solution can lead to large differences between the chemical potentials of free A and B at equal concentration, resulting in correspondingly large differential alterations of the relative standard free energy changes associated with the binding of A and B to X, and hence the relative affinities of X for A and B. A general thermodynamic formalism for the effect of macromolecular crowding (volume exclusion arising from high concentrations of macromolecules) upon macromolecular association in solution and upon association of a soluble ligand to a stationary site is briefly reviewed. Two specific examples of crowding effects upon reaction specificity are then presented: (1) the preference of a site for one of two competing ligands and (2) competitive inhibition of the binding of a virus to a cell surface.

**M-Pos241**

**USE OF BINDING ENERGY AND RECEPTOR ACTIVATION.**

**((C.J. Ritz-Gold)) Biomolecular Sciences, Fremont, CA 94536.**

**For many kinds of membrane receptor, the process of activation is thought to involve an agonist-induced conformational change. This conformational change has, in turn, been represented as an agonist-binding reaction in which: 1) rapid formation of an initial low-affinity agonist-receptor complex is followed by 2) slower isomerization to a final high-affinity complex. It is suggested here that this 2-step binding-reaction description may be used to gain further insight into two distinct but related types of activation process. In the case of neurotransmitter receptors such as the nicotinic ACh receptor, the initial complex would represent a transient active state and the final complex, a desensitized state. In the case of hormone receptors such as the β-adrenergic receptor, the initial complex would represent an inactive state and the final complex, an active state.**

**Using this binding-reaction description, we seek a better understanding of receptor activation by looking at how agonist binding energy is used during each of these two types of activation process. In particular, for each type of process, we look at the kind of changes in receptor structure and free energy one might expect to occur during each step of the agonist-binding reaction. The approach taken here is based on concepts drawn from both induced-fit theory and from strain or distortion theory [W.P. Jencks (1987) "Catalysis in Chemistry and Enzymology," Dover, N.Y.]. It also follows from, and extends, previous theoretical efforts to understand receptor activation in terms of induced-fit theory and the use of binding energy [e.g., T.J. Franklin (1980) Trends Pharm. Sci. 1, 430; A. Gero (1983) J. Theor. Biol. 103, 17].**

**M-Pos242**

**CONFORMATIONAL CHANGES IN PROPOSED BINDING POCKET OF THE HUMAN 5-HT$_{1D\alpha}$ RECEPTOR.**

**((A. Smolyar and R. Osman))** Department of Physiology and Biophysics, Mount Sinai School of Medicine, CUNY, New York, NY 10029.

The structure of a three dimensional model of the 5-HT$_{1D\alpha}$ receptor was optimized by energy minimization. A selective drug, sumatriptan, was docked inside the helical bundle by positioning the protonated side chain amine next to the carboxylate of Asp$^{118}$ in helix (Hx) 3, the N-H group of the sulfonamide of sumatriptan next to Asp$^{339}$ in Hx 7 and the S-O group next to the Oγ-H of Thr$^{342}$. The structure of the ligand-receptor complex was optimized by energy minimization and then heated to 300K followed by 200 ps of constant temperature molecular dynamics (MD) simulation with a distance dependent dielectric function. The sumatriptan was withdrawn and the remaining helical bundle was optimized and heated to 300K followed by 250 ps of MD simulations. Analysis of the average minimized structures and the MD trajectories from both simulations show that the contribution of non-polar residues to the molecular surfaces for each separate helix was 67-87% 0f the total surface area. The area of 4Å distance map between constructed surfaces shows that non-polar residues contribute 33-66% of the interfacing molecular surfaces. An inspection of a zone 3.5 Å around all polar residues shows specific intra- and interhelical polar-polar interactions that contribute to the stability of the bundle. The binding site is made up of 14 residues, 7 of which interact directly with sumatriptan with energetic contributions exceeding 2.5 Kcal/mol. An analysis of the conformational changes in the receptor upon binding of the ligand shows that major rearrangements occur in apolar residues in Hx 6, in polar residues in Hx 2, and in the binding pocket.

*Supported by NIDA Training Grant DA-07135 and grant DA-06620.*

**M-Pos243**

CHARACTERIZATION OF HIGH AFFINITY CALCIUM-ANTAGONIST BINDING SITES IN GUINEA-PIG LIVER: POSSIBLE RELATIONSHIP TO SIGMA RECEPTORS. ((F.F. Moebius, M. Hanner, J. Striessnig and H. Glossmann)) Institut für Biochemische Pharmakologie, Universität Innsbruck, A-6020 Innsbruck, Austria

The arylazide phenylalkylamine (PAA) $Ca^{2+}$-antagonist [$^3$H]azidopamil was used for the biochemical and pharmacological characterization of PAA binding polypeptides in guinea-pig liver. This PAA specifically photoaffinity labeled two polypeptides with apparent molecular masses of 22 and 27 kDa, respectively, which were highly enriched in the endoplasmic reticulum membrane. Pharmacological studies revealed that the 22 kDa polypeptide carries the previously described cation-sensitive binding site for the verapamil-like PAA emopamil. Both polypeptides displayed high affinity for azidopamil (Kd=13 nM) and emopamil (Kd=10 nM) as well as for other drugs, like opipramol and ifenprodil. As we and others found that the latter drugs also possess high affinity for [3H]DTG-labeled sigma binding sites (SBS) we investigated the relationship of the photolabeled polypeptides to SBS. The sigma ligands DTG (Ki=19 nM), pentazozine (Ki=2.6 nM), (+)-SKF10,047 (Ki=51 nM), and haloperidol (Ki=0.8 nM) inhibited specific photolabeling of the 27 but not of the 22 kDa polypeptide with high affinity and a pharmacological profile typical for SBS. This high affinity and the selectivity for (+)-benzomorphans (Ki > 1μM for (-)-SKF10,047) indicate that the 27 kDa polypeptide carries a sigma site of the sigma$_1$-subtype. As the 22 kDa polypeptide shares some pharmacological (i.e. identical affinity for azidopamil, emopamil, opipramol) as well as biochemical (subcellular localization, similar molecular mass) properties with the 27 kDa polypeptide, we propose the possibility of a structural and perhaps functional relationship with sigma binding sites.

This work was supported by Boehringer-Ingelheim fellowship (F.F.M.) and grants (S6601, P9351) by the Fonds zur Förderung der Wissenschaftlichen Forschung, Austria (H.G., J.S.).

**M-Pos244**

SEDIMENTATION EQUILIBRIUM DETERMINATION OF THE STOICHIOMETRY FOR FORMATION OF THE HUMAN GAMMA INTERFERON ($\gamma IFN_2$) : RECEPTOR (EXTRACELLULAR DOMAIN) COMPLEX. ((David A. Yphantis, Jeff Lary, Rosalinda Syto*, Stephen Tindall*, Paul P. Trotta* and William T. Windsor*)) Molecular and Cell Biology and National Analytical Ultracentrifuge Facility, Univ. of Connecticut, Storrs, CT 06268 and Schering Plough Research Institute*, Kenilworth, NJ 07033

$\gamma IFN_2$, a 36-kg $mole^{-1}$ homodimer, is a cytokine modulator of the immune system and inflammation. The activities of $\gamma IFN_2$ are initiated following its binding to a cell surface receptor ($\gamma$IFN-R). $\gamma$IFN-R contains a ~26-kDa extracellular binding domain (ECD), a ~2.4-kDa single transmembrane region and a ~25-kDa intracellular domain which becomes phosphorylated following $\gamma$IFN binding. Complex formation between recombinant E. coli derived $\gamma$IFN-R(ECD) and $\gamma IFN_2$ was examined in dilute solutions (~0.1mg/ml) in 0.1M ammonium acetate pH 6.9 (8°C) to estimate the initial stoichiometry of the complex formation. Least squares analysis of long-column (~2.6mm) sedimentation equilibrium experiments with mole-ratios of $\gamma$IFN-R(EDC):$\gamma IFN_2$ of 0.32, 0.52 and 2.16 at equilibrium speeds of 15, 22, and 30 K RPM indicated the initial stoichiometry to be 2.03+/-0.03 $\gamma$IFN-R(EDC):1.02+/-0.04 $\gamma IFN_2$. The association constant for complex formation was too large to be determined under the present conditions. [Supported in part by NSF Grants #DIR-8612159 and BIR-921867.]

**M-Pos245**

CLASSICAL RAMAN SPECTROSCOPIC STUDIES OF BIOPTERIN BOUND TO E. COLI DHFR BY DIFFERENCE TECHNIQUES. ((Y. Q. Chen, J. Kraut and R. Callender)) Dept of Physics (Y.C. and R.C.), CCNY of CUNY, NY, NY 10031 and Dept of Chemistry (J.K), University of California, San Diego, La Jolla, CA 92093

Current models of the catalytic pathway in dihydrofolate reductase require that the C=O bond of substrate is polarized to varying degrees as a proton is shuttled from solvent to substrate's N5 via Asp-27 and structural water molecules. We have used classical Raman difference spectroscopy to obtain the spectrum of biopterin bound in wild type DHFR and in the mutant D27S in order to investigate this issue directly. We found that bound biopterin in wild type DHFR-$NADP^+$-biopterin ternary complex exists as a mixture of the enol/enolate form and two keto forms (with pteridine ring's carbonyl stretches at 1693 and 1653 $cm^{-1}$). However, biopterin in D27S-$NADP^+$-biopterin exists only as a single keto form, virtually the same one as found in aqueous solution (keto stretch at 1700 $cm^{-1}$). The bound keto 1693 $cm^{-1}$ form represents a relatively small admixture of $^+C\text{-}O^-$ into the keto's C=O bond while the 1653 $cm^{-1}$ form is very strongly polarized. These results will be discussed in terms of the catalytic mechanism proposed by several groups, in which Asp-27 functions as promoting pteridine ring enolization.

**M-Pos246**

INFLUENCE OF VISCOSITY AND TEMPERATURE ON THE CONFORMATIONAL DRIFT IN MONOCLONAL ANTI-FLUORESCYL ANTIBODIES (Mab) 4-4-20 ((Joachim D. Müller*, Chester D. Eng, Sergey Y. Tetin, Theodore L. Haslett, Edward W. Voss Jr. & G. Ulrich Nienhaus)) Department of Physics, Biophysics & Microbiology, University of Illinois at Urbana-Champaign, IL 61801, *Technische Universität München, Germany.

Ligand titration studies with fluorescein reveal conformational changes in the monoclonal anti-fluorescyl antibody (Mab 4-4-20) upon binding. We used anisotropy and fluorescence quenching techniques to study the influence of viscosity upon the equilibrium binding at various temperatures. The experimental data for each temperature and viscosity failed to be represented by the Langmuir isotherm equation expected for ligand-receptor titration studies with a unique dissociation coefficient. We observe a decrease in the dissociation coefficient with increasing degree of association of the protein ligand complex and fit the data to an empirical model. Cooperativity between the two binding sites was excluded to be responsible for the observed binding curves by measurements performed on Fab fragments. Viscosity has a marked effect on the equilibrium binding, whereas temperature only induces small changes. We attribute the changes in the observed dissociation coefficient to conformational transitions on the same time scale as the lifetime of the protein ligand complex. Supported by NIH.

**M-Pos247**

SITE-DIRECTED SPIN LABELING OF THE FERRIC ENTEROBACTIN RECEPTOR, FEPA ((Jun Liu*, J. M. Rutz*, Phillip E. Klebba†, and Jimmy B. Feix*)) †Department of Microbiology, and *National Biomedical ESR Center, Biophysics Research Inst., Medical College of Wisconsin, Milwaukee, WI, 53222. (Spon. by Dr. C. Narasimhan)

Site-directed spin labeling is a powerful technique for probing structure-function relationships in proteins. The ability to introduce cysteine labeling sites at desired locations, rather than relying on endogenous cysteines, makes the spin labeling approach both general and systematic. We have initiated site-directed spin labeling studies of the *E. coli* ferric enterobactin receptor, FepA. This outer membrane receptor, which is responsible for iron uptake in the vast majority of enteric bacteria, contains two native cysteine residues that can only be labeled following thiol reduction, indicating that they are disulfide-linked. We have created two new mutants of FepA, each with an additional cysteine in the ligand-binding domain. These mutants are readily labeled with sulfhydryl-specific spin labels without prior thiol reduction, and retain full functional activity. The motional characteristics of spin labels bound to these sites indicate a highly structured environment. Accessibility to paramagnetic relaxation agents demonstrate that one mutation site is exposed to the aqueous phase, while the other occupies an interfacial location near the membrane surface. Systematic application of this approach can be used to develop a comprehensive structure for the ligand-binding domain of FepA.

**M-Pos248**

INTERACTION OF ANTINEOPLASTIC DRUGS WITH HEMOGLOBIN. (( Samira Barghouthi and Linda Munchausen)). Department of Chemistry and Physics, Southeastern Louisiana University, Hammond, LA 70402

In our research we are studying the interaction of some selected antineoplastic drugs such as podophyllotoxin and vinblastine with myoglobin and hemoglobin. Fluorescence spectrophotometry is used to monitor changes in emission spectra of the drugs upon binding to hemoglobin. UV-visible spectrophotometry is also employed to monitor conformational changes to the target protein in the presence of these drugs. By studying individual ligands and comparing their chemical and thermodynamic behavior we hope to gain a better understanding of the cytotoxicity of these potent antineoplastic drugs.

**M-Pos249**

STRUCTURE AND DYNAMICS OF α-TRANSDUCIN DETERMINED BY INTRINSIC TRYPTOPHAN FLUORESCENCE. ((Y.Manevich and P.A.Liebman))Univ. of Pa. Medical Center, Philadelphia, Pa. 19104-6058

295nm excitation of tryptophans 127 and 207 of transducin alpha subunit yielded steady state emission best fitted as the sum of peaks at 330nm (small) and 347nm (larger) suggesting apolar and polar trp environments respectively. $Cs^+$ quenching selectively reduced the polar emission, leaving the apolar emission unchanged consistent with a relatively exposed surface location of trp 127 and a buried location of trp 207. Emission decay was triexponential with lifetimes of ca. 0.25, 1.6, and 4.2ns. $Cs^+$ quenching effected only the 4.2ns amplitude, while $NO_3^-$ also effected the 1.6ns amplitude. This selectivity had its counterpart in steady state quenching as well. 8M urea denaturation gave increased intensity with the same decay times of 5.1ns, 1.4ns, and 0.25ns and emission maximum shift to 352nm. GDP/GTP exchange selectively enhances the apolar trp emission consistent with a tilt/rotation of the helix bearing trp 207 away from the protein hydrophobic core and nucleotide binding site. Time resolved anisotropy showed specific lipid selectivity in protein binding to vesicles. Supported by EY00012, EY01583 and by RR01348 to Penn's RLBL for the lifetime work.

M-Pos250

**CHLORIDE ACTS AS A NOVEL HETEROTROPIC EFFECTOR OF HEMOGLOBIN ROTHSCHILD (β37 TRP→ARG) IN SOLUTION**

((R.M. Kelly, H.L. Hui and R.W. Noble)) Depts. of Medicine and Biochemistry, State University of New York, University at Buffalo and Veterans Administration Medical Center, Buffalo, N.Y. 14215.

The effects of chloride ion concentration on the rate constants for association of carbon monoxide with human hemoglobin A and a synthetic form of the mutant hemoglobin Rothschild (β37 Trp→Arg) have been investigated by stopped-flow techniques. Previous studies of the structure (Kavanaugh et al. (1992) Biochemistry 31, 4111) and functional properties (Rivetti et al. (1993) Biochemistry 32, 2888) of hemoglobin Rothschild crystallized in the T state have demonstrated that the mutant arginine residues create new chloride ion binding sites and that chloride ions act to lower the oxygen affinity of hemoglobin Rothschild in these crystals. We have demonstrated a parallel effect of chloride ions on the rate of carbon monoxide association with deoxygenated hemoglobin Rothschild in solution. Although in solution the kinetics of this hemoglobin exhibit a Bohr effect, the chloride effect is independent of pH. In addition, other halide ions alter the rate constants for the association of carbon monoxide with this hemoglobin variant in a similar manner. Supported by funds from the USPHS NIH Program Project Grant PO1 HL40453 and the Veterans Administration.

M-Pos251

**HEMOGLOBIN TETRAMERS SHOW STRUCTURAL ASYMMETRY IN RESPONSE TO SINGLE-SITE MUTATIONS AND HEMESITE LIGATION.**

((Gary K. Ackers, Vince J. LiCata, Paula M. Dalessio, and George Lew)) Dept. of Biochemistry & Molecular Biophysics, Washington University School of Medicine, St. Louis, MO 63110.

Techniques of subunit hybridization [Perella *et al.* (1981) Methods Enz. 76, 133; LiCata *et al.* (1990) Biochem. 29, 9771] have made it possible to study the energetics of human hemoglobin tetramers containing a single modified amino acid residue and simultaneously ligated with any combination of ligated and unligated hemesites (CN-met). Recent experiments with 19 single-residue modifications have revealed dramatic asymmetry in the responses of the dimeric half-molecules within the same tetramer (i.e. the $\alpha^1\beta^1$ and $\alpha^2\beta^2$ dimers separated by the symmetry plane of the "$\alpha^1\beta^2$ interface"). It is found that: (a) ligation and mutation on opposite dimers (i.e. separated by the $\alpha^1\beta^2$ interface) are totally independent, while (b) ligation and mutation on the same dimer are coupled "globally", i.e. within the dimer. Implications of these findings for the mechanism of cooperative free energy transduction in the hemoglobin system will be discussed. (Supported by NIH Grant GM24486 and NSF Grant DMB9107244.)

M-Pos252

**INTERACTION OF ODORANTS WITH THE ODORANT BINDING PROTEIN.**

((Gabrielle Bains#, Ernesto Freire*, and L. Mario Amzel#))
#Department of Biophysics and Biophysical Chemistry, School of Medicine, *Department of Biology, The Johns Hopkins University, Baltimore MD 21205 (Spon. by Ed Lattman)

The thermal denaturation of the bovine odorant binding protein (bOBP) has been studied by differential scanning calorimetry (DSC). DSC of the homodimer in the absence of ligand demonstrates that the denaturation is partially reversible with an enthalpy on the order of 300 kcal/mol and a Tm of 87.4°C. The crystal structure of the protein is currently being determined in this lab and reveals a ß-barrel fold similar to that of the retinol binding protein. DSC performed in the presence of odorant reveals that the dimer is stabilized (Tm=88.4°C) and that the cooperativity of denaturation increases when odorant is present suggesting a change in the interaction energetics at the dimer interface. In other experiments, isothermal titration calorimetry has been used to characterize the binding of odorant to bOBP. The binding experiments indicate that the interaction between bOBP and the odorant (l)-carvone is enthalpically favorable (ΔH=-11.3 kcal/mol) and entropically unfavorable (ΔS=-9.4 cal/K.mol) at 25°C despite the hydrophobic and rigid nature of the ligand. The results of the binding experiments lend support to the idea that conformational changes in the protein or protein dimer interface may play a role in the binding of odorant ligands to this protein. (Supported by grants GM44692 and RR04328).

M-Pos253

**1H-NMR SOLUTION STUDIES OF AN EPIDERMAL GROWTH FACTOR-LIKE DOMAIN FROM THE MARFAN SYNDROME PROTEIN FIBRILLIN.**

((Vicky L. Bevilacqua*, Yu-Sung Wu+, and Jeremy M. Berg*))
Department of Biophysics and Biophysical Chemistry*, Johns Hopkins University, Baltimore, MD 21205 and Department of Chemistry+, Johns Hopkins University, Baltimore, MD 21218.

The connective tissue disorder Marfan syndrome (MFS) is manifested by skeletal, ocular, and cardiovascular abnormalities. Various studies have implicated mutations in the EGF-like repeats of the protein fibrillin as the cause of MFS and related disorders. One such mutation, Arg239-->Pro (R239P) has been found in fibrillin's fourth EGF-like repeat (hfib4) in two MFS patients. hfib4 and its homologous repeats in fibrillin contain a calcium-binding consensus sequence common to some EGF-like domains. The defect in fibrillin function could result from the inability of the mutated domains to fold, to fold properly, to bind calcium, or to self-assemble. We have synthesized and characterized 42 amino acid peptides corresponding to the wild type (wt) and R239P hfib4 domains. Using one and two-dimensional $^1$H-NMR, we have determined the low resolution structure of calcium-free wt hfib4 and are refining the structure with more distance constraints. We show here a comparison of the hfib4 wt structure with those of other EGF-like domains. In addition, we have determined the $K_d$ for calcium binding to wt hfib4 and are currently carrying out studies on R239P hfib4.

M-Pos254

**BIOPHYSICAL CHARACTERIZATION OF THE METAL-DEPENDENT CONFORMATIONAL CHANGE OF HUMAN PAPILLOMAVIRUS (HPV) TYPE 16 E7 PROTEIN.**

((A. Aulabaugh and W. Phelps.)) Burroughs Wellcome Co., Research Triangle Park, NC 27709

HPV16 E7 is a small (98 amino acid) viral oncoprotein characterized by an unusual C-terminal zinc-binding domain -Cys58-X2-Cys61-X28-Cys91-X2-Cys94-. Through residues in the amino-terminal half, E7 associates with several cell cycle regulatory proteins including the retinoblastoma tumor suppressor protein. Previous work from this laboratory (Pahel et al, J. Biol. Chem, in press) revealed that metal binding to HPV16 E7 induced a conformational change consistent with stabilization of a hydrophobic core in the bidomain protein. To more fully characterize the conformational change associated with metal binding we have used endogenous tyr fluorescence to monitor metal-dependent conformational changes in E7. E7 contains 4 tyr residues in the N-terminal half of the molecule which served as fluorescent probes to monitor conformational changes in solution with the assumption that the fluorescence quantum yield of a tyr residue in the protein is dependent on its local environment. Addition of zinc chloride resulted in a decrease in tyr fluorescence intensity and a concomitant change in the circular dichroism spectrum. Fluorescence quenching experiments with potassium iodide yielded additional information about the metal-dependent solvent accessibility of the tyr residues. In the presence of quencher, an increase in the fraction of accessible fluorophor from 0.6 to 1.0 was observed upon zinc-binding indicating the tyr residues were highly exposed in the metal-bound form. The fraction of solvent accessible tyrosine fluorescence of the metal-free protein was the same within error in the presence of the charged quencher KI or acrylamide indicating the inaccessibility of KI is not due solely to local charge effects around the tyrosinyl side chains but also burial of the residues. Apparent dissociation constants for the metal binding reaction are being calculated from the observed quench.

M-Pos255

**ASSOCIATION OF THE TERBIUM BINDING PROTEIN WITH CISPLATIN RESISTANCE.**

((R.G. Canada, *P.A. Andrews and K.M. Mack)) Howard Univ., Dept. of Physiology and Biophysics, Washington, D.C. 20059 and *Georgetown Univ., Dept. of Pharmacology, Rockville, MD 20850.

The objective of this investigation was to determine whether there is a relationship between the terbium ($Tb^{3+}$) binding protein and the accumulation of cisplatin (CDDP) in CDDP-sensitive (2008) and CDDP-resistant (C13*) human ovarian tumor cells. CDDP has been shown to interact with a specific $Tb^{3+}$ binding protein in the plasma membrane of cancer cells. Time-resolved phosphorescence and atomic absorption spectrophotometry were used to obtain equilibrium binding constants for the receptor binding of $Tb^{3+}$ and to measure the cellular accumulation of CDDP, respectively. The $\Delta I_{max}$ for the $Tb^{3+}$/C13* complex was significantly greater (by 78%) than the $\Delta I_{max}$ for the $Tb^{3+}$/2008 complex ($P < 0.002$). The $K_d$ for the $Tb^{3+}$/2008 complex was the same as that for the $Tb^{3+}$/C13* complex ($P > 0.4$). $Tb^{3+}$ was found to increase the cellular accumulation of CDDP. The $Tb^{3+}$-induced uptake of CDDP in C13* cells was 24% greater than in 2008 cells ($P < 0.004$). The receptor binding of $Tb^{3+}$ and the cellular uptake of CDDP were also examined in the RH4 CDDP-revertant cells. Our results suggest that the $Tb^{3+}$ binding protein correlate with CDDP resistance and may modulate CDDP accumulation.

**M-Pos256**

SPECIFICITY OF INTERACTION OF CALMODULIN WITH TARGET SEQUENCES. W.A.Findlay, G.J.Hipkin, S.R.Martin and P.M.Bayley. National Institute for Medical Research, Mill Hill, London NW7, U.K.

Calmodulin (CaM) binds with high affinity to a number of cellular targets, resulting in calcium-dependent activation of different enzymes. Different CaM binding sequences contain substantial variations in amino-acid composition, but are generally predicted to adopt an amphipathic $\alpha$-helical conformation. The specificity of the target interaction has been studied using a series of 18-residue peptides corresponding to residues 577-594 of skeletal muscle myosin light-chain kinase, with substitutions of the aromatic residues W,F,and F in positions 4, 8, and 17. Based on the nmr co-ordinates (Ikura et al., Science 256:632 (1992)), W4 is predicted to be approximately 13 Å from calmodulin Y138. Fluorescence energy transfer (FET) consistent with this has been observed in the complex of *Drosophila* calmodulin with the native sk-MLCK peptide (WFF). By contrast the complex of CaM with peptide FFW shows little or no FET, as well as having a characteristically different near-UV Trp CD spectrum. For both complexes, the Trp fluorophore is substantially protected against acrylamide quenching. These results are consistent with the binding of peptide FFW in the same sense as WFF, implying interaction of W17 of the peptide with residues of the N-terminal domain of calmodulin.

**M-Pos257**

FLUORESCENCE STUDIES OF THE COMPLEX BETWEEN CALMODULIN AND THE PEPTIDE CORRESPONDING TO THE CALMODULIN BINDING DOMAIN OF NEUROMODULIN. ((Mark R. Ehrhardt, Leonardo Erijman, G. Weber and A.J. Wand)) Department of Biochemistry, University of Illinois-Urbana/Champaign, Urbana, IL 61801

The interaction between the peptide corresponding to the calmodulin-binding domain of neuromodulin (Nm-p) and calcium free calmodulin (CaM) has been studied by fluorescence spectroscopy. Both neuromodulin and Nm-p are unusual among calmodulin binding proteins in that they bind to CaM in the absence of $Ca^{2+}$. The acidity of calmodulin and the seven basic amino acids of Nm-p (QASWRGHITRKKLKGEK) indicate electrostatic interactions are likely to dominate complex formation. This hypothesis was strongly supported by the observation that the CaM-Nm-p complex is 50% dissociated in 30 mM KCl. High pressure between 0.2 and 2.4 kbar red shifted of the Nm-p tryptophan emission center of mass indicating a regional change in polarity. This event was shown to be unimolecular (no dissociation of complex) by anisotropy measurements and concentration independence suggesting that water is forced into the structure at high pressure. Water presumably weakens the electrostatic interactions, driven by volume reduction resulting from electrostriction. If, however, the complex is first poised (free energy barrier to dissociation reduced) by KCl, pressure is able to push the equilibrium toward dissociation. NMR investigations are in progress to elucidate the structure of complex. (Supported by grant DK-39806 from the NIH to A. J. W.)

**M-Pos258**

NUCLEAR MAGNETIC RESONANCE STUDIES OF COMPLEXES BETWEEN CALMODULIN AND CALMODULIN BINDING PEPTIDES FROM PHOSPHORYLASE KINASE. ((Jeffrey L. Urbauer and A. J. Wand)) Department of Biochemistry, University of Illinois-Urbana/Champaign, Urbana, IL 61801

Calmodulin is an integral, tightly bound subunit of the phosphorylase kinase multisubunit complex. Many potential calmodulin binding sites on the various phosphorylase kinase subunits have been determined. Two peptides derived from the catalytic ($\gamma$) subunit show very high affinities for calmodulin and have been implicated in the transduction of the calmodulin-dependent regulation of catalytic activity by calcium. Complexes between calmodulin and these peptides are being studied using nuclear magnetic resonance (NMR) techniques. Heteronuclear 2D and 3D NMR studies show that the complex between calcium loaded calmodulin and the peptide corresponding to residues 302-326 of the $\gamma$-subunit is a tight, structurally well-behaved complex in slow exchange with its constituent components. In contrast, the complex with the peptide corresponding to residues 342-366, while in slow exchange with its components, is divided into structurally sound regions and regions of poorly resolved structure. Additonal support from results of resonance assignment studies using triple resonance techniques will be presented. (Supported by grant DK-39806 from the NIH to A. J. W.)

**M-Pos259**

CHARACTERIZATION OF THE CALMODULIN BINDING OF A 22 mer PEPTIDE FROM A M13 PHAGE LIBRARY. ((B. K. Kay[1], I. D. Clark[2], J. D. Brennan[3], & A. G. Szabo[2,3])) [1]Department of Biology, Univ. of North Carolina, Chapel Hill, NC, 27599-3280, [2]Institute for Biological Sciences, National Research Council, M54 Montreal Rd., Ottawa Canada K1A 0R6, [3]Department of Biochemistry, Univ. of Ottawa, Ottawa Canada.

The modulation of the activity of a number of proteins by Calmodulin in a $Ca^{2+}$ dependent manner is the subject of considerable interest. By screening a M13 phage library which displays random peptides consisting of 22 amino acids, the sequence determinants of high affinity interaction with Calmodulin were explored. Acid-elutable phage which bound to bovine brain calmodulin were recovered, amplified, and rescreened twice to yield binding phage. These isolates bound three orders of magnitude stronger to Calmodulin coated plates than to BSA coated plates. When sequences of the isolates were determined they were found to all be the same recombinant. Interestingly, the peptide sequence displayed by the pahge contained a tryptophan residue and had similarity to the Calmodulin binding domain of skeletal muscle light chain kinase. The interaction of the synthetic 22mer peptide with bovine brain Calmodulin was studied by steady state and time-resolved fluorescence methods. It was shown that the peptide bound to Calmodulin in a $Ca^{2+}$ dependent manner, and that there was a significant change in the structure of the peptide on binding to Calmodulin. A blue shift in the spectral maximum shows that the tryptophan enters into a more hydrophobic environment in the complex with Calmodulin. In the absence of $Ca^{2+}$ and/or Calmodulin the fluorescence decay parameters indicated that the tryptophan residue was in a random coil conformation. In the complex the pre-exponential terms suggest that the peptide may adopt a conformation in which the tryptophan is either in a $\beta$-turn or $\beta$ sheet type structure. The interaction of shorter peptides based on the original 22mer sequence allowed the description of the minimum peptide length and critical sequence for the efficient binding. This work was supported by Cytogen Corp., Princeton NJ (B.K.K.) and NSERC (A. G. S.).

**M-Pos260**

CHARACTERIZATION OF A BIFUNCTIONAL FUSION PROTEIN CONSISTING OF A SINGLE-CHAIN ANTIBODY AND AN EF-HAND $CA^{2+}$-BINDING PROTEIN. ((I.D. Clark, I. Hill, A.G. Szabo, S. Narang, M. Young, J.P. MacManus and R. MacKenzie)) Institute for Biological Sciences, National Research Council of Canada, Ottawa, Ontario, K1A 0R6.

A fusion protein (scFv-C1) was prepared containing two domains. One domain was the single-chain Fv fragment (scFv) of an anti-body specific for Salmonella seragroup B O-polysaccharide. The other domain was construct 1 (C1), a mutated form of the EF-hand $Ca^{2+}$-binding protein, oncomodulin, which had increased metal affinity engineered into the CD loop. C1 has the ability to bind $Tb^{3+}$ with very high affinity and to give a strong, sensitised $Tb^{3+}$ luminescence signal via excitation of the Trp residue in the CD loop. A second fusion protein (scFv-30mer) was also prepared, using a 30 residue helix-loop-helix as the metal-binding component. From the level of $Tb^{3+}$ luminescence, $Tb^{3+}$ binding to scFv-C1 was judged to be stronger than binding to scFv-30mer and was as good as with C1 alone. This suggested that C1 in the fusion protein still maintained its structural integrity. The scFv was also found to retain its antigenicity.

**M-Pos261**

STRUCTURAL DYNAMICS OF TROPONIN-C MUTANTS WITH CALMODULIN-LIKE PROPERTIES ((F. Pitici[1], J. Gulati[2], E.L. Mehler[1] and H. Weinstein[1])) Dept. Physiology/Biophysics: [1]Mt. Sinai Sch. Med., NY,NY 10029; [2]Albert Einstein Coll. Med., Bronx, NY 10461.

Mutant constructs of skeletal troponin C (sTNC), but not the fully $Ca^{2+}$-loaded sTNC (sTNC4) exhibit calmodulin-like (CAM-like) properties in phosphodiesterase (PDE) activation assays[Gulati et al., J. Biol. Chem. 268: 11685, 1993]. The mutants include (1) **M1**: deletion of residues $^{88}$KGK$^{90}$; (2) **M2**: $^{85}$EDA$^{87}$ residues converted to DTD; and (3) **M3**: the double mutant (DTDAKGK). Relative to CAM (100%), these mutants showed PDE activities of 5%, 61% and 90%, respectively, while their sTNC-like activities in muscle contraction are 100%, 68%, and 94% [Gulati et al., loc. cit.]. Computational simulations were used to assess the relation between the structural and dynamic properties of the mutants and those considered responsible for physiological actions of CAM [Weinstein & Mehler, Ann. Rev. Physiol. 1994]. The model of Herzberg et al. [J. Biol. Chem. 261: 2638, 1986] was used as the starting structure for sTNC4 and the mutants. Simulations of CAM[Mehler et al., Prot. Eng. 4:625,1991; *ibid.*, Mol. Sim. 10:309,1993] had resulted in a decrease in the radius of gyration (Rg) by ~4Å due to the bending of the tether helix that brings the two globular $Ca^{2+}$-binding domains closer, and a reorientation of the two domains away from the crystal structure toward that found by NMR for a CAM-MLCK complex[Ikura et al., Science 256:632,1992]. In contrast, we now find the Rg of sTNC4 decreased by only 1Å with no reorientation of the $Ca^{2+}$-binding domains, consonant with its negligible CAM-like activity. The change in Rg of **M1** and **M2** is limited, as in sTNC4, but Rg of **M3** is reduced by ~2Å showing additional compaction. Moreover, the orientation of the domains of **M2** is close to that in the CAM-MLCK complex, whereas the **M1** structure is very different. These initial simulations suggest correlations between structural features and observed CAM-like and/or sTNC-like activities. *Supported by NIH grants GM-41373 and AR-33736.*

M-Pos262

## MUTATIONAL TESTING OF A MODEL FOR CALMODULIN COMPACTION

((B. Weyer, C. Kephart, D. Tinker and M. A. Shea))
Dept. of Biochemistry, U. of Iowa College of Medicine, Iowa City, IA 52242-1109 (madeline-shea@uiowa.edu)

On the basis of molecular dynamics simulations, Weinstein and coworkers (*Mol. Eng.* 1: 231-247, 1991) proposed that R74, R86 and R90 in calmodulin play prominent roles in a ratcheting mechanism of compaction. The goal of our study was to test this hypothesis experimentally by mutating R90 to Ala or Gly in the wild type rat calmodulin sequence. CaM-R90A and CaM-R90G, overexpressed in *E. coli* Lys S cells, were purified using phenyl sepharose hydrophobic interaction chromatography. CaM-R90A and CaM-R90G were characterized using amino acid analysis, SDS-PAGE, $Ca^{2+}$-shift gels, and iso-electric focusing.

We have begun to determine how these mutations at R90 affect the equilibrium distribution of conformations of calmodulin. Fluorescence spectroscopy was used to compare the calcium-dependent properties of the mutant proteins to wild type calmodulin. These studies indicated that wild type CaM and CaM-R90A have similar calcium binding properties; however, CaM-R90G appeared to have enhanced affinity for calcium. CD and UV-Vis spectroscopy were used to monitor structural differences in the apo- and calcium-saturated proteins. The magnitude of the decrease in ellipticity at 222 nm upon loss of calcium was in the order R90G>R90A>WT; UV-Vis spectra suggested this decrease reflects differences in the apo forms of calmodulin.
(NSF MCB 9057157, AHA 91014980)

M-Pos263

## ION BINDING PROPERTIES & CONFORMATIONS OF FLAGELLAR CALCIUM BINDING PROTEIN

((S. D. Harmon and M. A. Shea*)) Dept. of Biochemistry, U. of Iowa College of Medicine, Iowa City, IA 52242-1109 ( Spon. by C. A. Swenson )

Flagellar Calcium Binding Protein (FCaBP) was originally identified at the gene level in the protozoan parasite *Trypanosoma Cruzi* which causes Chagas' Disease. FCaBP was immunologically localized to the flagellum of the parasite and was found to have sequence homology with other calcium binding proteins. Analysis of the primary sequence showed the presence of four regions with significant homology to calcium-binding sites of the EF-hand family of proteins. Preliminary studies of domain structure and calcium-linked conformational change indicated that FCaBP differed from many of the well-studied helix-loop-helix calcium binding proteins. Small zone gel permeation chromatography studies showed that FCaBP forms higher order oligomers; however, this phenomenon was not $Ca^{2+}$-dependent. The estimated molecular weight of the most abundant (and smallest) species was significantly greater than that calculated from the amino acid composition of a monomer. Circular dichroism studies showed that the conformation of FCaBP was sensitive to calcium, and a loss of helical secondary structure occurs upon calcium binding. Divalent cation titrations of FCaBP monitored by intrinsic fluorescence enhancement showed low affinity binding of $Ca^{2+}$ and $Mg^{2+}$ at pH 7.4, 22°C, 100 mM KCl. The apparent $K_{dssn}$ values were 1.8 mM for $Ca^{2+}$ and 61 mM for $Mg^{2+}$ binding. Calcium did not appear to bind cooperatively to FCaBP as it does to calmodulin, troponinC and calbindin.
(NSF MCB 9057157, AHA 91014980)

M-Pos264

## SUBSTRATE RECOGNITION BY SMOOTH MUSCLE MYOSIN LIGHT CHAIN KINASE.

((Gang Zhi and James T. Stull)) UT Southwestern, Dallas, TX 75235.(Spon. by K.Kamm)

The consensus phosphorylation motif for smooth muscle myosin light chain kinase shows an R residue N-terminal of the phosphorylatable serine at the p-3 position in smooth muscle light chain (SmLC) is important. The skeletal muscle light chain (SkLC) is a poor substrate possibly due to the replacement of the R with E. To understand the structural basis for these differences, site directed mutations and chimeric light chains were examined for changes in phosphorylation properties. Exchanging the 29 N-terminal residues of human SmLC for rabbit SkLC changed phosphorylation properties to those observed for SkLC. Likewise exchanging the 26 N-terminal residues of SkLC for SmLC changed phosphorylation properties to those observed for SmLC. Mutating E at p-4 position in SkLC to R increased the rate of phosphorylation modestly. However exchange of the C-terminal half with SmLC in this mutant increased the rate of phosphorylation similar to that observed for SmLC. Thus a primary determinant for substrate recognition is in the N-terminus of SmLC, but the C-terminus also appears to contribute.

M-Pos265

## Volatile Anesthetics Alter The Calcium Binding Properties Of Calmodulin.

Aaron Levin, B.S. and Thomas J.J. Blanck, M.D., Ph.D., Department of Anesthesiology, Cornell University Medical College, New York, NY 10021

The effects of the volatile anesthetics, halothane and isoflurane, on the calcium binding properties of bovine brain calmodulin were measured by fluorescence spectroscopy. Fluorescence spectra for calmodulin were obtained at a range of calcium concentrations (pCa 8-pCa 6), in the presence and absence of halothane and isoflurane. The intrinsic tyrosine fluorescence of calmodulin was measured at an emission wavelength of 320 nm and an excitation wavelength of 280 nm. Fluorescence measurements were carried out in 50mM Hepes, 100 mM KCl, and 2mM EGTA at pH 7.0, and 37.0°C. Experiments were performed in sealed cuvettes so that the volatile anesthetic concentrations were at equilibrium. The titration data were fit to the Hill equation using the Enzfitter program and non-linear regression analysis.

The presence of volatile anesthetics altered the calcium binding affinity of calmodulin in a dose dependent biphasic fashion. At low concentrations of both halothane (0.25mM) and isoflurane (0.33mM) the affinity of calmodulin for calcium was significantly decreased. However, at higher concentrations of both anesthetics the affinity for $Ca^{2+}$ was significantly increased. In the presence of 1.0mM halothane the $K_d$ for $Ca^{2+}$ decreased from 5.89 ± $0.14 \times 10^{-7}$M to 5.02 ± $0.14 \times 10^{-7}$M. Similar results were found with isoflurane. These data indicate a complex interaction of the hydrophobic volatile anesthetics with calmodulin. The volatile anesthetics have been shown in other systems to alter calcium homeostasis, but this is the first report of the modification of a calcium binding protein by the halogenated hydrocarbon anesthetics.

M-Pos266

## HYDRODYNAMIC PROPERTIES OF COMPLEXES FORMED BY CALMODULIN WITH THE REGULATORY PEPTIDES OF GLYCOGEN PHOSPHORYLASE KINASE.

(D. Juminaga, R.F. Steiner, and S. Albaugh) Department of Chemistry and Biochemistry, University of Maryland Baltimore County, Baltimore, MD 21228

The hydrodynamic properties of the complexes formed by calmodulin with the regulatory peptides of the γ-subunit of glycogen phosphorylase kinase have been monitored by means of the fluorescence anisotropy decay measurements. The complex of calmodulin with the nonamphipathic PhK13 peptide has a longer global rotational correlation time than the complex with the amphipathic PhK5 peptide. This is the case both for the intrinsic fluorescence of tryptophan-containing peptides and the extrinsic fluorescence of labels attached to calmodulin. Also, in all cases, the contribution to anisotropy decay of the more rapid rotational modes, which arise from localized motion of the fluorophore, is partially suppressed, reflecting increased molecular rigidity. However, significant internal mobility persists, as is reflected by the necessity of assuming a distribution of separations between an energy transfer donor tryptophan in the peptide and an acceptor nitrotyrosine in calmodulin in order to account for the observed time decay of donor fluorescence in the presence of acceptor. The efficiency of transfer between a donor pyrene group located at Cys-27 of wheat germ calmodulin and an acceptor nitrotyrosine-139 group is altered upon complex formation, indicating a change in extension of calmodulin.

M-Pos267

## PURIFICATION AND N-TERMINAL SEQUENCING OF A HIGH AFFINITY 22 KDA CALCIUM-ANTAGONIST BINDING POLYPEPTIDE FROM GUINEA-PIG LIVER.

((M. Hanner, F.F. Moebius, M. Grabner, H.-G. Knaus, F. Weber, J. Striessnig and H. Glossmann)) Institut für Biochemische Pharmakologie, Universität Innsbruck, A-6020 Innsbruck, Austria

The verapamil-like phenylalkylamine (PAA) $Ca^{2+}$-antagonist [$^3$H]emopamil reduces infarct size in experimental models of cerebral ischemia. It reversibly labels a cation-sensitive site associated with a 22 kDa polypeptide in the endoplasmic reticulum of guinea-pig liver, adrenal gland, kidney and lung. This polypeptide also binds other anti-ischemic drugs (trifluperazine, ifenprodil, amiodarone, opipramol) with high affinity and could therefore represent a common molecular target for antiischemic drugs (Moebius et al., *Molecular Pharmacology* 43:139, 1993). As a first step towards the identification of its physiological function we purified this polypeptide from guinea-pig liver microsomes. Reversible [$^3$H]emopamil binding activity was enriched about 250-fold after solubilization in digitonin by sequential chromatography on DEAE-sepharose, hydroxyl apatite, S-sepharose, dye-sepharose and metal chelate sepharose. The final preparation contained the 22 kDa polypeptide at >95% purity. The purified polypeptide was specifically photoaffinity labeled by the PAA arylazide [$^3$H]azidopamil and bound [$^3$H]emopamil with high affinity (Kd=6 nM, Bmax=7 nmol/mg of protein). Its pharmacological properties, i.e. its high affinity for a variety of anti-ischemic drugs and divalent cations, were unchanged as compared to liver microsomal membranes. The amino acid sequence of the 33 N-terminal residues was determined by gas phase sequencing and used to raise a site-directed antibody, that specifically immunoprecipitated the photolabeled 22 kDa polypeptide. The N-terminus did not reveal homology to other known protein sequences.

This work was supported by Boehringer-Ingelheim fellowship (F.F.M.) and grants (S6601, P9351) by the Fonds zur Förderung der Wissenschaftlichen Forschung, Austria (H.G., J.S.).

M-Pos268

## OXIDATION OF ONE METHIONINE ALTERS THE CALCIUM INDUCED CONFORMATIONAL COUPLING BETWEEN THE OPPOSING GLOBULAR DOMAINS OF CALMODULIN.

((Y. Yao*, D. Yin*, T.C. Squier*, and C. Schöneich+)) *Department of Biochemistry & +Pharmaceutical Chemistry, University of Kansas, Lawrence, KS 66045-2106.

Calmodulin (CaM) may be a major target of reactive oxygen species (ROS) under conditions of oxidative stress, which are characterized by a loss of calcium homeostasis. Therefore, we have investigated the sensitivity of CaM to ROS, and have identified relationships between oxidative damage, CaM's ability to bind and activate the plasma membrane $Ca^{2+}$-ATPase, and structural changes associated with calcium activation of CaM. Using HPLC and mass spectroscopy to identify tryptic fragments isolated from CaM, we find that either $Met_{146}$ or $Met_{147}$ are selectively oxidized by $H_2O_2$ (a major ROS). Oxidation results in a small decrease in binding affinity to both target peptides and the $Ca^{2+}$-ATPase, accompanied by a large reduction in $V_{max}$. Measurements of collisional quenching, fluorescence anisotropy, and resonance energy transfer indicate that upon oxidation CaM's two globular domains adopt a more open conformation, and move closer together. In addition, oxidation suppresses the calcium-dependent structural changes normally associated with CaM activation. This suggests that oxidized CaM binds in a nonproductive manner to the $Ca^{2+}$-ATPase.

M-Pos269

## RESOLUTION OF STRUCTURAL CHANGES OF CALMODULIN UPON BINDING TARGET PEPTIDES USING FREQUENCY-DOMAIN FLUORESCENCE SPECTROSCOPY.

((Y. Yao, and T. Squier)) Department of Biochemistry, University of Kansas, Lawrence, KS 66045-2106.

We have used fluorescence quenching, anisotropy, and resonance energy transfer (FRET) to identify structural changes both within the globular domains of calmodulin (CaM) and in their physical relationship to one another (i.e., the conformational heterogeneity). We have investigated both calcium activation and the subsequent binding of CaM to target peptides derived from melittin, myosin light chain kinase, and the plasma membrane $Ca^{2+}$-ATPase. Calcium activation at physiological pH involves i) a more extended and rigid central helix and ii) an unfolding of the globular domains bringing them into closer proximity. Upon peptide binding to CaM ($K_d \approx 1\ \mu M$) i) the central helix adopts a restricted range of conformations that brings the two globular domains into closer proximity (i.e., a bent conformation), and ii) the globular domains adopt a more open conformation. This is consistent with previous suggestions that both globular domains participate in the association with the target peptide. We are currently investigating the structural changes associated with calmodulin binding to the plasma membrane $Ca^{2+}$-ATPase from erythrocyte ghosts.

M-Pos270

## TEMPERATURE-FAVORED ASSEMBLY OF PROTEINS: A HYDROPHOBIC OR A HYDROPHILIC EFFECT?

((S. Leikin, D.C. Rau and V.A. Parsegian)) DCRT & NIDDK, NIH, Bethesda, MD 20892.

Both heat triggered self-assembly of proteins and cold denaturation of proteins are usually associated with a hydrophobic effect, the entropically favorable removal of water structured around exposed non-polar residues. Fairly common and quite striking, both phenomena are often considered to be good tests of folding/assembly theories. But are they really understood? The hydrophobic effect might not be the only explanation. For example, some other, "hydrophilic" mechanism must be responsible for the temperature-induced assembly of $Mn^{2+}$-DNA.

To address this problem, we now directly measure temperature-dependent forces between soluble proteins, specifically between triple helices of type I collagen. An exponential repulsion seen from 0 to 8 Angstrom separation is balanced by a longer-range attraction responsible for specific recognition and temperature-favored assembly into fibers. An observed pH dependence of the net force and a complete removal of both the attraction and the temperature sensitivity by added glycerol practically rule out any significant contribution from the hydrophobic effect. The long-range attraction appears to be caused by water-mediated hydrogen bonding between *polar* residues. The entropic effect and concomitant temperature dependence can be either a result of reorganizing water around these hydrophilic residues or a result of the increased conformational freedom of the water-bridged structure.

## SKELETAL MUSCLE ACTOMYOSIN

M-Pos271

## ACTIN-FILAMENT VELOCITY IS PERIODIC

((Evert L. deBeer*, Annemiek (M) A.T.A. Sontrop*, Miklos M.Z. Kellermayer, Csaba Galambos, Gerald H. Pollack)) Center of Bioengineering, University of Washington, Seattle.

Crossbridges are thought to interact independently of each other—without memory. To test this we measured the velocity of the front end, rear end and centroid of actin-filaments with high precision by numerical differentiation of the spatial coordinates. Velocity proved to be periodic. Peak-to-peak variation was ~5 μm/s (resolution 0.3-0.4 μm/s). To investigate the frequency content of the velocity signal, auto-correlation functions of the speeds were calculated. The auto-correlation functions were well fitted with a single sine wave (period 380 ± 80 ms) in seven out of eleven filaments; the others were fitted with two sine waves. Clear phase shifts between the three parts of the actin filament were observed. The life time of the waves of the auto-correlation functions was on the order of seconds, implying a deterministic process. When the actin filaments were stopped by an increase in osmolarity, the filaments actively wiggled with the same period (310 ± 30 ms; n=6). The hypotheses of independence of the force generator and the absence of memory are challenged by our findings: (1) the motion of actin filaments is periodic; and (2) the waves persist on a long (second) time scale. Our observations can be understood either if: binding of one crossbridge enhances formation of adjacent crossbridges; or, the driving force is a propagated transition along the actin-filament.

* On leave from the department of Medical Physiology, Utrecht University, Utrecht, The Netherlands

M-Pos272

## COMPETING EFFECT OF ATP AND IONIC STRENGTH ON *IN VITRO* ACTIN MOVEMENT

((M.S.Z. Kellermayer* and G.H. Pollack)) Bioengineering, University of Washington, Seattle, WA 98195 *Present address: Central Laboratory, University of Pécs, Medical School, Pécs, Szigeti ut 12. H-7624 Hungary

The combined effects of ATP concentration and ionic strength were studied in an actomyosin *in vitro* motility assay using skeletal and cardiac myosin. The velocity of actin filaments increased up to a critical ionic strength, where filament sliding stopped. Above the critical ionic strength, filaments did not translate, but wiggled while focally attached to the surface. At ionic strengths above the critical value, when the ATP concentration (originally 1 mM) was progressively reduced (down to 100 nM) by rigor-solution washes, the stationary, wiggling actin filaments promptly started to translate. The effect was reversible; upon adding ATP again, the sliding movement stopped, and wiggling began. The ATP-washout induced motility at high ionic strength may be explained by an electrostatic mechanism which determines the affinity of myosin to actin.

The critical ionic strength was significantly different for skeletal and cardiac myosin. For skeletal it was 60 mM, while for cardiac it was only 40 mM. Cardiac myosin's lower critical ionic strength implies a lower affinity to actin.

**M-Pos273**

*IN VITRO* MOTILITY ASSAYS USING *DROSOPHILA* FLIGHT MUSCLE PROTEINS.

((J.E. Molloy, A. Razzaq, J.C. Sparrow, D.C.S. White)) Dept. Biology, University of York, Heslington, York, YO1 5DD, U.K.

For our studies of mutant actins we have developed two methods to isolate the flight-muscle specific isoform of actin (Act88F) from *Drosophila*. 1). We use a scaled down purification method (based on Pardee & Spudich, 1982, *Meth. Cell Biol.* **24**, 271) on dissected indirect flight muscles. From 10 flies, we obtain a yield of 5$\mu$g of actin, which is sufficient for thousands of *in vitro* motility assays. The filament sliding velocity of rabbit actin moving on rabbit skeletal HMM was faster than that of *Dros.* wild type and the *Dros.* actin mutant, G368E, which was slower than **wt** (5.8, 5.1 & 4.8$\mu$ms$^{-1}$ resp.). This is consistent with mechanical measurements on skinned muscle fibres in which tension generation was slower in G368E than **wt** (Drummond *et al*, 1990, *Nature* **348**, 440). 2) To produce larger quantities of mutant actins we use a yeast expression system and separate expressed isoforms from the endogenous yeast actin by hydroxyapatite chromatography. From the actin null mutant (KM88), we have also prepared native *Dros.* **thick** filaments. Using this genetic background we will study a variety of *Dros.* myosin mutants. Rabbit actin filaments move at about 2$\mu$ms$^{-1}$ on the native, **wt**, *Dros.* thick filaments, slightly slower than that measured using synthetic rabbit thick filaments.

(This work supported by SERC and The Royal Society)

**M-Pos274**

THREE-DIMENSIONAL RECONSTRUCTION OF THICK FILAMENTS FROM RAPIDLY FROZEN, FREEZE-SUBSTITUTED TARANTULA MUSCLE. R. Padron[1], L. Alamo[1], M. Granados[1], J.R. Guerrero[1], P. Uman[2], N. Gherbesi[2], and R. Craig[2]. [1]Structural Biology Laboratory, IVIC-Biofisica, Caracas 1020A, Venezuela. [2]Dept. of Cell Biology, U. Mass. Medical School, Worcester, MA.

We have studied the structure of the myosin filaments of tarantula leg muscle *in situ* by rapid freezing and freeze-substitution. Longitudinal and transverse sections show clear preservation of the myosin crossbridge array. Computed Fourier transforms of individual filaments in longitudinal sections show 6 layer lines indexing on the 43.5 nm repeat of myosin helices. Phases of the main peak on either side of the first layer line are similar, implying that the number of crossbridge helices is even. 3D reconstructions of filaments show 4 continuous strands of density on the filament surface modulated by density at 14.5 nm intervals, corresponding to the myosin heads aligned approximately along the helical strands. In transverse view, the reconstruction shows 4 protruding crossbridges similar in profile to direct and averaged images of transverse sections of myosin filaments. This reconstruction is similar to that obtained from negatively stained isolated filaments of tarantula except that in the latter there is an additional modulation of the helix density, which better resolves the two heads of each myosin crossbridge (Crowther et al, J. Mol. Biol. 184:428-439). Thus the arrangement of the myosin heads in the rapidly frozen specimens is moderately well preserved, but finer details of structure such as individual myosin heads are lacking. These observations show that the relaxed structure of the myosin filaments can be preserved and suggest that rapid freezing can trap transient crossbridge states. Supported by NIH and MDA.

**M-Pos275**

USING SYNTHETIC PEPTIDES TO STUDY THE MYOSIN HEAVY CHAIN-LIGHT CHAIN INTERACTIONS.((Renne Chen Lu and Anna Wong)) Boston Biomedical Research Institute, Boston, MA 02114

As part of our study to monitor the effect of light chain phosphorylation on the light chain-heavy chain interactions, the segment of myosin heavy chain, designated as RS-R798, corresponding to the amino acid sequence of rat skeletal myosin from Arg-798 to Ile-847 (Strehler et al., JMB 90:291, 1986) was synthesized. In the crystal structure of chicken skeletal S1, this region is part of the long helix and is wrapped around with two light chains (Rayment et al., Sci. 261:50, 1993). CD measurement indicated that RS-R798 indeed has a high content of $\alpha$-helical structure by itself and the addition of helix-inducing solvent 2,2,2-trifluoroethanol (TFE) further increased the helical content to nearly 100%. To examine the interaction between RS-R798 and light chains, the two sulfhydryl groups, Cys-803 and Cys-824, were labeled with fluorescence probe acrylodan or bifunctional crosslinkers. Our data showed that the presence of light chain 2 (LC2) resulted in a blue shift of the emission spectrum and an increase in fluorescence intensity whereas light chain 1 (LC1) has no effect. RS-R798 was crosslinkable to either LC1 or LC2 via benzophenone iodoacetamide and the crosslinking pattern was not affected by divalent cations. However, in the presence of TFE, the crosslinking between RS-R798 and LC2 was significantly enhanced in the absence of divalent cations, whereas that between RS-R798 and LC1 was unaffected. Current efforts are focused on the use of other peptide analogs with Cys residues placed at strategic positions to study the heavy chain-light chain interactions. Supported by NIH Grants AR-28401 and AR-41637

**M-Pos276**

ACTO-HEAVY CHAIN EDC CROSS-LINKED SITES SHOW $Ca^{2+}$-REGULATION IN WEAK CROSS-BRIDGE STATES OF REGULATED ACTO-S1. ((J. Shi and P. Dreizen)) Physiology & Biophysics, SUNY Brooklyn, Brooklyn, NY.

During reaction of EDC with regulated acto-S1, the predominant cross-linked product is acto-heavy chain complex, A*HC, with 170K and 180K bands on SDS gel electrophoresis, as found with acto-S1 alone. In 10mM KCl, 0.1mM $Ca^{2+}$, the amount of A*HC is the same at ATP concentrations from 0 to 5mM; but in 1mM $EGTA_4$ there is a sharp transition with no A*HC at ATP > 1mM. Some $Ca^{2+}$ sensitivity is found with AMP-PNP, but no $Ca^{2+}$ sensitivity at ADP concentrations up to 10mM. $Ca^{2+}$ titration of A*HC formation at 3mM ATP shows a transition at ~1 $\mu$M $Ca^{2+}$, which can be fit to known constants for $Ca^{2+}$ binding sites of TN-C. In the absence of EDC, regulated actin-S1-ATP shows similar $Ca^{2+}$ dependence for MgATPase, while actin-S1 binding is $Ca^{2+}$-insensitive. The findings are consistent with a modified steric blocking model, in which TN-C $Ca^{2+}$ binding results in a minor shift of TM which opens the actin N-terminal EDC site to interaction with S1 in weak cross-bridges and thereby activates S1 ATPase, without affecting A·S1 binding otherwise. EDC reaction with regulated A·S1 was also done in 0.1M KCl, where A·S1 binding is greatly reduced. The amount of A*HC shows $Ca^{2+}$ sensitivity as ATP is increased, but much less $Ca^{2+}$ sensitivity with ADP and AMP-PNP. For all 3 nucleotides, the pCa profiles show separate transitions at 2-100$\mu$M and < 1$\mu$M. The findings cannot be attributed to heterogeneous $Ca^{2+}$-binding sites on TN-C, but are consistent with an intermediate TM position between "On" and "Off" states, evident at high ionic strength.

**M-Pos277**

THERMALLY-DEPENDENT $Mg^{2+}$-INDUCED SELF-ASSOCIATION OF HEAVY MEROMYOSIN. I. KINETICS. ((U. Ghodke and P. Dreizen)) Physiology & Biophysics, SUNY Brooklyn, Brooklyn, NY 11203.

Heavy meromyosin (HMM) undergoes self-association to large n-mers, closely dependent upon temperature and $Mg^{2+}$ concentration. We here report kinetic analysis of HMM self-association as determined from turbidity measurements. Above 34°, HMM shows a biphasic pattern of aggregation with a large peak at 10 to 20mM $MgCl_2$ and a small peak in 1mM EDTA. HMM aggregation in the presence of EDTA appears linked to 1 $Mg^{2+}$-site with $K_i \approx 16\mu M$, presumably due to stabilization of native conformation upon $Mg^{2+}$ binding to the LC2 high-affinity site. HMM association at high $MgCl_2$ shows distinct phases of activation and growth. The activation phase is largely concentration-independent, whereas the early growth phase fits bimolecular kinetics, with $k \approx 0.1/m/\mu M$ at 40°. The rate constants for activation and growth phases are both linked to binding at 2 $Mg^{2+}$ sites with $K_{Mg} \approx 2mM$. Aggregation is partly reversible at high salt concentration and fully reversible in SDS. Turbidity data obtained during prolonged incubation suggest that HMM self-association involves a more complex model than a simple bimolecular reaction. The data have been fit to a polymerization model of reversible association and dissociation, which indicates single-step rate constants $k_+ \approx 5x10^5/s/M$ and $k_- \approx 10^4/s$. These rate constants are comparable with those previously reported for subunit association of several multimeric proteins, but the forward rate constant is considerably less than the rate constant proposed for association of actin and S1 in the presence of MgATP.

**M-Pos278**

THERMALLY-DEPENDENT $Mg^{2+}$-INDUCED SELF-ASSOCIATION OF HEAVY MEROMYOSIN. II. STRUCTURE. ((U. Ghodke and P. Dreizen)) Physiology & Biophysics, SUNY Brooklyn, Brooklyn, NY 11203.

The products obtained following $Mg^{2+}$-induced self-association of heavy meromyosin (HMM) were negatively stained and observed in the electron microscope. Incubation of HMM in 20mM $MgCl_2$ at 40° for 2 hours reveals the formation of 2 kinds of structures: (1) fuzzy-balls, well-defined globular structures of ~100 nm diameter, many with hair-like extensions and often connected in a network; and (2) long filaments having a chain-like or beaded appearance with ~40 nm period. The filaments often branch into networks, mainly in a linear arrangement. Individual filaments show substructure below 40 nm period, with segments of knob-like repeats at approximately 15 nm. After incubation of HMM in 20mM $MgCl_2$ at 40° for shorter times or at lower protein concentrations early forms of fuzzy-balls or long filaments are observed. Control experiments on HMM in 20mM $MgCl_2$ at 25° show short beaded filaments, which appear to be prototypes of the long filaments obtained at high temperature. In contrast to the findings at 20 mM $MgCl_2$, HMM incubated in 1 mM EDTA at 40° for 2 hours results in the formation of irregular, variably-sized aggregates without obvious substructure. From these data we conclude that thermally-dependent, $Mg^{2+}$-induced self-association of HMM generates 2 characteristic structures: fuzzy-balls which involve self-association of myosin heads into distinct globular structures, and long filaments which appear to involve an organized arrangement of HMM heads and rods with the suggestion of an helical period of ~40 nm and a protein repeat of ~15 nm.

**M-Pos279**

PHOTOAFFINITYLABELLING OF THE MYOSIN : MANT-2-AZIDO-ADP : FLUOROMETAL TERNARY COMPLEXES.

((Taketoshi Kanbara and Shinsaku Maruta )) Department of Bioengineering, Soka University, Hachioji, Tokyo 192 JAPAN. (Spon. by T. Mitsui)

Myosin in the presence of $Mg^{2+}$-ADP forms stable ternary complex that mimic transition state with phosphate analogues of fluoroberyllate ($BeF_n$) and fluoroaluminate ($AlF_4^-$) [Maruta et al. (1993) J. Biol. Chem. 268, 7093-7100]. Fluorescence labelled ADP analogue, 3'-O-(N-methylanthraniloyl)-2-azido-ADP (Mant-2-$N_3$-ATP), which binds to 25kDa N-terminal tryptic fragment of skeletal muscle myosin subfragment-1 by non-trapping photo irradiation [Maruta et al. (1989) Eur. J. Biochem. 184, 213-221], was synthesized and used to study the differences between these complexes as transition state analogue and application for photoaffinitylabelling. Mant-2-$N_3$-ADP was trapped by these new type phosphate analogues into ATP binding site of skeletal muscle and smooth muscle myosin as well as by vanadate (Vi). The differences on formation and stability of ternary complexes between $BeF_n$ and $AlF_4^-$, and skeletal and smooth muscle myosin were observed. The complexes of myosin-ADP-fluoroaluminate and fluoroberyllate were stable against UV irradiation in contrast with complex of vanadate. When skeletal muscle myosin subfragment-1 / Mant-2-$N_3$-ADP / BeFn or $AlF_4^-$ were irradiated, approximately 18% of trapped Mant-2-$N_3$-ADP was incorporated into 25kDa N-terminal fragment covalently. On the other hand, 1-2% of trapped Mant-2-$N_3$-ADP was incorporated into smooth muscle myosin S-1. These results suggest that the conformations on ATPase sites of skeletal muscle and smooth muscle myosin are different. BeFn trapping methods are applicable for photoaffinity labelling on myosin. (Supported by grants from The Japan Science Society)

**M-Pos280**

FORMATION OF THE MYOSIN- PHOTO REACTIVE ADP ANALOGUE - FLUOROALUMINATE, FLUOROBERYLLATE AND VANADATE TERNARY COMPLEXES.

((Shinsaku Maruta)) Department of Bioengineering, Soka University, Hachioji, Tokyo 192 JAPAN.

Myosin forms a stable ternary complexes with ADP and fluoroberyllate, fluoroaluminate or vanadate which are thought to be phosphate analogue. Study of actin interaction with these three ternary complexes showed that the possibility of these three complexes are not identical state as transition state analogue[1]. Moreover, $^{19}$F-NMR experiments showed that the binding conditions of ADP in each ternary complexes are different[2] .To study the differences further in detail on these ternary complexes of Myosin - ADP - fluoroaluminate ($AlF_4^-$), fluoroberyllate ($BeF_n$) or vanadate (Vi), 3'-O-(N-methylanthraniloyl)-8-azido-ATP (Mant-8-$N_3$-ATP) which has "syn" conformation at N-glycoside bond and bind to the 20kDa C-terminal tryptic fragment of skeletal muscle myosin subfragment-1 in a ATP sensitive manner by no trapping methods [Maruta et al. (1989) Eur. J. Biochem. 184, 213-221], was synthesized and used. Mant-8-$N_3$-ADP was trapped into ATP binding site by $AlF_4^-$, BeFn and Vi , and the ternary complexes were formed. However, apparent differences among these three complexes on the formation and stability were observed. The ternary complexes of smooth muscle myosin were more stable than skeletal muscle myosin complexes especially on Vi complex. Photoaffinity labelling of myosin on these complexes was also performed. When Skeletal muscle myosin S-1/Mant-8-$N_3$-ADP/BeFn are irradiated, Mant-8-$N_3$-ADP was covalently photo incorporated into 20kDa C-terminal fragment. On the other hand, on smooth muscle myosin (SAP)S-1, Mant-8-$N_3$-ADP bound to 29kDa N-terminal fragment as well as it binds by non-trapping method.

1) Maruta et al. (1993) J. Biol. Chem. 268, 7093-7100. 2) Maruta et al. (1993) Biophys. J. 64, 141a. (Supported by Japan Science Society)

**M-Pos281**

DIVALENT CATIONS IN STABLE MYOSIN-NUCLEOTIDE COMPLEXES.

((Y.M.Peyser[1],M.M.Werber[2], and A.Muhlrad[1])) [1]Hebrew University-Hadassah School of Dental Medicine, Jerusalem 91010 and [2]Biotechnology General, Rehovot 76236, Israel.

The predominant intermediate of the myosin-catalysed ATP hydrolysis is the M**-MgADP-Pi complex whose dissociation is accelerated by actin during the cross-bridge cycle. We studied the role of the divalent cation in the transition complex by substituting $Mg^{2+}$ with $Fe^{2+}$ and $Co^{2+}$. These cations have been found to be good analogues of $Mg^{2+}$, since in their presence the low ATPase activity of myosin subfragment-1 (S1) was substantially activated by addition of actin. $Fe^{2+}$ and $Co^{2+}$ have also been found to substitute for $Mg^{2+}$ in stable ternary S1 complexes, containing vanadate (Vi), or beryllium fluoride (BeFx) as phosphate analogues. In these $Fe^{2+}$ or $Co^{2+}$ containing complexes, like in those containing $Mg^{2+}$, the ATPase activity was abolished. The rate of the complex formation from the time course of the activity disappearance was determined. The activity was recovered upon addition of actin or EDTA, which caused fast or slow decomposition of the complex, respectively. The slow EDTA-induced recovery was much faster in the presence of $Co^{2+}$ or $Fe^{2+}$ than with $Mg^{2+}$. The stability of the complexes was assessed from the rate of formation and from the rate of EDTA-induced decomposition. In the case of $Mg^{2+}$ the stability of the BeFx containing complex was higher than that of the Vi complex while with $Fe^{2+}$ and $Co^{2+}$ the Vi containing complexes were more stable. These results support the notion that the ADP- or ATP-bound metal cations significantly affect the structure of the myosin-nucleotide complexes.

**M-Pos282**

ATP HYDROLYSIS AND STRUCTURAL DYNAMICS IN ACTO-S1 FILAMENTS.

((Choi-man Ng and Richard D. Ludescher)) Department of Food Science, Rutgers University, New Brunswick, NJ 08903

Rabbit skeletal muscle F-actin labeled at cys-374 with the triplet probe erythrosin-5-iodoacetamide has a steady-state phosphorescence anisotropy (rp) of 0.090(±0.005) (at 20°C, 100 mM KCl, pH 7.0). Titration with skeletal muscle S1 fragment increased rp to 0.140(±0.008) at a mole ratio of 1:1. The increase in rp was not due to changes in the lifetime or in the orientation of the probe on the surface of F-actin. ATP addition initially decreased the anisotropy of the acto-S1 complex to 0.05(±0.005), a value significantly smaller than rp of pure F-actin; rp subsequently increased to 0.126(±0.002). The time course of the increase at different ATP concentrations matched that expected from the measured actin-activated ATPase of S1. The plateau value of rp (0.126) was identical to that of Acto-S1 in the presence of exogenous ADP and Pi. ATP hydrolysis by acto-S1 thus appeared to induce novel rotational motions of or within F-actin on the phosphorescence time scale (300 μs). Recent descriptions of the behavior of F-actin in motility assays indicate that myosin can induce torsional twisting motions about the long axis of F-actin; we speculate that the phosphorescence anisotropy provides a direct measurement on the microsecond time scale of the same long axis motions. In our measurements, however, the induced twisting motions were generated in isotropic solution by untethered myosin heads. (Supported by MDA and AHA-NJ.)

**M-Pos283**

ENHANCED ELECTROPHORETIC SEPARATION OF MYOSIN HEAVY CHAINS IN MAMMALIAN AND AVIAN SKELETAL MUSCLES

((Fanjie Zhang[1], Eric Blough[2], & Peter J. Reiser[1,2])) [1]Oral Biology and [2]Exercise Science, The Ohio State University, Columbus, OH 43210.

Electrophoretic separation of myosin heavy chains (MHC) has been utilized in several laboratories to quantitatively determine the MHC composition of single muscle fibers. Relatively recent reports of the expression of a third fast-type of MHC (i.e., "IID" or "IIX"), in addition to the long-recognized fast-type IIA and IIB and slow-type I MHCs, has spurred efforts to improve the separation and resolution of four MHCs in adult mammalian muscle. We have developed an SDS polyacrylamide gel electrophoresis protocol that reliably results in the separation of four MHC isoforms in adult mouse diaphragm and seven MHC isoforms that are expressed among several adult chicken skeletal muscles. The results of attempts to identify each MHC band, utilizing analyses of fiber-type composition of muscles and of immunoblots, will be presented. A complete description of the electrophoretic protocol including the preparation and composition of solutions and the gel running conditions will be provided. Supported by NIH grant AR39652.

**M-Pos284**

$^1$H-NMR EXPERIMENTAL EVIDENCE FOR A MgADP BINDING SITE LOCATED ON THE N-TERMINAL PART OF THE LC1 LIGHT CHAIN ASSOCIATED TO SKELETAL MYOSIN SUBFRAGMENT-1

((F. Andre, J.M.Neumann and M. Garrigos)) SBPM, DBCM/CEA, CE Saclay, F-91191 Gif/Yvette Cédex, France.

The H8 and H2 proton signals of the MgADP adenine ring were studied by $^1$H-NMR spectroscopy using a AM-500 Bruker spectrometer. All experiments were performed at 20°C in 10 mM Phosphate buffer $p^2H$ = 7.0, 100 mM NaCl, 10 mM $MgSO_4$, 1 mM DTT in $D_2O$ and using chymotryptic S1 from skeletal muscle myosin at concentrations between 0.5 and 0.8 mM. The difference spectra obtained by subtracting the S1 proton spectrum recorded at 20°C in the presence of increasing amounts of MgADP from a nucleotide free S1 proton spectrum display two pairs of H8 and H2 signals, one having the same chemical shifts as free MgADP ($\delta$H8 = 8.53 ppm and $\delta$H2 = 8.27 ppm), the second attributed to a MgADP molecule bound to S1 ($\delta$H8 = 8.59 ppm and $\delta$H2 = 8.23 ppm). The transverse relaxation time ($T_2$) measured by a $^1$H-Spin Echo experiments (CPMG pulse sequence) of the H8 proton resonance corresponding to the bound nucleotide is 80 ms. This $T_2$ value is also observed for some protons belonging to the N-terminal part of LC1 light chain. When the same type of titration experiments were conducted on purified S1 isoforms (S1(LC1) and S1(LC3)) the H8 and H2 proton signals attributed to the bound MgADP molecule is only observed for the S1(LC1) isoform. In conclusion, the N-terminal part of the LC1 associated to S1 offers a low affinity binding site for MgADP.

**M-Pos285**

PHOTOCHEMICAL MODIFICATION OF MYOSIN S1 TRYPTOPHANS ((S.J. Papp and S. Highsmith)) Department of Biochemistry, Univ. of the Pacific, S.F., CA, 94115

U.V. irradiation in the presence of 2,2,2-trichloroethanol (TCE) modifies protein tryptophans. Myosin subfragment 1 with light chain one present (S1A1) was irradiated in the presence of 40 mM TCE at pH 7, 25°C. During the first three minutes, the intrinsic fluorescence intensity at 334 nm decreased rapidly to a plateau. The fluorescence intensity of the photochemically modified S1A1 from the plateau region, when denatured, was 79% of denatured unmodified S1, suggesting one of the five tryptophans was eliminated as a fluorophore.

The MgATPase activity of the modified S1A1 was 60% above normal, after the excess TCE was removed. Preliminary data suggest there is limited sulfhydryl group modification. There were no indications of aggregation or internal cross-linking on SDS-PAGE.

The ATP-induced increase in tryptophan fluorescence intensity for the modified S1A1 was similar to that of the native S1A1 (~35%). This suggests that the photochemically hyperactive tryptophan is not a primary contributor to the ATP response. (NIH AR37499)

**M-Pos286**

HYDRATION PERTURBATIONS AFFECT MYOSIN ATP INTERACTIONS ((S. Highsmith)) Department of Biochemistry, Univ. of the Pacific, S.F., CA, 94115

Steady state MgATPase activities and intrinsic fluorescence intensity increases for S1.MgADP.$P_i$ formation were measured for S1(Mg) in the presence and absence of 10% by weight polyethylene glycol (PEG, MW1450) at 25°C, pH 7, in 200 mM KOAc, 10 mM Mops, 1 mM $MgCl_2$.

Preliminary measurements suggest that PEG reduces Vmax, increases Km, and reduces the apparent equilibrium constant for the formation of S1.MgADP.$P_i$. The decrease in Vmax is only about 20%. However, the increase in Km and the decrease in the apparent equilibrium constant are at least ten-fold.

Assuming that the observed effects are not due to PEG binding to S1(Mg) or to changes in viscosity, the results can be interpreted in terms of "osmotic stress", which reduces the water available for hydration of the S1-nucleotide intermediates (Parsegian et al., 1986, Meth. Enzymol. 127:400). Our preliminary data suggest that hydration by over 200 $H_2O$ molecules favors the formation of S1.MgADP.$P_i$ and of the product of the rate determining step of the steady state cycle.(NIHAR37499)

**M-Pos287**

NEUTRON SCATTERING FROM REDUCTIVELY METHYLATED MYOSIN SUBFRAGMENT 1. ((D. B. Stone[1], D. K. Schneider[2] and R. A. Mendelson[1])) [1]Cardiovascular Research Institute and Dept. Biochem. & Biophys., Univ. Calif. San Francisco, CA 94143; [2]Biology Dept., Brookhaven National Laboratory, Upton, NY 11973.

Reductive methylation was employed as an aid in the recent crystallization of myosin subfragment 1 (Rayment *et al.*, Science 261: 50, 1993). In the present study, neutron scattering has been used to assess the effect of reductive methylation on the structure of subfragment 1 in solution. The lysine residues of chicken papain S1 were reductively methylated by reaction with dimethylamine borane complex and formaldehyde (Rayment *et al.*, 1993). This modification inhibited the $K^+$(EDTA)-ATPase by more than 90% and activated the $Ca^{++}$-ATPase 2.5 fold. The neutron-scattering patterns of reductively methylated and unmodified S1 were compared in 50 mM Imidazode (pD 7.5), 110 mM KCl, 1 mM $MgCl_2$, 99% $D_2O$. Preliminary measurements indicate no significant difference in apparent $R_g$ over a protein concentration range of 0.5 - 6 mg/ml. These findings indicate that reductive methylation causes no large scale changes in the structure of S1. During the course of these experiments it was observed that reductively methylated chymotryptic and papain S1 are more resistant to proteolysis than unmodified S1.
(Supported by NIH grant AR 39710.)

**M-Pos288**

MEASUREMENT OF THE INTER-RLC DISTANCE IN SCALLOP MYOSIN BY NEUTRON SCATTERING. ((Satoru Fujiwara, Deborah B. Stone, & Robert A. Mendelson)) CVRI & Dept. of Biochem./Biophys., University of California, San Francisco, CA 94143 (sponsored by R. Vale)

The neutron scattering method combined with selective isotopic labeling and contrast matching is suitable for obtaining *in situ* structural information on particles embedded in a matrix. The observed intensities, however, may be distorted by inter-complex interference and by scattering-length-density fluctuations of the (otherwise) contrast-matched matrix. In order to measure the distance between a pair of RLCs in scallop myosin, we employed a method by which such distortion can be eliminated. In this method, the difference intensity of complexes bearing deuterated particles with a random distribution and a mixture of complexes bearing only deuterated particles and only protonated particles yields inter-particle distance information. Myosin synthetic filaments were formed by dialyzing *Placopecten* myosin, bearing appropriately deuterated RLC, against a solution containing 10 mM Imidazole (pH 7.0), 0.1 M NaCl, 1mM $MgCl_2$, 0.1mM EGTA, 1mM ATP, 1mM DTT, 42 % $D_2O$. Preliminary experiments on the pelleted myosin filaments were done at BNL and at NIST. In both the mixture and the randomly labeled samples, a peak at s = 1/14.3 $nm^{-1}$ from the myosin thick filament was observed. The interference function suggests that the two RLCs are far apart. This is consistent with the EM studies (Vibert, 1992; Levine, 1993) which suggest that the two heads of each myosin are splayed apart and oppositely oriented in thick filaments of relaxed muscle. (Supported by NIH grant AR 39710)

**M-Pos289**

THERMODYNAMIC LINKAGE OF ION BINDING AND HYDRATION OF BOVINE MYOFIBRILLAR PROTEIN AND MYOSIN IN SOLUTIONS DETERMINED FROM MULTINUCLEAR SPIN RELAXATION STUDIES. ((I.C. Baianu, T.F. Kumosinski, A. Mora-Gutierrez, E.M. Ozu and P.J. Bechtel)) AFC-NMR Facility, University of Illinois at Urbana, Urbana, IL 61801-3852.

NMR transverse relaxation rates of water and ions in myofibrillar protein and myosin solutions exhibit complex nonlinear variations on salt concentration. Such curves are modeled at all salt concentrations by a relatively simple model for the activity of myofibrillar proteins and ion binding to myosin. In this model, myofibrillar protein hydration is linked to salt binding in the sense of Wyman's theory of linked functions (Wyman, 1964, 1984). Ligand(ion)-induced association is highly cooperative and involves binding of n=4 moles of ions to myofibrillar protein sites. The values of the preferential ion binding coefficient obtained from the $^{17}O$ NMR data are close to those obtained from $^{23}Na$ NMR suggesting that hydration water is exchanged as the hydrated ion species in both myofibrillar protein and myosin solutions. Additional experiments with purified myosin may allow one to check the latter possibility, and further refine the ligand-induced protein association model that was here proposed. The understanding of muscle protein interactions with ions is important in the study of chemomechanical energy transduction in muscle. $^{35}Cl$ NMR measurements of chloride binding to myofibrillar proteins would allow one to further specify our thermodynamic linkage model that relates the hydration of myofibrillar proteins and myosin to cooperative anion binding.

**M-Pos290**

THE EFFECT OF METHYL GROUP ON 2-[(2,4-DINITROPHENYL)AMINO] ETHYL PHOSPHATES IN THE INTERACTION WITH SKELETAL MYOSIN ((D. Gopal*, J. P. Schwonek+, C. R. Sanders II+, M. Ikebe+ and M. Burke*)) *Dept. of Biology and +Dept. of Physiology and Biophysics, Case Western Reserve University, Cleveland, OH 44106.

Di- and triphosphate analogs of 2-[(2,4-dinitrophenyl)amino]ethanol (NODP and NOTP) and its methyl analog (MNODP and MNOTP) were synthesized to study the structural requirements of organic triphosphates to act as substrates for myosin and actomyosin and for their $Mg^{2+}$ complexes to support in vitro motility. Assuming that the activity observed with ATP is 100%, the S1 NTPases were 166% and 216% in the presence of $Ca^{2+}$ and 440% and 1960% in the presence of $Mg^{2+}$ for NOTP and MNOTP respectively. In the presence of EDTA both NOTP and MNOTP were only 30% and 8% respectively of the ATPase activity. While the MgNOTPase in the presence of actin was similar to that observed for MgATP, actin showed very little ability to activate the S1 MgMNOTPase. In vitro motility assays with F-actin on adsorbed myosin showed that while addition of the MgNOTP supported movement of the actin, additions of MgMNOTP were unable to support such movement. These observations are similar to studies with other analogs in that those that show low levels of hydrolysis by myosin S1 in the presence of EDTA and high levels in the presence of $Mg^{2+}$ with little activation by actin, are unable to support movement of F-actin in the in vitro motility assay. The differences in these triphosphate analogs as substrates is also observed in the ability of their diphosphate forms to be trapped in S1 using beryllium fluoride. Whereas MgNODP is easily trapped in S1 at 4°C, no trapping of the MgMNODP could be detected in the time required to separate the S1 from excess reagents by SEC HPLC. Molecular modeling studies and energy minimization analysis indicate a marked difference in the conformational states of these two analogs in the free state. (Supported by NIH NS15319)

**M-Pos291**

**AN UNUSUAL EF HAND DOMAIN FROM MOLLUSCAN ESSENTIAL LIGHT CHAINS IS REQUIRED FOR CALCIUM BINDING AND REGULATION OF MOLLUSCAN MYOSINS.** **((S. Fromherz and A.G. Szent-Györgyi)) Brandeis Univ., Dept. of Biology, Waltham, MA 02254. (Spons. by P. Vibert)**

A unique feature of molluscan muscle is that contraction is triggered by $Ca^{2+}$ binding to myosin. A variety of studies have indicated that the specific, high-affinity $Ca^{2+}$ binding site may be located in the molluscan myosin essential light chain (ELC), which is composed of four EF hand-like domains. We have previously used mutant ELCs to show that neither domains III nor IV constitute the $Ca^{2+}$ binding site (S. Fromherz and A.G. Szent-Györgyi (1993) *Biophys. J. 64a*: 7). However, these are the only two domains predicted from sequence analysis to be competent to bind $Ca^{2+}$ (J.H. Collins, et al. (1986) *Biochem. 25*: 7651). Here we report that when the EF hand-like domains of scallop ELC and rat cardiac ELC are interchanged, $Ca^{2+}$ binding and $Ca^{2+}$ sensitivity are retained only if the source of ELC domain I is from scallop. Furthermore, the crystal structure of scallop RD (X. Xie et al., in preparation) suggests that $Ca^{2+}$ is bound to this domain. We note a striking cluster of molluscan-specific residues (FWDGR) in the loop of domain I, and propose that these residues may account for the functional differences between molluscan and nonmolluscan ELCs. We have constructed several point mutations in the loop of domain I, and their effects on $Ca^{2+}$ binding and regulation will be presented.

**M-Pos292**

**THE DIFFERENT ATPASE ACTIVITIES OF CATCH AND STRIATED MYOSINS ARE CONFERRED BY ALTERNATIVE EXONS OF THE HEAVY CHAIN.**
((C.L. Perreault, A. Jancso, L. Nyitray and A.G. Szent-Györgyi)) Brandeis University, Waltham, MA 02254.

We explored the influence of the regulatory light chain (RLC), essential light chain (ELC) and the heavy chain (HC) on the ATPase activity of *Placopecten* striated and catch muscle myosins. Catch myosin had a lower ATPase activity than striated myosin (actin-activated=1.3vs.0.9; K-activated=1.5vs.0.8; Ca-activated=0.7vs.0.2,μM/min/mg). In hybrid studies ATPase activity depended on the HC-ELC complex and was independent of RLC. The contribution of ELC and HC was examined by cloning and sequencing the full length cDNA for the ELC and the S1 portion of the HC (up to nucleotide 2675) of catch and striated myosins. ELC from catch and striated myosins had identical nucleotide and deduced protein sequences. Sequence comparisons of the HC revealed three alternative exons. The first exon (5a,b) encoded the consensus P-binding loop and the 25-50 kD proteolytic junction, the second (6a,b) encoded part of the ATP binding site and the third (13a,b) encoded a region near a putative actin binding site. The different ATPase of catch and striated myosins therefore is most likely due to alternative exons in the HCs and is independent of RLC and ELC composition. Supported by NIH AR15963 and MDA.

**M-Pos293**

**UNFOLDING DOMAINS OF A 59 KDA EXPRESSED C-TERMINAL RABBIT SKELETAL LIGHT MEROMYOSIN.** ((S.S. Lehrer & Y. Maeda)). Boston Biomedical Research Institute, Boston, MA & International Institute for Advanced Research, Matsushita Electric Ind., Kyoto, Japan.

Light meromyosin (LMM) an α-helical coiled-coil, consists of the C-terminal 2/3 of myosin rod (amino acid sequence 441-1097) and contains 2 Trp residues at positions 533 and 618. Our previous CD and fluorescence studies showed that the LMM helix unfolds in a sharp transition with $T_{1/2}$ = 43° and a broad transition centered at 53°, and 2 fluorescence transitions with $T_{1/2}$ = 43° and 56° (King & Lehrer, Biochemistry, 28, 3498 (1989)). To determine if each Trp is located in a different unfolding domain, the unfolding properties of a purified C-terminal recombinent LMM (LMM59, sequence 591 - 1097, Maeda et al., J. Mol. Biol., 205, 269 (1989)), which only contains Trp 618 was studied under similar conditions as native LMM. LMM59 showed 2 clearly separated cooperative unfolding transitions at $T_{1/2}$ = 43° and 56°, representing about 40% and 60% loss of the α-helix, respectively. The Trp fluorescence only showed one cooperative transition with $T_{1/2}$= 56°. Assuming independent domains, these data suggest that LMM contains at least 3 unfolding domains: i) an N-terminal domain containing Trp 533, with $T_{1/2}$ = 47°; ii) a middle domain containing Trp 618 with $T_{1/2}$ = 56°, and a C-terminal domain with $T_{1/2}$ = 43°. (Supported by NIH HL-22461).

**M-Pos294**

STRUCTURAL AND FUNCTIONAL PROPERTIES OF SKELETAL MUSCLE MYOSIN FRAGMENTS EXPRESSED IN NONMUSCLE CELLS.
((Fumi Kinose, Carole L. Moncman and Donald A. Winkelmann))
Robert Wood Johnson Medical School, Piscataway, NJ 08854.

A full length skeletal muscle myosin heavy chain (MHC) cDNA and truncations corresponding to heavy meromyosin (HMM), subfragment 1 (S1), and S1(1-784) were expressed alone or in combination with skeletal muscle light chain 3 (LC3) in COS cells, a nonmuscle simian cell line. The expressed proteins were detected by immunofluorescence microscopy and immunoprecipitation using monoclonal and polyclonal antibodies. The fluorescent staining pattern of the HMM and S1 fragments expressed in COS cells is diffuse and distributed throughout the cytoplasm but not specifically aligned with other cytoskeletal elements. In contrast, the full length MHC assembles into short cytoplasmic filament bundles, and appears to be segregated from nonmuscle myosin filaments. When co-expressed with the muscle MHCs, the muscle myosin light chain (LC3) is found associated with the muscle as well as the nonmuscle myosin. The muscle MHCs and LC3 copurify through Triton and/or high salt extraction of transfected cells and ammonium sulfate fractionation. The muscle subunits co-sediment with actin in a binding assay. The endogenous nonmuscle regulatory light chains are also found assembled with the muscle MHCs. These results suggest limited selectivity in the association of myosin light chains with the heavy chains. However, neither the full length muscle myosin nor the myosin subfragments are found associated with the endogenous nonmuscle myosin by double label immunofluorescence microscopy, indicating myosin isotype selectivity in the association of intact molecules. (Supported by grants from the NIH and the American Heart Association-NJ Affiliate)

**M-Pos295**

SYNTHESIS OF A SPIN-LABELED ATP ANALOG AND ITS PHOTOAFFINITY LABELING OF MYOSIN IN SKELETAL MUSCLE FIBERS (( D.Wang†, Y. Luo*, E. Pate*, R.G. Yount†)) Depts of Biochem/Biophys.† and Mathematics*, WA. ST. U., Pullman, WA 99164

A new photoaffinity analog of ATP (SL-$Bz_2$ATP) in which a TEMPO spin label is attached to the benzophenone moiety of $Bz_2$ATP (3'(2')-O-(4-benzoyl)benzoyl adenosine 5'-triphosphate) has been synthesized and used to photolabel myosin in muscle fibers. Previous work has shown that $Bz_2$ATP specifically photolabels Ser-324 of the 50-kDa tryptic fragment of the skeletal S1 heavy chain (Mahmood *et al., Biochemistry* 28, 3989 (1989)). In our work, [$\alpha$-$^{32}$P]-SL-$Bz_2$ATP was trapped with $Co^{2+}$ and orthovanadate at the active site of myosin in rabbit psoas muscle fibers. After UV irradiation, the myosin heavy chain was the only protein band found to be significantly photolabeled after analysis by SDS gel electrophoresis and radioactivity counting. The labeling was further localized by SDS-PAGE analysis after brief trypsin treatment to be on the 50-kDa tryptic fragment of the S1 heavy chain. In three sets of experiments 34% to 43% of myosin in fibers was covalently photolabeled. The fibers photolabeled with SL-$Bz_2$ATP had the same active tension and maximum shortening velocity as the control fibers. This work indicates the feasibility of utilizing active site binding and photoaffinity labeling to introduce covalent spectroscopic probes on a specific and non-critical site on myosin in a fiber. Supported by MDA and NIH; DK05195 (R.Y.) & AR39643 (E.P.). E.P is an Established Investigator of AHA.

**M-Pos296**

A PROPOSED MECHANISM FOR THE VANADATE MODERATED PHOTOCLEAVAGE OF MYOSIN. ((Jean C. Grammer and Ralph G. Yount)), Dept. of Biochem. and Biophys., Washington State University, Pullman, WA, 99164-4660.

Myosin subfragment 1 (S1) is known to undergo photomodification of Ser-180 upon irradiation of the S1·MgADP·Vi complex (Grammer *et al.*, (1988) *Biochemistry* **27**, 8408; Cremo *et al.*, (1988) *Biochemistry* **27**, 8415, and (1989) *J. Biol. Chem.* **264**, 6608). The photomodified S1 can retrap MgADP·Vi and upon irradiation, the S1 heavy chain is cleaved at Ser-180 into 21 kDa N terminal and 74 kDa C terminal fragments. Ser-180 has been shown to be the site of cleavage by isolation and sequencing of the C terminal CNBr peptide ($R_1$') from the 21 kDa fragment (Grammer and Yount, (1993) *Biophys. J.* **64**, 142a). $R_1$' was C terminally blocked with an amide derived from the Ser-180 amino group. Isolation and characterization by amino acid analysis and mass spectrometry of the N terminal tryptic peptide ($R_1$) of the 74 kDa fragment showed that the N terminus of $R_1$ was blocked with an oxalyl group derived from carbons 1 and 2 of Ser-180. A plausible mechanism for photocleavage is proposed in which Vi is reduced and $O_2$ adds to the α-carbon of Ser-180. A subsequent rearrangement and two cleavage steps yields formate from carbon 3 of Ser-180 and the two peptide fragments. The presence of formate at levels equivalent to the amount of photocleavage was confirmed. No cleavage occurs in the absence of $O_2$. The mechanism also offers an explanation for the oxidation of Ser-243 known to be next to Ser-180 in the S1 structure (Rayment *et al.*, (1993) *Science* **261**, 50). Supported by NIH (DK-05195) and MDA.

M-Pos297

## AFFINITY PURIFICATION OF SKELETAL MYOSIN SUBFRAGMENT-1 (S1).

((Tamera Gallagher-Stobb*, Louis Riccelli*, Ivan Rayment#,. and Ralph Yount*)) *Department of Biochemistry & Biophysics, Washington State University, Pullman WA 99164 and #Department of Biochemistry and Institute for Enzyme Research, University of Wisconsin, Madison WI 53705.

An ATP-Affi Gel 10 (Bio-Rad) affinity column was previously shown to be useful in purifying S1 from rabbit skeletal muscle, (Braxton, PhD Thesis, Washington State University, 1988). We report here improvements in column preparation and performance. Improved methods for monitoring coupling were developed and coupling efficiency was improved 2.5 fold. The affinity column is stable for at least 9 months and can be used more than 50 times. When rabbit skeletal S1 is purified on the affinity column, two peaks result. Peak 1 contains approximately 15-20% of the protein, appears to contain more impurities by SDS-PAGE, and has an ATPase activity that is 30-80% less than the pre-column protein. Peak 2 contains 70% of the protein and has an ATPase activity that is 100-120% of the pre-column protein. Parallel experiments were done with reductively methylated chicken skeletal S1 (White and Rayment, *Biochemistry* 32, 9589, 1993). In this case, peak 1 contains ~75% of the protein and has an ATPase activity that is essentially the same as the pre-column protein. Peak 2 contains 5-15% of the protein and has an ATPase activity that is 260-300% of the pre-column protein. The purification of reductively methylated chicken skeletal S1 demonstrates that this protein is heterogeneous. Affinity column purification of S1 may yield more homogeneous protein samples that will aid in future crystallographic studies.

M-Pos298

ORIENTATION OF MYOSIN SUBFRAGMENT-1 IS DIFFERENT WHEN IT FULLY OR PARTIALLY DECORATES MYOFIBRILS. ((J. Borejdo and O.A. Andreev)) Baylor Research Institute, Baylor University Medical Center, 3812 Elm St., Dallas, TX 75226.

Myosin heads (S1) were labeled near the N-terminus by 9-ANN, near the center of the molecule by CPI and near the C-terminus by 1,5-IAEDANS. The dyes were immobilized on the surface of S1 showing that changes in orientation of transition dipoles of the dyes indicated changes in orientation of S1. Labeled S1 was added to myofibrils either at nanomolar or at micromolar concentrations, i.e. under conditions where it partially or fully saturated myofibrillar thin filaments. Orientation was measured by polarization of fluorescence. The orientation was different when muscle was irrigated with nanomolar and with micromolar concentration of S1. The values of horizontal polarization of fluorescence (exciting light parallel to myofibrillar axis) are shown in the Table. The difference in the mean values of polarization in myofibrils which were irrigated with nanomolar and micromolar concentrations of S1 was statistically significant ($P<10^{-3}$) for each dye. These results show that the orientation of S1 added to myofibrils depends on the degree of saturation of thin filaments, and support our earlier proposal that, depending on molar ratio, S1 could form two different rigor complexes with F-actin. Supported by NIH and AHA.

| S1 label | $P_h$(100 nM S1) | $P_h$(2 μM S1) |
|---|---|---|
| 9-ANN | 0.398±0.008 | 0.423±0.009 |
| CPI | 0.361±0.008 | 0.410±0.006 |
| IAEDANS | 0.461±0.010 | 0.366±0.009 |

M-Pos299

KINETICS OF BINDING OF MYOSIN SUBFRAGMENT-1 TO F-ACTIN DEPENDS ON THE MOLAR RATIO. ((O.A. Andreev, V.S. Markin and J. Borejdo)) Baylor Research Institute, Baylor University Medical Center, 3812 Elm St., Dallas, TX 75226 and Department of Cell Biology and Neuroscience, University of Texas Southwestern Medical Center, 5323 Harry Hines Blvd., Dallas, TX 75235.

We studied the kinetics of association of S1 with F-actin. S1 was labeled at Cys-707 by 5-(iodo-acetamido)-fluorescein (5-IAF). Fluorescence intensity of IAF-S1 increases when labeled S1 binds to F-actin (Ando, Biochemistry 23, 375, 1984). Stopped-flow experiments showed that the kinetics depended on the molar ratio of S1 to actin: when the ratio was large, fluorescence increase occurred rapidly in one exponential step. When the ratio was small, the rapid increase was followed by a second, slower exponential step. The same result was obtained earlier, when binding was monitored by quenching of fluorescence of pyrene-labeled F-actin (Andreev et al., Biochemistry 1993, in press). To explain these findings, we developed the model which assumed that binding of S1 to F-actin occurred in two steps: (i) initial rapid binding to one monomer of F-actin, A+M ⟷ A·M, and (ii) consequent slow binding to neighboring monomer, A·M+M ⟷ A·M·A, where A stands for actin and M for myosin subfragment 1. The second reaction could proceed only if the neighboring actin site was unoccupied. The model fitted very well the data monitoring changes both in S1 (IAF-S1) and in F-actin (pyrene-F-actin). The results confirm our earlier conclusion that when actin is in molar excess over subfragment-1, S1 is able to bind to two actin monomers in a filament. Supported by NIH and AHA.

M-Pos300

LOCAL CONFORMATION OF MYOSIN ROD FILAMENTS PROBED BY INTRINSIC TRYPTOPHAN FLUORESCENCE. ((Yoke-chen Chang and Richard D. Ludescher)) Department of Food Science, Rutgers University, New Brunswick, NJ 08903.

We have used fluorescence from the two tryptophans per chain of rabbit skeletal myosin rod to probe the influence of polymerization on the local conformation of the N-terminal region of LMM. Fluorescence spectra were unaffected by polymerization. Quenching by acrylamide was biphasic for both monomers and filaments; one species was readily quenched and thus solvent accessible while the other was very poorly quenched. Intensity decays were fit by a bimodal distribution with a discrete long lifetime and a broad Gaussian distribution of short lifetimes; polymerization had no effect on the long lifetimes (5.4 ns) while decreasing the mean of the Gaussian distribution from 0.9 ns in monomers to 0.1 ns in filaments. Only the discrete long lifetime component was quenched by acrylamide in either monomers or filaments. Tryptophan anisotropies in both monomers and filaments exhibited essentially identical decays to a constant. A fast ( 1 ns) correlation time probably corresponded to fast tryptophan wobble on the surface of the coiled-coil while a slower (6 ns) component reflected an unidentified segmental motion. The local environment of the two pairs of tryptophans was thus unaffected by filament formation suggesting that the N-terminal region of LLM was only loosely aggregated into the body of the thick filament or actually formed part of the crossbridge.

M-Pos301

## NUCLEOTIDE-INDUCED CONFORMATIONAL CHANGES OF THE SH1-SH2 SEQUENCE IN S-1 DURING ATP HYDROLYSIS.

((B. C. Phan & E. Reisler)) Depart. of Chemistry and Biochemistry, UCLA, Los Angeles, CA 90024.

The sequence 697-707 which includes the two most reactive thiols of S-1 (SH1 and SH2) has been implicated in actomyosin interactions. The two thiols can be crosslinked by bifunctional reagents of varying lengths in the presence of nucleotides (1). The recent atomic structure of the myosin head has assigned an α-helical structure to this region (2), suggesting its reorganization upon nucleotide binding. In this work, the conformational changes of this helix have been probed by monitoring the modification of the SH1 group and the crosslinking of the SH1 to SH2 in the presence and absence of nucleotides and nucleotide analogs corresponding to different stages of the ATP hydrolysis. Modifications of the SH1 group with the fluorescent monofunctional reagent 7-diethylamino-3-(4'-maleimidyl phenyl)-4-methyl coumarin (CPM) have shown that the reactivity of the SH1 group depends greatly on the nucleotide bound to S-1. The rate of SH1 modification in 40mM KCl, 25mM Pipes, pH 7.0 at 4 °C was faster in the presence of ATPγS , slower for ADP and slowest for ATP. The differences in SH1 modification rate in the presence of nucleotides suggest conformational changes of this region during ATP hydrolysis. Also, the reactivity of the SH1 group showed a strong temperature dependence. In the presence of ADP and beryllium fluoride, but not aluminum fluoride, the reactivity of the SH1 site is very similar to that observed in the presence of ATP. This supports the observations that S-1.ADP with beryllium and aluminum fluoride represents different S-1.ATP complexes. The SH1-SH2 crosslinking was examined by a variety of bifunctional reagents. The rate of crosslinking also showed a strong dependence on the presence of nucleotides bound to S-1. These results show state-specific changes in the SH1-SH2 sequence during ATP hydrolysis.

References: 1.Wells et al., (1980) *Jour. Biol. Chem.*, 255:11135-11140; 2.Rayment et al., (1993) *Science*, 261:50-58.

M-Pos302

## A KINETIC REEVALUATION SUPPORTS THE STRUCTURAL TWO STEPS MODEL FOR ATP BINDING TO ACTOMYOSIN.

(( J.A. Biosca*, C. Lionne, F.Travers and T. Barman)) INSERM U 128, CNRS, BP5051, Montpellier 34033, France and * Department of Biochemistry and Molecular Biology, Universitat Autonoma de Barcelona, 08193 Bellaterra, Spain.

Recently there was proposed a model for the interaction of ATP with actoS1 (Rayment et al, 1993, Science 261, 58-65) which is seen as a two step process. ***First***, the phosphates of the ATP bind to the base of the ATPase pocket of the S1. This leads to the opening up of the cleft between the upper and lower domains of the 50kD segment of S1, thereby disrupting the strong S1-actin interactions. At moderate ionic strengths and actin concentrations the acto-S1 complex dissociates. ***Second***, the nucleotide binding pocket closes in upon the ATP which becomes tightly bound.

We have transient kinetic evidence that supports this model. We measured actoS1 dissociation by turbidimetry (stopped-flow) and tight ATP binding by the cold ATP chase method (rapid flow quench). At 15°C, pH8 and 50mM ionic strength, the kinetics of the two processes were identical and increased linearly with [ATP] to the limits of the methods. But when the buffer contained 40% ethylene glycol the kinetics were different : at 100 μM ATP, k(diss) = 300$s^{-1}$ and k(binding) = 49 $s^{-1}$. Whereas k(diss) varied linearly with [ATP], saturation was obtained for k(binding) with Kd = 28μM and k(max) = 63$s^{-1}$. These results show that the steps by whioh ATP dissociates and binds tightly to actoS1 are *kinetically distinct*.

Interestingly, the ATP binding kinetics to S1 alone were different with Kd = 9μM and k(max) = 16$s^{-1}$. This implies that the ATPase site of the S1 freshly released from actoS1 is *different* from that of S1 alone.

Supported by the ECC (stimulating action).

**M-Pos303**

KINETIC MECHANISM OF BINDING OF A SERIES OF MYOSIN-S1-MANT-NUCLEOSIDE DIPHOSPHATE (mNDP) COMPLEXES TO ACTIN ((Wei Jiang and Howard White)) Department of Biochemistry, Eastern Virginia Medical School, Norfolk, Va. 23507.

We have measured the rate constants for binding of a series of myosin-S1-mNDP complexes to actin. The observed change in fluorescence of the mNDP bound in the active site of the myosin-S1 upon binding to actin is evidence for a change in the environment of the nucleotide produced by actin binding to myosin-S1. The time dependence of the increase in fluorescence enhancement can be approximately fit by a single exponential equation but is fit much better by a double exponential equation. The dependence of kobs upon actin concentration are fit by a hyperbolic equation to obtain a maximum rate of binding and an $K_{app}$. The dependence of the maximum rate upon mant-NDP is CDP > ADP > GDP. Under similar conditions the observed rate of binding measured by light scattering increases linearly until it is too rapid for measurement. These results are consistent with a mechanism in which the S1-mNDP binding to actin is followed by one or more conformational changes between ternary acto-S1-mNDP complexes. This mechanism is similar to the mechanism previously proposed by this laboratory and others for the mechanism of binding of S1-nucleotide complexes to actin labeled with pyrene-maleimide. However, the maximum rate constants measured using mant-NDPs are two to four times as rapid as those measured using pyrene labeled actin. This work was supported by HL41776.

**M-Pos304**

RATE AND EQUILIBRIUM CONSTANTS OF THE HYDROLYSIS OF A SERIES OF NUCLEOSIDE TRIPHOSPHATES BY MYOSIN-S1 ((Betty Belknap, Xing-Qiao Wang and Howard White)) Department of Biochemistry, Eastern Virginia Medical School, Norfolk, Va. 23507 (Spon by A. Robinson)

We have measured the presteady state hydrolysis of a series of nucleoside triphosphate substrates (NTPs) ATP, CTP, 2-aza-1-N6--etheno-ATP (aza-ATP), and GTP by myosin-S1 and actomyosin-S1 using rapid chemical quench methods. Single turnover measurements ([S1] > [NTP]) provide a direct measurement of the equilibrium constant of hydrolysis of myosin bound substrate. The dependence of single turnover hydrolysis of ATP and CTP was fit by two rate processes. The rapid initial hydrolysis of phosphate is proportional to the amount of M-NTP and the slow hydrolysis is proportional to M-NDP-P. The myosin bound hydrolysis of CTP is more rapid (measured by tryptophan fluorescence enhancement) and more in the direction of products than is ATP. The single turnover hydrolysis of GTP and aza-ATP are fit well by a single kinetic process. For GTP the single turnover rate is similar to the steady state rate, which indicates that M-GTP is the principal steady state intermediate. For aza-ATP the single turnover rate of hydrolysis is several times more rapid than the steady state rate but may be partially rate limiting. Although there are small substrate dependent changes (2-3 fold) in the rates of some other first order steps of the mechanism of the actomyosin NTP pathway, the changes in the rate and equilibrium constants of the bond splitting step are the only changes thus far measured that are adequate to produce the large substrate dependent differences (50-100 fold) in steady state rates of NTP hydrolysis by actomyosin and muscle fibers. This work was supported by HL41776.

**M-Pos305**

NUCLEOTIDE ANALOGS PHOTOINCORPORATED INTO MYOSIN S1 ACT AS MOLECULAR PROBES OF THE ACTIVE SITE: EVIDENCE FOR DISTINCT ROLES OF ACTIN AND MgATP IN THE PRODUCT RELEASE STEPS OF ATP HYDROLYSIS ((Y. Luo*, D. Wang†, C. Cremo†, E. Pate*, R. Cooke‡ and R. Yount† ))Depts of *Mathematics and †Biochem/Biophys., Washington State Univ., Pullman, WA 99164, ‡Dept. Biochem/Biophys & CVRI, UCSF, San Francisco, CA 94143

Bz2εADP, fluorescent photoreactive ADP analog, is known to be trapped with vanadate at the active site of skeletal myosin S1 and photoincorporated upon UV irradiation. In this work we examined the effects of actin on the properties of S1 photolabeled with Bz2εADP. In the absence of actin, vanadate trapped and photolabeled S1 was inactive but after addition of actin, essentially 100% of MgATPase activity was recovered. In addition, after actin and MgATP treatment to release Vi, purified and photolabeled S1 alone had full MgATPase activity. Fluorescence polarization studies of Bz2εADP-labeled S1 showed that the εADP fluorophore decreases its polarization upon addition of actin and MgATP. Actin (or actin plus $K^+$-EDTA-ATP) alone did not decrease the polarization but did promote the loss of vanadate. Again, if the trapped Vi was removed by actin-MgATP treatment, MgATP alone was able to decrease the polarization. These results indicate that actin acts alone to displace trapped Vi but MgATP is required to displace covalently attached εADP. The other indication of the experiments is that probes can be placed on specific amino acids, Ser-324 in this case, and can be used to measure the individual and combined effect of actin, metal ions, and/or ATP on the release of nucleoside diphosphate analogs trapped or bound at the active site. Supported by MDA and NIH; DK05195 (R.Y.), AR39643 (E.P.) & HL32145 (R.C.). E.P. is an Established Investigator of AHA.

**M-Pos306**

STUDIES OF THE INTERACTION BETWEEN TITIN AND MYOSIN. ((A. Houmeida*, J. Holt+ and J. Trinick*)) *Dept. of Clinical Veterinary Science, Bristol University, BS18 7DY, UK and +Rhone-Poulenc Rorer Central Research, King of Prussia, PA 19406, USA.

The A-band region of the titin (also known as connectin) molecule is thought to be an integral thick filament protein and to be bound through interactions with the LMM part of the myosin molecule and C-protein. The apparent binding constant of the interaction with LMM was found to be ~$5.10^{-9}$ M, determined by coupling the probe dansylchloride to LMM via a cysteine residue and observing the fluorescence depolarisation on addition of titin. A similar value was obtained by coating ELISA plates with LMM and reacting with titin, which was detected by monoclonal antibodies. The fact that binding is relatively strong suggested that the sites on titin should saturate once LMM is in excess, even at low protein concentration. This proved to be the case and titin:LMM stoicheometry at saturation was ~1:50. This value is close to the predicted ratio of titin:myosin in situ of 1:49, assuming that there are three titin molecules per half thick filament. A titin binding cyanogen bromide fragment of LMM was identified and separated by passing the CNBr digest through a titin affinity column. The fragment was further purified by reverse phase HPLC. Interaction with titin was confirmed by solid phase assays on nitro-cellulose paper and ELISA, using antibodies to detect bound titin. The fragment has a chain molecular weight in the range 10-15 kDa. Its sequence begins EQTVKDL which corresponds to position 528 in the 676 residue sequence of LMM. This binding region is therefore in the C-terminal part of LMM.

**M-Pos307**

ELECTRON PARAMAGNETIC RESONANCE OF SPIN-LABELED SINGLE CRYSTALS OF CHICKEN MYOSIN S1. ((Edmund C. Howard, Ivan Rayment, and David D. Thomas)) University of Minnesota Medical School, Minneapolis, MN 55455 and University of Wisconsin-Madison, Madison, WI 53706.

We are studying single crystals of chicken myosin S1 spin-labelled with 4-(2-iodoacetamido)-[$^2$H]TEMPO in order to determine the orientation of the spin label on the myosin head, and, in turn, the docking angle of S1 on actin in muscle. We have developed a loop-gap resonator with an integral computer-controlled goniometer with both high sensitivity and high angular resolution for this project. We plan to acquire EPR spectra of these crystals in January 1994; results will be reported at the meeting.

**M-Pos308**

*EFFECTS OF CHARYBDOTOXIN, APAMIN, AND TETRAETHYLAMMONIUM ON $Ca^{2+}$-SENSITIVE K+ CURRENT IN ISOLATED CORONARY SMOOTH MUSCLE CELLS.* ((N. Buljubasic, J. Marijic, J.P. Kampine and Z.J. Bosnjak)) Department of Anesthesiology, Medical College of Wisconsin, Milwaukee, WI 53226.

This study characterizes $K^+$ current in canine coronary artery and investigates its role in regulation of vascular smooth muscle tone during the resting and activated states. Isolated rings and whole-cell $K^+$ current as well as single $K^+$ channels were studied. Tetraethylammonium (TEA, <3 mM) did not increase the resting tension in isolated rings, however 0.3 mM TEA increased the tension in vessels that were precontracted by elevated $[K^+]_o$. The whole-cell $K^+$ current showed voltage and $Ca^{2+}$ dependency and sensitivity to TEA (31±7%, 72±2% and 83±4% depression by 1, 10 and 30 mM TEA, respectively). A large-conductance (100 pS) $K^+$ channel was identified in the cell-attached patches with open time distribution fitted with two exponentials. Calcium ionophore A23187 (10 μM) increased the probability of opening (Po), mean open time (MOT) and amplitude of this channel in the cell-attached patches. In inside-out patches, increase in cytoplasmic side $[Ca^{2+}]$ from $10^{-7}$ to $10^{-6}$ M increased both the Po and MOT, without changing its conductance. TEA (1 mM) on the cytoplasmic side caused reversible decrease in the current amplitude. Charybdotoxin (100 nM) decreased the Po, MOT and increased mean closed time, while apamin (100 nM) did not have significant effect on the channel kinetics. In summary, this study demonstrates the existence and important functional role of a large-conductance, $Ca^{2+}$-sensitive $K^+$ channel in the regulation of membrane potential and cell excitability, as well as some aspects of regulation and kinetics of this channel in canine coronary arterial cells.

**M-Pos309**

WHOLE-CELL, ATP-SENSITIVE $K^+$ CURRENT IN FRESHLY DISPERSED, PORCINE CORONARY SMOOTH MUSCLE ((D.K. Bowles and M. Sturek)) Vascular Cell Biophysics Laboratory, Dalton Cardiovascular Research Center and Department of Physiology, Univ. of Missouri, Columbia, MO 65211.

We measured ATP-sensitive $K^+$ currents ($K_{ATP}$) utilizing whole-cell voltage-clamp. Cells were superfused with normal physiological saline solution ($[K^+]$ = 5 mM). Pipette solutions contained (in mM), 125 $K^+$, 10 $Na^+$, 132 $Cl^-$, 1 $Mg^{2+}$, 20 HEPES, 0.2 EGTA, 0.1 mM fura-2 $K_5$, 0.5 GTP and either 3 ATP or 0.5 ADP. Step depolarizations (10 mV) from a holding potential of -80 mV were recorded. At potentials more negative than -40 mV only time-independent current was observed. At potentials more positive than -40 mV, time-dependent currents appeared superimposed on the time-independent current. Omission of ATP from the pipette dramatically increased the time-independent current. These results demonstrate significant whole-cell $K_{ATP}$ current near resting membrane potential in porcine coronary smooth muscle. (Supported by NIH HL41033, RCDA HL02872 and AHA 9310500)

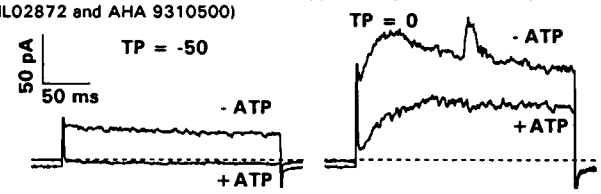


**M-Pos310**

INCREASED MYOSIN LIGHT CHAIN KINASE CONTENT IN RAGWEED POLLEN SENSITIZED SMOOTH MUSCLE FROM CANINE SAPHENOUS VEIN ((Gang Liu, Kang Rao, He Jiang, and Newman L. Stephens)) Dept. of Physiol. University of Manitoba, Winnipeg R3E 0W3 Canada.

Our previous studies had shown that ragweed pollen resulted in a generalized sensitization of smooth muscles from many different loci such as airway, blood vessels, and ureters. This model is thus suitable for studying not only the airway but also vascular hyperresponsiveness; the latter is important in anaphylactic shock. Mechanical data revealed that the smooth muscle from sensitized canine saphenous vein possessed greater active shortening capacity, and maximum shortening velocity. Relaxation of crossbridges in early shortening was also impaired. These functional changes may be responsible for the venous hyperresponsiveness observed in anaphylactic shock. Since smooth muscle crossbridge cycling is a function of actomyosin ATPase activity which is in turn regulated by phosphorylation of the 20 kDa myosin light chain($MLC_{20}$) by myosin light chain kinase (MLCK), $MLC_{20}$ phosphorylation, MLCK content and specific activity were assessed in saphenous vein smooth muscle of ragweed pollen-sensitized dogs and their littermate controls. Phosphorylation of $MLC_{20}$ in sensitized saphenous vein (SSV) was significantly increased, which resulted from higher MLCK content. The specific MLCK activity was similar in both groups. The results of our study suggest that MLCK content elevation is likely the key change that is responsible for the increased responsiveness of sensitized venous smooth muscle in anaphylactic shock. They are very similar to those we have reported for airway smooth muscle from the same animal model and support the idea that the sensitization process and associated changes in biophysical and biochemical properties likely involve smooth muscle from all the organs. (Supported by Manitoba Heart Found.; GL was supported by funds from Inspiraplex (Natl. Centres of Excellence, Canada)

**M-Pos311**

MYOSIN ISOFORMS, CONTENT AND TISSUE STRESS IN RAT CAROTID WITH DEVELOPMENT. ((T.J. Eddinger)) Biology Department, Marquette University, Milwaukee, WI 53233

Correlations between myosin heavy chain (MHC) isoforms, myosin protein content and stress production were examined in rat carotid tissue rings from animals between 10 and 150 days of age. Stress production ranged from a low of $1.5X10^4$ N/M$^2$ in the 10-day old animals to a high of $6.3X10^4$ N/M$^2$ in the adults. The myosin content present in these tissues was lowest in the 10-day old animals (1.2 mg myosin/gm tissue) and highest in the 20-day old animals (2.1 mg myosin/gm tissue) with the adults having 1.6 mg myosin/gm tissue. The ratio of media to total vessel weight was lower in the adult animals (0.46) than in the younger groups examined (10- to 30-day old, 0.57-0.66). Normalization to eliminate the adventitial content of the tissue showed the adult group to have the highest myosin content at 3.5 mg myosin/gm muscle. The ratio of non-muscle (NM) to smooth muscle (SM) MHC content decreased with increasing age from a high of 0.25 in the 10-day old animals to a low of 0.06 in the adult animals. The ratio of SM1/SM2 MHCs was low in both the young (10-day) and adult (<1.5) and peaked in the 25-day old group (2.7). These results indicate only a moderate level of correlation between either myosin content/muscle weight or NM/SM MHC ratio and stress production in these tissues ($0.45 \leq r^2 \leq 0.55$) and suggests that other factors must be included to account for the change in stress production observed with development. This work is supported by the American Heart Association, Wisconsin Affiliate and Marquette University's Committee on Research.

**M-Pos312**

EFFECTS OF $[K^+]_o$ ON THE SINGLE-CHANNEL PROPERTIES OF MAXI-$K_{Ca}$ CHANNELS RECORDED IN SINGLE VASCULAR SMOOTH MUSCLE CELLS. ((E. Morales, C. Rémillard, W.C. Cole, and N. Leblanc)) Montréal Heart Institute, Montréal, Québec, CANADA H1T 1C8, and University of Calgary, Calgary, Alberta, CANADA T2N 4N1.

The effects of altering the $K^+$ gradient on unitary currents through single maxi-$K_{Ca}$ channels were studied using the patch clamp technique in rabbit portal vein myocytes. When the cells were bathed in normal external solution (5.4 mM $K^+$ and 1.8 mM $Ca^{2+}$), $Ca^{2+}$- and charybdotoxin-sensitive maxi-$K_{Ca}$ channels were routinely recorded at the resting membrane potential (RMP; $V_p$ = 0 mV) in cell-attached mode with 140 mM $K^+$ in the pipette solution ($\gamma$ = 120-130 pS). With 5.4 mM $K^+$, maxi-$K_{Ca}$ activity was nearly undetectable at RMP ("apparent" $NP_o$ = 0) but increased at positive potentials, although difficult to resolve as they appeared as low conductance "noisy" channels. These effects of $K^+$ were still observed with 2 mM 4-aminopyridine in the pipette solution, or low chloride media to suppress delayed rectifier $K^+$ and $Cl^-$ channels, respectively. In cell-attached patches in which maxi-$K_{Ca}$ channels could be resolved with 5.4 mM $K^+$, patch excision into a medium containing 140 mM $K^+$ ($Ca^{2+}$ buffered to 100 nM) led to a marked increase in the slope conductance of the channel (from ~ 20 to 110 pS at 0 mV assuming RMP = -50 mV). Similar results were obtained in coronary artery myocytes. These data suggest that intracellular factors may significantly depress single-channel conductance of maxi-$K_{Ca}$ in a manner not previously described in inside-out patch experiments (~ 100 pS), which likely overestimated its contribution under physiological $K^+$ gradient.

**M-Pos313**

HIGH $[Na^+]_i$ STIMULATES $Ca^{2+}$-ACTIVATED $Cl^-$ CHANNELS VIA ENHANCED $Ca^{2+}$ ENTRY THROUGH $Na^+/Ca^{2+}$ EXCHANGE IN RABBIT PORTAL VEIN MYOCYTES. ((N. Leblanc, and P.M. Leung)) Montréal Heart Institute, Montréal, Québec, CANADA H1T 1C8.

Macroscopic currents were recorded in freshly dissociated smooth muscle cells from the rabbit portal vein using the tight seal whole-cell recording mode (22°C). In these experiments, TEA (pipette and bath) and Nifedipine (1-10 μM) were used to inhibit $K^+$ and L-type $Ca^{2+}$ channels, respectively. Cell dialysis with 30 mM $Na^+$ and low EGTA (0.1 mM) induced changes in membrane current consistent with activation of $Ca^{2+}$-activated $Cl^-$ channels ($I_{Cl(Ca)}$). From holding potential (HP) of -60 mV, high $[Na^+]_i$-induced current was instantaneous during 0.5-5 sec voltage clamp steps from -80 to +20 mV; steps ≥ +40 mV evoked slow time-dependent outward current ($I_t$) which was superimposed on the instantaneous current; upon return to HP, slow inward tail current appeared which reflected deactivation of $I_t$. Both current components: *1)* exhibited outward rectifying properties, *2)* reversed near the calculated equilibrium potential for $Cl^-$, *3)* were stimulated by elevation of $[Ca]_o$, *4)* were abolished when the cells were dialysed with 5 mM EGTA, and *5)* were potently inhibited by extracellular application of Niflumic acid (50 μM). Dialysis with either 0 mM Na and 0.1 mM EGTA, or 30 mM Na and 5 mM EGTA failed to evoke $I_{Cl(Ca)}$, suggesting the role of $[Na^+]_i$ was indirect. In contrast, $I_{Cl(Ca)}$ increased following complete replacement of $[Na]_o$. High $[Na^+]_i$-induced $I_{Cl(Ca)}$ was suppressed in the presence of 2 mM $Ni^{2+}$. Our results are consistent with an indirect mechanism of stimulation of $I_{Cl(Ca)}$ which involves reverse-mode electrogenic $Na^+/Ca^{2+}$ exchange activity.

M-Pos314

**LYSOPHOSPHATIDYLCHOLINE (LPC) IS AN ENDOTHELIUM-MODULATED RELAXANT OF PULMONARY ARTERIAL SMOOTH MUSCLE.** *((J.E. Duncan and J. Belik)) Department of Physiology and Pediatrics, University of Manitoba, Winnipeg, Manitoba CANADA R3E 0W3*

The effect of LPC, an endothelium-dependent relaxant of systemic vessels, was investigated on the pulmonary vasculature given the limited data available. Guinea pig pulmonary arterial rings, with endothelium intact (+Endo) and mechanically denuded (-Endo), were precontracted to 50% maximal force with phenylephrine (3μM) and exposed to cumulative doses of Acetylcholine (ACh) ($10^{-10}$-$10^{-3}$M) and LPC ($10^{-10}$-$10^{-4}$M). Synthesis of endothelium-derived relaxing factor (EDRF) was blocked with $N^G$-methyl-L-arginine. In +Endo maximal relaxation induced by LPC was 63±5% (mean±SE) as compared with 16±9% with ACh (10μM). The response to LPC was attenuated by endothelium denudation but not by EDRF blockade. LPC is an endothelium-modulated relaxant of pulmonary vessels in vitro, its maximal relaxing effect greater than that induced with ACh. (Supported by a grant from MRC Canada)

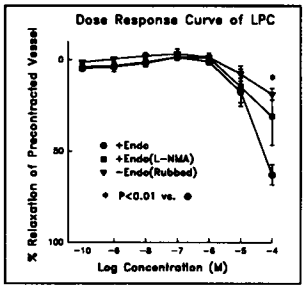


M-Pos315

EFFECT OF + 1-OLEOYL-2-ACETYLGLYCEROL (OAG) ON L-TYPE CALCIUM CURRENTS IN THE A7R5 SMOOTH MUSCLE-DERIVED CELL LINE.

((M. Auslender, C. Obejero-Paz and A. Scarpa)) Dept. Physiol. & Biophys., Case Western Reserve University. Cleveland OH 44106. (Spon. by J. Whittembury)

L-type calcium channel activity play a key role in the regulation of vascular tone. The modulation of these channels by protein kinase C (PKC) has been proposed with conflicting results. We characterized the effect of 100 uM OAG, a PKC activator, on L-type calcium channels, using the cell attached configuration of the patch clamp technique. Single channel currents carried by 110 mM $Ba^{2+}$ were elicited by pulses to + 10 mV from a holding potential of -40 mV. OAG increased the averaged probability (including null sweeps) from (mean±SE) 3.7 ± 0.7% to 7.4 ± 1.4% in 6 out 11 patches. In two patches with high channel activity under control conditions, 6.7% and 8%, the averaged probability decrease by 69% when the cells were exposed to OAG. In 3 patches no effect was noticed (control: 5.8 ± 1.0 %, OAG: 5.8 ± 0.6%).Those cells stimulated by OAG showed a late decrease in the channel activity after 10 min of being in contact with the drug. The observed increase in current was due to an increment in the open probability during the pulse and a decrease in the number of null sweeps. OAG did not affect the single channel current. Our results suggest a dual modulatory effect of OAG on L-type calcium channel, with early activation followed by late inhibition.

C.O-P and M. A. are Research Fellows of the American Heart Assoc., Northeast Ohio Affiliate, Inc.

M-Pos316

CALCIUM CURRENTS AT RESTING MEMBRANE POTENTIAL IN THE A7R5 SMOOTH MUSCLE-DERIVED CELL LINE.

((C. Obejero-Paz, M. Auslender, S.W.Jones, and A. Scarpa)) Dept. Physiol. & Biophys., Case Western Reserve Univ. Cleveland OH 44106.

Using the cell attached patch clamp technique, we have observed two types of calcium channels at resting membrane potential in A7r5 cells. Using 110 mM $Ba^{2+}$ as current carrier the slope conductances and extrapolated reversal potentials were (mean ± SD) 5.5 ± 0.5 pS and 50.7 ± 6.3 mV (n=5), and 13.1 ± 2.4 pS and 20.8 ± 11.0 mV (n=5). The 13 pS channel does not discriminate between $Ba^{2+}$ and $Ca^{2+}$ since the slope conductance and reversal potential in 110 mM $Ca^{2+}$ were 11.8 ± 1.0 pS and 17.7 ± 5.1 mV (n=4), respectively. Assuming the reversal potential measurements reflect $Ba^{2+}$ and $K^+$ permeations, and the single channel current to voltage relation is linear above 0 mV, we calculate a $P_{Ba}/P_K$ - 2 and 20 for the 5 and 13 pS channel, respectively. The 5 pS and 13 pS channels were observed in 10 % of the patches. Both channels are characterized by bursts of activity separated by long closures. The open probability of the 13 pS channel is voltage independent. We also observed whole cell currents in $Ca^{2+}$ and $Ba^{2+}$ blocked by 100 uM $Gd^{3+}$. It remain to be established whether this whole cell current result from the activity of channels like those observed in the cell-attached configuration. These experiments indicate that A7r5 cells have selective pathways for $Ca^{2+}$ entry in resting conditions, which could be involved in the setting of the cytosolic $Ca^{2+}$ concentration or the steady refilling of intracellular stores.

C.O-P and M. A. are Research Fellows of the American Heart Assoc., Northeast Ohio Affiliate, Inc.

M-Pos317

**MODULATION OF SMOOTH MUSCLE L-TYPE $Ca^{2+}$ CHANNELS BY PROTEIN KINASE C AND INTRACELLULAR $Ca^{2+}$**

K. Groschner and K. Schuhmann,
Dept. of Pharmacology und Toxicology, Univ. of Graz, Austria.

We investigated the regulation of smooth muscle L-type $Ca^{2+}$ channels by protein kinase C (PKC) and intracellular $Ca^{2+}$, and tested the hypothesis of a interdependence of these putative regulatory mechanisms. The function of single L-Type $Ca^{2+}$ channels was studied by recording unitary $Ba^{2+}$ currents in cell-attached patches of smooth muscle cells isolated from human umbilical vein. Stimulation of endogenous PKC with 100nM 12-O-tetradecanoyl phorbol-13-acetate (TPA) resulted in a transient increase in the mean number of open channels ($nP_O$) during depolarizing voltage steps, which was followed by a sustained suppression of L-type channel activity. Voltage-ramp experiments indicated that the transient, TPA-induced increase in channel activity was due to both an increase in the maximum number of available channels and a shift of the voltage dependence. At low TPA concentrations (10nM) clear inhibition of channel activity was observed without preceding stimulatory effects. The PKC inhibitor H7 (10μM) by itself slightly increased channel activity and prevented the inhibitory effects of TPA. Increasing the $Ca^{2+}$ concentration within the cells by elevation of extracellular $Ca^{2+}$ to values above 30 μM in the presence of the $Ca^{2+}$ ionophore A23187 (1μM), resulted in a reduction of channel activity which was further suppressed by TPA. $Ca^{2+}$-dependent inhibition of L-type channels in the presence of A23187 was partially prevented by H7 (10μM). Our results provide evidence for a dual regulatory role of PKC, and suggest a close linkage between PKC- and $Ca^{2+}$-dependent regulation of smooth muscle L-type $Ca^{2+}$ channels.

Supported by the Austrian Research Funds (S6605)

M-Pos318

**Properties of single calcium channels in smooth muscle cells from resistance-sized cerebral arteries using low calcium concentrations as the charge carrier**

((Michael Rubart, Adrian Bonev, and Mark T. Nelson)). Univ. of Vermont, Dept. of Pharmacology, Medical Research Facility, Colchester, VT 05446

To understand the membrane potential dependence of arterial tone, it is necessary to define the voltage dependence of Ca channels in resistance arteries under physiological conditions.

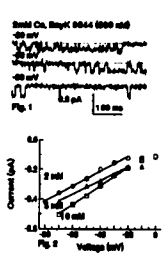

Single dihydropyridine - sensitive calcium channels were studied in cell-attached patches on cells isolated from resistance-sized branches of posterior cerebral arteries from rats. Ca (10, 5 and 2 mM) was used as the charge carrier. Openings of single calcium channels could be observed with nearly physiological Ca concentration (2 mM) as the charge carrier during steady state membrane voltages (Fig. 1). Lowering Ca from 10 to 2 mM shifted the single-channel current-voltage relationship in a hyperpolarizing direction and slightly changed single channel slope conductances at membrane voltages from -80 to -20 mV (Fig. 2; 2mM Ca, 5.0 pS; 5 mM Ca, 4.6 pS; 10 mM Ca, 6.3 pS). At voltages > -20 mV, the current-voltage relationship becomes non linear. We suggest 1) unitary currents through dihydropyridine-sensitive Ca channels can be resolved at low concentrations of the charge carrier and at the range of constant membrane voltages occurring in intact, pressurized arteries. Ca entry through these channels can regulate intracellular Ca levels and thus tone of resistance arteries; 2) the reduction in unitary current may result from the shift of $E_{Ca}$ as predicted from the Nernst equation; and 3) the small decrease in slope conductance may be indicative of local Ca activity held elevated by fixed negative surface charges. *Supported by NSF and NIH*

M-Pos319

A VOLTAGE WINDOW FOR SUSTAINED ELEVATION OF CYTOSOLIC CALCIUM IN SMOOTH MUSCLE CELLS. ((B.K. Fleischmann, R.K. Murray, and M.I. Kotlikoff)) Depts. of Animal Biology and Medicine, University of Pennsylvania, Philadelphia, Pa 19104.

The role of voltage-dependent calcium channels (VDCC) in the regulation of cytosolic calcium in cells that do not depolarize to membrane potentials sufficient to activate a substantial fraction of the available current has been controversial. We investigated the effect of sustained depolarizations on $[Ca^{++}]_i$ to determine whether VDCC activity at potentials near the threshold of channel activity regulate $[Ca^{++}]_i$ in non-spiking smooth muscle cells. Freshly dissociated equine tracheal myocytes were loaded with fura 2AM (2 μM, 15 min) and voltage-clamped at 35°C using the nystatin method to retain physiologic calcium buffering. Sustained depolarizations to potentials over a narrow voltage window near the resting potential, but not to more positive values, resulted in a sustained rise in cytosolic calcium. This calcium window corresponded well with the predicted window current measured under equivalent conditions (peak at -30 mV), could be augmented and shifted to more negative potentials by BAY K8644, and was blocked by nisoldipine (20 μM). The calcium window existed over the voltage range -40 to -20 mV in all cells (n=16). Sustained depolarizations to the peak of the calcium window (-30 mV) produced an averaged sustained increase in calcium of 97±11.5 nM (n=10). Despite a substantial rise in $[Ca^{++}]_i$, macroscopic currents were barely detectable over the course of the depolarizing step (less than -2 pA). Sustained depolarizations to potentials more positive than the calcium window resulted in a transient rise in $[Ca^{++}]_i$ that decayed below resting levels. Measurements of the calcium efflux rate constant indicate that a steady-state current on the order of -0.5 pA would be sufficient to produce a sustained increase in $[Ca^{++}]_i$ from 100 nM to 200 nM. Voltage-dependent, L-type calcium channels are capable of substantially elevating cytosolic calcium in the range of the predicted window current even though macroscopic currents are barely detectable. These data suggest that VDCC function near the apparent threshold of the macroscopic current play an important role in the regulation of $[Ca^{++}]_i$. Supported by NIH 45239.

**M-Pos320**

cAMP INCREASES INTRACELLULAR $Na^+$ IN VASCULAR SMOOTH MUSCLE CELLS via $Na^+$ PUMP INHIBITION ((M.L. Borin)) Dept. of Physiol., Univ. of Maryland Med. Sch., Baltimore, MD 21201.

The effect of the increase in cAMP on intracellular free $Na^+$ ($[Na^+]_i$) was studied in cultured rat aortic myocytes. The cells were loaded with the $Na^+$-sensitive fluorescent indicator SBFI. The membrane permeant cAMP analogue, 8-Br-cAMP, caused $[Na^+]_i$ to rise, with a net gain of 5 mM $[Na^+]_i$ achieved in 20 min. This rise in $[Na^+]_i$ might result either from inhibition of $Na^+$ efflux and/or from stimulation of $Na^+$ influx. When $Na^+$ pump-mediated $Na^+$ efflux was inhibited by ouabain, 8-Br-cAMP had no effect; i.e., $Na^+$ influx was not stimulated. Similar results were obtained when the cAMP level was raised by a mixture of the adenylate cyclase activator, forskolin, and the phosphodiesterase inhibitor, IBMX. These results suggest that the cAMP-induced rise in $[Na^+]_i$ in aortic smooth muscle cells is caused by suppression of $Na^+$ efflux. Such mechanism of cAMP effect on $[Na^+]_i$ is opposite to the cAMP-induced activation of the $Na^+$ pump and corresponding decrease in $[Na^+]_i$ observed in intestinal smooth muscle cells (Moore & Fay, PNAS,90, 8058-8062,1993). Earlier we demonstrated that increase in $[Na^+]_i$ causes accumulation of $Ca^{2+}$ in stores; therefore, cAMP may cause an intracellular $Ca^{2+}$ sequestration mediated by the rise in $[Na^+]_i$.

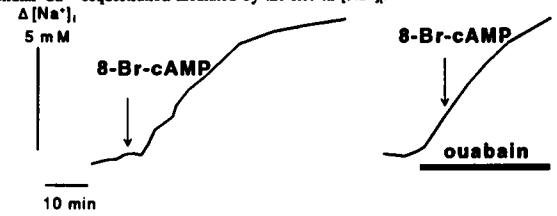


## CARDIAC MUSCLE PHYSIOLOGY

**M-Pos321**

CURRENT OSCILLATIONS IN RESPONSE TO CALCIUM OSCILLATIONS IN RABBIT VENTRICULAR MYOCYTES. ((Michael A. Laflamme and Peter L. Becker)) Dept. of Physiology, Emory University, Atlanta, GA.

Studies of $Ca^{2+}$ homeostasis in heart cells often involves conditions that allow measurement of $I_{Ca}$ along with detection of the resulting $[Ca^{2+}]$ changes. The presence of $Ca^{2+}$-activated currents can obscure the characteristics of the $I_{Ca}$. We have studied the current oscillations resulting from spontaneous $[Ca^{2+}]$ oscillations to determine their ionic basis and the impact of such currents on our ability to assess $I_{Ca}$. Single rabbit ventricular myocytes were voltage clamped using the whole-cell technique with a pipette that normally contained (in mM): 0.1 fura-2, 140 CsCl, 3.3 $Na_2$-ATP, 3.0 MgCl, 5 HEPES, and 5 NaCl, pH=7.2 with NaOH. The extracellular solution initially contained 115 NaCl, 20 CsCl, 1 $MgCl_2$, 1.5 $CaCl_2$, 0.3 $CaHPO_4$, 10 HEPES, 5 TEA, 5 glucose, pH=7.4. $[Ca^{2+}]$ was monitored with a high-time resolution microfluorimeter. Cells were held at +40 mV to elevate the $[Ca^{2+}]$ via the Na/Ca exchanger, which initiated spontaneous $Ca^{2+}$ oscillations. These $[Ca^{2+}]$ oscillations were associated with outward current oscillations. At +40 mV, the outward current, but not the $[Ca^{2+}]$ oscillations, was inhibited by the reversible $Cl^-$ channel blocker DNDS. The current reversed at about +20 mV under these approximately symmetrical $Cl^-$ conditions, but shifted about +25 mV when $E_{Cl}$ set at +30 mV. Replacing all $Cl^-$ with aspartate in both the pipette and bathing solutions resulting in oscillating *inward* currents at all potentials (up to +80 mV). We conclude that this oscillating current represents the combination of a calcium-activated $Cl^-$ current (Zygmunt & Gibbons, Circ. Res. 68:424, 1991) and a Na/Ca exchanger current (Lipp and Pott, J. Physiol. 397:601, 1988). The apparent synchrony of these two currents, as evidenced by the relatively steady current record at the reversal potential, suggests that these two currents may both sense the same $[Ca^{2+}]$.

**M-Pos322**

ACTION POTENTIAL PROLONGATION BY DEFIBRILLATION SHOCKS MAY BE DUE TO REACTIVATION OF THE RAPID SODIUM CURRENT. ((S.M. Dillon)) Dept. of Pharmacology, College of Phys. & Surg. Columbia University, New York, NY, 10032.

We have shown that defibrillation threshold strength shocks applied during the plateau phase caused action potential prolongation (APP) (Circ. Res. 69:842, 1991). Here, the mechanisms of APP were investigated by optical recordings of membrane voltage changes at the tips of isolated, coronary perfused rabbit papillary muscles during application of 5 msec electrical shocks in the plateau phase of a paced rhythm. It is known that externally applied electrical shocks cause membrane depolarizations (MD) and membrane hyperpolarizations (MH) of cardiac cells. Shocks applied along the longitudinal axis of the papillary muscle caused either MD or MH at the tip, depending upon the shock polarity. Fig 1 shows that neither MH or MD alone produced APP. However, Fig 2 shows that a shock applied across the width of the muscle tip, where MD and MH was produced in closely adjacent patches of myocardium, caused APP. It is thought that the shock removed sodium channel inactivation in cells undergoing MH such that they were promptly restimulated by current flow from cells undergoing MD, thus giving the appearance of APP. In Fig 3, two sequential pulses of alternate polarity produced the appearance of APP by first restoring excitability through strong MH and then stimulating an action potential by a small MD. This shows that sodium current kinetics permit APP to occur through action potential stimulation in refractory myocardium according to the mechanism described above.

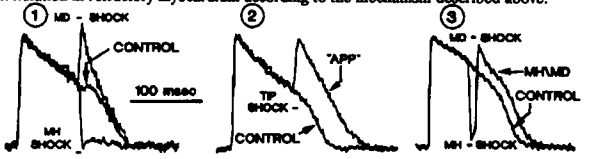


**M-Pos323**

CALCIUM SENSITIVITY OF TENSION IS INCREASED IN EXPERIMENTAL HEART FAILURE. ((Matthew R. Wolff and Richard L. Moss)) Departments of Medicine and Physiology, University of Wisconsin, Madison WI 53706.

To examine the role of myofibrillar pathophysiology in chronic heart failure, we determined isometric tension-pCa relations in a canine model of dilated cardiomyopathy (DCM) produced in 4 dogs by chronic rapid pacing at 250/min for 28.2 ± 8.8 days. Echocardiographic short-axis area ejection fraction decreased by 58% and left ventricular end-diastolic pressure increased from 7.5 ± 1.5 to 25.0 ± 3.8 mm Hg after development of DCM (for both, $p<0.05$). Isometric tension-pCa relations were measured using mechanically disrupted and permeabilized myocyte-sized preparations obtained from LV biopsies before (BASE, n=6) and after (DCM, n=7) chronic pacing. Resting sarcomere length (SL) was set at 2.35 μm, and preparations had low end-compliance (SL was 2.24 ± 0.04 μm during maximal activation). Passive (2.3 ± 1.2 vs 2.4 ± 0.4 mN/mm²) and maximal $Ca^{2+}$-activated tensions (28.4 ± 7.6 vs 30.3 ± 6.2 mN/mm²) were similar for BASE and DCM. However, tension-pCa relations were shifted leftward with DCM ($pCa_{50}$ = 5.86 ± 0.04 BASE vs 5.94 ± 0.04 DCM, $p < 0.05$). This *increased* calcium sensitivity of isometric tension may serve in part to compensate for decreases in systolic calcium transients in DCM, but may also play a role in the diastolic dysfunction that accompanies this condition.

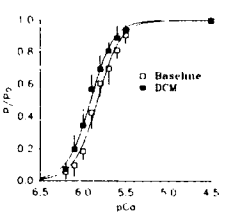


**M-Pos324**

THE EFFECT OF pH ON THE $Ca^{2+}$ AFFINITY OF THE $Ca^{2+}$ REGULATORY SITES OF SKELETAL AND CARDIAC TnC IN SKINNED MUSCLE FIBERS ((#B. Parsons, #J. Zhao, #G. Van Slooten, *W.G.L. Kerrick, +J.A. Putkey, #J.D. Potter)), #Dept. of Mol. & Cell. Pharmacology, Univ. of Miami School of Med., and *Dept. of Physiology & Biophysics, Miami, Florida 33101, +Univ. of Texas Med. School, Dept. of Biochem. & Mol. Biol., Houston, TX 77225

It is known that intracellular pH drops rapidly after the onset of ischemia and may play some role in the rapid drop in force that ensues. Lowering pH shifts the $Ca^{2+}$ dependence of force development in muscle fibers toward higher $[Ca^{2+}]$. The precise mechanism of this shift is unknown. To investigate this we have used skinned skeletal or cardiac muscle fibers whose endogenous troponin C (TnC) has been replaced with $STnC_{DANZ}$ or CTnC3 $(C84)_{IAANS}$, respectively. The fluorescence of the labeled TnC is enhanced by $Ca^{2+}$-binding to the $Ca^{2+}$-specific (regulatory) site(s) of STnC or CTnC and when incorporated into skinned fibers was measured simultaneously with force. When the pH was lowered from 7.0 to 6.5 ($[Mg^{2+}]$ = 1mM) the $Ca^{2+}$-dependence of force (T) and fluorescence (F) shifted in parallel toward higher $[Ca^{2+}]$. At higher $[Mg^{2+}]$ (5mM) the effect of lowering the pH from 7.0 to 6.5 was attenuated but the shifts in the $Ca^{2+}$-dependence of T and F were again in parallel. Since the T and F shift in parallel as the pH is lowered, it can be concluded that these changes in $Ca^{2+}$-sensitivity are caused by a decrease in the $Ca^{2+}$ affinity of the $Ca^{2+}$-specific sites of TnC. Since lowering the pH also results in lower maximal $Ca^{2+}$-activated force it is possible that $H^+$'s may act indirectly as well by reducing the number or type of crossbridges and thereby alter the crossbridge induced elevation of TnC $Ca^{2+}$ affinity (Guth & Potter, JBC 262, 1987). (Supported by NIH AR37701, AR40727, HL42325 and the AHA Florida Affiliate)

**M-Pos325**

**ANALYSIS OF THE IONIC BASIS FOR COCAINE'S DUAL EFFECTS ON REPOLARIZATION IN GUINEA PIG VENTRICULAR MYOCYTES.**

((Y-Q. Xu, C. Chang, C.H. Follmer, and C.W. Clarkson)) Department of Pharmacology, Tulane University School of Medicine, New Orleans, LA, 70112

The effects of cocaine on the duration of the cardiac action potential (APD) were investigated in isolated guinea pig ventricular myocytes at 37°C. At a paced cycle length of 5 sec, low concentrations of cocaine produced a significant increase in $APD_{90\%}$ (e.g. +22±5% at 3μM cocaine; n=6)(Mean±SE). In contrast, higher (30-100μM) concentrations produced a concentration-dependent, and fully reversible decrease in $APD_{90\%}$ (e.g. -53±2% at 100 μM cocaine; n=8). Pre-treatment of cells with 10 μM TTX changed the effect of 30μM cocaine on $APD_{90\%}$ from one of APD-shortening (-24±6%, n=5) to one of APD-lengthening (+16±5%, n=5, P<0.05). This suggests that block of a TTX-sensitive window current may contribute to cocaine's effect to shorten APD. Cocaine's effects were further investigated using the whole cell voltage-clamp technique at 37°C. Exposure to 10μM cocaine reduced the amplitude of delayed rectifier tail currents at -50 mV by 70±4% (n=4). The kinetics and voltage dependence of the cocaine-sensitive (difference) current indicated that cocaine blocks a rapidly activating, inwardly rectifying current similar to $I_{Kr}$. Cocaine also produced a concentration-dependent outward shift of the steady-state $I_m$ current-voltage relationship at plateau potentials in cells held at -90 mV (pulse duration = 400 msec), consistent with a drug effect to reduce inward plateau current(s). In Cs-loaded cells held at -40 mV, exposure to 100 μM cocaine produced a reversible reduction in peak $I_{Ca}$ at +10 mV of -36.5±6% (n=13). The effect of 100 μM cocaine to reduce the residual $I_{Ca}$ measured at the end of a 320 msec pulse to +10 mV was similar (-35.5±5%). We conclude that: 1) cocaine produces a biphasic concentration-dependent effect on repolarization in guinea pig ventricular myocytes; and 2) this biphasic effect on repolarization results from differences in the sensitivity of inward and outward currents to the blocking effects of cocaine, with low concentrations of cocaine producing a greater effect on outward vs. inward currents.

**M-Pos326**

**ENDOTHELIAL CELL FACTOR(S) MEDIATE MATCHING OF CARDIAC CONTRACTION AND OXYGENATION**

((A.M. Shah*#, A. Mebazaa¶#, G. Cuda§, R. Xiao#, J.R. Sellers§, J.L. Robotham¶ and E.G. Lakatta#)) #Lab. Cardiovasc.Science, NIH, & ¶Pulm. Anesth. Lab., Johns Hopkins Hospitals, Baltimore, MD; §NHLBI, NIH, Bethesda, MD; & *Dept. Cardiology, Univ. Wales Coll. Med., Cardiff, UK.

Endothelial cell (EC) factors, eg, nitric oxide, mediate *feedback* coronary vascular dilation during cardiac hypoxia. We determined whether hypoxic EC also influence myocardial contraction. Sheep cultured vascular and endocardial EC were superfused with hypoxic buffer ($pO_2$<70 mmHg), and reoxygenated superfusate (ECS) tested for its effect on rat cardiac myocyte contraction (diode array) and $[Ca^{2+}]_i$ (indo-1 fluorescence ratio, R). ECS induced rapid, marked, reversible reduction in twitch amplitude (-67.0±4.9%), and decreased diastolic length (L, -1.5±0.3μm; both p<0.001; n=18), but did not alter $Ca^{2+}$ transients (Fig). ECS also markedly depressed isometric force in ferret cardiac papillary muscle. The effects are attributable to a novel EC factor(s) acting independent of sarcolemmal receptors or known second messengers. Thus, (a) microinjection of ECS into myocytes induced similar effects, (b) diluted ECS (1/25) virtually completely but reversibly inhibited F-actin sliding over cardiac myosin in vitro, and actin-activated S1 ATPase, but had no effect on smooth muscle myosin. The data suggest a novel EC-mediated *feedforward* matching of contraction, and thus oxygen demand, to oxygen supply via factor(s) that alter cardiac myosin ATPase and crossbridge cycling.

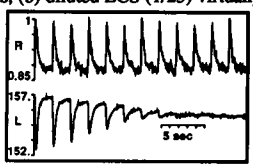


**M-Pos327**

**FLECAINIDE INHIBITS THE HYPERPOLARIZATION ACTIVATED CURRENT ($I_f$) IN SINGLE SINOATRIAL NODE CELLS FROM THE RABBIT.**

((Bernard Fermini)) Montreal Heart Institute, Montreal Quebec, Canada H1T 1C8.

Flecainide, a class Ic antiarrhythmic agent has been shown to cause sinus node bradycardia in patients; however, the ionic mechanism underlying this depressant effect is unknown. The whole cell voltage clamp technique was used to study the electrophysiological effects of flecainide acetate on the hyperpolarization activated current ($I_f$) in freshly dissociated sinoatrial (SA) node cells from the rabbit. $I_f$ was elicited by 1 sec hyperpolarizing voltage clamp steps from a holding potential of -40 mV. Rundown of the current was minimal over the recording period. Flecainide inhibited $I_f$ in a concentration-dependent fashion. When studied at -100 mV, the inhibition of $I_f$ averaged 55 ± 3% (n=3) and 67 ± 6% (n=3) for 15 and 30 μM, respectively. Flecainide apparently did not alter channel selectivity since the reversal potential for $I_f$ remained unchanged in the presence of both concentrations of the drug. Blockade of $I_f$ by flecainide was not use-dependent between 0.5 and 2.0 Hz, and the effects of the drug were partially reversed upon washout in all the preparations studied. **Conclusions**: 1) these results indicate that flecainide can inhibit $I_f$ in the SA node and 2) inhibition of $I_f$ by flecainide may partially explain the depressant effect of this drug on sinus node function.

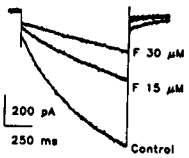


**M-Pos328**

**IBUTILIDE IS A POTENT BLOCKER OF $I_{Kr}$ IN CULTURED ATRIAL TUMOR MYOCYTES (AT-1 CELLS).**

((Tao Yang, Dirk J. Snyders and Dan M. Roden)). Departments of Medicine and Pharmacology, Vanderbilt University, Nashville, TN

AT-1 cells are derived from atrial tumors in mice expressing an ANF promoter-SV40 large T antigen transgene. The cells appear to retain a well-differentiated cardiac phenotype by biochemical and morphological criteria; they beat spontaneously in culture and cardiac action potentials can be recorded. We have recently reported that in >85% of AT-1 cells the major repolarizing current is a rapidly-activating delayed rectifier strongly resembling $I_{Kr}$ initially described in guinea pig myocytes. This current displays prominent inward rectification and nanomolar sensitivity to the methanesulfonanilide blocker dofetilide; unlike in guinea pig, $I_{Kr}$ in AT-1 cells can be observed directly, without the necessity of subtracting overlapping outward currents. Ibutilide is also a methanesulfonanilide which in guinea pig prolongs cardiac action potentials, an action which has been attributed not to $I_{Kr}$ block but to activation of a slow inward $Na^+$ current. In this study, we compared the effects of dofetilide and ibutilide on $I_{Kr}$ in AT-1 cells. Overlapping inward currents were eliminated by holding at -40 mV, and using the blockers nisoldipine and $Ni^{2+}$. Both agents blocked $I_{Kr}$: the $EC_{50}$ for ibutilide block with depolarizations to +20 mV was 27 nM (n=10) and for dofetilide 12 nM (n=8). Use of ibutilide in dofetilide-pretreated preparations did not result in augmented or altered block. Ibutilide block of $I_{Kr}$ was most prominent at plateau potentials: 20 nM reduced $I_{Kr}$ 12±8% at -30 mV, 37±9% at 0 mV, and 47±8% at +40 mV (n=7, each P<0.05). Block was frequency-independent, assessed with trains of 1 sec pulses and interpulse intervals from 0.2 to 2 sec. Thus, in this system, both ibutilide and dofetilide are potent blockers of $I_{Kr}$.

**M-Pos329**

**CARDIAC ACTION POTENTIAL SHORTENING AND ARRHYTHMIA DURING REPERFUSION AFTER ISCHEMIA: ROLE OF CORONARY VASOCONSTRICTION DUE TO OXY-RADICAL STRESS.**

((E.A. Aiello, R.I. Jabr and W.C. Cole)) Department of Pharmacology and Therapeutics, Faculty of Medicine, University of Calgary, Calgary, Alberta, Canada T2N 4N1.

Altered electrical activity due to oxygen-derived free radical (O-R) stress results in arrhythmias during reperfusion of the heart after ischemia. However, whether the changes in activity are due to direct effects of O-R on cardiomyocytes, and/or indirect effects resulting from coronary vasoconstriction (i.e. no-reflow phenomena) is not clear. We measured the changes in action potential duration (APD) and contractions during reperfusion of arterially-perfused guinea pig right ventricular walls. Right ventricular walls were dissected from hearts and perfused via the right coronary artery with Krebs-Henseleit solution (36-37°C) for 60 min before 30 min no-flow ischemia and 60 min reflow. Electrical activity was initiated from a point source at the base of the wall via 2 msec square pulses delivered at 2 Hz. APD at 90% repolarization ($APD_{90}$), measured with conventional microelectrodes, declined below ischemic values during early reperfusion. This was associated with pronounced arrhythmias (extrasystoles & tachyarrhythmia). Although reflow caused contracture and poor recovery of developed tension, $APD_{90}$ recovered to pre-ischemic value at 60 min. Perfusion with O-R scavengers (SOD, catalase & mannitol) inhibited reflow-arrhythmias and changes in $APD_{90}$. O-R from xanthine:xanthine oxidase (X:XO - 2mM:0.01 U/ml) caused decline in $APD_{90}$ in normoxia and enhanced $APD_{90}$ shortening on reflow in arterially perfused tissues. However, X:XO caused prolongation of APD in papillary muscle. Vasodilation due to nitroprusside (10μM) inhibited reflow- and X:XO-mediated decline in $APD_{90}$, arrhythmias and contracture but had no effect on AP on its own. These data provide evidence for O-R induced vasoconstriction in arrhythmogenic changes in cardiac AP during reperfusion after ischemia. Supported by MRC. RJ is a CHSF trainee.

**M-Pos330**

**THE EFFECT OF THYROID STATUS ON PHOSPHOLAMBAN PROTEIN EXPRESSION IN RAT HEARTS.**

((E. Kiss, I. Edes and E.G. Kranias)) Univ. of Cincinnati, Cincinnati, OH 45267. (Spon. by W.J. Ball)

Hyperthyroidism is associated with increases in the speed of cardiac relaxation while hypothyroidism results in decreases in this parameter. The present study was designed to determine whether the altered cardiac function in different thyroid states is associated with altered expression of the sarcoplasmic reticular (SR) proteins (phospholamban and $Ca^{2+}$-ATPase) responsible for $Ca^{2+}$ uptake. Quantitative immunoblot analysis revealed that the phospholamban protein level was depressed (76%) in hyperthyroid but increased in hypothyroid (135%) compared to euthyroid (100%) hearts. An opposite trend was found for the SR $Ca^{2+}$-ATPase. The $Ca^{2+}$-ATPase protein level was increased (135%) in hyperthyroidism and decreased (78%) in hypothyroidism. Consequently, the relative phospholamban/$Ca^{2+}$-ATPase ratio was lowest in hyperthyroid and highest in hypothyroid hearts. To examine whether the observed changes in this ratio reflected altered SR function, the $V_{max}$ and $EC_{50}$ of the SR $Ca^{2+}$ uptake for $Ca^{2+}$ were determined. The maximal SR $Ca^{2+}$ uptake rates were 21.4±0.7, 15.5±0.9 and 12.8±1.1 nmol $Ca^{2+}$/min/mg cardiac homogenate from hyperthyroid, euthyroid and hypothyroid hearts, respectively. A close correlation was observed between the relative phospholamban/$Ca^{2+}$-ATPase ratio and the $EC_{50}$ of SR $Ca^{2+}$ uptake in hyperthyroid (0.30±0.02 μM), euthyroid (0.41±0.04 μM) and hypothyroid (0.76±0.05 μM) hearts. These findings indicate that phospholamban and SR $Ca^{2+}$-ATPase protein levels change in different thyroid states. These changes lead to alterations in SR $Ca^{2+}$ uptake rates, which may contribute to alterations in the speed of cardiac relaxation.

**M-Pos331**

EFFECT OF BIDISOMIDE ON ACTION POTENTIALS RECORDED FROM ISOLATED CANINE ATRIUM AND VENTRICLE

((Cynthia Lee Martin and Kevin Chinn)) Searle, Skokie, IL 60077.

Bidisomide is a new class I antiarrhythmic agent in Phase III clinical trials. In addition to its sodium channel blocking properties, previous work demonstrated bidisomide significantly prolonged refractory period in the intact canine atrium, but only slightly in the ventricle (Garthwaite et al. Drug Dev. Res. 27:329-344). In isolated tissue studies, bidisomide shortened action potential duration (APD) in guinea pig ventricle and canine Purkinje fibers but had no effect on guinea pig atrial APD (Martin et al. Drug Dev. Res. 17:51-61; 1989). In the present studies, the effect of bidisomide on intracellular action potentials recorded from isolated canine cardiac atrium and ventricle was examined. At 30 μM, bidisomide prolonged atrial but not ventricular $APD_{90}$ and ERP. The effect was frequency-independent (ΔERP =24 ms at 1 Hz, 20 ms at 5 Hz, n=7). These data indicate that bidisomide may have two competing effects on APD, one which shortens APD and one which prolongs APD. The overall effect on APD (prolongation vs shortening) may reflect differences in channel densities in different regions of the heart and in different species.

**M-Pos332**

IS HYPERPOLARIZATION-ACTIVATED INWARD CURRENT THE "PACE-MAKER" CURRENT IN THE SINOATRIAL NODE? ((A. Zou, R.A. Powell and R.D Nathan)) Department of Physiology, Texas Tech University HSC, Lubbock, TX 79430.

Single pacemaker cells isolated from the rabbit S-A node and cultured for 1 - 3 days were employed to test the hypothesis that the hyperpolarization-activated current ($i_h$, $i_f$) is the only inward current that generates diastolic depolarization. To approximate physiological conditions, we used the perforated patch technique (300 μg/ml nystatin) and superfused the cells with a Tyrode's solution that contained 16 mM $NaHCO_3$, 95% $O_2$ and 5% $CO_2$. Measurements of $i_h$ were made at 150 ms, a diastolic period when the membrane potential is normally greater than -50 mV. When the holding potential (HP) was -50 mV, the threshold for $i_h$ was -55 mV (n = 8). Between -65 and -55 mV, the normal range of diastolic depolarization, $i_h$ varied from -16 ± 6 pA to -2 ± 2 pA. At these same potentials, time-independent or "background" inward current ($i_{bg}$) varied from -132 ± 30 pA to -89 ± 15 pA. This current was sometimes outward if the HP was -40 mV, possibly due to activation of delayed rectifier current. At -65 mV, 2 mM CsCl reversibly reduced $i_h$ by 92 ± 5% and $i_{bg}$ by 32 ± 13% in 5 cells; however, $Cs^+$ did not alter beat rate (BR) consistently (ΔBR = 0 ± 8%). In contrast, non-patched cells were slowed 22 ± 3% (n = 7) by $Cs^+$. If $i_h$ contributes to pacemaker activity, it should be enhanced by isoproterenol (ISO) and reduced by acetylcholine (ACh) at physiological concentrations. ISO (0.1 nM) accelerated BR in 4 cells (ΔBR = 40 ± 13%); however, $i_h$ increased in only 2 of these cells ($\Delta i_h$ = -1 ± 3 pA at -60 mV) and $i_{bg}$ increased in only 3 ($\Delta i_{bg}$ = 71 ± 73 pA). In 6 non-patched cells, ΔBR = 24 ± 10%. ACh (10 nM) slowed BR in 3 cells (ΔBR = -68 ± 20%); however, $i_h$ was reduced in only 2 of these cells ($\Delta i_h$ = -4 ± 5 pA at -60 mV) and $i_{bg}$ was reduced in only 2 ($\Delta i_{bg}$ = -36 ± 42 pA). These results demonstrate that $Cs^+$ does not block $i_h$ selectively and that $i_h$ may not be the only inward current that contributes to pacemaker activity. Supported by the Texas Advanced Research Program (#010674-039) and the NIH (HL48836).

**M-Pos333**

PHASE RESETTING AND DYNAMICS OF ATRIOVENTRICULAR NODAL CELL CLUSTERS ((Andrew Munk, Arkady Kunysz, Leon Glass, and Alvin Shrier)) Departments of Physiology and Physics, McGill University, Montréal, Québec, CANADA, H3G 1Y6

Cell clusters isolated from the rabbit atrioventricular (AV) node beat with a stable rhythm (cycle length: 200-550 ms) and are characterized by slow action potential upstroke velocities. The goal of this study is to better characterize the phase resetting and dynamics of this slow inward current system. Single and periodic depolarizing current pulses (5-30 ms) were injected into AV nodal cell clusters using microelectrodes or patch clamp electrodes. Phase resetting curves of both the strong, weak as well as discontinuous types were obtained by applying single current pulses of different intensities at increasing latencies following every ten action potentials. The transition point of the phase response curves typically occurred between 0.30 to 0.80 of the intrinsic cycle length depending upon stimulus intensity. Graded responses were elicited for certain ranges of stimulus phase and amplitude. Sustained periodic stimulation, at rates faster than the intrinsic beat rate resulted in various N:M (stimulus frequency:action potential frequency) entrainment rhythms as well as periodic or irregular changes in action potential morphology. Cessation of pacing was followed by a slight increase (15 to 40 %) of the intrinsic cycle length which dissipated almost completely after 5 beats and was roughly independent of the number of stimuli applied. These results provide a basis for understanding the modulation of the rhythmicity and excitability in the AV node.
This research was supported by the Canadian Heart and Stroke Foundation.

**M-Pos334**

**DEPENDENCE OF IMPULSE CONDUCTION ON THE GEOMETRY OF THE UNDERLYING EXCITABLE TISSUE: MULTIPLE SITE OPTICAL RECORDING OF TRANSMEMBRANE VOLTAGE (MSORTV) IN PATTERNED GROWTH HEART CELL CULTURES.**

((S. Rohr and B.M. Salzberg)) University of Bern, Bern, Switzerland and University of Pennsylvania School of Medicine, Philadelphia, PA, USA.

We have characterized impulse propagation across abrupt expansions of excitable tissue on a microscopic scale by investigating the spatio-temporal evolution of the shape of a propagating action potential as it traversed geometrically defined cellular patterns in monolayer cultures of neonatal rat heart cells. Cultures exhibiting defined structures (photo-lithographically patterned substrates) were stained with the voltage-sensitive dye di-8-ANEPPS and were mounted in a temperature controlled chamber on the stage of an inverted microscope. The preparations were stimulated by extracellular electrodes placed sufficiently distant that only propagated impulses could invade the recording site which was imaged onto a 12X12 photodiode array (spatial resolution = 15 μm in the object plane). The signals from the central 124 detectors were digitized at a frame rate of 2 kHz. An arbitrarily selectable subset of 16 signals was processed in parallel by a fast (1 MHz) analogue-to-digital converter (62.5 kHz frame rate) and was used to construct an activation map. The basic cellular pattern consisted of a narrow cell strand (up to 80 μm wide) inserting into a large rectangular cell region (width and length > 1500 μm). In order to vary the electrical load encountered by the propagating action potential at the junction, the transitional zone was formed either as a funnel, as a rectangular expansion (twice the load of the funnel), or as an incisure in the large rectangular region (three times the load of the funnel). While the funnel shaped expansions generally did not affect impulse propagation, delays of up to 1 ms were encountered at rectangular expansions. These delays corresponded to a local decrease in conduction velocity from 0.3 m/s to 0.03 m/s. Even greater delays (up to 4 ms) were recorded in the case of the incised patterns. In accordance with recently published 2-dimensional computer simulations, the maximal decreases in conduction velocity invariably occurred immediately after the abrupt expansions. These conduction disturbances were most probably related exclusively to the passive electrical properties of the patterns of myocytes, because the active membrane characteristics of individual cells are expected to be uniform in this cell culture system.
Supported by Swiss NSF grant 823A-028424 (SR) and USPHS grant NS16824 (BMS).

**M-Pos335**

ELECTRICAL INTERACTIONS BETWEEN THE SINOATRIAL NODE AND ATRIAL MUSCLE : CELL COUPLING EXPERIMENTS USING AN EXTERNAL CIRCUIT ((E. Watanabe, H. Honjo, T. Anno, I. Kodama, J. Toyama)) Department of Circulation, Research Institute of Environmental Medicine, Nagoya University, Furo-cho, Chikusa-ku, Nagoya, 464-01, Japan

To investigate the influence of the atrial muscle in pacemaking activity of the sinoatrial node (SAN) , we connected enzymatically isolated SAN cells with a membrane model (RC circuit) of a single atrial cell through an external circuit which mimics the electrical connection with variable coupling conductance (Gc). This circuit is composed of a dual preamplifier and a dual voltage/current converter(V/I) (Tan and Joyner 1990). In the present study a single atrial cell was substituted by a membrane model; input resistance of 220 MΩ, input capacitance of 51 pF and resting membrane potential of -80 mV. Trans-membrane potential of the SAN was recorded by the patch pipette under current clamp mode. At Gc of 0 nS average spontaneous cycle length (SCL) was 310±67 msec (mean±SD, n=15). Capacitance of the SAN cell preparations depended on the number of cell included, and ranged from 22 to 210 pF.Average single cell capacitance was calculated to be 28±4 pF. Step increase of Gc was associated with a progressive prolongation of SCL and alteration of action potential configuration.We measured the critical value of Gc which caused an index of SCL irregularity (defined by SD/mean of SCL) to be over 0.3. There was a linear relationship between the critical level of Gc and cell capacitance reflecting the number of cell included. The critical Gc level for single SAN cell with mean capacitance of 28 pF was calculated to be 0.3 nS. Parasympathetic neurotransmitter, acetylcholine (ACh) (0.05-0.2μM) reduced the value of Gc in a dose-dependent manner.The critical Gc at 0.1 μM ACh was 0.1 nS. These findings suggest that a regular pacemaking activity of a single SAN cell is easily inhibited when it is coupled directly to atrial cell. Atrial cell may act as current sink and ACh may increase the electrical load through an increase of membrane conductance.

**M-Pos336**

AN EXPERIMENTAL MODEL OF EARLY AFTER DEPOLARIZATIONS PRODUCED BY INJURY CURRENT FROM AN ISCHEMIC REGION.

((Rajiv Kumar and Ronald W. Joyner)), Department of Pediatrics, Emory University School of Medicine, Atlanta, GA, 30322

"Injury current" which flows between depolarized ischemic cells and normal myocardial cells has been proposed as a mechanism of the initiation of arrythmias. We devised a model system in which an isolated guinea pig ventricular cell is electrically coupled to a model depolarized cell to test the effects of "injury current" on the electrical properties of a normal cell with drugs which increase Ca current or decrease K current. Action potential (AP) duration was lengthened by low doses of isoproterenol (10 nM), Forskolin (1 μM), Bay K-8644 (0.5 μM) or intracellular cAMP (200 μM), but early after depolarizations (EADs) were not produced unless the cell was coupled to a depolarized cell model. Quinidine (5 μM) also prolonged the AP, but EADs were produced only after coupling to a depolarized model cell. Without these drugs, EADs were not produced in any cells with coupling to a depolarized cell model. Higher concentrations of isoproterenol produced EADs and spontaneous activity without coupling to the depolarized cell model. In such cells, coupling to a cell model with normal resting potential stopped spontaneous activity and inhibited EADs at high resistive coupling. We suggest that a localized depolarized region electrotonically produces EADs if the Ca current is increased or K current is decreased, which would occur with sympathetic innervation or quinidine, respectively, and may explain the antiarrythmic effects of β-blockers and proarrythmic effects of quinidine.

**M-Poe337**

RED BLOOD CELL FLOW THROUGH A MICROFABRICATED STRUCTURE. ((Jim Brody, Bob Austin, and Mark Bitensky)) Department of Physics, Princeton University, Princeton NJ and LANL, Los Alamos, NM.

Microlithographic techniques were used to fabricate an environment with a series of narrow channels followed by wide openings. A hydrodynamic flow carried human red blood cells through this environment, and this is recorded using bright-field video microscopy. As the cells move through the environment, they are repeatedly forced to squeese through 4 micron wide passageways, motion similar to their passage through the capillary bed. We measure the velocity of red blood cells through this environment and find a large and unexpected dispersion. We also observed cases where the rigidity of a cell increased by more than a factor of 50 over a few seconds. This rigid state is maintained for minutes, then the original rigidity returns in less than 100 milliseconds. When the red blood cell is in this rigid state, it cannot go through the 4 micron passages. If it becomes rigid inside a narrow passage, it *backs out* against the hydrodynamic flow. We will present video highlights of our findings and discuss the biological implications.

A human red blood cell flowing through a microfabricated structure.

**M-Poe338**

STRUCTURAL ANALYSIS OF DISTAL VALINE MUTANTS OF SPERM WHALE MYOGLOBIN BY X-RAY CRYSTALLOGRAPHY. ((M. L. Quillin, T. Li, J. S. Olson, and G. N. Phillips, Jr.)) Department of Biochemistry and Cell Biology, Rice University, Houston, TX 77251.

The role of the distal valine (E11 Val) in regulating ligand binding to sperm whale myoglobin has been studied extensively in recent years using the techniques of site-directed mutagenesis and laser photolysis. In an effort to understand functional differences among mutants in terms of structural perturbations, we have determined the crystal structures of several distal valine mutants at high resolution: E11 Ala, E11 Ile, E11 Leu, and E11 Phe. In myoglobins with β-branched amino acids (Val and Ile) at the E11 position, the E11 residues are oriented toward and partially obscure the iron atom, giving rise to unfavorable steric interactions with ligands. In contrast, E11 residues which are not branched at the β-carbon (Leu and Phe) point toward the back of the ligand binding pocket, reducing the volume accessible to the ligand but not directly hindering binding. These results explain the observed kinetic constants, suggesting that the E11 Ala and Ile mutations modulate the inner barrier to ligand association through steric efffects, while the E11 Leu and Phe mutations influence the outer barrier through changes in available pocket volume.

Supported by NIH GM08280 (MLQ), GN35649 (JSO), and AR40252 (GNP), the Robert A. Welch Foundation, and the W. M. Keck Center for Computational Biology.

**M-Poe339**

OPTICAL DETECTOR FOR NON-INVASIVE TISSUE SPECTROSCOPY. ((S. Fantini, M. A. Franceschini, S. Walker and E. Gratton)) Laboratory for Fluorescence Dynamics, Dept. of Physics, Univ. of Illinois at Urbana-Champaign, 1110 West Green St., Urbana, IL 61801.

The determination of the optical properties of tissues is of great importance in medicine, both for diagnostics and monitoring. Since tissues are strongly scattering media, the spectroscopic study of tissues deals with the problem of separating the effects of absorption and scattering. A simultaneous, independent measurement of the absorption coefficient ($\mu_a$) and the scattering coefficient ($\mu_s'$) of a strongly scattering media can be accomplished by frequency-domain spectroscopy. We designed a frequency-domain spectrometer that uses eight light emitting diodes (LEDs) as the light sources. Four of them emit light whose peak wavelength is 710 nm, while the others have a peak wavelength of 850 nm. They are arranged in two rows of four LEDs, one row for each wavelength, and are turned on one at a time in order to realize the multiple source-detector separation condition which provides a fast and accurate determination of $\mu_a$ and $\mu_s'$. The measured values of $\mu_a$ and $\mu_s'$ at the two wavelengths, obtained non-invasively by placing the detector on the tissue of interest, can be used to calculate the concentrations of oxy- and deoxy-hemoglobin, and hence the hemoglobin saturation and total blood volume. Preliminary *in vivo* measurements show good quantitative agreement with results obtained by invasive techniques. Supported by National Institutes of Health CA57032 and UIUC.

## SKELETAL MUSCLE E-C COUPLING

**M-Poe340**

THE EFFECT OF MAGNESIUM ON DEPOLARIZATION-INDUCED CALCIUM RELEASE IN ISOLATED SKELETAL MUSCLE TRIADS ((N.A. Rituccl and A.M. Corbett)) Department of Physiology & Biophysics, Wright State University, Dayton, OH 45435

Studies have shown that low myoplasmic $Mg^{++}$ potentiates depolarization-induced $Ca^{++}$ release in cut muscle fibers (Jacquemond and Schneider, 1992, J.Gen Physiol, 100:137) and skinned muscle fibers (Lamb and Stephenson, 1991, J. Physiol. 434:507). We examined the effect of different free $Mg^{++}$ concentrations (1 μM, 50 μM, 100 μM, 200 μM, 1.0 mM and 1.4 mM) on depolarization-induced $Ca^{++}$ release in isolated skeletal muscle triads/terminal cisternae. These vesicles were $Ca^{++}$ loaded in a solution containing 100 mM $K^+$-propionate, 36 mM imidazole, 1 mM $Na^+$-azide, 10 μM Fura, an ATP regenerating system, 2 mM $MgCl_2$, and either $Na_2ATP$ or MgATP (total of 2 mM) to yield the desired free $Mg^{++}$ concentrations (total $Cl^-$ concentration of 4 mM; total $K^+$ concentration of 100 mM). The $Ca^{++}$ loaded vesicles were diluted into release solutions which give maximal depolarization: final $[K^+]$ of 4 mM, $[Cl^-]$ of 100 mM, and varying amounts of $Mg^{++}$ to yield the desired free $Mg^{++}$ concentrations. No effect on depolarization-induced $Ca^{++}$ release was seen by increasing free $Mg^{++}$ up to 100 μM. Experiments using 200 μM free $Mg^{++}$ and above showed evidence of increased Ca-ATPase activity in the sarcoplasmic reticulum, which would antagonize our detection of $Ca^{++}$ release. In these experiments, thapsigargin was added to the release solutions to inhibit the Ca-ATPase of the vesicles. The addition of thapsigargin alone reduced our $Ca^{++}$ release 20%. $Mg^{++}$ levels of 200 μM or above in the presence of thapsigargin displayed a 75% reduction in $Ca^{++}$ release. It is not clear if high free $Mg^{++}$ directly inhibits $Ca^{++}$ release or does not allow complete inhibition of the Ca-ATPase by thapsigargin. This work supported by State of Ohio Research Challenge.

**M-Poe341**

**PARALLEL ASSAYS OF T-TUBULE DEPOLARIZATION AND INDUCED SR CALCIUM RELEASE IN TRIADS ISOLATED FROM RABBIT SKELETAL MUSCLE.** ((N. Ikemoto[1,2], and B. Antoniu[1])). 1, Boston Biomed. Res. Inst.; 2, Dept. Neurology, Harvard Med. Sch., Boston, MA.

Two types of chemical depolarization methods ($K^+ \rightarrow Cl^-$ and $K^+ \rightarrow Na^+$ replacement protocols) used to induce contraction in the skinned fiber system were employed with minor modifications for the studies of T-tubule-mediated SR $Ca^{2+}$ release in the isolated triads. Upon incubation of the triads in a priming solution with MgATP, the T-tubule moiety was polarized making the cytoplasmic side more negative, as determined by the $[^{14}C]SCN^-$ distribution method. Various degrees of ionic replacement of the polarized triads were made, and the process of T-tubule membrane depolarization was monitored with the fluorescent potential-sensitive probe WW781 in a stopped-flow fluorometric system. Depolarization-induced $Ca^{2+}$ release was monitored in the same system with fluo-3 in the presence of BAPTA-calcium buffer. It has been found that there is a close parallelism between the magnitude of T-tubule depolarization and the activation of SR $Ca^{2+}$ release (increase in both the rate and the magnitude of release). The voltage-dependence pattern of the SR $Ca^{2+}$ release kinetics derived from these studies shows a striking similarity to that of an intact fiber system. (Supported by grants from NIH and MDA).

**M-Pos342**

ISOLATION AND TISSUE DISTRIBUTION OF THREE TRIADIN ISOFORMS IN RABBIT SKELETAL MUSCLE

((*M. Peng, *R. Diebold, #H. Fan, #A. Caswell, *T. Kirley, *J. Wang and *A. Schwartz.))
*Dept. of Pharmacology & Cell Biophysics, University of Cincinnati, Cincinnati, OH 45267-0575 and #Dept. of Molecular and Cellular Pharmacology, University of Miami School of Medicine, Miami, Florida 33101*

It has been suggested that Triadin(Tr) may be an important link in skeletal muscle excitation-contraction coupling. The location and abundance of Tr in skeletal muscle sarcoplasmic reticulum membranes make it a likely candidate. An anti-Tr antibody has been shown to inhibit calcium release from SR vesicles. In the present study, three isoforms of Tr cDNA (Tr1, Tr2 and Tr3) were isolated from rabbit skeletal muscle by screening a cDNA expression library with the anti-Tr monoclonal antibody GE 4.90. The sequence of Tr1 is identical with that published by Knudson et al, 1993. Tr2 has two deletions which make the deduced protein 16 amino acids shorter than Tr1. The two deletions are located at cDNA sequence 1247-1273 (27bp) and 1754-1774 (21bp). Tr3 has one deletion located at nucleotides 1754 to 1774 (21bp). Northern blot analysis with Tr cDNA probes showed that Tr is in both skeletal muscle and heart, but not present in stomach, kidney and brain. The message size is 6.7 kb in the heart and 4.6 kb in skeletal muscle. These finding suggests that Triadin may not only perform a skeletal muscle-specific function in E-C coupling as postulated by Knudson et al, but is probably also involved in cardiac function.

**M-Pos343**

MORPHOLOGICAL CHARACTERIZATION OF A TRIAD FRACTION HIGHLY ENRICHED IN RYANODINE- AND DHP-BINDING ACTIVITY.

((D.G. Ferguson§, S.A. Lewis Carl§ and A.M. Corbett¶)) Department of Physiology and Biophysics, University of Cincinnati§, Department of Physiology and Biophysics, Wright State University¶

Heavy skeletal muscle microsomes, obtained by the rehomogenization of a 1000 x g pellet, were separated on a continuous sucrose gradient and pooled according to % sucrose (w/w). The highest PN200-100 binding was observed in pooled fractions (PF) 1-3 (>35 pmol/mg; 19-32% sucrose) while the highest ryanodine binding was observed in PF3-6 (>20 pmol/mg; 29-41% sucrose). Samples from PF1-6 were either pelleted and prepared for routine thin section electron microscopy or were etched and rotary shadowed. Thin section images indicated that PF1 was rather heterogeneous and had numerous very large vesicles, presumably of sarcolemmal origin, because some contained gap junctions. In the spaces between the larger vesicles there were pockets of smaller vesicles in which heavy SR and triads were visible. PF2 did not have any of the large vesicles but appeared to be a mix of T-tubules, heavy SR, light SR and some triads. PF 3 appeared to be highly enriched in triads. Rotary shadowing of this fraction produced images in which many of the vesicles had the characteristic domed appearance of heavy SR but feet structures often appeared to be masked by overlying T-tubules. PF4 and PF5 were enriched in triads but also appeared to contain increasing amounts of heavy SR. PF6 was enriched in heavy SR with relatively few triads. In the shadowed images, junctional feet were visible on the surface of most of the vesicles in PF6.

**M-Pos344**

PURIFICATION OF TRIADS THROUGH ALTERATIONS OF SKELETAL MUSCLE HOMOGENIZATION AND DIFFERENTIAL CENTRIFUGATION

((J.W. Kramer, N.A. Ritucci, and A.M. Corbett)) Department of Physiology & Biophysics, Wright State University, Dayton, OH 45435

The homogenate from fast twitch skeletal muscle was spun at 1,000 x $g_{av}$, the supernatant decanted and the pellet rehomogenized in Sucrose EDTA. The rehomogenized pellet was spun at 1,000 x $g_{av}$ and the supernatant retained. Supernatant A (1st homogenization) and Supernatant B (2nd homogenization) were spun at 12,000 x $g_{av}$, to obtain heavy microsomes. Pellet B contained a greater percentage of total binding sites (45% DHP and 39% Ryanodine) with approximately one half the total protein compared to pellet A. Pellet B heavy microsomes were separated on a continuous sucrose gradient, fractionated, pooled according to % sucrose, and assayed as follows. PF 1 and 2 (19-28% sucrose) contain high PN200-110 (40 pmol/mg avg), Adenylate Cyclase (70 pmol/mg/min avg), Ouabain (16 pmol/mg avg.), and Ouabain sensitive Na/K ATPase (16 $\mu$mol/h•mg) activities, but lower Ryanodine activity (15 pmol/mg avg.), characteristic of free T-tubules and Sarcolemma. PF 3 (29-32% sucrose) contained high PN200-110 (48.3 pmol/mg), Ryanodine (48.6 pmol/mg), Ouabain (15.6 pmol/mg), Adenylate Cyclase (33.5 pmol/mg/min), and Ouabain sensitive Na/K ATPase (6 $\mu$mol/h•mg) activities, characteristic of enriched Triadic Vesicles. PF 4 and 5 (33-36% sucrose) contained lower PN200-110 (19.5 pmol/mg avg.), Ryanodine (30.5 pmol/mg avg.), Ouabain (6.8 pmol/mg), Adenylate Cyclase (22.5 pmol/mg/min), and Ouabain sensitive Na/K ATPase (3 $\mu$mol/h•mg) activities, characteristic of less enriched Triadic Vesicles. PF 6 (37-41% sucrose) contained only high Ryanodine activity (22 pmol/mg), characteristic of isolated Terminal Cisternae. These triads had 5-10 times more PN200-110 and Ryanodine activity than our previous preps. Supported by State of Ohio Research Challenge.

**M-Pos345**

EFFECTS OF INTRACELLULAR CALCIUM ON CHARGE MOVEMENT IN FROG SKELETAL MUSCLE.

((K. Polakova and J.A. Heiny)) Department of Physiology & Biophysics, University of Cincinnati College of Medicine, Cincinnati, OH 45267-0576.

We studied the effects of intracellular Ca on charge movement measured in cut frog muscle fibers voltage-clamped with a vaseline gap method. The fibers were perfused extracellularly with 80 $TEA_2SO_4$, 5 MOPS, 1 $CaSO_4$, 0.5 $MgSO_4$, $10^{-6}$ g/ml TTX (pH 7, 10 C). The intracellular solution contained 70 CsGlutamate, 10 MOPS, 5 creatine phosphate, 5 ATP, 6.4 $MgSO_4$, and 10-20 EGTA or BAPTA; $CaSO_4$ was added to buffer resting intracellular Ca to the desired level. At resting $pCa \leq 9$, fibers perfused with BAPTA had significantly less $Q_{max}$ than fibers buffered with EGTA to the same $pCa_i$. Raising $pCa_i$ to a physiological range of 6.5-7 reduced these differences, suggesting that the effect of BAPTA on $Q_{max}$ is related to its Ca buffering action. Starting from $pCa_i$ levels in the physiological range, $Q_{max}$ can be increased further by repetitive depolarizations when EGTA, but not BAPTA is used. Because of its faster ON rates, BAPTA is expected to be a more effective buffer than EGTA for released Ca ions at distances close to the release sites. These results suggest that there is a Ca binding site in the triadic space which can modulate the amount of charge available to move. The postulated site is partially bound at rest and can become further saturated upon depolarization when triadic Ca rises. (Supported by NIH and AHA)

**M-Pos346**

THE SLOW CALCIUM CURRENT IS RELATED WITH THE $Q_\gamma$ CHARGE IN TWITCH SKELETAL MUSCLE FIBERS OF THE FROG.

((F. Francini, C. Bencini and A. Centonze)) Dpt. di Scienze Fisiologiche, Università di Firenze, 50134 Firenze, Italy.

In previous works it has been shown that only a small fraction of the dihydropyridine (DHP) receptors in skeletal muscle conducts $Ca^{2+}$ during a depolarization. Most of the intramembrane charge movement (ICM) measurable above -50 mV has been correlated with the hump ($Q_\gamma$), the fraction of ICM sensitive to DHPs, while $Ca^{2+}$ current appeared only at potentials positive to -40 mV. In this work the kinetics of the slow $Ca^{2+}$ current ($I_{Ca}$) were reinvestigated by tail currents analysis, and the voltage threshold and the time onset of both $Q_\gamma$ and $I_{Ca}$ were evaluated. Single cut twitch muscle fibers of *Rana esculenta* were voltage clamped in a double Vaseline-gap chamber. All ionic currents except for $I_{Ca}$ were minimized. Voltage test and control pulses were applied from a holding potential of -100 mV and 0 mV, respectively. The curve of total time integral of tail currents vs. voltage showed various humps, while $Cd^{2+}$ (2 mM) added to the external solution suppressed two humps elicited at voltages positive to -40 mV. The fit with two Boltzmann functions on the difference between these two plots, gave half-maximal potential near -30 and 20 mV, respectively. The voltage threshold for both $Q_\gamma$ and $I_{Ca}$, evaluated either with long (3-5 s) depolarizing pulses or with the running time integral of the currents during each pulse, was similar (-57 ± 2 and -56.5 ± 2 mV, respectively). To determine the time onset of $I_{Ca}$ we used voltage pulses with different duration to test for the beginning of the ON and OFF disequality. This appears ($Q_{OFF} > Q_{ON}$) for pulse duration of about 2 ms, a time comparable with $Q_\gamma$ onset. The present results agree with the hypothesis that in skeletal muscle the DHP receptor has a dual function as a voltage-sensing device for the voltage-dependent $Ca^{2+}$ channel, and as a voltage-sensor for ryanodine receptor. Supported by grant n° 239 from Telethon-Italy.

**M-Pos347**

BLOCKADE OF CHARGE MOVEMENT REPRIMING BY RYANODINE

((Adom González and Carlo Caputo)). Centro de Biofísica y Bioquímica. IVIC. Caracas. Venezuela.

We have studied the effect of Ryanodine, at high concentrations, on intramembrane charge movement, Q, in the frog cut fiber preparation using the triple vaseline gap voltage clamp technique. The solutions were (mM), Internal: Cs-Aspartate, 110; EGTA, 15; ATP-Mg, 5; Phosphocreatine, 5; Hepes, 5; Ca, 0.79 and Glucose, 5; External: TEA-Methanesulphonate, 110; Mg, 10; Hepes, 10; 3-4 DAP, 1; TTX, 0.001. Ryanodine at [100 µM] had not effect on the Qmax, nor on the voltage distribution of Charge 1 and Charge 2. This result suggests that Ryanodine has not direct effect on the voltage sensors for excitation-contraction coupling. Repriming of Charge 1 was measured using a pulse protocol ( A. Gonzalez and Caputo, C. Biophys. J. 64: a36,1993 ) designed to avoid contamination from Charge 2. In the presence of Ryanodine at [100 µM], repriming was diminished by about 65%. This fact suggests a retrograde interaction between the Ryanodine receptors and the voltage sensors. Even at higher concentrations of Ryanodine, up to 300 µM, repriming was not completely abolished, indicating the presence of a Ryanodine insentive component in the reprimed charge. Supported by Conicit S1-1248 and CEE CI1-CT92-0020.

**M-Pos348**

**MEMBRANE REPOLARIZATION STOPS CAFFEINE-INDUCED $Ca^{2+}$ RELEASE IN SKELETAL MUSCLE CELLS** ((N. Suda, C. Heinemann and R. Penner)) Max-Planck-Institut für biophysikalische Chemie. Am Fassberg, D-37077 Göttingen, Germany

There is no strict evidence that the calcium-induced calcium release (CICR) channel functions as the physiological depolarization-induced $Ca^{2+}$ release (DICR) channel. We have combined the patch-clamp technique with fura-2 measurements in order to investigate this in rat myoballs. Here, we report that CICR induced by 10 mM caffeine is turned off by membrane repolarization, a novel phenomenon, that we term RISC (repolarization-induced stop of $Ca^{2+}$ release) (B). The RISC is observed in the absence of external $Ca^{2+}$ or in the presence of 0.5 mM $La^{3+}$. The RISC is voltage and time dependent and is abolished in the presence of 0.5-1 uM nifedipine or PN 200-110. The results suggest that there exists direct coupling between the DHP receptor and the release channel and that the CICR channel is indeed the DICR channel.

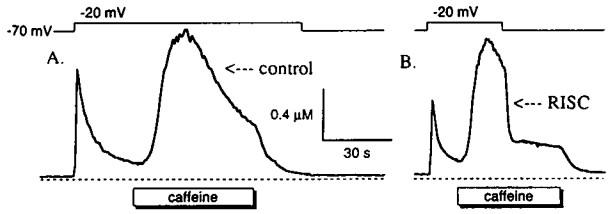


**M-Pos349**

**Ca TRANSFER FROM t WALL TO MYOPLASM DURING CONTRACTURE.** ((B.A. Curtis)), University of Illinois College of Medicine at Peoria, Peoria, IL 61656

The luminal surface of the transverse tubular system binds 12 pmol Ca/fiber, $Ca_{fast}$, which is released in proportion to activation and refills in proportion to repriming. 0.5 pmol Ca from this Ca store, $Ca_{transfer}$, enters the fiber coincident with activation-contraction. Drugs were applied for 3 min immediately after $Ca_{fast}$ was loaded with $^{45}Ca$. Depolarization after 0.25 mM ("low" dose) tetracaine reduced contractures to 12.5% of control, released $Ca_{fast}$, and $Ca_{transfer}$ was 0.58±.2 pmol(9). 5mM BDM reduced tension to 23%, and $Ca_{transfer}$ was 0.47±.17 (4). Both block only the SR Ca release channel: release of $Ca_{fast}$ and $Ca_{transfer}$ appear related to depolarization-activation of DHPR. 2.5 mM ("high" dose) tetracaine blocked the second contracture, $Ca_{fast}$ did not turnover, and $Ca_{transfer}$ was -0.03±.10 pmol (9). 5-10 mM diltiazem likewise blocked the contracture, release of $Ca_{fast}$, and $Ca_{transfer}$ was 0.05±.16 pmol Ca (6). The latter block charge movement and hence DHPR activation. 0 Ca (4-80 mM EGTA) in the external solution before and during depolarization resulted in a 25% t-T contracture, no turnover of $Ca_{fast}$ and a $Ca_{transfer}$ of 0.34±.13 pmol Ca (5).

Supported by The Illinois Affiliate, American Heart Association.

**M-Pos350**

**RESTING MYOPLASMIC FREE $[Mg^{2+}]$ ($[Mg^{2+}]_r$) MEASURED WITH MAG-FURA RED IN INTACT TWITCH FIBERS FROM FROG SKELETAL MUSCLE.** ((Mingdi Zhao, S. Hollingworth and S. M. Baylor)) Department of Physiology, University of Pennsylvania, Philadelphia, PA 19104.

$K_3$Mag-fura Red (Molecular Probes, Inc.) was pressure-injected into the myoplasm of single fibers. Although this indicator was difficult to inject, myoplasmic concentrations ≥ 0.3 mM were attained in 3 experiments (sarcomere length, 3.8-4.0 μm; normal Ringer's solution; 16°C). The o's in Fig. 1 show the absorbance spectrum, A(λ), of 0.8 mM Mag-fura Red in a resting fiber. The dashed curve shows that A(λ) was well-fitted by a linear combination of zero and saturating $Mg^{2+}$ calibration spectra determined in salt solutions (solid curves: pH 7.0, ionic strength=0.15 M). The fraction of the indicator in the $Mg^{2+}$-bound form estimated from the fit was 0.30. If the value of the indicator's dissociation constant for $Mg^{2+}$ is the same in the myoplasm as measured in the calibration solutions (9.3 mM), $[Mg^{2+}]_r$ is estimated to be 4.0 mM. The average value of $[Mg^{2+}]_r$ from the 3 fibers, 4.0 ± 0.1 mM, is substantially higher than the ca. 1 mM value often reported or assumed for frog fibers. *Supported by NIH NS-17620.*

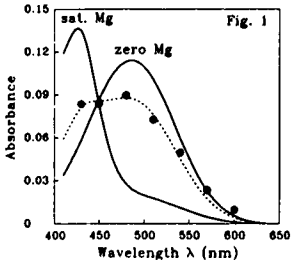


**M-Pos351**

**MEASUREMENT OF THE RAPIDLY AVAILABLE PROTON BUFFERING POWER IN FROG CUT MUSCLE FIBERS** ((W. K. Chandler, D.-S. Jong, and P.C. Pape)) Department of Cellular and Molecular Physiology, Yale University School of Medicine, New Haven, CT 06510.

Fibers (sarcomere length, 3.4-3.8 μm) were mounted in a double Vaseline-gap chamber and exposed to an internal solution that contained 20 mM EGTA, 0.63 mM phenol red, and 2 mM fura-2. The external solution was Ringers, 14-15°C. After an action potential, most of the Ca that is released from the sarcoplasmic reticulum into the myoplasm is expected to be complexed by either EGTA or fura-2. Because fura-2 binds and releases Ca much more rapidly than EGTA, some of the Ca that is initially bound by fura-2 dissociates during the next 200-300 ms and becomes bound by EGTA. EGTA releases two protons for each Ca that is bound, which leads to a change in internal pH given by $\Delta pH = -(2/\beta)\Delta[CaEGTA]$; β represents the proton buffering power of myoplasm. Δ[Cafura-2] and ΔpH are detected optically and the value of β is estimated from the relative magnitudes of the Δ[Cafura-2] and ΔpH signals on the assumption that Δ[CaEGTA] = -Δ[Cafura-2]. The value of β showed no significant dependence on internal pH between 6.7 and 7.0. Its mean value was 22 mM/pH unit (SEM, 1 mM/pH unit; n = 7), of which 4-5 mM/pH unit was estimated to be due to the internal solution and 17-18 mM/pH unit, to the immobile buffers inside the fibers. The latter value agrees with that estimated in intact fibers, 21 mM/pH unit (Irving et al., 1990, *Biophysical Journal*, **57**, 717), based on values of β obtained by others from measurements that required several minutes to complete. *Supported by NIH grant AR-37643.*

**M-Pos352**

**CALCIUM GREEN-2: THE PERFECT FLUORESCENCE $Ca^{2+}$ INDICATOR FOR STUDYING THE RELATIONSHIP BETWEEN $Ca^{2+}$ CONCENTRATION, FORCE AND ATPase ACTIVITY IN SKINNED FIBERS** ((W. Glenn L. Kerrick)) Department of Physiology and Biophysics, Univ. Miami Sch. of Med., Miami, FL 33101

A comparison of the various fluorescence $Ca^{2+}$-indicators was done in order to determine which indicators are the most useful for studying the activation of force and ATPase activity in skinned skeletal and cardiac muscle fibers. It was found that most of the indicators (Indo-1, Fura-2, Fluo-3, Calcium Orange, Calcium Crimson, Fura Red, Mag-fura-2, Mag-indo-1, and Calcium Green 5N) bound $Ca^{2+}$ over a concentration range of $Ca^{2+}$ which does not coincide well with the $Ca^{2+}$ concentration necessary for activation of force and ATPase activity. In contrast, Calcium Green-2 was found to have an affinity for $Ca^{2+}$ which is perfect for measuring the $Ca^{2+}$ concentration over the range which is required for the activation of force and ATPase activity. Calcium Green-2 fluorescence was used to monitor the $Ca^{2+}$ concentration surrounding skinned fibers in the Guth Muscle Research System while running a gradient of $Ca^{2+}$ through the 1 $mm^2$ cuvette containing the skinned fiber. The ability to continuously monitor $Ca^{2+}$ over the whole range required for activation of force and ATPase activity revealed striking differences between fiber types and 2 to 3 phases of $Ca^{2+}$-activation which cannot be fit to a simple Hill equation. It was possible to simultaneously measure the ATPase activity, $Ca^{2+}$ concentration, and force because the emission spectra of Calcium Green-2 and NADH (used to measure ATPase activity) overlap and the excitation spectra do not overlap. (Supported by grants from the American Heart and Muscular Dystrophy Associations)

**M-Pos353**

**VOLTAGE DEPENDENCE OF SARCOPLASMIC RETICULUM (SR) CALCIUM RELEASE IN FROG CUT MUSCLE FIBERS EQUILIBRATED WITH 20 mM EGTA.** ((P.C. Pape, D.-S. Jong, & W.K. Chandler)) Department of Cellular and Molecular Physiology, Yale University School of Medicine, New Haven, CT 06510.

SR Ca release was measured with the EGTA-phenol red method in voltage-clamped fibers mounted in a double Vaseline-gap chamber with a Ca-free external solution (Chandler et al., 1992, *Biophysical Journal*, **61**, A130; sarcomere length, 3.4-3.8 μm; temperature, 14-16°C). From -75 to -55 mV, the rate of release increased *e*-fold every 3.5 mV (SEM, 0.2 mV; n = 4). With a depolarization to -75 mV, the rate of release was 0.010 μM/ms (SEM, 0.003 μM/ms; n = 4) and the increment in free [Ca] above the resting level was 0.21 nM (SEM, 0.07 nM; n = 4). With a depolarization to 60 mV, the rate of release was 69.5 μM/ms (SEM, 1.5 μM/ms; n = 2). Thus, the rate of SR Ca release is steeply voltage dependent when only one Ca channel in $10^4$ is open and the value of myoplasmic bulk free [Ca] is increased <1 nM above the resting level. If the open channels are distributed randomly, this open probability implies that 97% of them are located ≥0.6 μm from any other open channel. Ca flux through a channel is expected to produce a local increment in [Ca]. A theoretical analysis shows that 20 mM EGTA is expected to reduce this increment to ≤1 nM at distances ≥0.6 μm. Thus, an open channel is expected to be isolated from the effects of Ca from another open channel if it is ≥0.6 μm away. Consequently, the steep voltage dependence of Ca release is likely due to the T-tubule voltage sensor rather than to a Ca feedback mechanism associated with SR Ca release. *Supported by NIH AR-37643.*

**M-Pos354**

**EFFECTS OF PRALIDOXIME AND BUTANEMONOXIME ON Ca RELEASE IN FROG SKELETAL MUSCLE FIBERS.** (( R. De Armas, S. Gonzalez, G. Pizarro and G. Brum)) Depto. de Biofisica, Fac. de Medicina, U. de la Republica, Montevideo, Uruguay.

We have previously reported that Butanedionemonoxime (BDM) inhibits Ca release in single skeletal muscle fibers (Biophys. J., 64, 1993). If this inhibition is due to the phosphatse activity of BDM other oximes should have similar effects. To test this hypothesis we studied the effect of 2-pyridine aldoxime (PAM) and butanemonoxime (BM) on myoplasmic Ca transients measured with APIII in single cut skeletal muscle fibers of the frog voltage clamped in a double vaseline gap. Both compounds were extracellularly applied at a concentration of 10 mM. The effect of these two oximes dramatically depended on the free $[Ca^{2+}]$ of the intracellular solution. At nominally 0 Ca ( 5 mM EGTA) both compounds supressed Ca release, evaluated by their effect on $dCa/dt_{max}$ : PAM reduced it by 90 % (sem=3%,n=4) and BM by 60 % (sem=20 %, n=5). With internal solutions containing 50 nM free $Ca^{2+}$ both compounds potentiated release at two different [EGTA] ( 0.1 and 5 mM). With 0.1 mM EGTA and 50 nM Ca PAM increased $dCa/dt_{max}$ by 350 % (sem= 68 %, n=4) and BM by 474 % (sem=265%, n=3). This in sharp contrast with the effect of BDM which was inhibitory independently of the intracellular $[Ca^{2+}]$. The fact that these two oximes have these complex effects suggest that phosphatase action is not the mechanism of BDM inhibition of Ca release.

Supported by a grant from CSIC.

**M-Pos355**

RELEASED CALCIUM AND SR CALCIUM CONTENT IN FROG CUT SKELETAL MUSCLE FIBERS CONTAINING BUFFERING CONCENTRATIONS OF QUIN-2. ((S.K. Dey, M.G. Klein, M.F. Schneider)) Dept. Biochem., UMAB, Baltimore, MD 21201

Quin-2 (2 - 5 mM; 30-60% Ca-complexed) was applied to the saponin permeabilized ends of fiber segments stretched to 3.1 - 4.0 μm/sarc in a double vaseline gap and voltage clamped at -90 mV. Fiber fluorescence for 380 and 358 nm excitation was used to calculate [Ca-quin-2] and [quin-2]. Transmitted light movement signals were eliminated as quin-2 entered the fiber. In some fibers AP III $[Ca^{2+}]$ signals were recorded and were greatly suppressed by quin-2. These results indicate effective buffering of myoplasmic $[Ca^{2+}]$ by quin-2 but movement or AP III $[Ca^{2+}]$ signals were sometimes observed during longer or larger pulses if quin-2 approached saturation. For a 50 ms pulse to 0 mV, Δ[Ca-quin-2] was 1.08 ± 0.26 mM (± sem; n=4; *R. temporaria*) and 1.05 ± 0.31 mM (n=4; *R. pipiens*). These values give the amount of $Ca^{2+}$ released from the SR during the pulse if quin-2 achieved full $Ca^{2+}$ buffering. Δ[Ca-quin-2] declined slowly after the pulse. Using two identical pulses separated by 1 - 2 s and assuming that the fractional suppression of Δ[Ca-quin-2] in the second pulse was only due to SR calcium depletion, the SR calcium content was calculated to be 3.42 ± 0.72 mmole/l fiber water (n=6; *R. temporaria*) and 2.43 (n=1; *R. pipiens*). Millimolar concentrations of quin-2 thus provide a means of buffering myoplasmic $[Ca^{2+}]$ and of directly monitoring SR calcium release during fiber depolarization. Supp. by NIH and MDA.

**M-Pos356**

THE RATE OF SR CALCIUM RELEASE IN QUIN-2-BUFFERED FROG CUT SKELETAL MUSCLE FIBERS. ((S.K. Dey, M.G. Klein, M.F. Schneider)) Dept. Biochem., UMAB, Baltimore, MD 21201

Fibers containing mM concentrations of quin-2 were voltage-clamped at -90 mV and quin-2 fluorescence signals were recorded (Dey et al, these abstracts). Assuming negligible $Ca^{2+}$ binding to other sites, the rate of calcium release ($R_{rel}$) from the SR is d[Ca-quin-2]/dt (=dCa-q/dt). For pulses to beyond about -40 mV, dCa-q/dt exhibited an early rise to a peak followed by first a fast and then a slower phase of decay, as calculated previously for $R_{rel}$ in unbuffered fibers. The peak value of dCa-q/dt for pulses to 0 mV was 26.5 ± 1.7 μM/ms (± sem; n=4; *R. temporaria*) and 41.8 ± 12.0 μM/ms (n=4; *R. pipiens*). Δ$[Ca^{2+}]$ at the time of peak dCa-q/dt was 168 ± 19 nM (n=8, all of above; calculated using rate constants for the Ca:quin-2 reaction from simultaneous quin-2 and AP III signals in other fibers with lower [quin-2]). For pulses to a given voltage, both the steady release permeability late in the pulse (= rate constant for the slow phase of decay of dCa-q/dt) and the peak dCa-q/dt remained constant or decreased as increasing quin-2 entered the fiber, providing no indication of removal of possible calcium-dependent inactivation of release with increased $Ca^{2+}$ buffering. The normal release wave form observed here when quin-2 buffered the myoplasmic $[Ca^{2+}]$ indicates either that $Ca^{2+}$ feedback was not essential for the normal release wave form or that [quin-2] as used here did not achieve local $[Ca^{2+}]$ buffering at the $Ca^{2+}$ regulatory sites for SR calcium release. Supp. by NIH and MDA.

**M-Pos357**

CALCIUM TRANSIENTS IN ENZYMATICALLY DISSOCIATED RAT SKELETAL MUSCLE FIBERS. ((S.L. Carroll, M.G. Klein, M.F. Schneider)) Dept. Biochem., UMAB, Baltimore, MD 21201

Intact fibers were dissociated from flexor digitorum brevis muscles by collagenase treatment, immobilized on polylysine coated cover slips, embeded in agarose Ringer and loaded with either fura-2 or mag-fura-2 using the acetoxymethyl esters. Fibers had sarcomere lengths of 1.94 ± 0.03 μm (± sem; n=15) and were studied at room temperature. Fiber fluorescence for 380 and either 358 or 350 nm excitation was used to calculate $[Ca^{2+}]$. Resting $[Ca^{2+}]$ determined by fura-2 ($K_D$ =70 nM in rat muscle) was 9.2 ± 3.8 nM in 30 fibers in 1 mM $Ca^{2+}$ Ringer and 100.4 ± 26.7 nM in 13 fibers in 2.5 mM $Ca^{2+}$. $[Ca^{2+}]$ transients (Δ$[Ca^{2+}]$) were recorded from individual fibers for single action potentials and for 10-200 ms trains of action potentials (100 Hz) evoked by external stimulation. When movement artifacts were present repeated applications of the same stimulation but alternating between 380 and 358 or 350 nm excitation were used to give fluorescence ratios for calculating Δ$[Ca^{2+}]$. Δ$[Ca^{2+}]$ was elevated during the train and decayed rapidly after the train. Fura-2 records indicated that Δ$[Ca^{2+}]$ then remained slightly elevated for 10's of s after the rapid decay and that the amplitude of this slowly decaying Δ$[Ca^{2+}]$ increased with the duration of the preceding train. Since fura-2 approached saturation during the trains Δ$[Ca^{2+}]$ was monitored in other fibers using mag-fura-2. This preparation is convenient for monitoring $[Ca^{2+}]$ in mammalian intact skeletal fibers. Supported by NIH and MDA.

**M-Pos358**

MYOPLASMIC CALCIUM CONCENTRATION IN PATIENTS WITH RHABDOMYOLISIS INDUCED BY EXERCISE. ((1B. Rojas, 2V. Parthe, 2J.R. Lopez)) 1Departamento de Medicina Interna, Hospital Militar Carlos Arvelo, Caracas, Venezuela. 2Centro de Biofisica, IVIC, Caracas, Venezuela.

We measured $[Ca^{2+}]_i$ with $Ca^{2+}$ selective microelectrodes in muscle fibers isolated from intercostal muscles of 6 patients during acute episodes of rhabdomyolisis and 4 patients 1 year after the acute episode. In all cases the episode of rhabdomyolisis was induced by exercise. Control values were obtained from subjects (n=8) without evidence of neurological diseases undergoing surgery. The $[Ca^{2+}]_i$ in the control subjects was 0.12±0.02μM (mean±SEM, n=25), while it was 1,345±128μM (n=24) in muscle fibers isolated from the rhabdomyolisis patients during the acute episode. Histologic studies showed muscle focal necrosis, edema and fatty infiltration. The $[Ca^{2+}]_i$ measured from those patients 1 year after the acute episode revealed a majority of muscle fibers with normal values (0.114±0.03μM, n=65) but some fibers had an elevated resting a $Ca^{2+}$ concentration (0.896±0.278μM), n=18). Histological studies from those biopsies revealed muscle fibers with fibrosis, edema, and focal evidence of necrosis. Dantrolene (50μM) produced a significant reduction in $[Ca^{2+}]_i$ regardless of the source of the muscle biopsy. The $[Ca^{2+}]_i$ after dantrolene was 0.062±0.01μM (n=12) in control muscle, 0.437±0.08μM (n=23) in muscle from acute episode, and 0.134±0.02μM (n=13) in muscle with a high resting $Ca^{2+}$ obtained a year after the acute episode. These results suggest that the underlying defects of rhabdomyolisis induced by exercise is related to a malfunction of calcium homeostasis. (Partially supported by Procter and Gamble.)

**M-Pos359**

SKELETAL MUSCLE CALCIUM CHANNEL DOMAIN I SLOWS DOWN $\alpha_1$ CARDIAC CHANNEL OPENING WITHOUT CHANGES IN THE VOLTAGE SENSOR. ((O. Delbono, M. Gopalakrishnan, A. Neely, R. Olcese, L. Bimbaumer & E. Stefani)) Dept. of Molec. Physiol. & Biophys., Baylor College of Med. Houston, Texas 77030.

An $\alpha_1$-subunit chimaera constructed with domain I plus amino terminal end from skeletal muscle $Ca^{2+}$ channel (Sk1-C3), and domains II-IV from cardiac $Ca^{2+}$ channel, was co-expressed with $\beta_2$-subunit in *Xenopus* oocytes. $Ba^{2+}$ current (in 10 mM $Ba(MeSO_3)_2$) and single channels activity (pipette: 79 mM $Ba(MeSO_3)_2$, 25 $BaCl_2$ and 5 μM BayK 8644, bath: $K(MeSO_3)_2$) were recorded using the cut-open oocyte voltage-clamp and the cell-attached configuration of patch-clamp techniques. Full length cardiac $\alpha_1$-subunit plus $\beta_2$ were used as control. Sk1-H3 had five times larger $Ba^{2+}$ current (1416±33 nA) than cardiac. Currents from chimaera activated following a single exponential function (25 ms) while cardiac presented a dual activation (4 and 43 ms). Ensemble averages of single channel traces reproduced the single and dual activation of Sk1-C3 (20 ms) and cardiac (0.7 and 12.7 ms), respectively. Mean open time histograms show one time constant for Sk1-H3 and two for cardiac. G-V relationship was shifted in cardiac to more negative potentials compared to the chimaera in about 9 mV, while Q-V relationships were almost superimposed.

**M-Pos360**

SLOW CALCIUM CURRENT ($I_{Ca}$) IS NOT REDUCED IN MALIGNANT HYPERTHERMIC (MH) PORCINE MYOTUBES. ((E.M. Gallant and K.G. Beam)) U. of Minnesota, St.Paul, MN 55108 and Colorado State U., Fort Collins, CO 80523.

Both MH adult muscles and MH myotubes have a lower than normal mechanical threshold (Biophys. J. 64:A37, 1993), and $I_{Ca}$ is reduced in muscles of adult MH pigs (Lamb et al., Muscle Nerve 12:135, 1989). We tested the hypothesis that there is a relationship between $I_{Ca}$ and mechanical activation by recording $I_{Ca}$ from MH and normal (N) myotubes using the whole cell patch-clamp technique. Extracellular solution contained (in mM): 145 TEA Cl, 10 $CaCl_2$, 10 HEPES, 3 $\mu$M TTX, pH 7.4, 24 ± 1°C. Pipettes (1.5-2.0 Mohms) were filled with (in mM): 140 Cs aspartate, 5 Mg aspartate, 10 $Cs_2$EGTA, 10 HEPES, pH 7.4. Recordings were from compact myotubes in 4-9 day cultures (21 N and 30 MH). Currents were recorded in response to 300 msec depolarizing pulses to potentials of -40 to +50 mV in 10 mV increments. Holding potential was at -80 mV. We found that current voltage relationships were similar with thresholds for $I_{Ca}$ at approximately 0 mV, and peak $I_{Ca}$ between +20 to +30 mV for both MH and N myotubes. Maximum $I_{Ca}$ amplitudes were not different (N: 4,990 ± 543 pA; MH: 6,102 ± 1,119 pA) nor were normalized $I_{Ca}$ (N: 8.9 ± 0.7; MH: 8.6 ± 1.0 pA/pF). Our findings in myotubes are consistent with the genetic defect underlying MH residing in the sarcoplasmic reticulum (SR) Ca-release channel (Fujii et al., Science 253:448, 1991) and with any changes in adult fiber $I_{Ca}$ being secondary to the SR defect. (Supported by NIH grant AR-41270.)

**M-Pos361**

THE ROLE OF NA/CA EXCHANGE ON TENSION DEVELOPMENT IN FROG PHASIC SKELETAL MUSCLE.((M. Rozyzcka, H. Gonzalez-Serratos, *H. Rasgado-Flores, and E. Castillo)). Dept of Biophysics, School of Medicine, Univ. of Maryland, Baltimore MD 21201 and *Dept of Physiol., UHS/The Chicago Medical School, North Chicago, IL 60064.

A net $Ca^{2+}$ influx exists in skeletal muscle at rest and during activation (J.Gen.Physiol.92:803, 1959), but since the SR has a limited capacity to store $Ca^{2+}$, a homeostatic mechanism must exist to regulate intracellular $Ca^{2+}$, otherwise contractures may occur. We have attributed this mechanism to the Na/Ca exchanger. The present experiments were undertaken to characterize the functional role of this mechanism. The experiments were done in isolated single muscle fibers of the frog Rana Pipiens. The Na/Ca exchanger was manipulated by altering $[Na^+]$ gradients across the sarcolemma. A decrease in $[Na^+]_o$ induced twitch potentiation which was proportional to the $[Na^+]_o$ reduction until action potential failed at 55 mM $[Na^+]_o$. Cross section images of $Ca^{2+}$ release showed that low $[Na^+]_o$ resulted in an increase of SR $Ca^{2+}$ release during the twitch activation. To assess the effect of $[Na^+] < 55$ mM, we studied K-contractures. Contractures in 10 mM $[Na^+]_o$ were up to three times (30 mM K) larger than in 100mM $[Na^+]_o$ with no change in mechanical threshold. Dichlorobenzamil amiloride (a Na/Ca exchanger inhibitor, Biochem. 70:1285, 1980) increased twitch tension by up to 67%. Low $[Na^+]_o$ potentiation could be increased with cyclopiazonic acid (CPA), a SR $Ca^{2+}$ ATPase inhibitor (Biochem. Pharmacol. 37:978, 1988). Twitch potentiation induced with CPA could be stopped with zero $[Ca^+]_o$. We propose that the Na/Ca exchanger contributes to maintain intracellular $[Ca^{2+}]$ in a steady-state.

**M-Pos362**

CONFORMATIONAL AND DYNAMIC CHANGES IN TROPONIN C ON METAL ION AND PEPTIDE BINDING. ((Martin Moncrieffe, Franklyn Prendergast and James Potter*)) Dept. of Biochem. and Mol. Biol., Mayo Foundation, Rochester, MN,55905; *Dept. of Mol. & Cell. Pharm., Univ. of Miami Sch. of Med., Miami, FL. 33136. (Sponsored by Franklyn Prendergast)

Troponin C (TnC) , a 18kDa protein has four calcium binding sites, two of which (sites III and IV) are thought to play a structural role while the other two (sites I and II) serve as regulators of calcium induced muscle contraction. In an attempt to determine the molecular basis for ligand induced changes in TnC conformation and dynamics, two mutants of chicken TnC (F154W and F78W) were constructed. The spectral results for F154W were similar to those reported by Smillie *et al* (Biophys. J. vol 61 #2 A157,1992). Correlation times extracted from the time resolved anisotropy decays of Trp fluorescence in both mutants reveal a progression towards a more spherical shape on binding $Ca^{2+}$. These results also suggest that there is considerable mobility of each domain about the central helix of the molecule. Molecular graphics and molecular dynamics simulations were used to predict the environment of the Trp residue in these mutants and an attempt is made to correlate the fluorescence lifetimes with the predicted environment of the Trp residue. Supported by GM 3487 (FGP) and AR 42727 (JDP)

**M-Pos363**

THE FLUORESCENT DYE bANS STIMULATES ATPase ACTIVITY OF NATIVE AND TnC-EXTRACTED SKELETAL MUSCLE MYOFIBRILS. ((John A. Putkey and Wen Liu)) Department of Biochemistry and Molecular Biology, University of Texas Medical School, Houston TX 77030.

Soluble fluorescent dyes and a variety of calmodulin (CaM) antagonists will bind to $Ca^{2+}$-dependent hydrophobic surfaces on CaM and both cardiac (cTnC) and skeletal (sTnC) troponin C. Several of these compounds have differential effects on the functional activities of CaM and TnC in that they inhibit CaM but sensitize TnC. We have used the compound 1,1'-bi(4-anilino)naphthalene-5,5'-disulfonic acid (bis-ANS or bANS) as a marker to monitor $Ca^{2+}$ binding to cTnC. To determine the functional consequences of bANS on the muscle activity we performed skeletal muscle myofibril assays under the following conditions: 1) unextracted myofibrils with bANS; 2) TnC-extracted myofibrils with bANS; and 3) TnC-extracted myofibrils reconstituted with either cTnC or sTnC that had be incubated with bANS. In the presence of $Ca^{2+}$, increasing concentrations of bANS induced a gradual decrease in the ATPase activity of both native and reconstituted myofibrils. At a concentration of 80 µM the ATPase activity was 90% inhibited. In the absence of $Ca^{2+}$, bANS induced an increase in ATPase activity of both native and reconstituted myofibrils that was maximal at about 20 µM and was about 50% of the maximal $Ca^{2+}$-dependent activity. At higher concentrations of bANS the ATPase activity was inhibited. This $Ca^{2+}$-independent ATPase activity was not due to an effect of bANS on TnC since extracted fibers alone showed a similar response in the presence and absence of $Ca^{2+}$. The ability of bANS to stimulate ATPase activity in these myofibrils appears to be an effect of binding to thick filament proteins or thin filament proteins other than TnC.

**M-Pos364**

EFFECTS OF GENETICALLY ENGINEERED TnC ON FORCE PRODUCTION IN SKINNED MYOFIBRILLAR BUNDLES FROM THE BARNACLE BALANUS NUBILUS. ((+C.C. Ashley, #T. Miller, +S. Lipscombe, #J.D. Potter)) +Univ. Lab. of Physiology, Oxford OX1 3PT, England/Friday Harbor Labs., Seattle, WA 98250, #Department of Molecular & Cellular Pharmacology, Univ. of Miami School of Med., Miami, FL 33101.

Recombinant $BTnC_2$ ($rBTnC_2$), containing small differences (M2V, L77I, D81G) in amino acid sequence (Collins et al., Biochem. 30, 1991) and a deletion mutant (TRUNC) of this which disrupted $Ca^{2+}$ binding site IV (del of 140-151 and T139C) were studied in TnC depleted muscle fibers. Previous studies (Collins et al., Biochem. 30, 1991) suggested that only sites II and IV bind $Ca^{2+}$ in $BTnC_2$. To test the function of site IV, reconstitution of the fibers with TRUNC was examined. Myofibrillar bundles (100-150$\mu$m diam) were isolated from single striated lateral depressor muscle. These bundles lost their $Ca^{2+}$ sensitivity, as judged by loss of force when challenged at pCa 3.0, when exposed to 10 mM orthovanadate in relaxing solution (pCa > 7.0, pH 6.8, I = 0.15 M, < 5', 20°C). Subsequent exposure (30' at 2 mg/ml) of native $BTnC_2$ and $rBTnC_2$ both in the absence of $Ca^{2+}$, or TRUNC in the presence of $Ca^{2+}$, restored force responses. Calmodulin (30$\mu$M) in the presence of $Ca^{2+}$ was unable to restore force in TnC depleted bundles. Thus orthovanadate effectively extracts TnC in these fibers. These results also suggest that site IV plays a structural role in $BTnC_2$ and is responsible for maintaining the interaction of $BTnC_2$ with BTnI. (Supported by MDA, NIH HL42325, AR37701, AR40727)

**M-Pos365**

EXPRESSION AND PURIFICATION OF RECOMBINANT TROPONIN T ALPHA AND BETA ISOFORMS FOR STRUCTURE-FUNCTION STUDIES. ((#T. Panavelil, +B-S. Pan, and #J.D. Potter)) #Dept. of Mol. & Cell. Pharmacology, Univ. of Miami School of Med., Miami, FL 33101, +MSD Research Labs, Dept. of Pharmacology, West Point, PA 19486.

Fast skeletal troponin T (TnT) has two carboxyl-terminal isoforms, α and β, which are expressed in a tissue-specific and developmentally regulated manner. Previous studies by us using truncated TnT fragments (J. Biol. Chem. 267, 23052) suggested that the α and β sequences may engender different $Ca^{2+}$ affinities to troponin. To further evaluate the functional difference of the isoforms, two pET-3b-based expression constructs were made, encoding respectively a full length TnT-α and TnT-β with identical $NH_2$-terminal sequences. The base sequence in the TnT-coding region of the constructs were verified by DNA sequencing. The TnT-α and β were then over-expressed in E-coli and purified by cation and anion exchange chromatography. The purity of the resulting TnT-α and β were established by SDS-polyacrylamide gels and western blots. The purified TnT-α and β are being tested using reconstituted regulated actomyosin to determine if the sequence of the carboxyl-variable region of TnT is a determinant of the $Ca^{2+}$-sensitivity of the contractile machinery. (Supported by NIH HL42325, AR37701 and AR40727)

**M-Pos366**

**DIAZO 2 RELAXATION TRANSIENTS IN SKINNED MYOFIBRILLAR BUNDLES FROM THE BARNACLE BALANUS NUBILUS: EFFECTS OF $P_i$ AND THE CARDIAC POTENTIATOR EMD 57033.** ((*S. Lipscombe, *J.D. Potter, *T. Miller, +C.C. Ashley)). +University Laboratory of Physiology, Oxford OX1 3PT, England/Friday Harbor Labs., University of Washington, Seattle, WA 98250, *Dept. of Molecular & Cellular Pharmacology, University of Miami School of Medicine, Miami, FL 33101.

Myofibrillar bundles (100-150 $\mu$m) were mechanically isolated under oil from single striated lateral depressor muscle fibers of the barnacle Balanus nubilus (Ashley et al., J. Musc. Res. 12(6), 532-542, 1991). These bundles, attached by aluminum T clips to a force transducer, were placed in a cooled (12°C) stainless steel trough containing either relaxing solution (pCa 7.0) or activating solution containing diazo 2 (2 mM, 20$\mu$M free $Ca^{2+}$, zero EGTA) (Ashley, Mulligan & Lea, Quart. Rev. Biophys., 1991). Initially maximal $Ca^{2+}$ activated force ($P_{max}$) was determined in Ca-EGTA solutions (pCa 3.0) and was depressed by 2.5 mM $P_i$ compared to control and increased by 10 $\mu$M EMD in DMSO (154 $\pm$ 16% SEM); DMSO alone had no effect. The relaxation transients initiated by laser flash photolysis of diazo 2 were slowed by $P_i$ (2.5 mM) and were essentially unaffected by EMD (10$\mu$M); again DMSO having no effect. These results suggest that EMD is affecting mainly $f_{app}$ with little effect on $g_{app}$, unlike ADP where force potentiation ($> P_{max}$) is associated with a marked slowing of the relaxation transient. (Supported by MDA, NIH HL42325, AR37701, AR40727)

**M-Pos367**

**THE EFFECT OF 2,5-DI-(*TERT*-BUTYL)-1,4-BENZOHYDROQUINONE ON THE CONTRACTILE APPARATUS AND FORCE RESPONSES IN SKINNED MUSCLE FIBERS OF THE RAT.** ((A.J. Bakker, G.D. Lamb, and D.G. Stephenson)) Department of Zoology, La Trobe University, Bundoora, Victoria 3083, Australia.

In this study, we investigated the effect of the sarcoplasmic reticulum (SR) $Ca^{2+}$ pump inhibitor, 2,5-di-(*tert*-butyl)-1,4-benzohydroquinone (TBQ) on the $Ca^{2+}$ sensitivity of the contractile apparatus, SR $Ca^{2+}$ loading and depolarization-induced force responses in mechanically skinned muscle fibers of the rat. Steady state force measurements showed a small decrease in maximum force in 20 $\mu$M TBQ (89.8 $\pm$ 2.5 % (n=4) of controls). A plot of % maximum force as function of pCa revealed a marked increase in the sensitivity of the contractile apparatus to $[Ca^{2+}]$ in the presence of 20 $\mu$M TBQ (50% force activation point shifted to left by 0.26 pCa units). SR loading experiments involved measuring caffeine-induced force responses in fibers previously depleted of $Ca^{2+}$ and then loaded for 2 min in a $Ca^{2+}$ loading solution (pCa 6). The integral of the caffeine-induced force response was taken to be equivalent to $Ca^{2+}$ loaded. Responses elicited in fibers loaded in the presence of 20 $\mu$M TBQ were 23.2 $\pm$ 6.2 % (n=3) of controls. As a similar level of $Ca^{2+}$ loading could be achieved in approximately 6.5 s under control conditions, $Ca^{2+}$ loading was at least 19 times slower in the presence of 20 $\mu$M TBQ (considering the effect of TBQ on the contractile apparatus). Depolarization-induced force responses elicited in the fibers were increased and prolonged in the presence of 5.0 and 20 $\mu$M TBQ, in a dose dependent manner. No effect was observed at 0.5 $\mu$M TBQ. While 7 or more similar responses could be elicited under control conditions, a second depolarization in 20 $\mu$M TBQ reduced force to 12.7 % of the first, and no force was observed by the third stimulation. The force response returned however, after exposure to a $Ca^{2+}$ loading solution, suggesting that the drop in force in consecutive depolarizations in 20 $\mu$M TBQ was due to SR $Ca^{2+}$ depletion. In conclusion, TBQ is a powerful inhibitor of SR $Ca^{2+}$ sequestration in skinned rat fibers. However, at a concentration of 20 $\mu$M, TBQ also increases the sensitivity of the contractile apparatus to $Ca^{2+}$.

**M-Pos368**

Effect of a $Ca^{2+}$ Channel Blocker on Calcium Sensitivity of Skeletal Fibers in Aged Rats. Ronglih Liao and Judith K. Gwathmey. Cardiovascular Disease and Muscle Research Laboratories, Harvard Medical School, Boston, MA 02115

Force development and $Ca^{2+}$ sensitivity of force were measured in single chemically skinned psoas fibers obtained from aged rats that were 26 - 29 months old. One group was served as the control (CON). The second group was given orally with a $Ca^{2+}$ channel blocker (CCB) served as the drug-treated group (EXP). Each of two groups contained male (M) and female (F) rats. Force-$Ca^{2+}$ relations were measured at sarcomere length of 2.8 $\mu$m at pH 7.0, and 20°C. The slope of the force-pCa curve and maximum force are greater for M than for F. The slope of force-pCa curves for the EXP fibers from M was 1.10 units less than that for CON. However, the drug shifted the $pCa_{50\%}$ to the left by 0.1 units. These results suggest that the $Ca^{2+}$ sensitivity of contractile force was enhanced by a CCB. Thus, the CCB utilized in this study may improve muscular contractility in skeletal muscle from senescent rats. Effect of native rabbit skeletal troponin C (RSTnC) in the skinned fibers of the aged rats was studied by first extracting endogenous TnC from the aged fibers and then reconstituting TnC-depleted fiber with RSTnC. Compared with CON fibers, the tension at pCa 4 for the reconstituted fibers from F and M was 80% and 86% $T_0$ (the maximal tension of unextracted fibers), respectively. The EXP fibers with RSTnC produced 95% $T_0$, which was close to the full force. This is additional evidence supporting the hypothesis that the CCB used may have beneficial in the skeletal muscle changes in senescence.

**M-Pos369**

ION CHANNELS AND RECEPTORS IN SKELETAL MUSCLE CELL LINES FROM DUCHENNE MUSCULAR DYSTROPHY PATIENTS ((P.Caviedes, R. Caviedes, J.L Liberona and E. Jaimovich)). Depto. Fisiología y Biofísica, Universidad de Chile and CECS, casilla 16443, Santiago 9 Chile.

A cell line (RCDMD), derived from a muscle biopsy taken from a 7 year old patient with Duchenne muscular dystrophy (DMD), was immortalized *in vitro*. Unlike other cell lines established by the same procedure, RCDMD cells were highly refractory to transformation and the resulting cell line grew slowly with a doubling time of approximately 48 hrs. Some characteristics of the cell line include lack of reaction with anti-dystrophin antibodies and the presence of receptors for the dihydropyridine PN200-110 (Kd = 0.3 $\pm$ 0.05 nM and Bmax = 1.06 $\pm$ 0.03 pmol/mg protein) and for $\alpha$-bungarotoxin (Kd = 1.02 $\pm$ 0.17 nM and Bmax = 4.2 $\pm$ 0.37 pmol/mg protein).

Patch-clamped cells lacked ion currents when growing in complete medium with high serum. After 5 days in differentiating medium, non inactivating, delayed rectifier potassium currents were seen. At day 12, A type, inactivating potassium currents as well as transient inward currents appeared. In conditions in which sodium and potassium currents were absent, a very fast activating and fast inactivating calcium current, much larger than those normally seen in muscle cells was evident.

This cell line has important electrophysiological differences when compared to muscle cells in primary culture as well as to other human muscle cell lines established in our laboratory. Financed by Fondecyt 931-1089, MDA, DTI B3390.

**M-Pos370**

POSSIBLE ROLE OF APAMIN-SENSITIVE $K^+$ CHANNELS IN MYOTONIC DYSTROPHY. ((M.I. Behrens, P.Jalil, A. Serani, F. Vergara and O. Alvarez)) Facultad de Ciencias Universidad de Chile and Centro de Estudios Científicos de Santiago, Chile. (Spon by R. Latorre)

Myotonic muscular dystrophy is a genetic disease characterized mainly by muscle atrophy and myotonia, a repetitive electrical activity of muscle. In the present study, the possible role of apamin-sensitive $K^+$ channels in the genesis of myotonia was investigated. Apamin is a peptide from bee venom that specifically blocks small conductance $Ca^{2+}$-activated $K^+$ channels. The injection of a small amount of apamin (20-30 $\mu$l, 10 $\mu$M) into the thenar muscle of myotonic dystrophy patients decreased the basal electrical activity during the electromyogram in the 6 patients studied. Myotonic discharges after muscle percussion were more difficult to be triggered and of smaller intensity and duration. In two controls and in two patients with generalized myotonia, as well as in one patient with myotonia congenita (where the defect is in chloride channels) apamin had no effect. These results suggest that apamin-sensitive $K^+$ channels participate in the mechanism that generates myotonia in myotonic dystrophy.

Support 296-1989, 1134-1992, 862-91, 193910-93, 1930912 FONDECYT Chile.

**M-Pos371**

EFFECTS OF ACTION POTENTIAL PROLONGATION ON $Ca^{2+}$ CURRENT, $[Ca^{2+}]_i$ AND CONTRACTION STUDIED USING THE ACTION POTENTIAL CLAMP TECHNIQUE. ((R.A.Bouchard, R.B.Clark,W.R.Giles)) Department of Medical Physiology, University of Calgary.

The action potential (AP) clamp technique was used to study the contributions of $Ca^{2+}$ current ($I_{Ca}$) and release of $Ca^{2+}$ from the sarcoplasmic reticulum (SR) to the positive inotropic effect of AP prolongation in Indo 1-loaded rat ventricular myocytes. APs recorded in the absence and presence of 4-aminopyridine were used as voltage-clamp command waveforms. $I_{Ca}$, $[Ca^{2+}]_i$ transients, and contraction (measured as unloaded cell shortening) were recorded simultaneously. AP prolongation produced a decrease in $I_{Ca}$, and a substantial slowing of the time-course of its decline. The increase in charge movement due to this slowing of $I_{Ca}$ was accompanied by enhanced mechanical activation and $[Ca^{2+}]_i$ transients, both of which were blocked completely by ryanodine. When AP duration was altered, the resulting changes in $I_{Ca}$ developed much more quickly than the inotropic effect. Taken together, these findings suggest that interventions which prolong the cardiac AP ($\alpha_1$-adrenoceptor stimulation, class III antiarrhythmics, stimulation frequency) can augment contractility indirectly by increasing uptake and release of $Ca^{2+}$ from the SR. (supported by the AHFMR and MRC).

**M-Pos372**

EC-COUPLING AND $[Ca^{2+}]_i$ HOMEOSTASIS IN RAT VENTRICULAR MYOCYTES STUDIED USING THE ACTION POTENTIAL CLAMP TECHNIQUE. ((R.A.Bouchard, R.B.Clark, W.R.Giles)) Department of Medical Physiology, University of Calgary.

An action potential (AP) was used as the command waveform for voltage clamping Indo-1 loaded rat ventricular myocytes. $Ca^{2+}$-dependent membrane current during the AP consisted of: 1) a rapidly activating component which peaked near +20 mV and was blocked completely by $Cd^{2+}$, suggesting it was due to $Ca^{2+}$ influx through L-type $Ca^{2+}$ channels ($I_{Ca}$). 2) an inward tail current ($I_{tail}$) which developed at membrane potentials negative to -25 mV during repolarization. The time-course for decay of $I_{tail}$ was very similar to that for decline of accompanying $[Ca^{2+}]_i$ transients measured using Indo-1 fluorescence. Superfusion of myocytes with ryanodine blocked $I_{tail}$, but had no effect on $I_{Ca}$. $I_{tail}$ was insensitive to the Cl channel blocker DIDS, but was suppressed completely when external $Na^+$ was replaced with $Li^+$, suggesting it was due to sarcolemmal $Na^+/Ca^{2+}$ exchange rather than a non-specific cation conductance or a $Ca^{2+}$-dependent $Cl^-$ conductance. Integration of $I_{Ca}$ yielded net charge movements which were approximately two times larger than those for $I_{tail}$, suggesting that most of the $Ca^{2+}$ entering the cell through L-type $Ca^{2+}$ channels can be extruded by the $Na^+/Ca^{2+}$ exchanger within a single cardiac cycle. Ryanodine completely blocked activation of cell shortening and $[Ca^{2+}]_i$ transients, despite having no effect on $Ca^{2+}$ influx during the AP. These findings argue against a direct role for trans-sarcolemmal $Ca^{2+}$ entry in the activation of myofilaments, and suggest that most of the $Ca^{2+}$ influx during $I_{Ca}$ is bound rapidly to high affinity ligands or that spatial gradients of $[Ca^{2+}]_i$ exist during EC-coupling. (Supported by the AHFMR and MRC)

**M-Pos373**

MYOPLASMIC Ca REMOVAL DURING RELAXATION IN FERRET VENTRICULAR MYOCYTES: A NOVEL Ca TRANSPORT SYSTEM? ((Rosana A. Bassani, José W.M. Bassani and Donald M. Bers)) Dept. of Physiology, Loyola University, Maywood, IL 60153

Simultaneous inhibition of SR Ca accumulation and Na-Ca exchange, during application of 10 mM caffeine in 0Na,0Ca solution, renders relaxation of the contracture (CafC) and $[Ca]_i$ decline very slow in rat and rabbit cardiac cells ($t_{1/2}$ ~8-10 s, Bassani *et al., J Physiol*, in press), but not in ferret myocytes ($t_{1/2}$ ~2.5 s). The rapid Ca transport was not into a thapsigargin (TG) sensitive pool, since complete inhibition of the SR Ca-pump with 2.5 $\mu$M TG did not alter $[Ca]_i$ decline. This relatively rapid $[Ca]_i$ decline was also not prevented by total removal of extracellular ions. Even additional inhibition of mitochondrial Ca uptake (with 3 $\mu$M FCCP) and the sarcolemmal Ca-pump (with 10 mM $[Ca]_o$ or 0.1 mM La), which virtually abolishes relaxation of the Na-free CafC in rabbit cells ($\tau > 80$ s), increased the $t_{1/2}$ of $[Ca]_i$ decline to only 4-5 s in ferret myocytes (see Fig)! Attempts to saturate a possible intracellular site of Ca transport (1 Hz twitches in a Na-free solution containing 10 mM caffeine and 10 mM Ca) also failed to alter $[Ca]_i$ decline or uncover a Ca pool releaseable with FCCP. We conclude that there might be an additional Ca transport system in ferret myocytes, probably a transsarcolemmal transport but neither an ion-exchanger, nor a Ca-ATPase with characteristics like that in cardiac cells from other species.

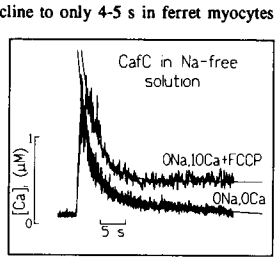


**M-Pos374**

A NEGATIVE REGULATORY MECHANISM WITH FEATURES OF ADAPTATION CONTROLS $Ca^{2+}$-INDUCED $Ca^{2+}$ RELEASE IN CARDIAC MYOCYTES. ((K.Yasui, P.Palade and S.Györke)) University of Texas Medical Branch, Department of Physiology & Biophysics, Galveston, TX 77555-0641

The mechanism of termination of $Ca^{2+}$-induced $Ca^{2+}$ release (CICR) from the sarcoplasmic reticulum (SR) has been investigated in patch-clamped rat ventricular myocytes loaded with fluo-3. During depolarizing steps evoking $Ca^{2+}$ currents ($I_{Ca}$), $Ca^{2+}$ release first activated, then the release rapidly declined, as evidenced by the rate of change (derivative) of the fluorescence signal. This rapid termination of release was not due to a depletion of $Ca^{2+}$ from the SR, since it also occurred at potentials eliciting submaximal $Ca^{2+}$ transients. To determine whether the termination of release was due to inactivation of "trigger" $I_{Ca}$, we used the $Ca^{2+}$ channel agonist FPL 64176 (Fisons Pharmaceuticals, Leicestershire, UK), which is known to reduce $I_{Ca}$ inactivation (Rampe & Lacerda, J. Pharmacol. Exp. Ther. 259, 982, 1991). In the presence of the drug (1 $\mu$M) at 20 mV the time constant of $I_{Ca}$ inactivation increased from 18.8±3.0 ms to 158.7±24.9 ms (M±SE, n=4); at the same time, the rate of release termination did not change significantly ($\tau \approx 14$ ms). Similar results were observed at other potentials. Large tail currents, obtained in the presence of FPL 64176 upon repolarization, elicited secondary releases from apparently inactivated stores (fig.). These results suggest that a negative control mechanism operates at the $Ca^{2+}$ release level which terminates CICR independently of the duration of the trigger $I_{Ca}$ and before $Ca^{2+}$ from the SR was depleted. The ability of release to be reactivated by incremental increases in trigger $I_{Ca}$ suggests that this negative feedback is not a conventional inactivation but is a mechanism which exhibits features of adaptation, as demonstrated recently in individual SR $Ca^{2+}$ release channels (Györke & Fill, Science, 260, 807, 1993). Supported by AHA (SG) and JHF fellowship (KY).

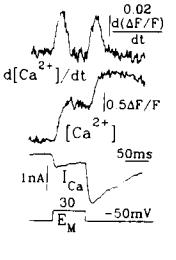


**M-Pos375**

Ica ACTIVATED SARCOPLASMIC RETICULUM (SR) $Ca^{2+}$ RELEASE IN CARDIAC MYOCYTES IS NOT DIRECTLY DEPENDENT UPON THE ABUNDANCE OF MORPHOLOGICAL "COUPLINGS" BETWEEN THE SR AND SARCOLEMMA (SL). ((A.M. Janczewski, K. Bogdanov, B.D. Ziman, H.A. Spurgeon and E.G. Lakatta)) GRC, NIA, Baltimore, MD. (Spon. by W.H. duBell).

We compared the relationship between peak $I_{Ca}$ and amplitudes of the corresponding $Ca^{2+}_i$ transients in whole-cell voltage clamped, indo-1 dialyzed adult ventricular myocytes of rat (R), which have an extensive T-tubular system and those of a bird, Finch (F), which lack T tubules and, compared to R, lack 80% of the morphological "couplings" between SR and SL. SR $Ca^{2+}$ depletion with caffeine showed that in both R and F, the $Ca^{2+}_i$ transients elicited by $I_{Ca}$ are similarly (by 75-85%) dependent on SR $Ca^{2+}$ release. Under the same experimental conditions (1 mM Ca, 30 uM TTX in the bath at 24° C; 100 mM Cs, 20 mM TEA, 0 Na in the pipette) the average dependence of $I_{Ca}$ and $Ca^{2+}_i$ transients on the voltage clamp potential (-50 to +90 mV) from a holding potential of -75 mV, were similar in R and F (Fig). Thus, neither T tubules nor complete anatomical "coupling" of SL $Ca^{2+}$ channels to SR $Ca^{2+}$ release channels are required for E-C coupling in mammalian cardiac cells.

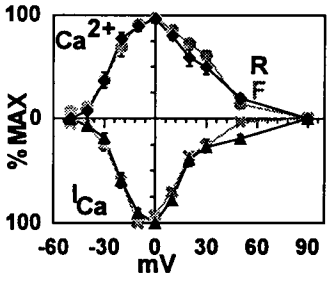


**M-Pos376**

INTRACELLULAR PROTEIN AND ACIDOSIS ALTER THE $K_d$ AND FLUORESCENCE SPECTRA OF THE CALCIUM INDICATOR INDO-1. ((AJ Baker, R Brandes*, J Schreur, SA Camacho, & MW Weiner)). Univ. Calif. San Francisco CA 94121 & *Loyola Univ. Chicago IL 60153.

Indo-1 is widely used to monitor cytosolic $[Ca^{2+}]$; however, quantitation is hampered by uncertain effects of intracellular milieu on the dissociation constant ($K_d$) for calcium and on fluorescence spectra. We measured the effect of protein (from frog or rat muscle) and acidosis on $K_d$ and on fluorescence spectra. **Results:** Fig.1 shows $K_d$ markedly increased with [protein] and acidosis (which had additive effects). Frog protein affected $K_d$ more than rat protein. Fig.2 shows that the ratio of fluorescence spectra for Ca-free/Ca-bound indo-1 (S-values) increased with [protein], and the isosbestic wavelength (at S=1) decreased. Acidosis had a smaller effect on fluorescence (not shown). **Conclusion:** $K_d$ and S-values of indo-1 are significantly affected by [protein] and pH, therefore, quantitation of $[Ca^{2+}]$ in-vivo using indo-1 requires calibration constants determined in the presence of appropriate [protein] and pH.

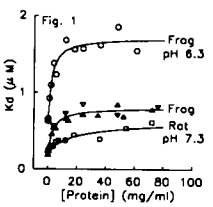


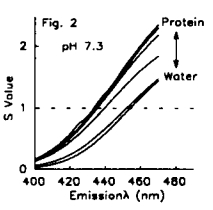

**M-Pos377**

Ca ENTRY DURING A TWITCH COMPARED WITH SR Ca CONTENT IN PATCH CLAMPED RABBIT VENTRICULAR MYOCYTES. ((L.M. Delbridge, J.W.M. Bassani and D.M. Bers)) Loyola University Chicago, Maywood, IL 60153.

Whole cell patch clamp technique was used to measure the Na-Ca exchange (Na-CaX) current due to SR Ca release during caffeine contracture (CafC) relative to the Ca influx associated with $I_{Ca}$ during steady state (SS) twitch in indo-1(FA) loaded ventricular myocytes (22°C). With a holding potential of -70 mV, a train of 6 clamp pulses from -40 to 0 mV was applied from rest to achieve SS twitch Ca transients (ratio 405/485). The final test clamp was preceded by a ramp to inactivate $I_{Na}$. Holding potential was maintained during two 10s-long CafCs (10 mM). K currents were blocked by the inclusion of Cs and TEA in the patch pipette. The first CafC was associated with peak inward currents of 40-100 pA. This current was not present during the second CafC, which was applied to confirm that the SR was completely depleted. The integrals of the CafC-induced Na-CaX current [71.0±13.3 nA·ms] and $I_{Ca}$ [28.4±3.6 nA·ms] for each myocyte were calculated. Thus, 0.736 fmol Ca is released from the SR during CafC and removed from the myocyte by Na-CaX, compared with the SS $I_{Ca}$ entry of 0.147 fmol Ca per twitch. Bassani *et al* estimated that the SR Ca content released by CafC is about 2x that released during a twitch *(Am J Physiol 265:C533-C540, 1993)*. The present result is consistent with the influx of Ca via $I_{Ca}$ supporting 28% of the twitch contraction in rabbit ventricular myocytes. (This work was done during the tenure [LMD] of an International Research Fellowship of the American Heart Association.)

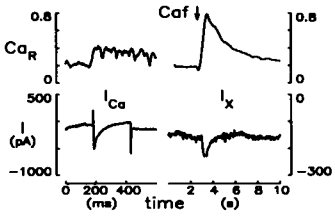


**M-Pos378**

CONTROL OF SARCOPLASMIC RETICULUM CALCIUM RELEASE DURING CALCIUM LOADING IN RAT VENTRICULAR MYOCYTES. ((C. I. Spencer and J.R. Berlin)) Bockus Research Institute, Graduate Hospital, Philadelphia, PA 19146. (Spon. by H. Martin)

The effect of intracellular $Ca^{2+}$ ($Ca_i$) load on regulation of sarcoplasmic reticulum (SR) $Ca^{2+}$ release was investigated in rat ventricular myocytes voltage-clamped with electrodes containing 60 μM indo-1 or a lower affinity $Ca^{2+}$ indicator, Ca Green-2 (5μM; with 250 μM carboxy SNARF-1 to correct for cell movement). $Ca_i$ loading was manipulated by changing $Na^+$, $Ca^{2+}$ and caffeine concentrations in the superfusion solutions. After depleting SR $Ca^{2+}$ with caffeine, trains of depolarizing pulses were produced in $Na^+$-free, $Ca^{2+}$-containing solutions in order to increase $[Ca^{2+}]_i$. The figure shows superimposed Ca Green-2 fluorescence transients elicited by consecutive 16 ms (dotted pulses) and 100 ms depolarizations early (left side) and late (right side) during a depolarization train. The amplitude of transients elicited early in the train were dependent on pulse duration and potential. Transients elicited later in the train, prior to spontaneous changes in $[Ca^{2+}]_i$, were larger in amplitude and less sensitive to pulse duration and potential. $Ca^{2+}$ saturation of the indicator is unlikely to explain these data. Instead, the relationship between sarcolemmal Ca current and SR $Ca^{2+}$ release appears to depend on the degree of $Ca_i$ loading.

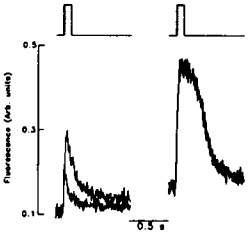


**M-Pos379**

INTRINSIC CYTOSOLIC CALCIUM BUFFERING IN SINGLE RAT CARDIAC MYOCYTES. ((J.R. Berlin, J.W.M. Bassani and D.M. Bers)) Bockus Research Inst., Graduate Hospital, Philadelphia, PA 19146 and Dept. of Physiology, Loyola University Stritch Sch. of Med., Maywood, IL 60153.

Intracellular $Ca^{2+}$ buffering was estimated in voltage-clamped rat cardiac myocytes. Cells were loaded with indo-1 ($K^+$ salt) to an estimated cytosolic concentration of 44 ± 4 μM (mean ± S.E.M., n=5), and $Ca^{2+}$ removal from the cytosol was inhibited by thapsigargin (10μM) and superfusion in a $Na^+$-free Tyrode's solution. In some experiments, the mitochondrial uncoupler "1799" (10 μM) was included in the superfusion solution. To titrate the cellular buffers, $[Ca^{2+}]_i$ was increased with a train of voltage clamp pulses from -40 to 10 mV (see figure), and the change in total cell $Ca^{2+}$ with each depolarization was calculated by integrating the Ca current. The change in total cell $Ca^{2+}$ was then analyzed as a function of $[Ca^{2+}]_i$ and the properties of the $Ca^{2+}$ buffers (including indo-1) were determined by assuming that all buffers behaved as a single Michaelis-Menton species. In 5 cells, $B_{max}$ was estimated to be 162 ± 15 μmoles/liter (cytosolic $H_2O$) with a $K_D$ of 0.63 ± 0.07 μM. Assuming that indo-1 had a $K_D(Ca)$ of 0.33 μM, intrinsic cytosolic $Ca^{2+}$ buffering capacity would be 124 ± 17 μmoles/liter with a $K_D$ of 0.96 ± 0.18 μM. These data indicate that a $[Ca^{2+}]_i$ transient which raises $[Ca^{2+}]_i$ from 0.1 to 1 μM adds ≥ 50 μmoles/liter $Ca^{2+}$ to the cytosol.

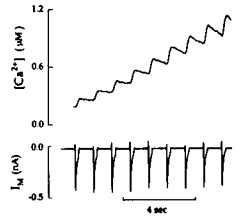


**M-Pos380**

EXTRACELLULAR HEPARIN BLOCKS CONTRACTION AND Ca TRANSIENTS IN MAMMALIAN CARDIAC MYOCYTES. ((M. C. Garcia, J. A. Sanchez, V. K. Sharma, and S-S. Sheu)) Department of Pharmacology, University of Rochester, Rochester, NY 14642, and Department of Pharmacology, CINVESTAV-IPN, A. P. 14-740, Mexico, D.F. 07000.

Heparin binds with high affinity to the dihydropyridine (DHP) receptor of cardiac muscle (Knaus *et al.*, JBC 265:156, 1990) where its effects on the L-type Ca currents are still controversial (Knaus *et al.*, *ibid.*; Lacinova & Morad, JP 465:181, 1993). Our experiments investigate the action of heparin on action potentials, Ca transients and contraction in ventricular myocytes from rat or guinea pig heart. Cells were loaded with Fura 2-AM (3 μM) and fluorescence signals were obtained at excitation wavelengths of 340 and 380 nm. Cell motion was measured with an edge detector. Tension and action potentials were measured in papillary muscles with conventional techniques. Heparin reversibly decreased Ca transients and cell motion in a dose-dependent manner. Half and complete blockade were obtained with 50 μg/ml and 200 μg/ml, respectively. The DHP agonist BAY-K (50 nM) antagonized this effect. Ca release elicited by caffeine (10 mM) was not affected by heparin. The amplitude of the plateau of the action potential and tension of papillary muscle were decreased by heparin, although at higher concentrations (5 mg/ml). BAY-K (500 nM) also antagonized these effects. These results suggest that heparin decreases Ca transient and muscle contraction of heart by inhibiting DHP-sensitive Ca channels.

**M-Pos381**

EFFECT OF INOTROPIC STIMULATION ON MITOCHONDRIAL CALCIUM IN THE ISOLATED PERFUSED HAMSTER HEART.
((CS Moravec, RW Desnoyer, M Milovanovic and M Bond)) Dept of Cardiovascular Biology, Cleveland Clinic Foundation, Cleveland, OH

We have previously demonstrated, using electron probe microanalysis (EPMA) on rapidly frozen hamster papillary muscles, that mitochondrial calcium content (MTCA) does not change during a single cardiac muscle contraction (Moravec & Bond, Am J Physiol 1991) or following inotropic stimulation (Moravec & Bond, J Biol Chem 1992). We have now extended these observations to the isolated, Langendorff-perfused heart, in which physiological temperatures and heart rates are employed. Isolated hearts from male hamsters at 110 days of age were perfused at 60 mm Hg perfusion pressure, using 37° Krebs-Henseleit buffer. The hearts were stimuated at 4 Hz and left ventricular pressure (LVP) was recorded via a transducer-tipped catheter. Three experimental conditions were used: control hearts (CTRL); hearts treated with $10^{-6}$M isoproterenol (ISO), which produced an average increase in LVP of 191 ± 28 (SEM)% and hearts in which perfusion pressure was raised from 60 to 100 mm Hg (PP), which produced an average increase in LVP of 60 ± 6%. Hearts were then rapidly frozen, using the PS-1000 metal mirror cryofixation device. The timepoint of the freeze during the contractile cycle was observed from the chart recorder and only hearts frozen at peak LVP were used for EPMA. Ultrathin (100nm) cryosections were cut from the surface of the heart, and EPMA used to measure MTCA. EPMA revealed no significant increase in MTCA in ISO (1.2 ± 0.1 mmol/kg dry wt; n=89) or PP (1.1 ± 0.1 mmol/kg dry wt; n=86) hearts as compared to CTRL (1.0 ± 0.1 mmol/kg dry wt; n=89). These data lend further support to the hypothesis that MTCA does not increase during inotropic stimulation of cardiac muscle, regardless of temperature and stimulation frequency, and argue against a role for MTCA in coupling energy use at the myofilaments to energy production in the mitochondria.

**M-Pos382**

MODULATION OF PHENYLEPHRINE EFFECTS ON $[Ca^{2+}]_i$ AND CELL SHORTENING BY ACIDOSIS/REALKALINIZATION. ((C.A. Ward and M.P.Moffat)) Dept. Pharmacology and Toxicology, University of Western Ontario, London, ON, CANADA N6A 5C1. (Spon. by O.F. Schanne)

Upregulation of $\alpha_1$-adrenergic receptors has been reported in the ischemic/reperfused heart. In addition, we have recently demonstrated that phenylephrine (PE) depresses post-ischemic recovery of isolated rabbit hearts. The present study was undertaken to elucidate the mechanism responsible for this phenomenon. Isolated rabbit ventricular myocytes were loaded with fura2-AM and the $[Ca^{2+}]_i$ transient amplitude (TA) and cell shortening were measured simultaneously. Cells were subjected to 10 min of lactate acidosis followed by realkalization (A/R). Under control conditions PE ($10^{-8}$-$10^{-4}$ M) caused a dose-dependent increase in $[Ca^{2+}]_i$ and cell shortening. When PE ($10^{-7}$ M) was added immediately upon realkalization, $[Ca^{2+}]_i$-TA was enhanced and cell shortening was decreased, however, these results were not significant. Treatment with $10^{-5}$ M PE immediately upon realkalization significantly increased $[Ca^{2+}]_i$ by 4 minutes and values were increased 30% above those in control cells after 10 minutes. Early hypercontractility associated with realkalinization was attenuated by this concentration of PE. Addition of PE ($10^{-5}$ M) following 10 min realkalinization significantly increased $[Ca^{2+}]_i$-TA by 50% compared to control cells; a value comparable to the response to this concentration of PE in cells not subjected to acidosis. Cell shortening was also significantly increased. The lower concentration of PE was without significant effect on either $[Ca^{-}]_i$-TA or cell shortening. The results of this study demonstrate that PE, a positive inotropic agent, depresses cell shortening following acidosis and enhances and prolongs the increase in $[Ca^{2+}]_i$. Supported by the Medical Research Council of Canada.

**M-Pos383**

EFFECTS OF ISOPROTERENOL ON INTRACELLULAR FREE $[Ca^{2+}]$ DURING RELAXATION IN RAT CARDIAC MYOCYTES. ((M. A. Movsesian, E. O. Palmer, B. L. Palmer, J. Y. Cheung and R. L. Moore)) Veterans Affairs Medical Center & University of Utah School of Medicine, Salt Lake City, UT, and Milton S. Hershey Medical Center, Pennsylvania State University, Hershey, PA.

Phosphorylation of phospholamban by cAMP-dependent protein kinase reduces the $K_m$ of oxalate-supported, ATP-dependent $Ca^{2+}$ transport in sarcoplasmic reticulum-derived microsomes prepared from ventricular myocardium without changing $V_{max}$ or Hill coefficient ('$n$'). To examine the relevance of this effect to the regulation of intracellular free $[Ca^{2+}]$ ('$[Ca^{2+}]_i$') during relaxation by isoproterenol, we measured the effect of 4 $\mu$M isoproterenol on $d[Ca^{2+}]_i/dt$ in isolated rat ventricular cardiac myocytes loaded with fura-2. Values for $-d[Ca^{2+}]/dt$ ('$v$') were determined for each $[Ca^{2+}]_i$ during relaxation, and data were fitted to the equation $v = V_{max}[Ca^{2+}]_i^n/(K_m^n + [Ca^{2+}]_i^n)$, which describes the steady state kinetics of the $Ca^{2+}$-transporting ATPase of the sarcoplasmic reticulum. Isoproterenol increased $V_{max}$ ($\mu$M/sec) from 7.45 to 11.46, but changed $K_m$ ($\mu$M) only from 0.84 to 0.76 and $n$ only from 2.2 to 2.6. These results suggest that the effect of isoproterenol on $[Ca^{2+}]_i$ during relaxation in cardiac myocytes cannot be explained by the effect of phosphorylation of phospholamban by cAMP-dependent protein kinase on oxalate-supported, ATP-dependent $Ca^{2+}$ transport by the sarcoplasmic reticulum.

**M-Pos384**

CONTRACTILE ARREST INCREASES SR Ca TRANSPORT AND SERCA2 GENE EXPRESSION IN CULTURED NEONATAL RAT HEART CELLS ((J.W.M. Bassani, M. Qi, A.M. Samarel and D.M. Bers)) Loyola Univ Chicago, Maywood, IL 60153.

We measured the effect of chronic verapamil-induced arrest (VA) on the function of SR Ca-ATPase, Na/Ca exchange (NaCaX) and slow Ca transport systems (mitochondria and sarcolemmal Ca-ATPase) using indo-1 in neonatal rat ventricular myocytes. We also measured expression of SERCA2 (mRNA & protein) and NaCaX mRNA. $Ca_i$ transients were recorded during caffeine-induced contractures (CafC, $\pm Na_o$) and twitches induced by brief depolarizations with Na-free, high $[K]_o$ solution (K-Twitches). The $t_{1/2}$ for $[Ca]_i$ decline when both the SR Ca uptake and NaCaX were prevented was the same for control and VA cells ($\sim$20s), indicating unaltered slow Ca transport. There was also no difference in the $t_{1/2}$ of CafC when NaCaX was the main mechanism for $[Ca]_i$ decline ($t_{1/2} \sim 1.5$ s). On the other hand, $[Ca]_i$ declined $\sim$2-fold faster during K-Twitches in VA cells ($t_{1/2} = 0.84 \pm 0.05$ *vs* $0.48 \pm 0.06$ s, $P < 0.001$), indicating an increase in SR Ca transport. This was also reflected by a 56% increase in the maximal SR Ca content. These results agreed with expression levels, where NaCaX mRNA was unchanged, but SERCA2 mRNA and protein in VA cells were markedly increased (to $166 \pm 10\%$ and $164 \pm 20\%$ respectively). Thus, VA induced an increase in SR Ca uptake (& SERCA2 expression) without affecting NaCaX or slow Ca transport systems.

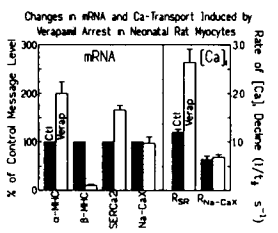


**M-Pos385**

**THYROID STATE AND RAT VENTRICLE MYOCYTE ACTIVITY. ((B.M.Wolska, V.Averyhart-Fullard and R.J.Solaro)). Dept. of Physiology & Biophysics, Univ. of Illinois, Chicago, IL, 60612-7342.**

**Many of the cellular mechanisms which are involved in excitation-contraction coupling are affected by thyroid hormone. Our hypothesis is that thyroid hormone changes cardiac contractility not only by an effect on $Ca_i^{2+}$ but also by an effect on intracellular $Na_i^+$ and $pH_i$. The role of changes in $Na_i^+$ and $pH_i$ in long term effects of thyroid hormone on cardiac myocytes is unknown. Hypothyroism decreases the shortening of rat ventricle myocytes from 12.1 ± 1.2% to 5.2 ± 2.0%. The time to peak contraction was prolonged from 150 ± 5ms (n = 25) to 296 ± 16ms (n = 24). Hyperthyroidism did not significantly change either the amplitude of the shortening or the time to peak contraction. To study $Ca_i^{2+}$, the myocytes were loded with fura-2/AM. In myocytes isolated from hypo-, eu-, and hyperthyroid rat hearts the amplitude of the 340/380 ratio was 1.65 ± 0.10 (n = 20), 2.45 ± 0.12 (n = 16), and 2.88 ± 0.12 (n = 28), respectively. The diastolic ratio was 0.85 ± 0.03 (n = 20), 0.95 ± 0.03 (n = 16), and 0.94 ± 0.02 (n = 28) in myocytes isolated from hypo-, eu- and hyperthyroid animals. To study $Na_i^+$, myocytes were loded with SBFI/AM. There was no difference in 340/380 ratio between myocytes isolated from hypo- and euthyroid rats. However hyperthyroidism resulted in an increase of SBFI ratio from 0.96 ± 0.02 (n = 24) to 1.16 ± 0.03 (n = 27). Further investigation to measure the $pH_i$ in different thyroid states and to test if the mechanism for changes in $Ca_i^{2+}$ and $Na_i^+$ involves altered expression of genes encoding membrane exchangers, pumps and channels are now in progress.**

**M-Pos386**

SPHINGOLIPID ACTIONS ON CARDIAC MYOCYTE $Ca^{2+}$ TRANSIENTS AND L-CHANNEL CONDUCTANCE.
((R. Sabbadini, P. McDonough, K. Yasui, P. Palade, C. Dettbarn, R. Betto, G. Salviati and C. Glembotski)) Dept. of Biology San Diego State University, San Diego CA 92182. Dipartimento Scienze Biomediche Sperimentali, University of Padova Italy. Dept. of Physiology and Biophysics University of Texas Med. Branch, Galveston TX 77550.

We have previously shown that the naturally occurring second messengers, sphingosine (SPH) and sphingosylphosphorylcholine (SPC), can modulate Ca release from skeletal muscle cells through direct actions on the SR ryanodine receptor (RyR) (Sabbadini et al., JBC 267:15475-15484, 1992). In this study, we demonstrate that SPH substantially blocks the indo-1 Ca transients of adult rat ventricular myocytes and cultured neonatal ventricular cells paced by electrical field stimulation. Whole cell patch clamping reveals substantial inhibition of L-channel currents by SPH and isolated SR studies show SPH inhibition of Ca release through the RyR. We conclude that SPH has dual actions in inhibiting EC-coupling by reducing the amount of 'trigger Ca' for Ca-induced Ca release (CICR) and by simultaneously raising the RyR's threshold for CICR. SPC has opposite actions to SPH and can induce Ca release from myocytes by direct action on the RyR. Other spingolipids, including ceramides were ineffective in controlling cardiac Ca levels. Consequently, we propose that sphingolipids produced by the sphingomyelin signal transduction pathway could be physiologically relevant regulators of cardiac Ca levels. Supported by the MDA, NIH, CNR, Telethon-Italy and Minestero della Pubblica Istruzione of Italy.

**M-Pos387**

POTENTIATION OF $CA^{2+}$ TRANSIENTS BY ENDOTHELIN AND ARACHIDONIC ACID IN RAT CARDIAC MYOCYTES IS MEDIATED BY K+ CHANNEL INHIBITION.
((D.S. Damron, D.R. Van Wagoner, C.S. Moravec and M. Bond)), The Cleveland Clinic, Cleveland, OH 44195.

Endothelin (ET) has been shown to enhance cardiac contractility, suggesting that ET alters intracellular $Ca^{2+}$ homeostasis via changes in trans-sarcolemmal $Ca^{2+}$ flux. We previously showed that both arachidonic acid (AA) and ET potentiate $Ca^{2+}$ transients evoked by extracellular ATP in adult rat ventricular myocytes and that this effect was attenuated by inhibitors of protein kinase C (PKC). However the source(s) of $Ca^{2+}$ involved in the potentiation of the ATP response by AA or ET were not known. To investigate the mechanism of ET- and AA-induced potentiation of ATP-stimulated $Ca^{2+}$ transients, we used suspensions of adult rat ventricular myocytes loaded with fura-2. Depletion of sarcoplasmic reticulum (SR) $Ca^{2+}$ with ryanodine (5 $\mu$M) pretreatment had no significant effect on the AA- or ET-induced potentiation of the ATP response, but nifedipine (10 $\mu$M) abolished the potentiated responses. This could be due to PKC-mediated activation of $Ca^{2+}$ channels or alternatively, to PKC-dependent inhibition of $K^+$ channels. Pretreating cardiac myocytes with the $K^+$ channel blocker, 4-aminopyridine (4-AP, 4 mM), enhanced the amplitude of the ATP-stimulated $Ca^{2+}$ transient by 107%. This potentiation was unaffected by incubation of ET or AA with 4-AP. In isolated isometrically contracting papillary muscles (PM) addition of 4-AP increased developed tension (DT) by 21%. Similarly, ET (50 nM) increased DT by 23% and this effect was inhibited by staurosporine (50 nM). Using the whole cell patch clamp technique, we found that AA inhibited the transient outward $K^+$ ($I_{TO}$) current whereas ET inhibited the delayed rectifier $K^+$ current ($I_K$). These results suggest that AA and ET may prolong action potential duration by inhibition of $K^+$ channels, thus increasing $Ca^{2+}$ entry into the cell and enhancing contractile function.

**M-Pos388**

SPATIO-TEMPORAL PROPERTIES OF CALCIUM SPARKS IN CARDIAC MYOCYTES. ((H. Cheng, *M.B. Cannell and W.J. Lederer)) Dept. Physiology, Univ. MD. Sch. Med., 660 W. Redwood St., Baltimore MD 21201 & *Dept. Pharm., St. George's Hosp. Med. Sch., Cranmer Terr., London SW17 ORE.

**Using the laser scanning confocal microscope (LSCM) and the fluorescent calcium indicator fluo-3 spontaneous local increases in $[Ca]_i$ are observed at rest (see Cheng, Lederer & Cannell, Science, In press). These calcium sparks result from spontaneous (stochastic) gating of the SR ryanodine receptor since they are not directly dependent on calcium fluxes through sarcolemmal calcium channels but are affected by ryanodine, which (at low doses) increases their probability of occurance and time course. Using the line scan mode of the LSCM, we have examined sparks at their initiation site. The figure (left) shows the distribution of fluorescence associated with a spark at the time**

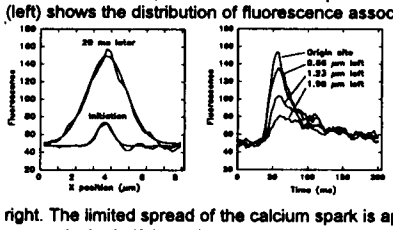


**of initiation (within the 2ms time resolution of the LSCM). 20 ms later the spark is approximately gaussian in profile with a half width of 2.7 μm. The time couse of the $[Ca]_i$ spark at various positions from its initiation site is shown on the right. The limited spread of the calcium spark is apparent as is its short time course (a the half time of decay of a normal $[Ca]_i$ transient is 160 ms).** **Supported by grants from the NIH, AHA and British Heart Foundation.**

M-Pos389

## TWO-SIDED SYMMETRY IN CARDIAC CA SIGNALING

((P. Lipp[1], J.Hüser[1,2], L. Pott[2] and E. Niggli[1])) [1]Dept. Physiology, University of Bern, Switzerland; [2]Dept. Cell Physiol; [3]Dept. Physiology, University of Bochum, Germany

In cardiac myocytes Ca release from the sarcoplasmic reticulum is the principal link in excitation-contraction coupling. The subcellular spatial organization of the SR network has been proposed to play an important role in this process. Indirect spatial information has been obtained by examining Na-Ca exchange currents ($I_{NaCa}$) activated by changes of [Ca] under the sarcolemma. In this study, subcellular spatial aspects of Ca-signaling in guinea-pig cultured atrial myocytes were investigated using ratiometric confocal microscopy with two Ca-indicators (Fluo-3 and Fura-Red). Membrane currents were measured with the whole-cell variant of the patch-clamp technique, the cells were dialyzed with a solution containing 60 mM citrate to partially uncouple SR Ca release from Ca influx. During trains of Ca currents different subcellular Ca release patterns were found to depend on the particular cell geometry. In spherical cells homogeneous Ca release alternated with failures and the relation between $I_{NaCa}$ and $[Ca]_i$ was unique. Additionally, in elongated cells linear Ca-waves propagating through the entire cell were observed. During wave propagation similar levels of subcellular [Ca] produced different $I_{NaCa}$ amplitudes depending on the particular subcellular region, giving rise to a variable relationship of $I_{NaCa}$ vs. [Ca]. The current was larger when the wave was near a cell end and smaller in the cylindrical cell body. In elongated cells propagation of Ca waves was frequently blocked by a subcellular unexcitable region (e.g. the nucleus), resulting in two components of $I_{NaCa}$. The results suggest a functional segmentation of the myocytes possibly arising from differences in the surface-to-volume ratio in different regions.

Supported by the SNF.

M-Pos390

## CELL GEOMETRY DETERMINES SUBCELLULAR CALCIUM SIGNALING IN SINGLE ATRIAL MYOCYTES

((J.Hüser[1,2], P.Lipp[1], L.Pott[3] and E.Niggli[1])) [1]Dept. of Physiology, University of Bern, Switzerland [2]Dept. of Cell Physiology; [3]Dept. of Physiology, Ruhr-University Bochum, Germany.

In cardiac myocytes release of Ca from the sarcoplasmic reticulum (SR) is mainly triggered by an influx of Ca through voltage-dependent Ca channels in the surface membrane. Spatial properties of Ca signaling were investigated in cultured guinea-pig atrial myocytes using ratiometric confocal Ca microscopy with a mixture of the fluorescent Ca-probes Fura-red and Fluo-3. Membrane currents were measured by means of the whole-cell patch-clamp technique. Cells were dialyzed with 60 mM citrate to partially uncouple SR Ca release from Ca influx. Under these experimental conditions activation of Ca current elicited two distinct types of Ca signals: Ca transients due to Ca influx via L-type Ca channels and transients caused by Ca release from the SR. With the confocal microscope subcellular regions could be identified which exhibited Ca entry transients of larger amplitude compared to the rest of the cell. During trains of repetitive Ca currents after a period of rest the first $I_{Ca}$ usually triggered a spatially homogeneous Ca release. Subsequent Ca currents frequently elicited Ca waves probably propagating by the CICR mechanism. It was a consistent finding that triggered or spontaneous Ca waves originated in subcellular regions characterized by large Ca entry transients. These regions were generally located at one or both ends of the myocyte, where the surface-to-volume (s/v) ratio is higher than in other cell segments. We propose that the diversity of the subcellular Ca signals results from the particular cell geometry. Local differences in the s/v-ratio cause spatially non-uniform Ca entry transients which locally determine the Ca loding state of the SR and provide the trigger signal for SR Ca release.

Supported by the SNF

M-Pos391

## MICRO-HETEROGENEITY OF SUBCELLULAR CA SIGNALING IN CARDIAC MYOCYTES: FOCAL RELEASE AND SPIRAL WAVES

((P. Lipp & E. Niggli)) Dept. of Physiology, University of Bern, Switzerland. (Spon. by W. Zhang).

The Ca-induced Ca release (CICR) mechanism is an important amplifier of signal transduction in heart muscle cells. This regenerative mechanism contributes to the Ca transient activating the mechanical contraction, but is also believed to drive Ca waves propagating within the cytosol. We investigated the subcellular Ca distribution in neonatal rat and adult guinea-pig ventricular myocytes using ratiometric confocal microscopy with a mixture of the fluorescent Ca indicators Fura-Red and Fluo-3. Resting cells in normal or elevated $[Ca]_o$ were found to exhibit spontaneous Ca release from the SR. Different patterns of subcellular Ca signals could be distinguished in individual myocytes: i) Focal Ca release with no or limited propagation; ii) Linear Ca waves propagating throughout the cell; iii) Spiral waves of Ca spinning around a nucleus or core-shifting along a subcellular region without entering it. Spontaneous transitions between the different release patterns were frequently observed, suggesting that a particular release pattern is not the property of an individual cell but reflects the functional state of the SR. The existence of focal release and refractory zones within a single cell suggests that the SR is not isotropic on the subcellular level. The SR seems to be composed of a network of SR elements, each of which can differ in its functional state with respect to CICR. The observed features of Ca signaling can be explained by a subcellular variability in the positive feedback of the CICR mechanism. The degree of positive feedback exhibited by a single SR element may depend on its Ca content.

M-Pos392

## CONFOCAL MICROSCOPIC DETECTION OF MEMBRANE POTENTIAL

((E. Niggli[1], J. Hüser[1,2] and P. Lipp[1])) [1]Dept. of Physiology, University of Bern, Switzerland. [2]Dept. of Cell Physiology, Ruhr-University Bochum, Germany.

The voltage-clamp technique has been widely used to control the membrane potential of cells. However, the voltage sensed by various proteins anchored in the cell membrane may be different because they are located inside the range of surface charge effects. During concentration changes of divalent cations (i.e. Ca) shifts of the surface potential profile are known to affect voltage-dependent proteins like ion channels and electrogenic transporters. Voltage-sensitive fluorescent dyes are inserted into the cell membrane and report the transmembrane field more directly. We used di-8-ANEPPS and di-4-ANEPPS and a confocal microscope in the line-scan mode to rapidly (up to 500 Hz) image the membrane potential which was simultaneously controlled by a voltage-clamp amplifier using whole-cell recording. Measurements in unexcitable SF9 cells revealed a linear relationship between voltage- and fluorescence-changes. When guinea-pig cardiac myocytes were voltage-clamped to evoke Na currents ($I_{Na}$), voltage-spikes were present on the optical voltage trace. These voltage spikes probably reflect changes of the transmembrane potential due to voltage-escape during the large $I_{Na}$, but may also contain a component arising from intracellular screening of surface charges by Ca accumulating under the sarcolemma. Ca has been proposed to enter via Na-Ca exchange after an increase of subsarcolemmal Na during the large $I_{Na}$. The results show that the membrane potential can be imaged with a confocal microscope and potential-sensitive probes. The technique may allow for the detection of surface-charge screening effects mediated by cations in the subsarcolemmal space.

M-Pos393

## MITOCHONDRIAL $Ca^{2+}$ OSCILLATIONS IN SINGLE LIVING CELLS REVEALED BY RHOD-2 AND LASER CONFOCAL MICROSCOPY.

((Mei-Jie Jou and Shey-Shing Sheu)) Department of Pharmacology, University of Rochester, 601 Elmwood Avenue, Rochester, NY 14642.

It has been proposed that the physiological role of mitochondrial $Ca^{2+}$ transport systems is to relay changes in the cytosolic free $Ca^{2+}$ concentration ($[Ca^{2+}]_c$) to the mitochondrial matrix to regulate the activities of mitochondrial dehydrogenases involved in oxidative metabolism. To test this hypothesis, the mitochondrial free $Ca^{2+}$ concentration ($[Ca^{2+}]_m$) must be measured in the intact living cell. In this study, cells were loaded with a cationic $Ca^{2+}$ dye, rhod-2 that localized primarily inside the mitochondria due to their negative membrane potential. The fluorescent signal of mitochondria was then detected using a laser confocal microscope that significantly reduced the undesired signal from out-of-focus planes. In cultured neonatal rat ventricular myocytes, when $[Ca^{2+}]_c$ was elevated by membrane depolarization or by $Na^+$-$Ca^{2+}$ exchange inhibition, the fluorescent signal of the mitochondrial area also increased to a peak factor of 1.78±0.20 (n=20) and 1.52±0.09 (n=7), respectively. During $[Ca^{2+}]_c$ oscillations that were induced by the spontaneous heartbeats, the fluorescent signal of mitochondria also oscillated concomitantly with a peak fluorescent intensity of 1.71±0.03 (n=77) fold higher than the baseline fluorescence. In addition, in the rat brain astrocyte cell line RBA-1, $[Ca^{2+}]_m$ responded to the oscillations of $[Ca^{2+}]_c$ induced by histamine with a peak fluorescent intensity of 1.78±0.13 (n=15) fold higher than the baseline fluorescence. We conclude that mitochondria of these two types of cells are able to relay oscillations of $[Ca^{2+}]_c$ into the matrix and, thus, may serve to regulate a variety of mitochondrial functions that have pronounced influences on cellular bioenergetics.

M-Pos394

## INTRA-SARCOMERE $[Ca^{2+}]$-GRADIENTS IN VENTRICULAR MYOCYTES REVEALED BY HIGH SPEED DIGITAL FURA-2 IMAGING

(G.Isenberg*, E.F.Etter, R.A.Tuft, F.S.Fay). Biomedical Imaging Group, UMMC, Worcester, MA 01605, *on leave from Dept. Physiology, Cologne, Germany

In mammalian ventricular myocytes, activator $Ca^{2+}$ is released through ryanodine-receptors of junctional and corbular SR localized in the I- but not the A-band of the sarcomere. Local SR $Ca^{2+}$ release should result in $[Ca^{2+}]$ gradients, at least at the onset of systole. In order to probe for the existence of $[Ca^{2+}]$ gradients we acquired 2 ms images of Fura 2 fluorescence at 351 and 383 nm in an UV laser-illuminated ultrafast digital imaging microscope. At 37 °C and 2 mM extracellular calcium, guinea-pig ventricular myocytes were potentiated by paired voltage clamp pulses. Images of 512x20 pixels were taken before and 10, 25, 40, 55, 70, 85, 100, 115 ms after start of the test-pulse to 10 mV. During initial 10 ms, mean $[Ca^{2+}]$ increased from 80 to 600 nM. $[Ca^{2+}]$ fluctuations, superimposed on this value, were correlated with the striations seen in the through-light image. Within the 0.3 µm pixel resolution, $[Ca^{2+}]$ was 100 -120 nM higher at the level of the I-band than at the A-band. This intra-sarcomere $[Ca^{2+}]$ gradient decayed 25 ms after start of the clamp step. 20 mM BAPTA in the electrode solution suppressed both systolic rise and intra-sarcomere $[Ca^{2+}]$ gradients. Autofluorescence shows a reversed intensity (higher at the A- than the I-band) and much smaller amplitude. Thus the observed $[Ca^{2+}]$ gradients appear to reflect real heterogeneities in $[Ca^{2+}]$ during excitation-contraction coupling.

**M-Pos395**

MULTIFUNCTIONAL CALCIUM/CALMODULIN-DEPENDENT PROTEIN KINASE (CAMK) MEDIATES CALCIUM-DEPENDENT AUGMENTATION OF CALCIUM CURRENT IN RABBIT VENTRICULAR MYOCYTES. ((Mark E. Anderson and Andrew P. Braun)) Stanford University School of Medicine, Stanford, CA 94305

Elevation of intracellular Ca2+ can augment the inward Ca2+ current (ICa) in cardiac myocytes. To examine the potential role of CaMK in ICa augmentation, isolated adult rabbit ventricular myocytes were dialyzed with peptide inhibitors derived from the regulatory domain of CaMK using whole cell voltage clamp. Ca2+ release by flash photolysis of Nitr-5 augmented peak ICa by 38.9%±5.2% above pre-flash levels. Dialysis of cells with CaMK derived peptides had no effect on Nitr-5 Ca2+ release, as shown by simultaneous Fluo-3 fluorescence. Ca2+-dependent augmentation of peak ICa was significantly less in cells dialyzed with CaMK inhibitory peptides derived from the pseudo-substrate region (13.2%, P=0.025) or the calmodulin binding region (3.2%, P=3x10-5); an inactive control peptide had no effect on Ca2+-dependent augmentation. These peptide inhibitors were selective, as they did not abolish the subsequent β-adrenergic enhancement of ICa. Peak ICa following flash was not significantly different from control levels (23.8%, P=0.101) in cells dialyzed with a pseudo-substrate inhibitory peptide derived from protein kinase C. These findings implicate CaMK in the mediation of Ca2+-dependent augmentation of cardiac ICa.

**M-Pos396**

L-TYPE CALCIUM CURRENT CHARACTERISTICS IN CARDIAC VENTRICULAR MYOCYTES WITH AND WITHOUT THE T TUBULES. ((K. Bogdanov, A.M. Janczewski, B.D. Ziman, H.A. Spurgeon and E.G. Lakatta)) Gerontol. Res. Ctr., NIA, Baltimore, MD 21224. (Spon. by M. C. Capogrossi).

Detailed histologic studies have shown that avian ventricular myocytes are devoid of the T tubules and that in strains such as the Finch (F), only about 20% of the sarcoplasmic reticulum (SR) forms junctions with the sarcolemma. We compared Ca current ($I_{Ca}$), the putative trigger for SR $Ca^{2+}$ release in mammalian cells, i.e. rat (R) myocytes with that in the F. Cell capacitance was 50 ± 4 pF (n=25) in F vs 145 ± 8 pF (n=38) in R. In cells bathed in 1 mM $Ca_o$ at 22° C, maximum $I_{Ca}$ density during voltage clamp from -45 mV (10 mM EGTA in pipette) averaged 10.5 ± 0.3 pA/pF in F (n=19) vs 6.9 ± 0.6 in R (n=21). $I_{Ca}$ inactivation kinetics also differed between F and R (Fig. 1): in F, the fast time constant of $I_{Ca}$ decay averaged 4.6 ± 0.3 ms vs 13.4 ± 1.3 ms in R; the slow $\tau$ for $I_{Ca}$ decay did not differ in F and R, and averaged 68 ± 6 and 66 ± 7 ms, respectively. The calculated $I_{Ca}$ time integral following depolarization increased more rapidly in F than in R (Fig. 2). These differences in $I_{Ca}$ characteristics between F and R may be of significance with respect to the coupling of excitation to SR $Ca^{2+}$ release in F and R cells, which vary markedly in size and structure.

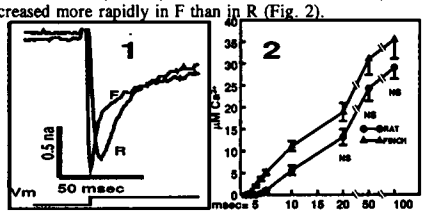


**M-Pos397**

DISTINCT VOLTAGE AND $Ca^{2+}$ DEPENDENT FACILITATION OF $I_{Ca}$ BY $Ca^{2+}$/CALMODULIN KINASE II IN CARDIAC MYOCYTES. ((R.-P. Xiao, H. Cheng, W.J. Lederer, T. Suzuki, and E.G. Lakatta)) Gerontology Research Center and University of Maryland, Baltimore, MD 21224.

While $Ca^{2+}$ dependent facilitation of L-type $Ca^{2+}$ channel current, $I_{Ca}$, has been described, a distinct voltage (V) dependence has not been established. In voltage clamped rat ventricular myocytes we found that a pure V stimulus (prepulse from -90 to +100 mV in the absence of $Ca^{2+}$ influx) potentiated $I_{Ca}$ amplitude and slowed its inactivation (Fig. A); these effects persisted with a $\tau$ of 1.7 sec. and were not blocked by BAPTA in pipette. A mixed Ca + V stimulus (prepulse from -90 to 0mV) had similar effects but these persisted with a $\tau$ of 9 sec. and were blocked by BAPTA. The V dependent facilitation (Fig. B) as well as the $Ca^{2+}$/V facilitation was blocked by a specific peptide inhibitor of CaMKII. Using confocal microscopy we found that autophosphorylated CaMKII is localized near sarcolemmal membranes and changes in its fluorescence due to $Ca^{2+}$/V stimuli are correlated with changes in $I_{Ca}$. Thus, the facilitation of the $I_{Ca}$ in heart constitutes a CaMKII-specific short-term memory of both previous membrane depolarization and of increased $[Ca^{2+}]_i$ and may provide a general model for the regulation of $I_{Ca}$ in excitable cells.

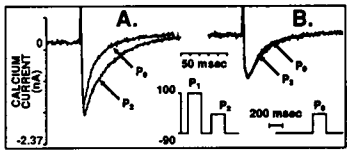


**M-Pos398**

EFFECT OF VOLATILE ANESTHETICS ON CARDIAC CALCIUM CURRENT KINETICS ((J.J. Pancrazio, and C. Lynch III)) Dept. of Anesthesiology, Box 238, University of Virginia, Charlottesville, VA 22908. Supported by a NIH grant R01-31144 to CL and a NRSA to JJP.

The inhalational anesthetic halothane has been shown to depress myocardial contractility in a dose-dependent manner in a variety of preparations. Recently, Bosnjak *et al.* [1] directly demonstrated anesthetic-induced reductions in the magnitude of voltage-activated Ca current of canine ventricular myocytes utilizing Ba as the charge carrier in place of Ca. We compared the effects of halothane and isoflurane on cardiac whole cell currents carried by either Ba ($I_{Ba}$) or by Ca ($I_{Ca}$). Isolated guinea pig ventricular myocytes were immersed in a bathing solution containing (in mM): 125 CsCl, 20 tetraethylammonium (TEA)-Cl, 1 $MgCl_2$, 2 $CaCl_2$ or $BaCl_2$, 10 HEPES, 2 mg/l tetrodotoxin, pH 7.4. Heat-polished patch pipettes were filled with a solution containing: 120 CsCl, 20 TEA-Cl, 11 EGTA-CsOH, 1 $CaCl_2$, 5 Mg-ATP, 10 HEPES, pH 7.3. Anesthetics were equilibrated in the bathing solution by bubbling filtered air through a calibrated vaporizer for at least 15 min and verified by gas chromatography. Application of halothane produced a similar dose-dependent depression of the peak magnitude of both $I_{Ca}$ and $I_{Ba}$ and increased the rate of inactivation. Halothane at 0.75% and 2.25% (0.40 and 1.40 mM) significantly decreased peak $I_{Ca}$ and $I_{Ba}$ by 29 ± 4% and 59 ± 3%. Equimolar concentrations of isoflurane depressed peak $I_{Ca}$ and $I_{Ba}$ to a lesser extent than halothane, although similar changes in $I_{Ca}$ inactivation were observed. The inactivation phase was well-fitted to the sum of a slow and a fast exponential decay function: $A_S\exp(-t/\tau_S)+A_F\exp(-t/\tau_F)$, consistent with the view that there are at least two pathways for Ca channel gating [2]. Under control conditions, slow time constant ($\tau_S$) ranged from 120-1000 msec and the faster $\tau_F$ ranged from 10-60 msec. Both halothane and isoflurane decreased the magnitude of the slow component ($A_S$) and reduced $\tau_S$. In contrast, comparatively little effect was observed on the fast component ($A_F$ or $\tau_F$). Reductions in $\tau_S$ may be partially attributed to shifts in steady-state inactivation; 1.5% halothane produced a slight (~3 mV) hyperpolarizing shift, whereas the voltage shift in the presence of 2.5% isoflurane was more pronounced (~8 mV). Enhanced buffering of intracellular Ca using BAPTA in place of EGTA partially inhibited the effect of halothane on $\tau_S$, however use of BAPTA had little effect on the isoflurane-induced change in $\tau_S$. A simple gating model is proposed to describe anesthetic-induced alterations in Ca channel inactivation kinetics.

[1] Bosnjak, *et al.* (1991) *Anesthesiol.* 74: 340. [2] Richard, *et al.* (1990) *Am. J. Physiol.* 258: H1872.

**M-Pos399**

T- AND L-TYPE CALCIUM CURRENTS AND EXCITATION-CONTRACTION COUPLING IN ISOLATED CARDIAC PURKINJE CELLS. ((Zhengfeng Zhou, Craig T. January)) Dept. of Medicine. University of Chicago, Chicago, IL 60637. (Spon. by A. Undrovinas)

Two types of $Ca^{2+}$ channels (T and L) have been found in many cardiac myocytes. In cardiac Purkinje cells T-type $Ca^{2+}$ current ($I_{Ca,T}$) is relatively larger compared to ventricular cells. The role of $I_{Ca,T}$ in cardiac Purkinje cells, however, is unknown. We used the amphotericin perforated-patch method to study the roles of $I_{Ca,T}$ as well as L-type $Ca^{2+}$ current ($I_{Ca,L}$) in excitation-contraction (E-C) coupling in isolated canine Purkinje cells. Cell shortening was monitored using an edge detector. $Na^+$ channel current was eliminated by using $Na^+$-free external solution and 10 μM TTX, and $[Ca^{2+}]_o$ was 1.8 mM. Under these conditions, from a holding potential of -80 mV, depolarizing clamp pulses to voltages between -50 and -30 mV elicited $I_{Ca,T}$ and contractions. The contractions were characterized by delay in onset, slow rate of shortening and reduced peak shortening. $I_{Ca,T}$ at these voltages was confirmed by replacing $Ca^{2+}$ with $Ba^{2+}$ as the charge carrier. Clamp steps to more positive voltages elicited $I_{Ca,L}$ and a different type of contraction. The onset of contraction occurred sooner, the rate of shortening became faster and amplitude was larger. Low concentrations (100-200 μM) of $Ni^{2+}$ inhibited $I_{Ca,T}$, decreased contraction amplitude and further delayed the onset of contraction at the $I_{Ca,T}$ voltage range. When $I_{Ca,T}$ and $I_{Ca,L}$ were abolished by removing $Ca^{2+}$ from external solution or by using high concentrations of both $Ni^{2+}$ and $Cd^{2+}$, no contractions were elicited by depolarizing clamp steps. Ryanodine (1μM) abolished contractions at all voltage ranges, however, the contractions elicited by $I_{Ca,T}$ were abolished first. These results suggest that under our experimental conditions both $I_{Ca,T}$ and $I_{Ca,L}$ contribute to E-C coupling in cardiac Purkinje cells.

**M-Pos400**

THE EFFECTS OF NiCl ON INTRACELLULAR $Ca^{2+}$ $Na^+$ AND $H^+$, DURING METABOLIC INHIBITION IN RAT VENTRICULAR CELLS. ((Simon M. Harrison & Mathew K. Lancaster)) Department of Physiology, University of Leeds, Leeds LS2 9NQ, U.K.

Metabolic inhibition (MI) was induced in freshly isolated rat ventricular myocytes by perfusion with a solution containing 5 mM deoxyglucose, 1 mM iodoacetic acid and 2 mM sodium cyanide (pH 7.4 at 36°C). The cells were paced at 1 Hz and contractions and either intracellular $Ca^{2+}$, $Na^+$ or pH ($Ca_i$, $Na_i$, $pH_i$) measured from the fluorescence of Fura-2, SBFI or BCECF, respectively. Contractile responses to MI were similar to those observed previously i.e. an initial small negative inotropic effect followed by a more sustained positive inotropic effect, followed by contractile failure. Following the failure of evoked contractions the cells remained relaxed for a short period before a contracture developed. The effects of NiCl (5 mM) on the contracture and intracellular ion levels was studied. The addition of 5 mM NiCl during the early phase of the contracture led to: i) a rapid fall of $Ca_i$; ii) the relaxation of the contracture, iii) a rapid decrease in $Na_i$ and iv) a rapid increase in $pH_i$. The effects of NiCl on $pH_i$ persisted in the presence of 1 mM amiloride suggesting that the rise of $pH_i$ was not mediated via Na-H exchange. One possible interpretation of these data is that the NiCl-induced fall of $Ca_i$ (due to block of Na-Ca exchange) releases Ca-H binding sites which are taken by protons. This would deactivate the Na-H exchanger such that the influx of $Na^+$ associated with proton extrusion is reduced allowing $Na_i$ to fall. Preincubation with Amiloride significantly delayed the onset of contractile failure and the subsequent contracture during metabolic inhibition. This may reflect the ability of amiloride to partially block Na-Ca exchange at the dose used (1 mM). *Supported by The Wellcome Trust.*

**M-Pos401**

DEVELOPMENTAL DIFFERENCES IN SARCOPLASMIC RETICULUM AND SODIUM-CALCIUM EXCHANGER FUNCTION IN RABBIT VENTRICULAR MYOCYTES. ((T.K. Chin, M.C. Barruga and W.H. Barry))
University of Utah, Salt Lake City, UT 84132. (Spon. by K.W. Spitzer)

The sarcoplasmic reticulum (SR) is rudimentary in the immature rabbit heart. To evaluate the functional importance of the $Na^+$-$Ca^{2+}$ exchanger and SR during development, contractions were measured in ventricular myocytes isolated from neonatal (ages 3-5 days) and adult (ages 8-10 weeks) rabbits. Using the whole cell disrupted patch clamp technique, cell shortening was measured at 32° C. during 2 second, 90 mV clamp steps from a holding potential of -80 mV. In adult cells (n=6) both phasic and tonic components of contraction were observed, and the phasic component was eliminated by 10 mM caffeine. In neonatal cells (n=8) only a single component of contraction was apparent during the clamp pulse, and the amplitude of contraction was unchanged by caffeine. SR-dependent relaxation was compared in neonatal and adult myocytes. Contractions were obtained by field stimulation ($C_{FS}$) or by rapidly switching to a solution containing (in mM) 145 $K^+$, 0 $Na^+$ and 0 $Ca^{2+}$ ($C_{RS}$). During $C_{RS}$, the cells were depolarized by high external $K^+$, and $Na^+$-$Ca^{2+}$ exchange was disabled simultaneously by 0 $Na^+$. Compared to relaxation after $C_{FS}$, relaxation after $C_{RS}$ in adult myocytes (n=6) was minimally changed. In contrast, relaxation following $C_{RS}$ in neonatal myocytes (n=7) was markedly delayed relative to relaxation following $C_{FS}$, indicating an increased dependence on the $Na^+$-$Ca^{2+}$ exchanger. These data support developmental differences in the contributions of the SR and $Na^+$-$Ca^{2+}$ exchanger to contraction and relaxation in rabbit myocardium. In neonates as compared to adults, the SR contributes less to contraction. Neonates also show an increased dependence on the $Na^+$-$Ca^{2+}$ exchanger for relaxation. (Supported by NIH Grant HD27827.)

**M-Pos402**

RAPID COOLING OF VOLTAGE-CLAMPED GUINEA-PIG CARDIAC MYOCYTES PRODUCES AN INWARD CURRENT WHICH COULD BE ATTRIBUTABLE TO Na/Ca EXCHANGE.
((R.U. Naqvi, C.M.N. Terracciano and K.T. MacLeod)) Natl Heart & Lung Inst, Dept Cardiac Medicine, University of London, London SW3 6LY, U.K

Rapid cooling of a cardiac cell from room temperature to 1 °C in < 1 sec causes a release of calcium from the SR and a cell contracture which is maintained due to the cold-induced slowing of the main mechanisms responsible for calcium removal and cell relaxation. A gradual decline in $[Ca]_i$ is often observed during the cooling period but full recovery of diastolic $[Ca]_i$ (and hence cell length relaxation) only occurs upon rewarming as the cold-induced suppression of SR Ca ATPase and Na/Ca exchange activity is removed. We found that cooling cells voltage-clamped at -80mV resulted in a maintained inward current [amplitude 84.3 ± 1.1 pA (mean ± SEM) n = 10]. Rewarming the cell resulted in a recovery of this current [time to 50% recovery (R50); 1.5 ± 0.1s]. The R50 of the associated decline in the indo-1 signal was 1.1 ± 0.1s (mean ± SEM). Repeating the protocol in a Na-free, Ca-free solution abolished this inward current whilst the addition of 10mM caffeine to the cooling and rewarming solutions resulted in an inward current of similar amplitude that first partially recovered upon rewarming then induced further transient inward current. These findings suggest that an inward current, dependent upon $Na_o$ and $Ca_o$, exists during cooling.

**M-Pos403**

ACIDOSIS AFFECTS $Na^+/Ca^{++}$ EXCHANGE BY INCREASING $Na^+$ VIA $Na^+/H^+$ EXCHANGE IN GUINEA-PIG VENTRICULAR MYOCYTES.
((C.M.N. Terracciano and K.T. MacLeod)) Natl Heart & Lung Inst, Cardiac Medicine, University of London, Dovehouse St, London SW3 6LY, U.K

The ability of $Na^+/Ca^{++}$ exchange to extrude $Ca^{++}$ from guinea-pig ventricular myocytes during intracellular acidosis was studied. In voltage-clamped cells, rapid application of 10 mM caffeine elicited a transient increase in Indo-1 fluorescence and a transient $Na_o$ and Ni-sensitive inward current. Under such conditions the rate of decline of $[Ca^{++}]_i$ is an index of $Na^+/Ca^{++}$ exchange activity. Using the $NH_4Cl$ rebound technique (15mM) we obtained an intracellular acidosis. In this condition (A) the decline of $[Ca^{++}]_i$ was significantly slower than in control (C) [C-$t_{50}$=0.73±0.03s (mean ± SEM); A-$t_{50}$=0.86±0.03s, n=7; p=0.014]. We also observed a slower decay of the transient inward current during acidosis [C-$t_{50}$=0.31±0.03s; A-$t_{50}$ = 0.48±0.06s, n=11; p=0.012]. To test whether such an effect was due to a direct effect of protons on the exchanger or to an increase in $[Na^+]_i$ brought about by $Na^+/H^+$ exchange, the effect of 1mM amiloride (Am) was investigated. In the presence of Am, which inhibits $Na^+/H^+$ exchange, the decay of the transient inward current was unchanged. [C-Am-$t_{50}$ = 0.45±0.05; A-Am-$t_{50}$=0.43±0.05, n=11; p=0.849]. We conclude that acidosis affects the activity of $Na^+/Ca^{++}$ exchange mainly by increasing $[Na^+]_i$ via $Na^+/H^+$ exchange.

## SMOOTH MUSCLE E-C COUPLING

**M-Pos404**

SARCOPLASMIC RETICULUM PROTEINS: DISTRIBUTION AND ABUNDANCE OF CALRETICULIN, $Ca^{2+}$-ATPASE AND BiP IN AORTIC AND CORONARY SMOOTH MUSCLE CELLS. ((D.M. Berman, T. Sugiyama, S.E. Cala and W.F. Goldman)) Dept. Physiol., Univ. Maryland Med. Sch.; GRECC, Baltimore VAMC, Baltimore, MD 21201 and Dept. Med., Indiana Univ. Sch. Med., Indianapolis, IN 46202.

Three markers of SR proteins were used to characterize and compare the SR $Ca^{2+}$ stores in cultures of rat aortic and coronary arterial myocytes. Using standard immunoblotting techniques with antisera directed against calreticulin, SR $Ca^{2+}$-ATPase, and BiP (Immunoglobulin heavy chain-binding protein) we determined the presence and compared the relative abundances of each of these proteins in both cell types. The 3 SR markers were readily observed and no differences in the relative abundances of the proteins were found between homogenates of the two cell types. On the other hand, in enriched crude microsomes, the abundance of SR proteins was greater in aortic than coronary preparations, likely reflecting the presence of more SR in aortic than coronary cells. In addition, the intracellular distributions of calreticulin and $Ca^{2+}$ATPase were dermined by examining deconvolved images of the distributions of the fluorescently labeled SR proteins. In both aortic and coronary cells, calreticulin labeling was uniform and appeared as a dense, reticular network of tubules (0.3-0.6 μm in diameter) which were most concentrated in the perinuclear region, and became more sparce toward the periphery. The labeling of $Ca^{2+}$-ATPase was similar to calreticulin in the perinuclear region, but was punctate in the periphery suggesting that $Ca^{2+}$ATPase was selectively localized to specific SR regions those areas of the cells.

**M-Pos405**

CALMODULIN DEPENDENT PROTEIN KINASE II IS RESPONSIBLE FOR A PERSISTENT ACCELERATION OF $Ca^{2+}$ REMOVAL IN SMOOTH MUSCLE.
R.M. Drummond, J.G. McCarron*, M. Ikebe†, J.V. Walsh Jr., and F.S. Fay. Department of Physiology, UMMC, Worcester, MA 01605, *Institute of Physiology, University of Glasgow, U.K. and †Case Western Reserve, Cleveland, OH 44106.

The increase in intracellular $Ca^{2+}$ concentration ($[Ca^{2+}]_i$) that occurs in response to stimulation is known to exert feedback on both $Ca^{2+}$ influx and reuptake processes. It has been shown that following a train of depolarizing pulses there is a persistent enhancement of the rate of removal of $Ca^{2+}$ from the cytoplasm (Science 244 211-214). The aim of the current study was to determine the biochemical pathway involved, and to identify the targeted removal mechanism. Freshly isolated smooth muscle cells from the stomach of *Bufo marinus* were loaded with the ratiometric $Ca^{2+}$ indicator Fura-2 and studied using tight-seal, whole-cell recording. $[Ca^{2+}]_i$ was increased by a 300 msec depolarization to +10 mV and $Ca^{2+}$ removal was then examined following repolarization to the holding potential of -110 mV. The rate of removal, calculated for a 300 msec depolarization pulse, was increased at all $[Ca^{2+}]_i$ when the stimulus was applied 15 sec after a train of depolarizations (-110 to +10mv; 2 pulses $sec^{-1}$). In the presence of ryanodine, thapsigargin or cyclopiazonic acid, cells continued to show an acceleration of the rate of removal suggesting that an enhanced reuptake by the sarcoplasmic reticulum is not responsible. When extracellular $Na^+$ was substituted for $Li^+$, cells continued to show an enhancement of $Ca^{2+}$ removal following the train; thus, the $Na^+$-$Ca^{2+}$ exchanger is not responsible. When cells were microinjected with CK3AA, a pseudo-substrate inhibitory peptide of CaM kinase II, the persistent enhancement of the rate of $Ca^{2+}$ removal which normally occurs following the train was inhibited. However, cells microinjected with CONCK3AA, a nearly identical but biologically inactive peptide continued to show enhanced removal following the train. These results indicate that CaM dependent protein kinase II is able to produce a persistent acceleration of $Ca^{2+}$ removal, thereby producing a more rapid return of $[Ca^{2+}]_i$ to resting levels. (Supported by NIH grant HL14523).

**M-Pos406**

**MITOCHONDRIA IN SMOOTH MUSCLE CELLS SEQUESTER $Ca^{2+}$ FOLLOWING STIMULATION OF CELL CONTRACTION.**

T.C.H. Mix, R.M. Drummond, R.A. Tuft and F.S. Fay. Biomedical Imaging Group, UMMC, Worcester, MA 01605.

The role of mitochondria in removing cytosolic $Ca^{2+}$ under conditions of extreme $Ca^{2+}$ overload is well established, but there is increasing evidence that mitochondria are involved in shaping the cellular $Ca^{2+}$ response during physiological stimulation. We have found that the mitochondrial inhibitors FCCP and cyanide significantly affected $Ca^{2+}$ reuptake in gastric smooth muscle cells from Bufo marinus, in which $[Ca^{2+}]_i$ was measured with Fura-2 while membrane potential was controlled via a patch pipette. Specifically, these inhibitors slowed reuptake of $Ca^{2+}$ following brief stimulation and prevented enhancement of rates of $Ca^{2+}$ removal, normally seen following higher, prolonged increases in cytoplasmic $[Ca^{2+}]$ (Science 244 211-214). As ATP was present in the patch pipette, the observed effects of the inhibitors suggested that mitochondria in smooth muscle may play a direct role in $Ca^{2+}$ removal. We have recently used the calcium sensitive indicator, rhod-2, to directly measure fluorescence changes in individual mitochondria with a high speed digital imaging microscope. Using this system, cells were imaged in seven focal planes at 20 msec intervals. The resultant images were processed using a constrained iterative deconvolution algorithm to move fluorescence back to its point of origin in the 3-D image, thereby making possible more accurate measurements of intensity changes within mitochondria. During stimulation with KCl (131 mM), caffeine (20 mM) or depolarization via patch pipette, the cell contracted and the fluorescence was seen to increase in mitochondria in 11 of 11 cells. These data suggest that mitochondria in smooth muscle are capable of sequestering $Ca^{2+}$, at least transiently, during physiologic stimulation. As mitochondria have been localized principally to the periphery of smooth muscle cells by the potentiometric fluorescent indicator TMRE, we suggest that the $Ca^{2+}$ taken up initially by mitochondria, following a rise in $[Ca^{2+}]_i$, may be transferred subsequently to $Ca^{2+}$ pumps of the nearby SR or plasma membrane. (Supported by HHMI Research Fellowship for Medical Students to TCHM and NIH grant HL14523 to FSF).

**M-Pos407**

**EFFECTS OF NEUROKININ A AND VASOPRESSIN ON CYTOSOLIC $CA^{2+}$ CONCENTRATION AND CONTRACTION IN COLONIC SMOOTH MUSCLE.** ((K. Sato, R. Leposavic, N.G. Publicover, W.T. Gerthoffer and K.M. Sanders)) Dept. of Physiology, Univ. of Nevada School of Medicine, Reno, NV 89557. (Sponsored by K.M. Sanders)

It is well known that contraction of smooth muscles is regulated by cytosolic $Ca^{2+}$ concentration ($[Ca^{2+}]_i$), but $[Ca^{2+}]_i$ is not the only determinant of contraction. Other mechanisms, besides the regulation of $Ca^{2+}$ homeostasis, are known to affect contractile force. We examined the effects of neurokinin A (NKA), a neuropeptide, and vasopressin (AVP), an excitatory endocrine substance, on the $Ca^{2+}$-tension relationship in canine colonic muscles loaded with fura-2 to measure changes in $[Ca^{2+}]_i$ or permeabilized by staphylococcal $\alpha$-toxin. NKA (1 nM to 0.3 $\mu$M) increased $[Ca^{2+}]_i$ and force in a dose-dependent manner. Higher concentrations of NKA (0.1 and 1 $\mu$M) induced contraction, but reduced $[Ca^{2+}]_i$. In the presence of high external $K^+$ (70 mM), NKA (0.5 $\mu$M) increased contractile force but decreased $[Ca^{2+}]_i$. The data suggest that NKA can increase force production of colonic muscles via a $Ca^{2+}$-sensitizing effect. AVP (1 pM to 0.1 nM) caused a dose-dependent increase in $[Ca^{2+}]_i$ and force without an obvious $Ca^{2+}$-sensitizing effect. Pre-incubation of muscles with threshold concentrations of NKA sensitized the muscles and increased responses to acetylcholine. Thus, a background of excitatory neuropeptides may increase motor responses to other excitatory agents. In $\alpha$-toxin permeabilized muscle, NKA (1 $\mu$M) with GTP (10 $\mu$M) increased $Ca^{2+}$-contraction and GDP-$\beta$S (10 $\mu$M) inhibited this contraciton. AVP (1 pM and 10 pM), however, had no significant effect on $Ca^{2+}$-contraction. These data suggest that the integrated output of colonic motor function results from several agonists regulating both $[Ca^{2+}]_i$ and the sensitivity of the contractile apparatus to $Ca^{2+}$ via G-proteins. (Supported by NIH DK 41315.)

**M-Pos408**

SYNERGISTIC INTERACTIONS IN SMOOTH MUSCLE BETWEEN $\alpha$-ADRENOCEPTOR MEDIATED RESPONSES AND THE EFFECTS OF ANGIOTENSIN II. ((X-F. Li, B.G. Allen, M.P. Walsh, and C.R. Triggle)) Departments of Pharmacology & Therapeutics and Medical Biochemistry, University of Calgary, AB, Canada, T2N 4N1. (Spon. by W.C. Cole)

Pressor responses in the absence or presence of angiotensin were recorded in the pithed rat. Intracellular $Ca^{2+}$ levels ($[Ca^{2+}]_i$) using fura-2, were measured in freshly dispersed single smooth muscle cells from the rat tail artery. Tension and myosin light chain phosphorylation measurements were obtained from ring preparations of the rat tail artery. Pressor subthreshold concentrations of angiotensin II (AII) did not potentiate responses to cirazoline ($\alpha_1$-agonist) or BHT933 ($\alpha_2$-agonist) unless the rat had been pretreated with the angiotensin-converting enzyme inhibitor, captopril. In isolated cells, low subthreshold concentrations of AII (10nM) enhanced the $[Ca^{2+}]_i$ signal obtained with BHT933, but only marginally enhanced the response to cirazoline. The effects of AII were inhibited by the protein kinase C (PKC) inhibitor, H7. In isolated ring preparations, 10 nM AII did not initiate tension development but did significantly enhance 20 kDa myosin light chain phosphorylation [MLCP]. This enhancement was inhibited by the PKC inhibitor, staurosporine. AII (10nM) also significantly enhanced BHT933, but not cirazoline, induced MLCP and the enhanced tension and MLCP was inhibited by either H7 or staurosporine. We conclude that AII contributes to the pressor responses mediated by postsynaptic $\alpha_1$ and $\alpha_2$ adrenoceptor activation by a PKC-mediated process involving enhanced $[Ca^{2+}]_i$ and MLCP. Supported by the Alberta Heart & Stroke Foundation and the MRC.

**M-Pos409**

IMMUNOGOLD LOCALIZATION OF CALSEQUESTRIN AND INOSITOL 1,4,5-TRISPHOSPHATE RECEPTORS IN SMOOTH MUSCLE ((G.F.Nixon, G.A.Mignery*, T.C.Sudhof* and A.V.Somlyo)) Dept. Molec. Physiology & Biological Physics, Univ. of Virginia Med. Center, Charlottesville, VA 22908, *Dept. Molec. Genetics, Univ. of Texas Southwestern Med. Center, Dallas TX 75235

The purpose of this study was to provide correlated information about the $Ca^{2+}$-releasing action of $IP_3$ and the distribution of the sarcoplasmic reticulum (SR), its $IP_3$ receptors and the luminal calcium binding protein calsequestrin (CSQ) in smooth muscle. The SR, selectively stained with osmium ferricyanide in guinea pig vas deferens, a phasic smooth muscle, was present at peripheral sites in close apposition to the plasma membrane and also included a small component of central, perinuclear SR. Strips of vas deferens permeabilized with $\beta$-escin in which the SR was preloaded with $Ca^{2+}$ contracted in response to caffeine (25mM), $IP_3$ (100mM), but not to cyclic ADP-ribose (100mM). Silver enhanced immunogold labeling(1.4nm gold particle covalently attached to a Fab' fragment) of primary antibodies to CSQ or to $IP_3$ showed the presence of the $IP_3$ and CSQ antibodies both at the peripheral and the central SR. Caveolae, mitochondria, nuclear and plasma membrane were not stained by either antibody. Cryosections of guinea pig aorta were similarly labeled (peripheral and central SR) with the anti-$IP_3$ antibody, but not with the anti-CSQ antibody. The (tonic) aortic smooth muscle contained a much larger volume of central SR at the nuclear pole than the phasic smooth muscle as reported in previous studies. In conclusion, we find $IP_3$ receptors present in peripheral and central SR in both guinea pig vas deferens and aortic smooth muscle, and confirm the presence of CSQ in vas deferens, but not in the SR of aortic smooth muscle. Supported by AHA fellowship (to GFN) and by PO1HL48807.

**M-Pos410**

TRACHEAL MUSCLE STIFFNESS DURING TONIC CONTRACTIONS GRADED BY CHANGES IN MUSCLE LENGTH OR BY ACETYLCHOLINE CONCENTRATION. ((Susan Gunst, Michael Rowe, Richard Meiss, and Ming-Fang Wu)). Dept. of Physiol. and Biophysics, Indiana Univ. Sch. Medicine, Indianapolis, IN 46202-5120.

The relationship between muscle stiffness and active force has been used to assess the proportion of attached crossbridges which contribute to active force generation in smooth muscle tissues. We measured tracheal muscle stiffness continuously during tonic contractions induced by acetylcholine (ACh) by imposing 25 micron, 40 Hz length oscillations on tracheal smooth muscle strips and measuring the force perturbation amplitude. Stiffness did not increase proportionally with force during force development, suggesting that the proportion of attached crossbridges contributing to force generation was increasing. However, during the plateau phase of contraction, the stiffness/force ratio (S/F ratio) was higher than during force development and continued to increase while force remained constant, suggesting a continuous decline in the proportion of attached crossbridges contributing to force maintenance. The S/F ratio during the plateau phase of contraction was lower at longer lengths of isometric contraction, suggesting that a higher proportion of attached crossbridges contribute to force maintenance at longer muscle lengths. Similar results were obtained when [ACh] was increased at constant muscle length, suggesting that a higher proportion of attached crossbridges contribute to force maintenance at higher levels of contractile activation. Cytostructural remodeling during activation under different conditions might also contribute differences in the S/F ratio. Supported by HL29289.

**M-Pos411**

EFFECTS OF HYPOXIA ON INTRACELLULAR CALCIUM CONCENTRATION IN SMALL PULMONARY ARTERIES ISOLATED FROM RATS. ((1E. Fermin, 2,3J.R. Lopez, 3P. Allen, 2C. Perez, 2H. Padrino)). 1Hospital de Clinicas Caracas, 2CBB, IVIC, Caracas, Venezuela. 3Department of Anesthesia Brigham and Women Hospital Boston, MA.

Hypoxia induces contractile responses in rat pulmonary arteries (Agrawal et al. 1992). We measured $[Ca^{2+}]_i$ during acute episodes of hypoxia. Sprague Dawley rats (200-250 g) were anesthetized with a mixture of $O_2$-$CO_2$ and halothane 2% and the heart and lungs were removed. The small pulmonary artery (SPA 100-300 $\mu$m) were dissected and mounted as rings preparation on the stage of a fluorescence microscope. SPA were loaded with fura-2, by incubation in fura -2 AM for 2 h at 37° C. Hypoxia was induced by gassing the bath with a mixture of 95% $N_2$ and 5% $CO_2$ for 10,15,30, or 45 minutes. Hypoxia induced a transient rise in the $[Ca^{2+}]i$ whose amplitude was related to the duration of hypoxia episode. The fura ratio (340/380) increased from 0.95 pre-hypoxia (n=12) to 1.05 at 15 min (n=7), 1.35 at 30 min (n=6), and 1.49 at 45 min (n=5) of hypoxia. Incubation in nitrendipine 5 $\mu$M blocked by 71% the changes in [Ca2+]i observed during hypoxia. After reoxygenation the $[Ca^{2+}]_i$ returned to the pre-hypoxia levels. These results show that acute episodes of hypoxia in SPA are related to transient increase in myoplasmic calcium concentration.(Partially supported by Parke Davis of Venezuela)

**M-Pos412**

ACTIONS OF POLYAMINES ON CONTRACTION IN SMOOTH MUSCLE
((P. Hellstrand, M. Gomez, B.-O. Nilsson, I. Nordström and K. Swärd)) Dept of Physiology and Biophysics, Univ of Lund, Sweden.

Polyamines (putrescine, spermidine, spermine) are associated with cellular growth and differentiation, but in addition have diverse actions, mainly thought to involve interaction of these positively charged molecules with negatively charged sites on phospholipids and proteins. Contraction in smooth muscle elicited by electrical spike activity is inhibited by spermine and spermidine, while putrescine has little effect. We have now shown in whole cell and single channel recordings from guinea-pig ileum cells that inward current through $Ca^{2+}$ channels is inhibited by spermine and spermidine, whether applied from the interstitial or cytosolic side of the cell membrane. In preparations permeabilized by β-escin, intracellular $Ca^{2+}$ release elicited in $Ca^{2+}$-free medium by carbachol (0.1 mM) or GTPγS (0.1 mM), but not $IP_3$ (40 μM) or caffeine (20 mM), is inhibited by spermine (1 mM). This suggests inhibited production of $IP_3$ from $PIP_2$ as a cause of the response. In high-EGTA solution (4-10 mM) and in the presence of A23187 (10 μM) spermine potentiates the contractile response to $Ca^{2+}$. Spermidine and putrescine potentiate less than spermine. Spermine had a minimal potentiating effect on preparations contracted in the absence of $Ca^{2+}$ after full or partial thiophosphorylation of 20 kDa myosin light chains ($LC_{20}$). Although potentiation of $Ca^{2+}$ sensitivity by spermine is quantitatively comparable to that by carbachol, the spermine effect does not appear to involve G-protein coupled receptors. Force potentiation at suboptimal pCa (6.25) is associated with increased $LC_{20}$ phosphorylation. Force-velocity relations obtained at pCa 6.25 after addition of 1 mM spermine showed similar force and $V_{max}$ as those at optimal pCa (4.5) in the absence of spermine. The results show effects of polyamines at different steps in the activation of contraction in smooth muscle, suggesting that naturally occurring polyamines, and variation in polyamine contents, may influence contractile function.

**M-Pos413**

Effect of nitric oxide vasorelaxation in smooth musle cells from cortical arterioles. ((Kirti Tewari and J. Marc Simard)) Div. Neurosurg. , Sch. of Med.,UMAB , Baltimore , MD 21201.

The discovery that the powerful cerebral vasodilator,NO, is generated by neuronal activity has led to the suggestion that this agent might be the long -sought mediator coupling neuronal activity and cerebral blood flow. Recently , we developed a new preparation of isolated smooth muscle cells from cortical precapillary arterioles of guinea pig. Here we report on patch clamp studies of these cells in which we investigated the effects of nitric oxide on ion channel activity. Using conventional patch clamp techniques, we found that in precapillary arteriolar cells, the number of Ca channels was greater and their voltage dependence of activation was shifted to more negative potentials compared to Ca channels in smooth muscle cells from the basilar artery. When membrane patches were studied in the cell-attached configuration at -10 mV , the nitric oxide donor Na nitroprusside ( 10 μM) caused a reversible reduction in Ca channel activity. The open channel activity was decreased by a factor of 2.6 , from 0.072 to 0.027. Also , this compound augmented activity of Ca-activated K ($K_{Ca}$ ) channels, an effect that would cause hyperpolarization of the cell and promote vasorelaxation. These effects on both Ca and $K_{Ca}$ channels were mimicked by 8-bromo-cGMP (100 μM ) , as would be expected if nitric oxide stimulates activity of guanylyl cyclase . Together, our findings provide the first evidence of ion channel mechanisms involved in the action of nitric oxide in cortical precapillary arterioles and fit well with the proposed role of nitric oxide in coupling neuronal activity with cerebral blood flow.

**M-Pos414**

$Ca^{2+}$ UPTAKE BY THE SARCOPLASMIC RETICULUM OF ISOLATED SMOOTH MUSCLE CELLS ((Margaret E. Kargacin and Gary J. Kargacin)) Department of Medical Physiology, University of Calgary, Calgary, Alberta, Canada T2N 4N1.

A method (Kargacin et al. Am. J. Physiol. 245:C694-C698, 1988) utilizing fura-2 to monitor $Ca^{2+}$ uptake by striated muscle sarcoplasmic reticulum (SR) vesicles was modified to study SR $Ca^{2+}$ uptake and release in saponin skinned smooth muscle cells. Suspensions of isolated cells took up $Ca^{2+}$ from the bathing medium in the presence of ATP. Uptake was inhibited by the SR $Ca^{2+}$ pump inhibitor, thapsigargin (2 -10 μM). Stored $Ca^{2+}$ was released by the $Ca^{2+}$ ionophore Br-A23187 or thapsigargin (20 - 50 μM). From cell density and SR $Ca^{2+}$ uptake rates, the rate at which the SR of a single cell could remove $Ca^{2+}$ from the bathing medium ($1.6 \times 10^{-17}$ moles/s) was calculated. From this, we estimate that the SR in an intact smooth muscle cell could lower intracellular $[Ca^{2+}]_{free}$ at a rate of 45 nM/s. We also estimate that the $Ca^{2+}$ gradient across the SR membrane in smooth muscle cells is greater than 25,000 and that the SR is capable of storing approximately 10 times the amount of $Ca^{2+}$ needed to trigger a single contraction. We conclude that $Ca^{2+}$ pumping into the SR in smooth muscle cells is capable of being the major mechanism for the removal of $Ca^{2+}$ from the cytoplasm of smooth muscle cells following contractile stimuli. (G.J.K. supported by NIH AR39678, AHFMR and the Heart and Stroke Foundation of Alberta; M.E.K. supported by MRC (Canada) PG-44).

**M-Pos415**

MICROMOLAR CALCIUM REDUCES AFFINITY OF INOSITOL TRISPHOSPHATE RECEPTOR IN VASCULAR SMOOTH MUSCLE. ((J. Watras, D. Benevolensky and I. Moraru)) University of Connecticut, Farmington, CT 06030

The mechanism by which calcium inhibits inositol trisphosphate ($InsP_3$)-induced calcium release from sarcoplasmic reticulum (SR) of vascular smooth muscle was investigated. $InsP_3$ binding to SR vesicles from canine aortic smooth muscle was inhibited 51±6% by 2 μM calcium in the presence of 10 nM [$^3$H]-$InsP_3$. Scatchard analysis indicated the presence of two $InsP_3$ binding sites in the absence of calcium ($K_d$=2.5±0.8 and 51±9 nM $InsP_3$). The low affinity site was more prevalent, representing 92±3% of the total number of binding sites. Calcium (2 μM) did not alter $InsP_3$ binding to the high affinity site, but increased the $K_d$ of low affinity site three-fold ($K_d$=150±3 nM). The total number of binding sites remained unchanged. The possibility that the apparent increase in $K_d$ was caused by calcium-dependent activation of an endogenous phospholipase C could be excluded because the inhibition of $InsP_3$ binding was completely reversible and insensitive to an inhibitor of phospholipase C. Moreover, calcium did not inhibit $InsP_3$ binding to the receptor partially purified by heparin-sepharose chromatography, though another fraction (devoid of $InsP_3$ receptor) restored calcium sensitivity of the partially purified $InsP_3$ receptor. Thus, calcium binding to a calcium-sensitizing factor associated with the $InsP_3$ receptor reduces the affinity of the receptor complex for $InsP_3$.

## ANION CHANNELS I

**M-Pos416**

INVOLVEMENT OF CARBOXYTERMINUS STRUCTURES IN SLOW VOLTAGE GATING OF THE *TORPEDO* VOLTAGE-GATED CHLORIDE CHANNEL. ((P. Fong and T. J. Jentsch)) Center for Molecular Neurobiology, University of Hamburg, Germany.

Membrane hyperpolarization normally results in slow gating of the *Torpedo* voltage-gated chloride channel, ClC-0. In order to elucidate the structural basis of this phenomenon, we constructed chimerae in which areas of ClC-0 were replaced by the corresponding regions of ClC-1, the major skeletal muscle chloride channel, and ClC-2, a ubiquitous volume-regulated chloride channel. Chimeric channels were expressed in *Xenopus* oocytes and resultant currents were measured using standard two-microelectrode voltage clamp techniques. We previously reported that a chimeric channel with the cytoplasmic interdomain stretch (IDS) between transmembrane domains 12 and 13 (D12, D13) replaced by the corresponding area of ClC-1 exhibited a half-maximal slow gate activation voltage that was shifted in the positive direction by ~30 mV. While a chimera having most of the carboxy-terminal cytoplasmic tail replaced by the analogous region of ClC-2 was devoid completely of slow gating, the more conservative substitution of only D13 by that area of ClC-2 did not gate significantly differently from wild type ClC-0. We now report that a chimera consisting of the backbone of ClC-0, the IDS of ClC-1, and the D13 of ClC-2 also exhibits altered slow gating. The half-maximal activation voltage for slow gating of this channel is also shifted by~+30 mV. Thus, the carboxyterminal tail, especially the region between D12 and D13, is important for normal slow gating of ClC-0.

**M-Pos417**

THE SKELETAL MUSCLE CHLORIDE CHANNEL, ClC-1, HAS A LOW SINGLE CHANNEL CONDUCTANCE OF 1 pS
((M. Pusch, K. Steinmeyer, and T.J. Jentsch)) Center for Molecular Neurobiology (ZMNH), Hamburg University, Hamburg, Germany

Expression of the major skeletal muscle chloride channel, ClC-1, in HEK293 cells induced chloride currents whose macroscopic properties were similar to those obtained after expression in Xenopus oocytes, except that faster gating kinetics are observed in mammalian cells. Instantaneous currents were inwardly rectifying and activation at positive voltages could be described by a Boltzmann-distribution with an apparent gating valence of 1. Outward and inward currents were reduced substantially in the presence of extracellular iodide. Non-stationary noise analysis revealed that both rat and human ClC-1 have a low single channel conductance of about 1 pS. This finding may explain the lack of single-channel data for chloride channels from skeletal muscle despite its high macroscopic chloride conductance.

**M-Pos418**

EFFECT OF ANGIOTENSIN II ON OK7A CELLS ((J.J. Guo, X.W. Guo and U. Hopfer)) Dept. of Physiology and Biophysics, CWRU, Cleveland, OH 44106

Angiotensin II (ANGII) plays important role in glomerular hemodynamic and renal tubular transport following binding to high affinity receptors. We studied the ANGII-receptors mediated currents in proximal tubular opossum kidney cell line (OK7A) by patch clamping technique. Interestingly, ANGII stimulated a transient increase in $Cl^-$ current in these cells. OK7A cells were seeded on 20% ethicon coated coverslips. 4-days old cells on the coverslips were used within four hours in the patch-clamp experiments. Cell passages used were from 4 to 14. Standard whole cell tight-seal patch-clamp technique were used. The basal current was 3-6 pA/pF at +50 mV and increased to 46± 16 pA/pF (n=6) with stimulation of 10 nM ANGII. The current lasted 1-2 min. The current and voltage relation was linear between -70 mV and +50 mV. The current must be carried mainly by $Cl^-$ because in symmetric $Cl^-$ solutions (145 mM), the reversal potential of the current was almost zero, and when the extracellular $Cl^-$ concentration was reduced from 145 mM to 35 mM, the reversal potential of this current was shifted to +25 mV. The latter value is close to the expected reversal potential, +36 mV. When the pipette/intracellular solution was highly buffered with 10 mM EGTA with free $[Ca^{2+}]_i$ at 100 nM,, the ANGII-dependent $Cl^-$ current was abolished. These Data suggest that this ANGII-stimulated $Cl^-$ conductance is dependent on elevated cytosolic calcium levels. Supported by NIH (HL-41618)

**M-Pos419**

THE 35 pS OUTWARDLY-RECTIFYING CHLORIDE CHANNEL IS INHIBITED BY SUBSTRATES FOR P-GLYCOPROTEIN TRANSPORT (( C.Li and C.E. Bear)) Hosp. for Sick Child., Toronto, CAN. M5G 1X8. (Spon. A. Klip)

P-glycoprotein functions as an ATP-dependent pump for a diverse spectrum of compounds The mechanism underlying this activity is unknown. Further, it has also been shown that P-glycoprotein may be bi-functional as its' over-expression leads to the expression a volume-regulated chloride conductance. So far, only the macroscopic properties of this conductance have been described, namely, it is outwardly rectifying in the presence of symmetrical chloride solutions and is inhibitable by subtrates for P-glycoprotein transport in an ATP-dependent manner. We hypothesize that the single channel underlying this response should also exhibit sensitivity to these compounds. Hence, we sought to determine if a 35 pS, outwardly-rectifying chloride channel, observed at high density in P-gp expressing CHO cells (B30 cells), is modulated by treatment with substrates for P-glycoprotein. We found that pretreatment of B30 cells with colchicine, vinblastine, daunomycin or verapamil (50$\mu$M) caused block of the channel. At least in the case of colchicine, this effect is independent of cytosolic ATP. Analysis of open time histograms revealed that blockade resulted primarily from a decrease in channel open time. The inhibitory effect of these compounds appeared specific for the 35 pS chloride channel as a large, 300 pS channel was unaffected by pretreatment with drug. These results may be explained by two possible hypotheses: either the 35 pS channel is P-glycoprotein or alternatively, this channel is not associated with P-glycoprotein but is related to this protein in that it can be modified by MDR-type compounds.

**M-Pos420**

SUBSTRATE TRANSPORT DOES NOT PREVENT P-GLYCOPROTEIN-ASSOCIATED $Cl^-$ CURRENTS ACTIVATED BY CELL SWELLING. ((E. Han, G. Altenberg and L. Reuss)) Department of Physiology and Biophysics, UTMB, Galveston, Texas 77555-0641.

Overexpression of P-glycoprotein (Pgp), which is thought to be a drug efflux pump, causes multidrug resistance. It has recently been suggested that Pgp is a $Cl^-$ channel. We tested for the presence of Pgp-associated $Cl^-$ currents by using the whole cell patch-clamp technique in breast cancer cells transfected with the human MDR1 cDNA (BC19/3) and the parental cell line (MCF-7; no detectable Pgp expression). Reducing bath osmolality from ≃280 to ≃230 mosmol/kg elicited a reversible increase in $Cl^-$ conductance ($G_{Cl}$) in BC19/3 but not in MCF-7 cells. These results are in agreement with previous observations by others (Valverde et al., Nature 355:830, 1992). A similar reversible $G_{Cl}$ increase in BC19/3 cells was obtained in isosmotic solutions by elevating the pipette pressure by ≃10 cm $H_2O$. The increase in $G_{Cl}$ was measurable 10 s after the pressure change and virtually complete by 1 min. The $G_{Cl}$ activation by hyposmotic solution was prevented by 100 $\mu$M vinblastine in the pipette solution. Other Pgp substrates, Adriamycin (100 or 250 $\mu$M) and rhodamine 123 (100 $\mu$M), had no effect. We conclude that: 1. Pgp either is a $Cl^-$ channel itself or regulates pre-existing $Cl^-$ channels. 2. Pgp-associated $G_{Cl}$ can be activated by changes in cell volume under both anisosmotic and isosmotic conditions, suggesting that it is mechanosensitive. 3. Transport of substrates does not prevent Pgp-associated volume-activated $G_{Cl}$. It is possible that the effect of vinblastine is due to its effect on microtubules. [Supported by the John Sealy Memorial Endowment Fund]

**M-Pos421**

CELL VOLUME REGULATION IN NIH 3T3 FIBROBLASTS AFTER SWELLING DEPENDS ON THE EXPRESSION OF $I_{Cln}$, A CHLORIDE CHANNEL CLONED FROM EPITHELIAL CELLS. (( M. Gschwentner, U.O. Nagl, A. Schmarda and M. Paulmichl )) Dept. Physiology University of Innsbruck A-6020 Austria - Europe.

Fibroblasts (NIH 3T3) are able to effectively regulate their cell volume after reduction of extracellular osmolarity by 50 mosM (omission of mannitol). Using the whole cell patch clamp method a characteristic outwardly rectifying chloride current ($I_{Cl}$) can be observed during this regulatory volume decrease (RVD) showing a pronounced inactivation after stepping to potentials more positive than +40 mV. RVD and $I_{Cl}$ can be blocked by known chloride channel blockers such as NPPB or DIDS. In addition, nucleotides like ATP, cAMP or cGMP, resp., added to the extracellular fluid are able to dramatically impair $I_{Cl}$ and/or RVD. Verapamil, a substance known to impede the multi-drug transporter, a protein believed to be a chloride channel involved in RVD, is unable to deteriorate $I_{Cl}$ in our preparation at concentrations of up to 100 µM. In its kinetics and sensitivity for different blockers $I_{Cl}$ resembles $I_{Cln}$, a chloride channel cloned from epithelial cells (MDCK) expressed in *Xenopus laevis* oocytes (Paulmichl et al., Nature 356: 238-241, 1992). Using RT-PCR and Western-blots $I_{Cln}$ can be detected in NIH 3T3 fibroblasts. Preincubation of the fibroblasts with oligonucleotides, disclosing a reverse-complementary nucleotide sequence from the beginning of the ORF coding for $I_{Cln}$ (antisense oligo), selectively reduces $I_{Cl}$. In addition, we can demonstrate a dramatic reduction of chloride flux in fibroblasts treated with antisense oligos by applying diH-MEQ, a fluorescence dye sensing free chloride concentration in living cells. In conclusion, our experiments show that $I_{Cln}$ is the major chloride channel involved in RVD in NIH 3T3 fibroblasts.

**M-Pos422**

$Cl^-$CURRENTS IN AMPHIBIAN SKELETAL MUSCLES. ((Guillermo Bertran, Basilio A. Kotsias and Paul Horowicz)). Inst. Inv. Médicas A. Lanari, Universidad de Buenos Aires, Argentina and Dept. of Physiology, Univ. of Rochester, NY.

Cl currents ($I_{Cl}$) were measured in short fibers (1-2 mm) from the lumbricalis muscle of toads (Bufo arenarum) with a two-microelectrode voltage clamp (15°C) in a K-free solution: $Cs_2SO_4$ 68; $Na_2SO_4$ 20; CsCl 60; $CaSO_4$ 8; HEPES 2.5 (pH 7.2). One and two pulses were used to estimate the availability and the inactivation of the instantaneous $I_{Cl}$ during a test pulse (I0, tp). The $I_{Cl}$ showed a weak voltage dependence. The currents were fitted using the constant field equation and the best fit was obtained with a $P_{Cl}$ of 4.3 x $10^{-6}$ cm/sec. When a two-pulse protocol was employed new insights in the $I_{Cl}$ appeared. After returning the potential to the holding potential for various times, tp's of the same amplitude and duration of the prepulses (pp's) were applied. The I0,tp was 70 % of the I0,pp and the recovery was complete in less than 300 msec with a linear relationship between the I0, tp and the amplitude of the preceding pp. When the tp's were preceded by a positive pp, the I0,tp for any given tp was larger than with a negative pp. If we assumed that I0,tp is a measure of the number of channels open at the end of the pp, these results suggest that hyperpolarizing pulses inactivate and depolarizing pulses activate the $I_{Cl}$ although another mechanism limits open channel conductance: this value declined from 1.3 mS/cm$^2$ with a +18 mV pulse to 0.9 mS/cm$^2$ for the +75 mV pulse.

**M-Pos423**

FLUCTUATION ANALYSIS OF A VOLUME-SENSITIVE CHLORIDE CONDUCTANCE IN T84 CELLS. ((M.W.Y. Ho, M. Duszyk, and A.S. French)) Departments of Physiology & Medicine, University of Alberta, Edmonton, Alberta, Canada. (Spon. by L.L. Stockbridge)

Regulatory volume decrease is achieved by increasing $Cl^-$ secretion through apical chloride channels in T84 cells. In this study we characterized the volume-sensitive $Cl^-$ channels by noise analysis of individual whole-cell currents. The volume-sensitive $Cl^-$ current appeared with normal bath solution and hypertonic pipet solution. It developed over a few minutes and showed significant inward rectification. The volume-sensitive $Cl^-$ current could be blocked by reversing the osmotic gradient or by using 20 $\mu$M DIDS in the bath solution. Development of the current was accompanied by an increase in the current noise variance which was well fitted by a double Lorentzian relationship with corner frequencies of ~1.8 Hz and ~63 Hz. Noise analysis indicated that the single channel conductance for these volume-activated $Cl^-$ channels was ~0.2 pS. Supported by the Medical Research Council of Canada, the Alberta Heritage Foundation for Medical Research, and the Canadian Cystic Fibrosis Foundation.

**M-Pos424**

DIFFERENT MODULATORY PATHWAYS INVOLVED IN ATP-ACTIVATED CHLORIDE SECRETION IN RAT EPIDIDYMAL EPITHELIUM H.C. Chan, C.W. Lau & P.Y.D. Wong *Department of Physiology, Faculty of Medicine, The Chinese University of Hong Kong, Shatin, Hong Kong*

In addition to neuronal and humoral control, electrolyte and fluid secretion across the epididymal epithelium is subject to local control by substances (e.g. ATP) released from sperm. Previous short-circuit current ($I_{sc}$) studies have shown that $Cl^-$ secretion across rat epididymal epithelium can be stimulated by apical addition of ATP. In the present study we further investigated the modulatory pathways involved in ATP-stimulated $I_{sc}$ response in the same preparation. $I_{sc}$ responded to ATP (1 $\mu$M) with two transient rising phases, one with an increase in $I_{sc}$ of 11.78 $\pm$ 1.46 $\mu A/cm^2$ peaked at 11 $\pm$ 1.06 sec and the other of 9.2 $\pm$ 0.73 $\mu A/cm^2$ at 52 $\pm$ 2.2 sec. Inhibitor of $P_1$ receptor, 8-phenytheophyline (10 $\mu$M) did not have any effect on both phases of the ATP-activated $I_{sc}$, indicating that the two phases in $I_{sc}$ were not due to the involvement of different purinoecptors, e.g., $P_1$ and $P_2$ receptors. Rather, different modulatory pathways might be involved. Pretreatment of $Cl^-$ channel blocker, DIDS (300 $\mu$M), resulted in a reduction in the first peak (4.1 $\pm$ 1.93 $\mu A/cm^2$) but did not significantly affect the second peak (9.3 $\pm$ 3.2 $\mu A/cm^2$). However, pretreatment of DPC (1 mM) reduced the first and second peaks, 2.39 $\pm$ 0.5 and 1.05 $\pm$ 0.31 $\mu A/cm^2$, respectively. Pretreatment of protein kinase inhibitor H-8 (20 $\mu$M) had a more pronounced effect on the second peak (3.81 $\mu A/cm^2$). It appeared that different modulatory pathways were involved in ATP-activated $Cl^-$ secretion. The DIDS-sensitive first phase might be mediated by $Ca^{2+}$-activated $Cl^-$ conductance, whereas, the DPC-sensitive second phase might be mediated by cAMP-dependent pathway, presumably CFTR. *Supported by the Croucher Foundation, the Research Grant Council, and the UPGC of Hong Kong.*

**M-Pos425**

RECOMBINANT CHLOROTOXIN: AN INHIBITOR OF GASTRIC $Cl^-$ CHANNELS ((D.H. Malinowska, A.M. Baker, K.M. Blumenthal and J. Cuppoletti)) Dept. Physiol. & Biophys., Univ. of Cinc. Coll. Med., 231 Bethesda Avenue, Cincinnati, OH 45267-0576.

Gastric HCl secretion involves an acid- and voltage-activated chloride channel. Chlorotoxin, a 36 amino acid polypeptide component of scorpion (*Leiurus quinquestriatus*) venom has been reported to be an inhibitor of epithelial $Cl^-$ channels. Recombinant chlorotoxin (CTX) was prepared as a gene 9 bacteriophage T7 fusion protein chimera in the vector pSR9 and expressed in *E. coli*. The fusion protein was isolated, purified by anion exchange chromatography, reoxidized, and cleaved. CTX was then purified by anion exchange chromatography and tested as an inhibitor of gastric chloride channels present in rabbit H/K ATPase-containing vesicles. Single chloride channel recordings in planar lipid bilayers were obtained as described (AJP 264:C1609-C1618, 1993). Sided additions of 3.6 uM CTX were carried out. CTX had no effect on the open probability (Po) or on mean open or closed times of the channel when added to the cytoplasmic face of the chloride channel (*cis* side). However, *trans* addition greatly decreased Po due to increased closing time. Similar findings were obtained in at least three different recording sessions. CTX also inhibited HCl accumulation in the same gastric vesicles without affecting ATPase activity. Photoaffinity labeling studies of proteins contained in gastric vesicles, which are enriched in H/K ATPase using [$^{125}$I]p-azidosalicyl,amido,ethyl,1,3'dithio propionylyl CTX in attempts to identify the gastric chloride channel protein are in progress. Supported by NIH DK43816 & DK43377 (JC & DHM); NIH GM48676 & HL41543 (KMB). AMB was supported by NIH training grant HL07571.

**M-Pos426**

ALKALINE PHOSPHATASE REGULATES EPITHELIAL ANION CHANNELS IN BOVINE TRACHEA. ((M. Duszyk, D. Liu, A.S. French and S.F.P. Man)) Departments of Medicine and Physiology, University of Alberta, Edmonton, Canada.

Bovine tracheal epithelium contains 105 pS chloride channels, that have a linear current-voltage relationship, and are not voltage-dependent. We studied the regulation of these channels in native epithelial cells and in liposomes containing apical membrane proteins by patch clamp. In silent patches, these channels could be activated by fluoride, and inhibited by alkaline phosphatase (AP). They showed no $Ca^{++}$-sensitivity, and could also be activated by cAMP-dependent phosphorylation. In other experiments, the peripheral membrane proteins from the apical fraction were removed, and the remaining proteins were used in single channel studies. This treatment made the channels insensitive to fluoride, but activation by cAMP-dependent phosphorylation was unchanged. These experiments showed that the apical membrane contains fluoride-sensitive proteins. However, several patches contained spontaneously active $Cl^-$ channels with a similar conductance but different activation properties. One group of channels were not sensitive to AP and showed clear voltage dependence, being mostly open at negative voltages. The other group were similar to AP-sensitive $Cl^-$ channels, but their activity could be restored when AP was washed away, and in the absence of PKA and ATP. This suggests that AP inhibits this $Cl^-$ channel by mechanisms other than dephosphorylation.

**M-Pos427**

CHARACTERIZATION OF AN ANION CHANNEL EXTRACTED FROM SUBMITOCHONDRIAL PARTICLES. ((G. Liu and A.D. Beavis)) Dept. of Pharmacology, Med. Coll. of Ohio, Toledo, OH 43699

The inner mitochondrial membrane contains an anion uniport pathway which catalyzes the electrophoretic transport of a wide variety of anions. This pathway (IMAC) has been well characterized using flux measurements in intact mitochondria. We have now begun a study to identify the protein and examine its electrophysiological properties in planar lipid bilayers. Submitochondrial particles prepared from rat liver mitoplasts were solubilized in 3% Triton and the solubilized proteins were reconstituted into proteoliposomes made from L-$\alpha$-lecithin and cardiolipin. These proteoliposomes were then fused with planar lipid bilayers (PS:PE:PC (1:1:1)) with 600 mM KCl and 60 mM KCl on the cis and trans sides respectively. An anion selective channel ($P_{Cl}/P_K \approx 7$) was most frequently observed when the fusion occurred at pH 7.8. Under these conditions, the conductance of the channel decreases from 110 to 85 pS between -80 mV and +20 mV (cis-trans). In addition, the open probability decreases from about 98% at -60 mV to 65% at 0 mV. This is due to a decrease in the mean open time from 1 s to 0.1 s and an increase in the mean closed time from 10 ms to 50 ms. The latter component appears to reflect the existence of two closed times, one of 3-5 ms which is voltage independent and one which is voltage dependent increasing to about 0.5 s at 0 mV. The properties of this channel suggest that it may be the 100 pS channel observed previously by others in patch-clamp experiments using both rat liver and brown adipose tissue mitochondria. This work was supported by NIH grant HL/GM 47735.

**M-Pos428**

NON-LINEAR AMPLIFICATION BY CALCIUM-DEPENDENT CHLORIDE CHANNELS IN OLFACTORY RECEPTOR CELLS. ((G. Lowe and G. H. Gold)) Monell Chemical Senses Center, Philadelphia, PA

Odorants induce an inward current in vertebrate olfactory receptor cells. For many odorants, this response is caused by cyclic AMP acting directly on cyclic nucleotide-gated cation-selective channels. Moreover, Kurahashi and Yau (*Nature* **363**, 71 (1993)) have recently shown in newt receptor cells that $Ca^{2+}$ influx through the cyclic nucleotide-gated channels activates $Ca^{2+}$-dependent $Cl^-$ channels, which pass an inward $Cl^-$ current that significantly augments the cyclic AMP-induced cationic current. We have combined photolysis of caged cyclic AMP with selective block of chloride channels to investigate the contribution of the $Cl^-$ current to the cyclic AMP-dose dependence of the transduction current. When cells were loaded with caged cyclic AMP, a brief flash (20 ms) of UV light caused a transient inward current (latency *ca.* 10 ms, duration at half peak amplitude *ca.* 0.5 s). The peak amplitude of this current varied with flash intensity according to the Hill equation with cooperativity *ca.* 3.5. However, in the presence of the $Cl^-$ channel blocker SITS, the peak amplitude of the current decreased by *ca.* 85% and the cooperativity decreased to *ca.* 1.5, close to that observed in excised patches. Thus, the $Cl^-$ current increases the total cyclic AMP-induced current in a highly non-linear manner. Consequently, the $Cl^-$current could serve to amplify supra-threshold responses relative to basal transduction noise.

**M-Pos429**

GROWTH HORMONE IMPROVES THE LOWERED CHLORIDE CONDUCTANCE OF RAT SKELETAL MUSCLE DURING AGING.
((A. De Luca, S. Pierno, D. Cocchi and D. Conte-Camerino)) Unit of Pharmacology, Department of Pharmacobiology, Faculty of Pharmacy, University of Bari, Via Orabona 4, Campus, 70125 Bari, ITALY.

The decrease of chloride conductance ($G_{Cl}$) in rat skeletal muscle during aging is partially restored (by 30%) by a 6-8 week treatment with biosynthetic growth hormone (GH), possibly by a protein synthesis mediated effect (De Luca et al. J. Pharmacol. Exp. Ther., in press). To better understand the mechanism of action of GH on $G_{Cl}$ of aged muscle, we prolonged the duration of the treatment and we performed a pharmacological characterization of the GH-treated rats with the enantiomers of 2-(p-chlorophenoxy) propionic acid (CPP), highly specific for muscle chloride channels (De Luca et al. Naunyn Schmied. 346: 601, 1992). 20-22 month old Wistar Kyoto female rats were treated daily for 4 months with 150$\mu$g/kg biosynthetic GH. The electrophysiological recordings were performed *in vitro* by means of computerized two intracellular microelectrode technique on extensor digitorum longus (EDL) muscles (De Luca et al.,1992). In the GH-treated aged rats we found a significant 55% increase of $G_{Cl}$ towards the adult value. Indeed, $G_{Cl}$ was 2492$\pm$93$\mu S/cm^2$ (n=33), 1258$\pm$97$\mu S/cm^2$ (n=68) and 1949$\pm$122$\mu S/cm^2$ (n=73) in adult, aged and GH-treated aged rats, respectively. S-(-) CPP was much less potent in decreasing $G_{Cl}$ in untreated aged ($IC_{50}$ = 63$\mu$M) with respect to adult rats ($IC_{50}$ = 15.4$\mu$M). The GH treatment significantly increased the sensitivity to S-(-) CPP which decreased $G_{Cl}$ with an $IC_{50}$ of 19.8$\mu$M. The R-(+) CPP, tested at 3$\mu$M and 500$\mu$M, produced in adult rats the typical biphasic effect (De Luca et al., 1992). In untreated aged-rats the R-(+) CPP increased $G_{Cl}$ by 48% and 17% at 3$\mu$M and 500$\mu$M, respectively. In GH-treated aged rats R-(+) CPP at 3$\mu$M increased $G_{Cl}$ by 20% whereas a decrease of $G_{Cl}$ (by 10%) was again detectable at 500$\mu$M. The partial restoration of $G_{Cl}$ observed upon prolongation of the treatment, as well as the adult-like pharmacology of $G_{Cl}$, suggest that a faulty growth factor, signaling control of muscle chloride channel expression, may account for the decreased $G_{Cl}$ value recorded during aging (Supported by Italian CNR P.F. Invecchiamento and 93-263).

**M-Pos430**

A $Cl^-$ CONDUCTANCE IN PANCREATIC ZYMOGEN GRANULES (ZG) WITH FUNCTIONAL AND MOLECULAR PROPERTIES OF MDR P-GLYCOPROTEIN.

((F. Thévenod,I. Anderie & I. Schulz)) Physiology II, Univ. Saarland, 66421 Homburg, FRG

Previous studies have demonstrated $Cl^-$ and $K^+$ permeabilities in the membrane of isolated pancreatic ZG which are modulated by ATP and its non-hydrolyzable analogs. Two Nucleotide Binding Fold (NBF) containing transporters with $Cl^-$ channel properties, the Cystic Fibrosis Transmembrane conductance Regulator (CFTR) and the MDR P-glycoprotein (Pgp) are also modulated by ATP binding and/or hydrolysis. In this study we have characterized further the regulation of $Cl^-$ and $K^+$ conductances in ZG by the non-hydrolyzable ATP analog AMP-PCP. ZG were purified from rat pancreas homogenate by Percoll gradient centrifugation. $Cl^-$ conductance was assayed by resuspending ZG in isotonic KCl/HEPES, addition of the $K^+$ ionophore valinomycin (val) and measurement of the kinetics of osmotic lysis of ZG at 540 nm induced by gradient-driven influx of KCl and $H_2O$. $K^+$ conductance was determined by measuring osmotic lysis of ZG suspended in isotonic $K^+$ acetate/imidazole buffer after addition of the protonophore CCCP, which generates an outside-directed $H^+$ diffusion potential to energize $K^+$ influx through endogenous channels and osmotic $H_2O$ flow. $Cl^-$ conductance was maximally stimulated by 0.5 mM AMP-PCP ~ 4-fold. Two different monovalent cation conductances were found in ZG membranes: A $K^+$ and $Rb^+$ selective conductance was completely blocked by 0.5 mM AMP-PCP; an AMP-PCP insensitive, nonselective cation conductance was inhibited by 0.1 mM $Ba^{2+}$. In the absence of val ZG were stable in KCl buffer up to 2 hours. AMP-PCP enhanced osmotic lysis dramatically (half-time of lysis ~ 30 min), due to activation of $Cl^-$ conductance by AMP-PCP and $K^+$ influx through the AMP-PCP-insensitive cation pathway. AMP-PCP induced lysis of ZG in KCl buffer without val was not blocked by a monoclonal antibody (mAb) against CFTR (M3A7; 5 μg/ml), but was strongly inhibited by two mAb against Pgp (JSB-1 and C219; 5 μg/ml). This inhibition occurs through block of the AMP-PCP activated $Cl^-$ conductance. The AMP-PCP insensitive monovalent cation conductance was not blocked by mAb against Pgp. We propose that the $Cl^-$ channel activated by the non-hydrolyzable ATP analog AMP-PCP in ZG membranes is either Pgp or a member of the family of NBF containing $Cl^-$ transporters which include Pgp.

**M-Pos431**

2-METHYLTHIO ATP ACTIVATES TWO DISTINCT CONDUCTANCES IN GUINEA PIG VENTRICULAR MYOCYTES. ((KE Parker and A Scarpa)) Case Western Reserve University, School of Medicine, Dept. Physiology and Biophysics, Cleveland, OH 44106.

Extracellular ATP affects heart function. It can have both positive and negative inotropic effects. When ATP is applied extracellularly to guinea pig ventricular myocytes, (assayed by patch-clamp in the whole-cell configuration; held at -70 mV; with a internal solution of 120 mM CsCl, 20 mM TEA-Cl, 3 mM $MgCl_2$, 10 mM EGTA-Cs, 10 mM HEPES, pH 7.2; and an external solution of 140 mM NaCl, 10 mM glucose, 5 mM KCl, 2.5 mM $CaCl_2$, 0.5 mM $MgCl_2$, 10 mM HEPES, pH 7.4), several conductances are evoked, including at least two inward conductances and one outward conductance. 100 mM 2-MT-ATP, an agonist for fewer classes of purinergic receptors than ATP, evokes only two conductances--one desensitizing inward current that activates as quickly as the agonist can be applied (average half-time of activation of 104 msec, n=3), and an outward current that activates after a delay of approximately 300 msec with an average half-time of activation of 185 msec, (n=3). In preliminary experiments the inward current reversed at -7 mV, consistent with a chloride or non-specific cation conductance, whereas the outward current reversed negative to -70 mV, consistent with a cesium or TEA conductance. When 2-MT-ATP is applied as a 500 msec puff, the inward current desensitizes but recovers to about 80% by 4 min over a time course that cannot be fit with fewer than two exponentials. Additional data from ion-replacement experiments, dose-response experiments and experiments with other ATP analogues will be presented.

**M-Pos432**

SINGLE CHANNEL STUDIES OF OUTWARDLY RECTIFING $CL^-$ CHANNEL IN HUMAN MYELOBLASTIC LEUKEMIA CELLS

((B.Xu and L.Lu)) Department of Physiology and Biophysics, Wright State University, School of Medicine, Dayton, Ohio 45435

Apical $Cl^-$ channels are important in the regulation of salt and water transport in a variety of secretory epithelial cells. It has been reported that the outward-rectifying $Cl^-$ channel (ORCC) plays a crucial role in $Cl^-$ secretion and cell volume regulation. Recently, using the inside-out patch clamp technique, we have identified and characterized a voltage-gated ORCC in patches from the membrane of cultured human myeloblastic leukemia cells (ML-1). Excised patches of cell membrane displayed no channel activity until they were depolarized at greater than +40mV. The current-voltage (I-V) relationship of the $Cl^-$ current showed an outward rectification in symmetrical $Cl^-$ solution with 48ps (at+60mV)in the outward direction and 27ps (at-60mV)in the inward direction. After high $Cl^-$ solution was perfused into the bath(300mM $Cl^-$ in bath /142 mM $Cl^-$ in pipette solutions), the reversal potential was shifted from near 0 to +14 mV, which is close to the +19mV predicted by Nernst equation. The $Cl^-$ current was activated by the cAMP-dependent protein kinase (PKA) catalytic subunit plus $Mg^{2+}$-ATP in the bath solution under physiological conditions. Biophysical analyses revealed that the ORCC in ML-1 cells has at last two sub-conductance states that were not affected by PKA catalytic subunit activation. Open time constants of this channel showed a voltage dependent manner to the membrane potential and is increased by PKA activation . Two anion transport inhibitors, anthracene-9-carboxylic acid (9-AC) and 4,4-diisothiocynatostilbene-2,2-disolfonic acid (DIDS) caused an reversible block of the channel. The half-inhibitory concentrations of 9-AC and DIDS were 174± 20 μM and 70± 16 μM. Our results provide new information about the characterizatics and distribution of ORCC, which serve as a useful model for studying the relationship between ORCC and cystic fibrosis transmembrane conductance regulator(CFTR).

## Na CHANNELS I: STRUCTURE-FUNCTION

**M-Pos433**

PERMEATION IN AN INACTIVATION-DEFICIENT SKELETAL MUSCLE (μ1) $NA^+$ CHANNEL ((J.R. Balser, H.B. Nuss, D.W. Orias, J.H. Lawrence, P.H. Backx, E. Marban, G.F. Tomaselli)) The Johns Hopkins University School of Medicine, Baltimore, MD 21204.

Fast inactivation complicates the study of $Na^+$ channel permeation and intra-pore block. To avoid the confounding effects of toxins or proteolysis, we slowed inactivation in μ1 channel α subunit using site-directed mutagenesis. Mutant RNA was expressed in *Xenopus* oocytes; channel function was assessed using whole-cell and single channel cell-attached and excised inside-out patch recording. Substitution of a hydrophobic amino acid (F1304Q) in the linker between domains III and IV (West *et al.*, 1992) prolonged the single-channel open time and slowed the decay of the whole-cell current. The single-channel i-V relationship in cell-attached patches was measured over a wide range of external [$Na^+$] (10-280 mM) from -100 to +50 mV. Similar to BTX-modified $Na^+$ channels (Green *et al.*, 1987), conductance at low external [$Na^+$] was high and deviated from a Langmuir isotherm. Although an external surface charge may be responsible, an alternative explanation is multi-ion occupancy of the channel pore (eg. Begenesich and Cahalan, 1980). We therefore simulated the concentration-conductance relationship over the entire voltage range using a two-site multi-occupancy barrier model incorporating coulombic interaction. The model predicts a deep energy well (G/RT= -11) at ~0.4 of the electrical distance from the external side of the pore and a second, more internal higher energy site (G/RT= -3). Multi-ion occupancy and electrostatic repulsion between permeating ions may partly explain the deviation from a Langmuir isotherm at low ionic strength that has been ascribed to surface charge screening.

**M-Pos434**

INTRA-PORE BLOCK OF INACTIVATION-DEFICIENT SKELETAL MUSCLE (μ1)$NA^+$ CHANNELS BY QX-314 ((J.R. Balser, K.A. Kluge, G.F. Tomaselli))The Johns Hopkins University School of Medicine, Baltimore, MD 21204.

Quaternary ammonium (QA) compounds are useful probes for establishing the structural basis of block by local anesthetic compounds via the hydrophilic pathway. The effects of QA on whole-cell $Na^+$ current has been extensively characterized, but rapid inactivation of $Na^+$ channels precludes single-channel quantification of intra-pore block. In order to study block, toxins or enzymes have been used to remove rapid inactivation; however, these agents may affect permeation and may interact with the QA. To avoid these complications, we have slowed inactivation in μ1 channel α subunit using site-directed mutagenesis to replace a hydrophobic amino acid in the linker between domains III and IV with glutamine (F1304Q; West *et al.*, 1992). These channels exhibit permeation properties that are indistinguishable from wild-type (Balser *et al.*, 1993). Inactivation-deficient channels were expressed in *Xenopus* oocytes and studied using inside-out patch recording. Patch electrodes contained 140 NaCl and the bath was $Na^+$ free (140 KCl). We used the permanently charged lidocaine QA analog QX-314 to examine block of the channel from the cytoplasmic side. QX-314 decreased the probability of channel opening and reduced the unitary current (i) in a voltage and concentration-dependent manner; both effects were completely reversible. At -60 mV, 0.5 mM QX-314 caused no reduction in i, while at 0 mV i was reduced by 21%. At 2 mM, i was reduced by 22% at -60 mV, 32% at -40 mV, 41% at -20 mV, and 50% at 0 mV. We conclude that F1304Q channels are an excellent tool for evaluating open-channel block. The voltage-dependence of block suggests an intra-pore binding site; future studies will focus on identifying the amino acids forming this site.

**M-Pos435**

CARDIAC SODIUM CHANNELS (HH1) ARE INTRINSICALLY MORE SENSITIVE TO TONIC BLOCK BY LIDOCAINE THAN ARE ($\mu$1) SKELETAL MUSCLE CHANNELS.

((H. Bradley Nuss and Eduardo Marban)) Johns Hopkins University, Baltimore, MD

When lidocaine is given systemically, cardiac Na channels are blocked preferentially over those in skeletal muscle and nerve. This apparent increased affinity is thought to arise solely from the fact that cardiac Na channels spend a large fraction of their time in the inactivated state. The oocyte expression system was used to compare systematically the sensitivities of skeletal ($\mu$1) and cardiac (HH1) Na channels to block by lidocaine, where the only difference was the choice of $\alpha$ subunit. To check for differences in tonic block, Na currents were elicited after 2-3 min of exposure to various lidocaine concentrations at -100 mV, a potential at which both HH1 and $\mu$1 channels were fully reprimed. Surprisingly, HH1 Na channels (n=12) were 3-fold more sensitive to rested-state block by lidocaine than were $\mu$1 Na channels (n=10, see figure). In contrast, the inactivated state binding affinities determined at partially depolarized holding potentials ($h_\infty \approx 0.2$) were similar ($K_i = 16 \pm 2\mu M$, n=9 for HH1 and $12 \pm 3\mu M$, n=5 for $\mu$1). These unexpected findings suggest that structural differences in the $\alpha$ subunits impart intrinsically different lidocaine sensitivities to the two isoforms.

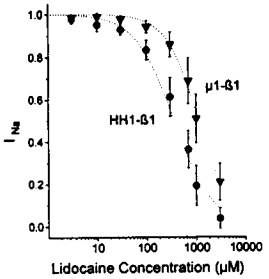


**M-Pos436**

CHARACTERIZATION OF FAST AND SLOW GATING MODES OF THE RIIA VOLTAGE-GATED SODIUM CHANNEL EXPRESSED IN OOCYTES WITH AN IMPROVED TWO-ELECTRODE VOLTAGE CLAMP.

((T.E. Hebert[1,2], P. Drapeau[2] and R.J. Dunn[2])) 1Department of Medical Genetics, University of Toronto, Toronto, ON, Canada; 2Centre for Research in Neuroscience, Montreal General Hospital, McGill University, Montreal, QC, Canada.

Fast and slow gating modes of rat brain IIA sodium channel $\alpha$ subunits expressed in *Xenopus* oocytes were isolated from one another due to their distinct inactivation properties. Sodium currents were measured by fast intracellular voltage clamping with large agarose-tipped electrodes and by excised membrane patch clamp recording. At holding potentials < -55 mV, fast mode currents inactivated within a few ms and could be isolated due to their rapid recovery from inactivation. Sodium channels opened early upon depolarization of membrane patches and rarely showed reopenings. At holding potentials > -55 mV, fast mode currents were inactivated, revealing slow mode currents which had slower activation and inactivation kinetics. When membrane patches were held at these lower potentials, single channels showed sustained activity during depolarizing pulses. The steady-state voltage dependencies of fast and slow mode activation were very similar. In contrast, slow inactivation was shifted to depolarized potentials compared to fast inactivation. The slow mode appears to be due to destabilization of a voltage-insensitive conformation. The fast gating process dominated at high current levels, perhaps due to $\alpha$ subunit interactions.

Supported by the MRC, FRSQ and FCAR.

**M-Pos437**

EVALUATING SODIUM CHANNEL MUTANTS: MACROSCOPIC CORRELATES OF MODE CHANGES.

((M.D. Rayner, D. Featherstone, M. Andres, J. Lu, M. Henteleff, P.C. Ruben and J.G. Starkus)) Bekesy Laboratory of Neurobiology, University of Hawaii, Honolulu, HI 96822.

Macroscopic sodium currents from single macropatches show time-dependent kinetic changes from slow to fast kinetic mode following patch excision (Fleig et al. 1993. *Biophys. J.* Abs). Furthermore, during steady-state inactivation in mixed-mode patches, fast kinetics preferentially disappear at more negative prepulse potentials, suggesting a separable population of fast-mode channels with left-shifted steady state inactivation. In addition to the long-term metabolic biasing of channel mode suggested by our previous data, there is also a very rapid, voltage-dependent, biasing mechanism. Thus, in macropatches from *Xenopus* oocytes expressing both wild-type and mutant Rat Brain IIA channels, we always see a greater proportion of slow mode properties at near threshold potentials and increasing proportions of fast behavior at more positive test potentials. However, we find that the voltage dependence of this mode-switching can be altered by S4 mutations in domains II, III and IV. We describe both right (e.g. R1312Q) and left shifts (e.g. L860F and R1638Q) resulting from S4 mutations, suggesting that kinetic effects induced by mode shifts should be carefully distinguished from more direct effects on the rates of activation and inactivation.

(Supported by PHS grants #NS-21151, #NS-29204, NIH RCMI grant #RR-03061 and grants from the American Heart Assoc. Hawaii Affiliate)

**M-Pos438**

DOMAIN III AND IV S4 CHARGE NEUTRALIZATIONS ALTER GATING PROPERTIES OF RAT BRAIN IIA SODIUM CHANNELS.

((D. Featherstone, M. Henteleff, M.D. Rayner and P.C. Ruben)) Békésy Laboratory of Neurobiology, University of Hawaii, Honolulu, HI 96822.

Sodium channel activation, fast inactivation, and slow inactivation are distinct properties that can be separated on the basis of their pharmacological and voltage sensitivities. We have studied the steady-state activation (F(V)) and slow inactivation ($F(V_h)$) gating properties of rat brain IIa channels (RBIIa) with charge neutralizations in the S4 transmembrane segments in domains III and IV. Replacement of the domain III arginine in position 1312 with glutamine (R1312Q) had little effect on the midpoint or slope of the F(V) curve, but decreased the slope valence of the $F(V_h)$ curve by *ca.* 1*e* and depolarized the midpoint by *ca.* 10 mV. By contrast, R1638Q in domain IV decreased F(V) slope valence by *ca.* 0.9*e* and hyperpolarized the $F(V_h)$ midpoint by *ca.* 15 mV. R1638Q had little effect on F(V) midpoint or $F(V_h)$ slope.

These data confirm our previous hypotheses that (i) activation and slow inactivation are controlled by separate voltage sensors, and (ii) these voltage sensors are electrostatically and/or allosterically coupled such that some, but not all, effects on activation voltage sensitivity also alter slow inactivation voltage sensitivity.

(Supported by PHS grant #R-01 NS29204 and American Heart Association Hawaii Affiliate to PCR)

**M-Pos439**

EFFECTS OF N-GLYCOSYLATION ON SODIUM CHANNEL GATING

((E. Bennett, V.V. Patel, S.S.Tinkle, M.S. Urcan, and S.R. Levinson)) Department of Physiology and Program in Neuroscience, UCHSC, Denver, CO, 80262

The effect of N-glycosylation on voltage-gated sodium channel function was studied through whole cell recording of the tetrodotoxin-sensitive rat skeletal muscle sodium channel, RSkM1, exogenously expressed in Chinese Hamster Ovary (CHO) cell lines. Wild type channels were expressed in a variety of CHO cell lines capable of varying degrees of glycosylation (*lec* and *ldlD* cell lines). Also, deletion mutants in which four and five putative N-glycosylation sites were removed from the channel clone were constructed and transfected into the parental cell line, CHO-K1. Thus, three different systems (the two cell line systems and the mutant constructs) were developed to determine and compare the functional characteristics of RSkM1 in the presence of full and reduced glycosylation. In all three systems, a reduction in channel glycosylation caused a depolarizing shift in steady state gating of the channel (e.g., shifts in the voltage of half activation ($V_a$) of 7-12 mV), indicating that glycosylation of the channel affects the voltage dependence of channel activation. At least two possible mechanisms may explain the phenomenon: 1) The negatively charged sialic acid residues that are in abundance at the ends of the channel carbohydrate structures alter the electric field sensed by the gating mechanism (electrostatic hypothesis), or 2) glycosylation of the channel affects the structural integrity of the channel thereby changing the level of depolarization required for activation (conformational effect). If the conformation of the carbohydrate domains were responsible for the effect of glycosylation on channel activation, then one might predict that the observed shift in $V_a$ with reduction in glycosylation would be different for each of the three systems described above (since the carbohydrate structures of the channels produced in each system are structurally different). However, the shifts in steady state gating observed for the three systems were very similar in both direction and magnitude, indicating that the negatively charged sialic acid residues attached to the ends of the carbohydrate structures play a primarily electrostatic role in channel activation by influencing the membrane potential sensed by the gating mechanism of the channel. Measurements of the effects of these manipulations on channel gating kinetics are also consistent with this hypothesis. Experiments are currently in progress to distinguish the two possible mechanisms more directly. Supported by NIH: NS15879 (SRL) and NS09327 (EB).

**M-Pos440**

SURFACE CHARGE VARIATIONS ACCOUNT FOR DIFFERENCES IN THE GATING OF RSkM1 SODIUM CHANNELS IN DIFFERENT CELLS.

((V.V.Patel, S.R. Levinson, and J.H. Caldwell)) Depts. of Physiology and Cell/Structural Biology and the Neuroscience Program, U. Colorado Medical School, Denver, CO 80262

Cloned voltage-dependent channels frequently exhibit altered behavior when exogenously expressed in different cells (c.f. Yang et al., *J. Neurosci. 12:268 (1992)*). We have compared the activation gating properties of the RSkM1 sodium channel expressed in *Xenopus* oocytes and Chinese hamster ovary (CHO) cells with those of the parent tissue. Significant differences in steady-state activation were seen as reflected in the activation midpoint $V_a$. Thus in 2mM $Ca^{2+}$ $V_a$ was -37,-31,-18, and -9 mV for rat FDB muscle fibers, oocytes, and 2 different CHO cell lines respectively. We next compared the ability of calcium to induce shifts in the steady-state activation vs. voltage relations. These measurements showed significant differences in both the total range of the shift and its sensitivity to $[Ca^{2+}]$ (as reflected in $K_{50}$'s). In particular, channels gating at more negative potentials (e.g. muscle fibers) exhibited larger shift ranges but with reduced calcium sensitivity than those gating at more positive potentials (CHO cells). Furthermore, the absolute values of the gating midpoints appeared to converge to similar values at saturating calcium concentrations. Taken together, these findings suggest that the differences observed in gating for RSkM1 channels expressed in different cells reflect variations in surface charge around channel gating elements. Since artificial manipulation of glycosylation (particularly sialic acid) can induce similar changes in channel gating (see Bennett et al., this meeting), it seems that differences in surface charge resulting from posttranslational modifications of channels in different cells could be the basis for the observed gating variations. If so, then variable glycosylation may be another means by which cells may modulate the function of voltage-gated ion channels. Supported by NIH NS15879 (SRL), NS07083 (VVP), and NS26505(JHC).

M-Pos441

**Calcium acts at multiple sites on skeletal muscle sodium channels.** ((V.V. Patel and S.R. Levinson)), Dept. of Physiology and Program in Neuroscience, University of Colorado Medical School, Denver, CO 80262

External calcium affects the function of sodium channels through two distinct actions, namely a voltage-dependent block of sodium current and a positive-going shift in the membrane potential required to gate the channel. Classically, block has been thought to be consequential to a voltage-dependent binding of calcium to a site within the channel pore, while gating effects (usually defined as shifts in steady state activation midpoint) have been considered to be caused by calcium interactions with negatively charged sites on the outer membrane surface. However, recent studies have found that for sodium channels in cultured GH3 cells the calcium concentration dependence for both effects was similar. On the basis of this finding, it has been proposed that both effects are mediated by single calcium binding site within the pore itself (Armstrong and Cota, *PNAS 88:* 6528 (1991)).

We have repeated these experiments on rat skeletal muscle sodium channels (RSkm1) expressed in transfected CHO cells. In this system,we find that there is a large difference in the concentration dependence between the block and activation shift effects ($K_{50}$(block) =7.2mM, $K_{50}$(shift)=0.5mM). It may also be argued on theoretical grounds that if the two calcium actions were indeed mediated by a single, voltage-dependent site, then the observed dose-response relations for the two effects should in fact differ. In particular, $K_{50}$ for the shift effect should be greater than that of the blocking action (whereas we have found the opposite to be true). Quantitative analysis further shows that the observed $K_{50}$ is about 40 times smaller than the value expected if the voltage-sensitive block site was responsible for gating shifts. Thus we conclude that calcium acts on separate sites on RSkm1sodium channels.

Other experiments presented at this meeting suggest that a significant proportion of the shift sites are sialic acid residues attached to the outside of the channel through N-linked glycosyl moieties (Bennett et al.; Patel et al.).Supported by NIH NS15879 (SRL) and NS07083(VVP).

M-Pos442

A COMMON PHENOTYPE FOR DIVERSE NA CHANNEL MUTATIONS IN PARAMYOTONIA CONGENITA. ((N. Yang, S. Ji, M. Zhou, M. Chahine, R. L. Barchi, R. Horn, and A.L. George, Jr.)) Dept of Physiol., Jefferson Med. Coll., Philadelphia, PA 19107; Dept. of Neurol. & Institute of Neurol. Sci., Univ. of Penn., Philadelphia, PA 19104; Dept. of Medicine & Pharmacol., Vanderbilt Univ., Nashville, TN 37232.

At least 6 different point mutations in the adult human skeletal muscle Na channel α-subunit are associated with the disease paramyotonia congenita (PC). We constructed 5 of these mutations in the recombinant human Na channel cDNA hSkM1, and expressed the channels in a mammalian cell line. A1156T (alanine→threonine) is in the cytoplasmic linker between S4 & S5 in domain 3 (D3). T1313M (threonine→methionine) is in the cytoplasmic linker connecting D3 and D4, a region believed to be the inactivation gate (Stühmer et al, '89, *Nature* **339**:597; West et al, '92, *PNAS* **89**:10910). L1433R (leucine→arginine) is near the extracellular end of segment S3 of D4 (S3/D4). R1448H and R1448C substitute histidine and cysteine for the outermost arginine in S4/D4. Although the phenotypes of these PC mutants differ in biophysical details, they have two common features: 1) little or no effect on the kinetics and voltage dependence of activation, and 2) an increase in the time constant of inactivation for decay of Na current in response to a depolarization. The latter effect is greatest in R1448C, which inactivates ~5-fold slower than wild-type at voltages near 0 mV. We postulate that i) the diverse mutations affect either the inactivation gate directly (i.e. T1313M) or its receptor, ii) the cytoplasmic ends of S4 helices contribute to this receptor, and iii) mutations at R1448 and L1433 inhibit the S4/D4 helix from responding to voltage.

M-Pos443

EXPRESSION OF THE SODIUM CHANNEL $\beta_1$ SUBUNIT IN RAT SKELETAL MUSCLE IS SELECTIVELY ASSOCIATED WITH THE TETRODOTOXIN-SENSITIVE α SUBUNIT ISOFORM. ((J. S. Yang, P. B. Bennett, N. Makita, K. Kirkland, S. D. Kraner, A. L. George and R. L. Barchi)) Mahoney Inst. of Neurological Sciences and Dept. of Neuroscience, Univ. of Pennsylvania, Philadelphia, PA 19104; Dept. of Pharmacology and Medicine, Vanderbilt Univ., Nashville, TN 37232

Transcripts homologous to the rat brain sodium channel β subunit ($\beta_1$) are predominently expressed in both innervated and denervated adult skeletal muscle and in heart, but not in neonatal skeletal or cardiac muscle. A β cDNA from rat skeletal muscle was cloned by PCR and found to be identical in sequence to the rat brain and heart $\beta_1$ subunits. Regulation of $\beta_1$ mRNA expression closely parallels that of SkM1 α but does not follow SkM2 expression under any condition examined. Level of the expression of both SkM1 and $\beta_1$ mRNA increase in parallel, while SkM2 decreases >100 fold between day 5 and 14, a time when the motor endplate is reported to mature. In the adult muscle, denervation increases SkM2 mRNA from levels below detection to comparable to the SkM1, while $\beta_1$ and SkM1 shows little change. In primary muscle culture, SkM2 is upregulated when cell electrical activity is blocked by TTX or adenyl cyclase is elevated, while $\beta_1$ and SkM1 are relatively insensitive to these changes. In oocytes, $\beta_1$ interacts functionally with SkM1 to modulate the abnormally slow inactivation kinetics observed with this α subunit expressed alone. We conclude that a common $\beta_1$ subunit is expressed in skeletal muscle, heart, and brain and that in skeletal muscle, this subunit is specifically associated with the SkM1, rather than the SkM2, sodium channel isoform.

M-Pos444

CHARACTERIZING THE μ-CONOTOXIN BINDING SITE ON NA CHANNELS WITH ANALOGS AND POINT MUTATIONS. ((M. Chahine, L.-Q. Chen, N. Fotouhi, R. Walsky, D. Fry, R. Horn, and R.G. Kallen)) Dept of Physiol., Jefferson Med. Coll., Philadelphia, PA 19107; Depts of Bronchopul. Res. & Molec. Sci., Hoffmann LaRoche, Nutley, NJ, 07110; Dept of Biochem. & Biophysiol., Univ. of Penn., Philadelphia, PA 19104.

μ-conotoxin (μCTX) is a 22-amino acid peptide that blocks Na channels of adult skeletal muscle, but not brain or heart. The block of μCTX was studied on Na currents expressed in *Xenopus* oocytes, using cRNA of a Na channel cloned from rat skeletal muscle (rSkM1). Analogs of μCTX were constructed by solid-state peptide synthesis. Block varied by >2 orders of magnitude for different analogs. Each of the 7 basic residues was individually substituted by glutamine; these substitutions reduced the potency of block. The magnitude of the effect depended on the residue, with Arg13 being most critical for potency and Lys9 the least critical. Charge alone was not a sufficient explanation for changes in toxin block; e.g. Arg13→Lys was almost as poor a blocker as Arg13→Gln. Also, Asp12→Asn had little effect, whereas Asp12→Glu greatly reduced toxin potency. 1-D NMR spectra show that the latter substitution caused a shift of the peak associated with a proton on Arg13, suggesting an interaction between Arg13 and Glu12 in this analog. Point mutations were constructed in putative extracellular residues of rSkM1. One of these, rSkM1(Y401C), located in the loop between S5 and S6 of domain 1 and known to make the channel tetrodotoxin-insensitive (Chen et al, *FEBS Lett* **309**:253), reduced the block by native μCTX. This mutant was tested with μCTX analogs. The results suggest that either or both of the basic residues at positions 13 and 19 on μCTX interact with the residue Y401 on rSkM1.

M-Pos445

SECONDARY STRUCTURE, MEMBRANE INTERACTION AND ASSEMBLY WITHIN PHOSPHOLIPID MEMBRANES OF SYNTHETIC H-5 SEGMENTS OF VOLTAGE-GATED SODIUM CHANNEL. ((Yehonathan Pouny and Yechiel Shai)). Department of Membrane Research and Biophysics, Weizmann Institute of Science, Rehovot, 76100, ISRAEL (Spon. by S. R. Caplan)

The α-subunit of voltage-gated $Na^+$ channels is composed of four homologous repeats, each of which contains six putative membrane-spanning α-helices. The linkers between the fifth and the sixth transmembrane segments of each repeat (termed H-5) are homologous. Models of voltage-gated channels suggest that the H-5 segments of four domains/subunits form the narrow part of the channel [Durell & Guy (1992) Biophys. J. 62, 238; Sato & Matsumoto (1992) Biochem. Biophys. Res. Comm. 186, 1158]. We have synthesized and fluorescently labeled two peptides resembling the H-5 regions of domains I and III of *Electrophorus electricus (eel)* $Na^+$ channel, and utilized a spectrofluorometric approach to investigate their interaction with phospholipid membranes. Structural characterization using CD spectroscopy revealed that both peptides adopt low level of α-helicity in hydrophobic environment (20-25%). Functional characterization of the peptides demonstrated that they bound strongly PC vesicles and permeate them. Fluorescence Energy Transfer experiments between donor/acceptor-labeled pairs of peptides revealed that membrane embedded H-5 peptides associate with each other but do not associate with unrelated membrane-bound peptides. These results support the hypothesis that H-5 segments are packed in close proximity and as such might contribute to the oligomerization and to the correct assembly of the protein to form a functional channel.

M-Pos446

DYNAMICAL MODEL OF SODIUM CHANNEL ACTIVATION. ((C.C. CHANCEY)) Physics Dept., Purdue University Calumet, Hammond, IN 46323-2094. ((S.A. GEORGE and H.-T. Huang)) Neuroscience Program and Biology Dept., Amherst College, Amherst, MA 01002.

We have modelled voltage sensing in the sodium channel by evaluating forces on the S4 α-helix portion of the channel molecule, which we assume moves outward during activation. The interaction between the S4 α-helix segment and its environment was modelled by 1) nearest neighbor Coulombic forces, 2) the electric force due to an external electric field, and 3) static mechanical and electrostatic terms arising during the segment's resting state. These terms collectively describe a depolarization-dependent effective potential within which the S4 segment moves. We have determined the center-of-mass motion energy states for this potential. Thermal transitions are modelled starting from the Boltzmann distribution, and the time evolution of the segment's position relative to the membrane is simulated. Combining the histories of four such processes simulates the activation history for a single channel. Our model simulation is in close qualitative agreement with single channel open and closed dwell time distributions and with the dependence of the open probability on depolarization. The model also predicts the results of site-specific mutagenesis experiments showing opposite effects of eliminating positive charges on the cytoplasmic and extracellular ends of the S4 segment.

**M-Pos447**

CLONING AND SEQUENCE OF A PUTATIVE SQUID SODIUM CHANNEL cDNA AND A PROPOSED TERTIARY STRUCTURE MODEL: OCTAGONAL CORE STRUCTURE MODEL.

((Chikara Sato, Kiyonori Hirota and Gen Matsumoto)) Super Mol. Sci. Div., Electrotechnical Laboratory, Tsukuba, Ibaraki 305, Japan

With polymerase chain reaction and recombinant DNA techniques, we have cloned DNA complementary to RNA which seems to encode a sodium channel protein of the optic lobe of squid *loligo bleekeri*. The total number of the amino acid residues deduced from the cDNA is 1,522, about three fourth of those of rat brain I, II and III. On the basis of the sequence, we have proposed a tertiary structure model of the sodium channel where the transmembrane segments are octagonally aligned and the four linkers of S5-6 between segments S5 and S6 play a crucial role in the activation gate, voltage sensor and ion selective pore, which can slide, depending on membrane potentials, along inner walls consisting of segments S2 and S4 alternately. The proposed model is contrasted with that of Noda *et al.* (Nature 320; 188-192, 1986). Furthermore, genomic analysis were performed and the position of the intron were analyzed.

**M-Pos448**

EXPRESSION AND KINETICS OF HUMAN MUSCLE MUTANT SODIUM CHANNEL V1589M CAUSING SODIUM CHANNEL MYOTONIA.

((N.Mitrovic, A.L.George, S.Wagner, U.Hartlaub, R.Heine, U. Pika, H.Lerche, F.Lehmann-Horn)) Department of Applied Physiology, University of Ulm, Germany. (Spon. by A.Herrmann-Frank)

Human muscle sodium wild type (WT) channel and mutant (V1589M) channel which causes sodium channel myotonia were expressed in human embryonic kidney 293 cells. Patch-clamp recordings in both whole-cell and single-channel mode showed altered inactivation of the mutant sodium channel while no change in activation curve or single channel conductance was seen. The main difference between mutant and WT sodium current was a relative proportion of steady-state to peak current ($I_{ss}/I_{peak}$). $I_{ss}/I_{peak}$ measured at the end of 35 ms depolarizing pulse in whole-cell mode was larger in cells expressing V1589M mutant (3.15±0.70 % at -15 mV) than in those expressing WT channel (0.87±0.10 % at -15 mV). Furthermore, late sodium currents recorded in single-channel mode were also increased in patches containing V1589M channels (1.95±0.37 % at -30 mV) compared to patches containing WT channels (0.40±0.08 % at -30 mV). These results were comparable to data obtained from biopsied muscle specimen of patient carrying the M1592V mutation which causes hyperkalemic periodic paralysis, another myotonic disease. Patch-clamp recordings on sarcolemal blebs from native M1592V muscle fibers revealed an increase (1.34±0.43 % at -30 mV) in late channel openings compared to normal controls (0.34±0.07 % at -30 mV). Both mutations are in the sixth transmembrane segment of the fourth domain confirming that this region is involved in the process of inactivation. We hypothesize that this channel part which is located close to the inner mouth of the pore, acts as an acceptor of the inactivation gate. Supported by DFG Le 481/3-1.

## K CHANNELS I

**M-Pos449**

FUNCTIONAL FOREIGN SODIUM CHANNELS ACCELERATE ENDOGENOUS ION CHANNEL EXPRESSION IN EMBRYONIC *XENOPUS LAEVIS* MYOCYTES.

((Paul Linsdell and William J. Moody)) Dept. Zoology, Univ. of Washington, Seattle WA 98195. (Sponsored by Mark S. Cooper).

*Xenopus* embryonic myocytes dissociated at the neural plate stage, approximately 17½ hours after fertilization, have no voltage gated currents. They develop inward rectifier, delayed rectifier, A-current and Na currents sequentially over the next 10 hours in culture. Injection of fertilized eggs with rat brain IIA Na channel mRNA leads to the expression of large Na currents in early myocytes before any endogenous currents are normally present, effectively reversing the normal developmental sequence of K and Na channels. Myocytes expressing these foreign Na channels also express inward rectifier and delayed rectifier channels at a developmental time at which no currents are normally seen. These effects were inhibited by growing embryos in the presence of 1μM TTX, indicating that functional Na channels are necessary to alter the expression patterns of other ion channels. Expression of mouse Kv1.1 delayed rectifier channels in myocytes failed to accelerate either inward rectifier or Na channel expression. These results suggest that increased excitability early in myogenesis accelerates the normal program of voltage gated ion channel expression.

**M-Pos450**

HETEROLOGOUS EXPRESSION OF SPECIFIC $K^+$ CHANNELS IN T LYMPHOCYTES: FUNCTIONAL CONSEQUENCES FOR VOLUME REGULATION.

((C.Deutsch and L.Q.Chen)) Departments of Physiology and of Biochemistry/Biophysics, University of Pennsylvania, Phila., PA 19104-6085.

It has been postulated that the $K^+$ channel isoform Kv1.3 plays a role in regulatory volume decrease (RVD) in response to hypotonic shock. We show that a mouse cytotoxic T-lymphocyte line, CTLL-2, is devoid of voltage-gated $K^+$ channels, and is unable to volume regulate. Transient transfection of these cells with Kv1.3 reconstitutes their ability to volume regulate. When cells were transfected with Kv3.1, an isoform believed to be expressed in a specific subclass of mouse thymocytes, the CTLL-2 cells did not show RVD. The difference in the ability of the two isoforms to confer the capacity for RVD is expected from differences in the voltage dependence for activation of the channels, according to our proposed model for RVD (Deutsch *et al.*, J.Physiol. 372:405, 1986). This model predicts that the volume-induced changes in membrane potential activate voltage-gated $K^+$ channels. Our experimental approach involved transient co-transfection of $K^+$ channel-encoding plasmids with a plasmid encoding an abundantly-expressed cell surface molecule to which an antibody was available, in this case, human CD4. Selection of positive transfectants is highly effective, having >95% efficiency. This method, and this cell line, constitute important tools in studying lymphocyte $K^+$ channels and their function *in situ*.
Supported by NIH GM41467.

**M-Pos451**

EFFECT OF WHOLE-CELL DIALYSIS UPON CUMULATIVE INACTIVATION OF THE n-TYPE $K^+$ CURRENT OF PRIMARY HUMAN T-LYMPHOCYTES.

((D.I. Levy and C. Deutsch)) Dept. of Physiology, Univ. of Pennsylvania School of Medicine, Philadelphia, PA 19104-6085. (Spon. by D. Wilson)

The n-type $K^+$ current of human T lymphocytes undergoes cumulative inactivation upon repetitive depolarization. A recent report showed that oocyte expression of Kv1.3, which is presumed to underlie the n-type $K^+$ current, produces $K^+$ currents that demonstrate cumulative inactivation in excised, but not cell-attached patches (Marom *et al.* Receptors & Channels, 1:81-88, 1993). These data suggest a role for cytoplasmic factors in the regulation of cumulative inactivation. We have explored this possibility by comparing perforated patch (using amphotericin B) and standard whole-cell recordings from primary human T lymphocytes. A significant difference in the rate of cumulative inactivation was revealed by a train of 24 20-ms depolarizing pulses generated at 5 Hz. The rates of cumulative inactivation 8-20 min after sealing were $0.415 \pm 0.044$ sec$^{-1}$ (n=8) and $0.640 \pm 0.059$ sec$^{-1}$ (n=8), for perforated patch and whole-cell recording, respectively ($p<.01$). If the K·Asp/KCl whole-cell pipette solution was replaced with a KF solution, cumulative inactivation was profoundly enhanced; with a rate of $1.20 \pm 0.10$ sec$^{-1}$ (n=5), ($p<.001$ *vs.* perforated cells). To test the hypothesis that membrane-bound phosphatases alter cumulative inactivation, we used the whole-cell K·Asp/KCl preparation to examine the effects of intracellular [$Ca^{++}$], [$Mg^{++}$], okadaic acid (4μM), microcystin (100nM), deltamethrin (100nM), or orthovanadate (1mM) with $H_2O_2$ (1mM). None of these had significant effects on cumulative inactivation. Additionally, no significant effect on this process was produced by intracellular exposure to the reducing agent dithiothreitol (2mM) or the oxidizing agent 5,5'-dithio-bis-2-nitrobenzoic acid (DTNB, 2mM), suggesting that cumulative inactivation is not regulated by the redox state of the channel. While it appears that the intact T lymphocyte can modulate the process of cumulative inactivation, the exact mechanism remains to be determined. Supported by NIH GM 41467 and T-32 GM 07170.

**M-Pos452**

TRUNCATED $K^+$ CHANNEL DNA SEQUENCES SPECIFICALLY INHIBIT Kv1.3 AND Kv3.1 EXPRESSION IN MOUSE T LYMPHOCYTES.

((L.Tu and C.Deutsch)) Department of Physiology, University of Pennsylvania, Phila., PA 19104-6085. (Spon. by A. Weber)

We have implemented a strategy first demonstrated in oocytes by Li *et al.* (Science 257: 1225,1993) for specific suppression of $K^+$ channels in T lymphocytes. Plasmids that contain either a truncated Kv1.3 or a truncated Kv3.1 sequence and a CMV promoter were made, each containing the S1 transmembrane segment. The truncated Kv1.3 sequence contains the first 671 bases of the $NH_2$-terminus and Kv3.1 contains the first 685 bases. When mouse cytotoxic T cells(CTLL-2), which are devoid of endogenous voltage-gated $K^+$ currents, were transfected with full-length Kv1.3 and truncated Kv1.3, functional expression, as determined by whole-cell patch-clamp recording was inhibited by 89%, when compared to transfection with Kv1.3 alone. This inhibition was specific: transfection with truncated Kv1.3 did not significantly inhibit the current due to transfected full-length Kv3.1, a $K^+$ channel isoform belonging to a different subfamily of $K^+$ channels. Similarly, when CTLL-2 were transfected with full-length Kv3.1 and truncated Kv3.1, functional expression was specifically inhibited by 90%. To determine the minimum DNA sequence requirements for intra- and inter-subfamily specificity of inhibition, we are studying several other truncated DNA sequences including ones that lack the S1 segment, and ones that contain both S1 and S2 segments. The results have implications regarding heteromultimer formation. Supported by NIH GM41467.

**M-Pos453**

THE PRIMARY SEQUENCE OF THE INWARDLY RECTIFYING POTASSIUM CHANNEL FROM A LENS EPITHELIUM. ((James L. Rae)) Mayo Foundation, Rochester, MN 55905.

We have determined the primary amino acid sequence of the inwardly rectifying potassium channel from lens epithelium. For these studies, we used the α-TN4 cell line of mouse lens epithelium whose inward rectifier currents we had studied previously both at the single channel and whole cell levels. We constructed 7 forward and 6 backward non-redundant PCR primers from the sequence of mouse macrophage inward rectifier publish by Kubo, et al., Nature 362:127, 1993. Using either total or messenger RNA extracted from the δ-TN4 cells, we synthesized a first strand cDNA which was then amplified by PCR using all appropriate combinations of the forward and backward primers. Products which made bands on an agarose gel were reamplified using nested primers. This produced a series of 11 distinct products which extended from the start codon to stop codon in overlapping fragments. Each of the PCR products was sequenced directly without subcloning using Promega's fmol cycle sequencing kit. The sequence obtained was essentially identical to that found for the mouse macrophage. Cloning and expression are presently underway.

Supported by EY03282, EY06005 and an unrestricted award from Research to Prevent Blindness.

**M-Pos454**

**MOLECULAR CLONING, FUNCTIONAL EXPRESSION AND LOCALIZATION OF AN INWARD RECTIFIER POTASSIUM CHANNEL IN THE MOUSE BRAIN**

((K. Morishige, N. Takahashi, H. Koyama, J. S. Zanelli and Y. Kurachi)) Mayo Clinic, Rochester MN 55905. ((I. Findlay)) Unviersite de Tour, Tour, France. ((N. A. Jenkins and N. G. Copeland)) NCI-Frederick Cancer Research and Development Center, Frederick, MD 21702-1201. ((C. Peterson and N. Mori)) University of Southern California, Los Angeles, CA 90089.

We have cloned an inward-rectifier potassium channel from a mouse brain cDNA library, studied its distribution in the brain by *in situ* hybridization and determined the chromosomal localization of the gene. A mouse brain cDNA library was screened using a fragment of the mouse macrophage IRK1 cDNA as a probe. Two duplicate clones of ~5.5 kb were obtained. The amino acid sequence of the clone was identical to that of IRK1 recently cloned from a mouse macrophage cell line. *Xenopus* oocytes injected with cRNA derived from the clone expressed a potassium channel with inwardly rectifying channel characteristics. *In situ* hybridization study showed the mouse brain IRK1 to be generally distributed throughout the brain,with particular prominent expression in periglomelular cells of the olfactory bulb and the molecular layer of the cerebellum. The gene was placed in the distal region of mouse chromosome 11, which contains several uncloned neurological mutations. These results provide the first demonstration of the cloning and distribution of an inward rectifier potassium channel from the central nervous system.

**M-Pos455**

CLONING AND DISTRIBUTION OF KV-1 TYPE POTASSIUM CHANNEL SEQUENCES IN THE SQUID STELLATE GANGLIA. ((M. A. Perri, J.J.C. Rosenthal, T. Liu and W.F. Gilly)) Hopkins Marine Station, Stanford University. Pacific Grove, CA 93950.

Although membrane K conductances have been studied extensively in the squid giant axon, the molecular structure of the underlying channels have yet to be determined. We have cloned multiple putative K channel cDNA's from *Loligo opalescens* by screening a stellate ganglion (SG) cDNA library with a partial clone isolated from giant fiber lobe (GFL) neurons using degenerate PCR primers. One clone, KZ4, has been completely sequenced and codes for a protein which bears over 50 % identity with the Kv1 K channel family. Partial sequencing of 35 additional clones has revealed 4 sequence classes as defined by differences in the 5' coding and untranslated (UT) regions. RNAse protection using class specific probes demonstrate that two classes, KZ4 and KZ18, are expressed in GFL neurons and thus may encode channel proteins which exist in the giant axon and/or its somata. KZ18 is also expressed in the SG. The two other classes, KZ21 and KZ39, were not detected in the GFL but appear to be expressed at low levels in the SG. *In situ* hybridizations on SG and GFL tissue sections confirmed that KZ4 mRNA is expressed only in the GFL. Attempts to express KZ4 in an heterologous system are underway. KZ4 mRNA levels in transiently transfected Human Embryonic Kidney 293 cells are extremeley low in comparison to Shaker B1 (ShB1) controls in the identical plasmid vector. Chimeras containing KZ4 and ShB1 coding regions coupled to a Xenopus ß-globin 5' untranslated region (UT) and a ShB1 3' UT demonstrate that elements in both the KZ4 5' UT and 5' coding region may confer message instability. Some of these chimeras form functional K channels.

**M-Pos456**

**DELAYED RECTIFIER $K^+$ CHANNEL SEQUENCES FROM THE SQUID *LOLIGO PEALEI*** ((Tania Silva and Francisco Bezanilla)) Dept. of Physiology , UCLA, Los Angeles, CA, 90024.

We have obtained several cDNA sequences of potassium channels from the squid *Loligo pealei*. The clones were isolated from cDNA libraries from squid brain and optic lobe. The first clones, that were used later as probes, were identified using medium stringency hybridization conditions with an heterologous probe containing the central core region of the rat brain $K^+$ channel DRK1. The screening yielded clones containing the 5' and 3' ends of the channel sequences, with none or very little overlap. Primers were designed based on this sequence information to obtain PCR fragments, using as a template cDNA derived from mRNA of the same tissue, which confirmed the sequence of little overlap. The squid sequences contain 6 putative transmembrane domains and the P region which are highly conserved in $K^+$ channels. The squid clones show a high degree of similarity to DRK1 (the original probe) and to Drosophila *Shab*-11, however outside this core region there is little similarity. The squid clones are nearly identical in the central core region of the channel sequence, but some differ from one another towards the amino and carboxy termini, sugesting that this channel may be part of a multigene family and/or is alternatively spliced. A full length clone, constructed from two of the cDNA clones, expresses $K^+$ currents when cRNA is injected into *Xenopus* oocytes. (See abstract by D. E . Patton et al). Supported by USPHS grant GM30376.

**M-Pos457**

**FUNCTIONAL EXPRESSION OF A DELAYED RECTIFER POTASSIUM CHANNEL CLONED FROM SQUID IN *XENOPUS* OOCYTES.** ((D. Earl Patton, Tania Silva, David DiGregorio and Francisco Bezanilla)) Department of Physiology, UCLA. School of Medicine, Los Angeles, CA 90024.

We have constructed a full length potassium channel from 2 cDNA clones isolated from a squid (*Loligo pealei*) optic lobe library described in the accompanying abstract (Silva and Bezanilla). It is possible that these 2 cDNA clones were derived from different mRNA species because they only had 14 base pairs of sequence overlap, which was in the middle of the S4 segment. The full length construct has an open reading frame of 2,724 nucleotides and contains the *Xenopus* β-globin 3' untranslated region following the open reading frame. Injection of cRNA transcribed from the full length construct into *Xenopus* oocytes resulted in the expression of a delayed rectifier potassium current. The currents expressed from this construct resemble currents through the DRK1 potassium channel except that the squid channel begins to activate at least 20 mV hyperpolarized relative to DRK1 and its activation kinetics are faster. We have also constructed a DRK1/squid chimeric channel consisting of DRK1 amino acids 17 through 303 followed by the squid channel sequence through the end of the open reading frame. The junction is in the middle of the S4 segment. This chimeric channel displays activation properties intermediate between the pure squid and DRK1 channels. Supported by USPHS grants GM30376 and NS07101.

**M-Pos458**

STRUCTURAL DETERMINANT FOR THE ASSEMBLY OF HETEROMULTIMERIC MAMMALIAN $K^+$ CHANNELS (T.E. Lee, L.H. Philipson, A. Kusnetsov and D.J. Nelson) University of Chicago, Chicago, IL 60637

$K^+$ channel function is regulated through the assembly of subunit isoforms into either homo- or heterotetrameric channel structures, each characterized by distinct pharmacologic and kinetic properties. We constructed a deletion mutant of hKv1.4 in which residues 28 through 283 were deleted ($hKv1.4_{\Delta 28\text{-}283}$), and examined the functional properties electrophysiologically in *Xenopus* oocytes. Deletion of 255 amino acids in the N-terminal domain of Kv1.4 prevented the formation of hybrid channels within the subfamily but had no effect on homomultimerization or voltage-dependent gating. The time course of inactivation was 40 ± 6 msec [n = 6] for $Kv1.4_{\Delta 28\text{-}283}$ and 43 ± 6 msec [n=6] for wild-type in a step to +40 mV. The threshold for current activation was -53 ± 4 mV [n=3] for $Kv1.4_{\Delta 28\text{-}283}$ and -50.9 ± 1.5 mV [n=3] for wildtype. The midpoint of steady-state invactivation for the mutant channel was shifted to slightly more hyperpolarized potentials (-68 ± 0.8 mV [n=4] versus -62 ± 1.2 mV [n=5]). Although $hKv1.4_{\Delta 28\text{-}283}$ could not form heteromultimers within the same subfamily, it could, however, form heteromultimers with $Kv2.1_{\Delta 1\text{-}139}$. $Kv2.1_{\Delta 1\text{-}139}$ exhibits a non-inactivating current with a midpoint of steady-state inactivation shifted positive relative to $Kv1.4_{\Delta 28\text{-}283}$. Heteromultimers of $Kv1.4_{\Delta 28\text{-}283}$ and $Kv2.1_{\Delta 1\text{-}139}$ were characterized by an inactivating current which was present at holding potentials in which all $Kv1.4_{\Delta 28\text{-}283}$ homomultimeric current was eliminated. We conclude that the amino-terminal region of mammalian $K^+$ channels functions to allow heteromultimer formation within a subfamily and prevent heteromultimer formation between subfamilies.

**M-Pos459**

**DOMINANT NEGATIVE EXPRESSION APPROACH TO THE STUDY OF FUNCTIONAL $K^+$ CHANNEL ASSEMBLY IN *XENOPUS laevis* OOCYTES.**

((A. Moscucci, H. Wang, T. Babila, G. Koren)) Cardiovascular Division, Brigham & Women's Hospital, Harvard Medical School, Boston, MA.

**The functional heterogeneity of $K^+$ channels is determined by the assembly of channel subunit polypeptides into tetrameric protein complexes. We previously showed that Kv1.1 (RCK1) and Kv1.5 (RMK2) form homo- or heteromultimeric $K^+$ channels, and that the S1 segment is essential for *in vitro* association of the $NH_2$-terminal domains of these proteins. We investigated the structural elements essential for channel assembly *in vivo*, by expression of $K^+$ currents in *Xenopus* oocytes microinjected with cRNAs of Kv1.1, Kv1.5, and several $NH_2$-terminal domain truncations of these polypeptides. $K^+$ currents were recorded by two-electrode voltage clamp 2-3 days post-injection. Overexpression (> 10X molar ratio) of constructs including the S1 domain (Kv1.1N206 and Kv1.5N314) had significant ($p<0.01$) negative dominant effect on wild type $K^+$ channels' expression, as did a Kv1.1 $NH_2$-terminal domain truncated construct without the S1 (Kv1.1N168). However, a Kv1.5 $NH_2$-terminal construct lacking the S1 (Kv1.5N242) had no significant dominant negative effect. Furthermore, overexpression (50X molar excess) of the S1 fragment itself (Kv1.1S1) significantly ($p<0.01$) blocked Kv1.1 current expression. Constructs consisting only of transmembrane domains (Kv1.1S1-S6 and Kv1.1S2-S6) produced no expressed current, as did none of the fragments above.**

**Our data show that the S1 segment is essential for multimerization of channel subunits. These studies refine and extend the current model of $K^+$ channel assembly, and suggest a structural model system in which the $NH_2$-terminal domain and the S1 allosterically promote $K^+$ channel subunit assembly.**

**M-Pos460**

CLONING AND EXPRESSION OF THE GENE ENCODING THE MURINE DELAYED RECTIFIER POTASSIUM CHANNEL KV1.5.

((B. London*#, J.A. Hill*, B. Nadal-Ginard*, and D.A. Logothetis+)) Harvard Medical School: Children's Hospital* and Massachusetts General Hospital#, Boston, MA and Mount Sinai School of Medicine+, New York NY

We have cloned the delayed rectifier potassium channel mKv1.5 from a mouse PCC4 genomic library. Sequencing of the clone showed the transcription start site ~150 BP downstream from a 50 BP dinucleotide (CA) repeat; the polyadenylation signal was 3.4 KB further downstream. This intronless gene is highly homologous to the previously reported rat cDNA clones, and codes for a protein 602 amino acids in length (96% amino acid identity to rat Kv1.5). Northern Blot analysis identified an abundant mRNA of the expected size in fetal and adult ventricles; lesser amounts were present in skeletal muscle and brain.

The coding region was subcloned into a high expression vector after addition of a consensus Kozak sequence. *In-vitro* transcribed cRNA was injected into Xenopus oocytes (50 ng/oocyte), and two microelectrode voltage clamp yielded delayed rectifier outward currents. Steady state activation curves (generated in 50 mM RbCl from isochronal tail current measurements) gave a total gating valence $z = 4.6\pm0.1$ $e^-$ and a voltage of 10% activation $V_{10\%} = 31.6\pm1.5$ mV (n=6). This gating valence is 23% lower and $V_{10\%}$ is shifted 20 mV to the right compared to the rat Kv1.1 channel, despite the fact that the S4 regions of the two channels are identical.

We plan to further investigate (1) those elements outside the S4 region which contribute to the channel's voltage sensor and (2) the *in-vivo* function of this channel in the mouse heart.

**M-Pos461**

PHARMACOLOGICAL CHARACTERIZATION OF FIVE CLONED VOLTAGE-GATED $K^+$ CHANNELS, Kv1.1, Kv1.2, Kv1.3, Kv1.5, AND Kv3.1, STABLY EXPRESSED IN MAMMALIAN CELL LINES

((A.N. Nguyen, S. Grissmer, D.C. Hanson, R.J. Mather, G.A. Gutman, M.J. Karmilowicz, D.D. Auperin and K.G. Chandy)). Department of Physiology and Biophysics and Microbiology and Molecular Genetics, UC Irvine, CA 92717 and Department of Immunology and Molecular Biology, Pfizer Central Research, Groton, CT 06340.

We have analyzed the biophysical and pharmacological properties of five cloned $K^+$ channels (Kv1.1, Kv1.2, Kv1.3, Kv1.5, Kv3.1) stably expressed in mammalian cell lines. Kv1.1 is biophysically similar to a $K^+$ channel in C6 glioma cells and astrocytes, Kv1.3 and Kv3.1 have electrophysiological properties identical to the types *n* and *l* $K^+$ channels in T cells, and Kv1.5 closely resembles a rapidly activating delayed rectifier in the heart. Each of these native channels may be formed from the homomultimeric association of the corresponding Kv subunits, and pharmacological compounds that selectively modulate them may be useful for the treatment of neurological, immune and cardiac disorders. The cell lines described in this report could be used to identify such drugs and we have therefore embarked on a pharmacological characterization of the five cloned channels. The compounds tested in this study include 4-aminopyridine, capsaicin, charybdotoxin, cromakalim, dendrotoxin, diltiazem, D-sotalol, flecainide, mast cell degranulating peptide, nifedipine, noxiustoxin, resiniferatoxin and tetraethylammonium. This work was supported by a grant from Pfizer Inc., Groton, CT (KGC), and from Pfizer Ltd., Sandwich, England (SG).

**M-Pos462**

**EXPRESSION OF THE Kv1.3 POTASSIUM CHANNEL IN VARIOUS CELLS OF HEMATOPOIETIC ORIGIN.**

((M. Strong, D.J. Nelson, B. Dethlefs, M. Sheng, L. Jan, K.G. Chandy and G.A. Gutman)). Depts. of Physiol. & Biophys., Microbiol. & Mol. Gen., UC Irvine; Dept. of Neurol., Univ. of Chicago; and HHMI, UCSF.

We report here that the Kv1.3 $K^+$ channel gene may be expressed in various cells of hematopoietic origin. The Kv1.3 gene has previously been shown to encode the type *n* channel in human and mouse T cells, and in a variety of T cell lines. Additionally, currents similar to the type *n* channel have been found in human tissue macrophages, mouse peritoneal macrophages, B cells, natural killer cells, mammalian platelets, the promonocyte lines U937 and THP1, and the ML1 myelomonoblast line.

The $K^+$ current $I_A$ expressed in human monocyte-derived macrophages and alveolar macrophages could be produced by the Kv1.3 gene product. An electrophysiological comparison of the cloned Kv1.3 channel, the type *n* channel, and the $I_A$ current reveals their similarity. These three channels exhibit use-dependent inactivation, have slow tail currents upon deactivation and have similar voltage-dependent activation and inactivation kinetics. PCR analysis using Kv1.3-specific primers on 7 day adherent macrophages reveal the predicted size band from cDNA. Genomic DNA was excluded as a source of contamination in this analysis.

In order to elucidate the distribution of the Kv1.3 channel, we are analyzing various hematopoietic cells for the presence of Kv1.3 functional channel and/or protein by Western blotting. Using a polyclonal rabbit anti-N-terminal-peptide antibody, we have detected a ~58kD membrane-associated protein in human platelets, U937, Jurkat, RBL and K562 lines. Positive controls are a Kv1.3 transfected NIH3T3 fibroblast line and a vaccinia virus/Kv1.3 infected CV1 line (see R. Spencer this meeting). Negative controls include the HL60 promyelocyte and CV1 kidney line. While this Ab does detect Kv1.3 protein, it also cross-reacts with proteins other than the ~58kD band, in whole cell preps and in CV1 membranes. These studies together with patch clamp analyses reveal that detection of channel protein by Western blotting does not necessarily *predict* functional $K^+$ channel expression. Supported by grants from Pfizer Inc. and USPHS GM36823.

**M-Pos463**

**HIGH LEVEL PROTEIN EXPRESSION AND POST-TRANSLATIONAL MODIFICATIONS OF AN INWARDLY RECTIFYING POTASSIUM CHANNEL.**

((Deborah L. Laidlaw, Stephan Grissmer, George A. Gutman*, K. George Chandy)) Dept. of Physiology & Biophysics, and *Dept. of Microbiology & Molecular Genetics, UC Irvine, CA 92717)

$K_{ir}2.1$ (IRK1), is an inwardly rectifying potassium channel cDNA clone from the J774.1 macrophage cell line. The 47 kDa protein contains two putative transmembrane regions and a pore region homologous to other $K^+$-selective ion channels. Studies on the structure and post-translational modifications of $K_{ir}2.1$ would be facilitated by the availability of substantial amounts of purified protein. For high-level protein expression in a mammalian system, we cloned the $K_{ir}2.1$ coding region into the pTM1-derived plasmid vector pTH1 to generate a $K_{ir}2.1$ fusion protein. This fusion protein consists of a histidine repeat ($His_6$) for $Ni^{2+}$-column purification, a portion of the gene 10 protein of phage T7, and an enterokinase cleavage site, fused in-frame to the $NH_2$-terminus of the $K_{ir}2.1$ protein. This vector includes the T7 promoter and transcription termination sequences. We expressed the $K_{ir}2.1$ fusion protein in Xenopus oocytes and the properties of the expressed channels were biophysically indistinguishable from those of the native protein. The construct was then transfected into African Green monkey CV-1 cells, simultaneously infected with a vaccinia recombinant virus expressing T7 RNA polymerase. Immunoprecipitation of the resulting $^{35}S$-met-labelled fusion protein with an anti-G10 monoclonal antibody, followed by SDS-PAGE, revealed two bands corresponding in size to 47 kDa (the predicted size of the $K_{ir}2.1$ protein) and 48 kDa. Using this transfection/infection procedure, we plan to extend our biochemical studies to determine the sites of various post-translational modifications and their relevance for functional protein expression. (Supported by grants from the NIH [AI-24783] and Pfizer Inc.)

**M-Pos464**

SUBUNIT INTERACTIONS IN *SHAKER* $K^+$ CHANNEL GATING

((Ling Lin, Ken McCormack, Fred J. Sigworth)) Dept. Cell. and Molec. Physiol., Yale Sch. of Med., New Haven CT 06510. (Spon. by R. K. Ayer, Jr.)

The A2 mutation (L382A in the *Sh*B sequence) shifts activation by more than +130 mV. Dimeric and tetrameric constructs of N-terminal-truncated, *Sh* 29-4 cDNAs were generated using 19-aa linkers. Eight tetrameric constructs contained one, two or three A2 protomers in various permutations. The figure compares the G-V curves for oocytes injected with RNA for wild-type truncated and A2 monomers, and the tetrameric constructs WAWW, AWAW and AWAA. Solid curves indicate fits of a model developed for the V2 mutation (L382V) that assumes independent voltage-dependent transitions in each subunit followed by a voltage-dependent concerted channel-opening step. Dotted curves show the predictions of this model for heteroprotomeric channels, assuming additive contributions of of the concerted transition. The lack of agreement between data and predictions suggests that one or more assumptions in this model may need to be modified.

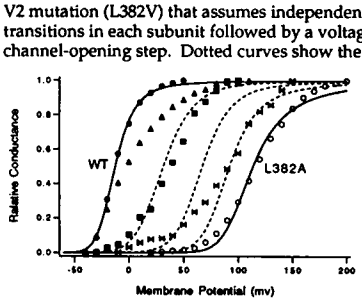

**M-Pos465**

MUTAGENESIS OF THE S3 REGION OF MKV1.2 ALTERS VOLTAGE-DEPENDENCE OF ACTIVATION.((S. Smart,W.Hopkins and B. Tempel))Pharmacology Dept., U. of Washington, Seattle, WA.

The mouse potassium channel mKv1.2 differs by only nine amino acids in protein sequence from its rat homologue RCK5. However, when expressed in Xenopus oocytes, RCK5 has been described as activating near -50 mV (EMBO J. 8:3235, 1989) whereas mKv1.2 activates near -40 mV (Hopkins, submitted). When expressed in CHO cells, mKv1.2 activates near -10mV, suggesting that in mammalian cells mKv1.2 activates at a yet more positive potential than seen in oocyte expression studies (Soc. Neurosci., 19:712A). We have used site-directed mutagenesis to investigate the structural basis for this apparent difference in the voltage-dependence of activation between these otherwise very similar channels. Two of the amino acids differing between mKv1.2 and RCK5 are in putative transmembrane regions, and we have substituted each of these residues in mKv1.2 with the corresponding residue found in RCK5. Specifically, alanine 262 in the S3 region of mKv1.2 and isoleucine 292 in the S4 region of mKv1.2 were each changed to threonine, as found in RCK5. When expressed in Xenopus oocytes, A262T appears to activate near -50mV, whereas I292T activates at -40mV and does not appear to differ from the wild-type mKv1.2 channel. To determine the characteristics of the amino acid residue at position 262 responsible for the observed shift in voltage-dependence of activation, we have further substituted the alanine at this position in mKv1.2 with valine, isoleucine, glycine, and serine.

**M-Pos466**

**PROLONGED DEPOLARIZATION CHANGES CHARGE MOVEMENT PROPERTIES IN SHAKER-IR W434F $K^+$ CHANNEL**
((R. Olcese#, L. Toro#, E. Perozo*, F. Bezanilla* & E. Stefani#)), #Dept. Molec. Physiol. & Biophys, Baylor Col. Med. Houston, TX 77030 and *Dept. of Physiol., UCLA, Los Angeles, CA 90024.

Prolonged depolarization induces a slow inactivation process (type C) in *Shaker* $K^+$ channel lacking the inactivating ball peptide (*ShH4IR*) (Hoshi et al., Neuron 7:547-56. We investigated how type-C inactivation affects transitions among closed states by measuring charge movement in a non-conducting mutant (*ShH4IR-W434F*) expressed in *Xenopus* oocytes. Gating currents were recorded using the cut-open oocyte voltage clamp technique. Due to the high expression levels, gating currents were directly recorded after analogical compensation of the linear capacity at +40 mV. The voltage-dependence of the charge movement (Q-V) when the membrane potential was held at -90 mV showed two components which can be described by the sum two Boltzmann distributions; the first with a shallower voltage dependence ($V_{½}$=-56 mV, z=2.2) and the second with a steeper voltage dependence ($V_{½}$=-37 mV, z=5.7) (*see* Perozo et al., this meeting). When the channels were inactivated at HP=0 mV, the Q-V curve was shifted to more negative potentials without changes in the total amount of charge moved (Bezanilla et al., J. Gen. Physiol. 79:21-40,1982). The first component had $V_{½}$=-85 mV, z=1.55 and the second component $V_{½}$=-55 mV, z=3.6. We found that both the installation and recovery of the slow inactivation takes several seconds. For example, at 0 mV, 10-20 sec are needed to reach a reduction of 50% in the charge movement for pulses to -60 mV. In conclusion, prolonged depolarization induces a slow inactivation process that is associated with a conformational change in the channel protein. A manifestation of this new conformation is the different voltage dependence and sensitivity of the charge movement. (Supported by NIH grants AR38970 and GM30376).

**M-Pos467**

**ON THE RELATIONSHIP BETWEEN GATING AND IONIC CURRENTS FROM THE DELAYED RECTIFIER $K^+$ CHANNEL IN SQUID GIANT AXONS. A SIMPLE MODEL OF $K^+$ CHANNEL GATING.**
((J.R. Clay)) NINDS, NIH, Bethesda, MD 20892.

The relationship between gating (Q-V curve) and channel activation (f-V curve) provides important constraints on gating models. For example, White and Bezanilla (J. Gen. Physiol., 1985, 85:539) reported a 40 mV difference in the midpoints of the two curves, suggesting that significant charge movement occurs amongst many closed states prior to channel opening. However, the f-V curve for the squid axon DR has, in my view, been significantly mismeasured beginning with HH, and subsequently. The $I_K$ open channel IV is a non-linear function of ($V-E_K$), consistent with GHK (J.R. Clay, J. Physiol. 1991, 444:449). Consequently, $I_K$ records should be normalized by GHK rather than by ($V-E_K$). Surprisingly, the results of this analysis superimpose with the Q-V results of White and Bezanilla, save for the foot of the curves (-70, -40 mV), suggesting that significant charge movement occurs as the channel opens. These results are well desribed by a model consisting of two closed and one open state, in which the forward rate parameter between the closed states is time dependent (semi-Markov). The model also describes the Cole-Moore effect and a rising phase of ON gating current.

**M-Pos468**

TESTING FOR MICROSCOPIC REVERSIBILITY IN THE GATING OF BK CHANNELS USING TWO-DIMENSIONAL DWELL-TIME DISTRIBUTIONS.
((L. Song, and K. L. Magleby)) University of Miami, School of Medicine, Miami, FL 33101-6430

An assumption often made when developing kinetic models for the gating of ion channels is that the transitions among the various states involved in the gating obey microscopic reversibility. When microscopic reversibility is obeyed, the number of forward and backward transitions per unit time for any given pair of connected kinetic states will, on average, be identical, and consequently the data must show time reversibility. To look for possible deviation from time reversibility, two-dimensional dwell-time distributions of adjacent open and closed intervals obtained from single-channel current records were analyzed in the forwards and in the backwards directions (Steinber, 1987, Biophysical J. 52:47-55). Two-dimensional dwell-time distributions of pairs of open intervals and of pairs of closed intervals were also analyzed to extend the resolution of the method to special circumstances in which intervals from different closed (or open) states might have similar durations. Analysis of several hypothetical models indicated that the method can detect deviations from microscopic reversibility for certain types of cyclic gating models. We then investigated whether the gating of large conductance $Ca^{2+}$-activated $K^+$ channels (BK channels) in cultured rat skeletal muscle displays non-equilibrium processes. No significant differences were observed between the forwards and backwards analysis of the various two-dimensional dwell-time distributions, consistent with time reversibility. Thus, we find no evidence to indicate that the gating of the examined BK channels violates microscopic reversibility. Supported by Grants from the NIH and the Muscular Dystrophy Association.

**M-Pos469**

ROLE OF SIDE CHAIN CHARGE, SIZE, AND CAPACITY TO FORM HYDROGEN BONDS IN S4 FUNCTION. ((Y. Huang and D.M. Papazian)) Department of Physiology, UCLA School of Medicine, Los Angeles, CA 90024. (Spon. by E.M. Wright)

Analysis of the S4 mutation, R368Q, at the voltage clamp, single channel, and gating current levels suggests that this residue is a key component of the voltage sensor of Shaker K channels. The amino acids N, D, E, C, and G have now been substituted for R at position 368. Each mutation generates functional channels, indicating that this position can tolerate positive, negative, and neutral amino acids with a wide range of sizes. These mutations affect the slope of the conductance-voltage (g-V) curve, which provides a rough estimate of the voltage-dependence of the channel, and the midpoint of the g-V curve, which may indicate the relative stability of the open and closed conformations of the protein. Changes in side chain charge are not sufficient to explain the results. The slope of R368D is similar to that seen in R368Q, N, C, and G. Side chain size also plays a role since R368E has larger effects on slope and midpoint than R368D, and R368Q shifts the midpoint more than R368N. However, charge and size are not the only factors that affect the relative stabilities of open and closed states. C and G, with small, neutral side chains, cause larger shifts in the midpoint than the larger, neutral N and acidic D. One possibility is that the decreased capacity for hydrogen bond formation by C and G compared to N and D decreases protein stability. Thus, the contribution of the amino acid at 368 to the stability or voltage-dependence of the channel may depend on side chain charge, size, and capacity to form hydrogen bonds. (Supported by the NIH (GM43459), the Klingenstein Fund, and the Pew Charitable Trusts.)

**M-Pos470**

CONSERVED CYSTEINES IN SHAKER K CHANNELS ARE NOT LINKED BY A DISULFIDE BOND. ((C.T. Schulteis, S. John, Y. Huang, and D.M. Papazian)) Department of Physiology and Program in Neuroscience, UCLA School of Medicine, Los Angeles, CA 90024.

Many voltage-activated K channels contain two conserved cysteine residues in the putative transmembrane segments S2 and S6. It has been proposed that these cysteines form an intrasubunit disulfide bond (Durrell & Guy, *Biophys. J.*, 62: 238-250, 1992). This proposal was tested by site-directed mutagenesis and electrophysiological and biochemical analysis of the Shaker K channel. Shaker protein contains 7 cysteine residues, the conserved ones being at positions 286 and 462. Each cysteine in the Shaker protein can be individually mutated to serine with the retention of functional activity as measured by expression in *Xenopus* oocytes. These results indicate that if the protein contains a disulfide bond, it is not essential for protein folding or the assembly of active channels. To determine biochemically whether the two conserved cysteines form a disulfide bond, HEK 293 cells were transfected with a plasmid containing the Shaker sequence under the control of a cytomegalovirus promoter. Intact transfected and untransfected cells were treated with trypsin, boiled in Laemmli sample buffer, and subjected to electrophoresis and immunoblot analysis. An antipeptide antibody directed against the C terminal end of the protein recognizes a tryptic fragment of approximately 38,000 daltons. The mass of this fragment and its reactivity with the C terminal antibody suggest that it extends from the putative extracellular loop between S3 and S4 to the C terminus of the protein, including cysteines 462 and 505. The migration of this fragment on SDS gels is identical under reducing and non-reducing conditions, indicating that the conserved cysteine at 462 is not involved in a disulfide bond with cysteines in the N terminal half of the protein, including the conserved cysteine at position 286. (Supported by the NIH (GM43459) and the Pew Charitable Trusts. CTS is a predoctoral fellow of the Howard Hughes Medical Institute.)

M-Pos471

**A MODULAR APPROACH TO OLIGONUCLEOTIDE-DIRECTED *IN VITRO* MUTAGENESIS FOR THE DESIGN OF MULTIPLE, SIMULTANEOUS MUTATIONS.**

**((M.S. Champagne and J.A. Drewe)) Baylor College of Medicine, Houston, TX 77030. (Spon. by H.A. Hartmann)**

Oligonucleotide-directed *in vitro* mutagenesis is a valuable tool for the targeted manipulation of cDNAs. A very high success rate of mutation can be obtained with a kit available from Amersham. However, if multiple, simultaneous mutations over a large region are needed, a single, long, mutant oligonucleotide is impractical due to size limitations on synthetic oligonucleotides and the decreased flexibility to choose different combinations of mutations within that region. The modular approach reported allows the formation of both long and short mutation ranges concurrently with the same oligonucleotides. The sixth putative transmembrane region (108 bp) of a *Drosophila* potassium channel clone, Kv1.1, was divided into three sections: S6′, S6″, and S6‴, each to be mutated to that of a related but phenotypically dissimilar rat potassium channel clone, Kv3.1. Three contiguous, non-overlapping oligonucleotides with the desired mutations of each subregion were designed, and the chimeras S6′, S6″, S6‴, S6′+S6″, S6″+S6‴, S6′+S6‴, and S6′+S6″+S6‴ were formed. We have achieved mutation rates of 95% for singles and 69% for doubles (9/13 samples). We sequenced four samples of the triple and found the mutation in one. We have found this modular approach to oligonucleotide-directed *in vitro* mutagenesis extremely useful for structure-function studies because of the ability to interchange several mutations easily and efficiently.

M-Pos472

THE β-SUBUNIT OF THE HIGH-CONDUCTANCE $Ca^{2+}$-ACTIVATED $K^+$ CHANNEL FROM SMOOTH MUSCLE.

((H.-G. Knaus[1], A. Eberhart[1], M. L. Garcia, M. Garcia-Calvo, G.J. Kaczorowski, M. Smith, K. Folander[2], and R. Swanson[2])) [1]Biochemical Pharmacology, Univ. Innsbruck, Austria; Dept. of Membrane Biochemistry & Biophysics and [2]Pharmacology Merck Research Laboratories, Rahway, NJ 07065; West Point, PA 19486.

The high-conductance $Ca^{2+}$-activated $K^+$ channel from bovine trachea smooth muscle consists of two non-covalently linked subunits, α and β, with Mr's of 62,000 and 31,000, respectively. The β-subunit represents the protein to which [$^{125}$I]charybdotoxin (ChTX) is crosslinked and it is a glycoprotein with a core Mr of 21,400. Amino acid sequence, obtained from isolated proteolytic fragments of the β-subunit, was used to identify bovine tracheal and aortic smooth muscle cDNAs encoding this protein. The cDNAs encode a deduced protein of 21,952 Da containing two hydrophobic (putative transmembrane) domains, two consensus sequences for N-linked glycosylation and a Thr residue within a consensus sequence for phosphorylation by protein kinase A. Northern blot analysis reveals strong hybridization of the cDNA to an 3.8 kb mRNA and weak hybridization to a 1.7 kb mRNA in both trachea and aorta. Site-directed antibodies raised against two of the putative extracellular domains of the β-subunit recognize this protein in Western blots and are able to immunoprecipitate not only the [$^{125}$I]ChTX crosslinked subunit but also, under nondenaturing conditions, the α/β complex. These results provide further evidence that the maxi-K channel exists, *in vivo*, as a complex of α- and β-subunits, and represent the first $K^+$ channel β-subunit cloned to date.

M-Pos473

MAPPING THE "BALL" PEPTIDE (BP) RECEPTOR OF $K_{Ca}$ CHANNELS

((M. Ottolia*, E. Stefani*, L. Toro* and R. Latorre§)) *Baylor College of Medicine, Houston, TX 77030. §CECS and Univ. Chile, Santiago 9, Chile.

The inactivating "ball" peptide (BP) of *Shaker* B K channels is able to interact with $Ca^{2+}$-activated $K^+$ channels. We designed 10 BP mutants with different charges and hydrophobicity to study the channel internal structure. The net charge of BP was either decreased by replacing arginine (R) and lysine (K) for glutamine (Q); or increased by exchanging glutamic (E) and aspartic (D) acids with asparagine (N), Q, or K. In general, an increase in the peptide positive charge was followed by an increase in both the affinity for the channel and the association rate constant ($k_{on}$) (*e.g.* a change from +1 in K18QK19Q to +7 in E12KD13K diminished the $K_d$ from 259±92 μM, n=2 to 3.6±0.3 μM, n=2, and increased $k_{on}$ from $3.5x10^5$ $M^{-1}s^{-1}$ to $4.3x10^6$ $M^{-1}s^{-1}$). Interestingly, the voltage dependence (zδ≈0.5) did not change by increasing the charge. Hydrophobicity of BP was varied by replacing alanines (A) or glycines (G) with valines (V). Increasing hydrophobicity affected mainly the time the peptide resides in the internal mouth, and not the frequency at which it hits the receptor (*e.g.* at concentrations of about twice the $K_d$, E12KD13K produced blocked times ≈10 ms, while the ones induced by A2VA3VA5VE12KD13K were of ≈300 ms and ≈2 s duration; whereas, $k_{on}$ values were $4.3x10^6$ $s^{-1}M^{-1}$ *vs.* $3.1x10^6$ $s^{-1}M^{-1}$). Common features to all peptides were: 1) blockade was relieved by increasing external [$K^+$], and 2) they were only active from the internal side. In addition, an increase in the ionic strength decreased the peptide affinity for its receptor. All our results can be explained assuming the existence of negative charges and a hydrophobic pocket in the internal vestibule of the channel. Supported by NIH grants HL47382, HL37044 and FNI 863-91.

M-Pos474

**STRUCTURAL STUDIES OF UNITARY CONDUCTANCE IN MAXI-K (*SLOWPOKE*) CHANNELS.**

((A. Lagrutta, K.-Z. Shen, R.A. North, and J.P. Adelman)) Vollum Institute, Oregon Health Sciences University, Portland, OR 97201.

*Slowpoke* channels are a structural prototype for large conductance, voltage-dependent, calcium-activated potassium channels. Using site-directed mutagenesis and expression in *Xenopus* oocytes, we assessed the contribution of amino acid residues flanking the P region to unitary conductance. Wildtype and mutant channels were recorded from inside-out membrane patches with [K]o = [K]i = 120 mM, [Ca]o = 1.8 mM, [Mg]i = 2 mM, [Ca]i = 1-30 μM. Under these conditions, there is a slight inward rectification of unitary current.

First, we tested the contribution of two aromatic residues on the S5-P region junction, at the external mouth of the channel pore (Tyr293 and Phe294). We substituted each residue by Trp, the homolog in *Shaker*, *Shab*, *Shal*, and *Shaw*. Outward currents were not affected. Inward currents for Y293W were ~40% smaller than wildtype; inward currents for F294W were identical in amplitude to the wildtype but were flickery, unlike the wildtype or the Y293W mutant. Similar findings were made with [Ca]o = [Mg]i = 0: at -100 mV unitary current was 26.9 ± 0.3 pA (n = 11) for wildtype, 10.0 ± 0.3 pA (n = 8) for Y293W, and 26.3 ± 0.9 pA (n = 9) for F294W. Unitary conductance was a saturating function of [$K^+$] for all three channel types; half-maximal [$K^+$] was not different among the three channel types: 6.8 ± 0.6 mM for wildtype, 9.0 ± 1.9 mM for Y293W, and 8.4 ± 1.7 mM for F294W.

Secondly, we tested the contribution of two negatively charged residues at the cytoplasmic end of S6, near the internal mouth of the channel pore (Glu335 and Glu338), by charge neutralization (Gln) or reversal (Lys). Compared to the wildtype, unit currents in E338Q, E338K, E335Q, and E335K had smaller amplitudes, with no obvious change in rectification. Unit conductance at 0 mV was 196 pS for wildtype, 178 pS for E338Q, 131 pS for E338K, 153 pS for E335Q, and 122 and 166 pS for E335K (two levels detected). Similar findings were seen with [Mg]i = 0.

Our results suggest that a ring of specific aromatic residues at the external mouth, and a negative charge ring at the internal mouth, of the *Slowpoke* pore are important contributors to the large unitary conductance displayed by this channel.

M-Pos475

EXPRESSION SYSTEM AFFECTS THE STEADY-STATE KINETICS OF HUMAN k⁺ CHANNEL Kv1.5

(B. Wible, D. Fedida* and A.M. Brown). Dept. of Molecular Physiology and Biophysics, Baylor College of Medicine, Houston, TX 77030, and * Dept. of Physiology, Queen's University, Kingston, Ont. Canada K7L 3N6

A human heart potassium channel gene, fHK (Kv1.5), cloned from a fetal heart library, has been stably expressed in three heterologous mammalian cell lines: HEK 293 (human embryonic kidney), U-373 MG (human glioblastoma), and mouse fibroblast L cells. Four fHK-expressing clonal HEK cell lines, J9, J10, J20 and J14, were examined with widely varying levels of fHK current. Peak current voltage relations were independent of the expression level in both whole cell and macropatch recordings, and revealed slope conductances of 16.3, 72.4, >333 and 183 nS for J9 to J20, respectively. While the level of expression did not affect the steady-state activation and inactivation kinetics of fHK, the particular cell type in which the channel was expressed did. In HEK cells, the midpoint potentials for activation (-1.67 ± 6.8) mV and inactivation (-2.51 ± 9.5) mV of fHK were significantly more positive (10 to 20 mV) than in mouse L cells. fHK in glioma cells exhibited kinetics that more closely approximate the HEK cell phenotype. In HEK cells, the limiting activation rate was fit by a monoexponential process and inactivation followed a biexponential time course. Recovery from inactivation also followed a biexponential time course. The phenotype of the current expressed by fHK channels in HEK cells most closely resembled the rapidly activating delayed rectifier $K^+$ current (IKur) recently described in human heart. These experiments emphasize the importance of the heterologous expression system in the interpretation of the physiological role of cloned channels in the native cells in which they are expressed. (Supported by HL37044-4, Texas APT0032, MRC Canada and HSFO).

M-Pos476

**DELETION OF THE CONSERVED C-TERMINAL TD(L/V) MOTIF IN THE KV1 K+ CHANNEL FAMILY DOES NOT PREVENT EXPRESSION OF WILD-TYPE CHANNELS IN MOUSE FIBROBLASTS.**

((V. Uebele, S.W. Yeola, D.J. Snyders, and M.M. Tamkun)) Depts. of Mol. Physiology and Biophysics and Pharmacology, Vanderbilt Medical School, Nashville, TN 37232. (Spon. by S.K. England)

The members of the Kv1 K+ channel family share high amino acid sequence identity within the six membrane spanning domains and pore forming sequence. In contrast, the intracellular N and C- terminal regions show little conservation between isoforms and the sequence within these regions defines the isoform. The exceptions are the last three C-terminal residues, TD(L/V), which are conserved within the Kv1 subfamily but absent from the Kv2, 3 and 4 subfamilies. These three amino acids are conserved in Kv1 family members from species as diverse as *Drosophila*, rat, and man. To address the role of C-terminal amino acids in channel function and biosynthesis, C-terminal truncations were performed on the human Kv1.5 channel and function assessed in transfected mouse L- cells. Control constructs and constructs with deletions of the 4, 16, and 57 C-terminal amino acids were made, with the largest deletion also removing 2 putative protein kinase A phosphorylation sites. Maximum whole cell current densities (at +60 mV) ranged from 0.7 to 5.6 nA with no significant differences between constructs. The midpoint of activation (-14 to -18 mV), degree of inactivation at 250 msec (17 to 19 %), and the activation kinetics (τ = 1.6 to 2.0 ms at +60 mV) were also unaffected by the truncations. Similar results were obtained with the rKv1.1 channel. Therefore, the conserved TD(L/V) motif, and most of the C-terminal amino acids, are not required for the expression of wild-type Kv1 channels. However, these sequences may function in cellular processes that are specific to electrically-excitable cells.

**M-Pos477**

VESICULAR TRANSPORT OF K AND NA CHANNELS TO THE SURFACE OF NEUROBLASTOMA CELLS. ((W.F. Wonderlin and S. Sattsangi)) Dept. Pharmacology & Toxicology, West Virginia Univ., Morgantown, WV 26506-9223.

Newly synthesized membrane proteins are delivered to the cell surface by transport vesicles formed in the *trans*-Golgi. We have developed a method for isolating these vesicles from cultured cells, so that we can study the delivery of voltage-gated ion channels to the cell surface. Confluent N1E-115 neuroblastoma cells were differentiated 4-6 days in 1%FBS/2%DMSO. The cells were washed with a pseudo-intracellular buffer (GGA: 38mM K-Gluconate/38mM K-Glutamate/38mM K-Aspartate/2mM EGTA/2.5mM $MgCl_2$ /1mM DTT/25mM HEPES/pH7.2) and permeabilized by incubation (20 minutes, 37°C) in GGA buffer containing saponin (75ug/ml) and either an ATP-generating system (1mM ATP/8mM creatine phosphate, 50ug/ml creatine kinase) or an ATP-depleting system (apyrase, 30 units/ml). A low-speed supernatant (6000xg, 20 min) of the incubation medium was underlaid with a 20:26:31:37:45% sucrose gradient (4:4:4:4:5ml) and centrifuged for 16 hours at 100,000xg. The distribution of membranes among 1ml gradient fractions was measured using a lipid-sensitive fluorescent dye, TMA-DPH (Molecular Probes). The fluorescence in fractions containing less than 35% sucrose was ATP dependent. Peak fluorescence was found near 29% sucrose, and a smaller peak was typically present near 24% sucrose. ATP-dependence was highest (91%) in the 24% fraction and somewhat lower (74%) in the 29% fraction. Negatively-stained (1% uranyl acetate) fractions viewed by electron microscopy revealed a homogeneous population of small vesicles (20-50nm dia.) in the 24% fraction with both small and larger vesicles (>100nm dia.) in the 29% fraction. Voltage-gated K and BTX-modified Na channels were incorporated into planar bilayers by vesicle fusion. Western blots of the 24% and 29% fractions revealed KV3.1 K channel proteins (pGEXdrk1 antibody from J. Trimmer). A subpopulation of vesicles carrying KV3.1 channels was isolated by immunoadsorption onto pGEXdrk1-coated polyacrylamide beads. (supported by PMA Foundation grants).

**M-Pos478**

THE N-TYPE INACTIVATION GATE OF SHAKER B POTASSIUM CHANNELS IS MADE OF FOUR FUNCTIONAL "BALL-AND-CHAIN" PEPTIDES. ((F. Gómez-Lagunas, and C. M. Armstrong)) University of Pennsylvania. Philadelphia, PA. 19104-6085. USA. and Instituto de Biotecnología. UNAM. Cuernavaca, Mor. 62271. Mexico. (Spon. by M. Hiriart)

Fast inactivation in ShakerB K channels results from pore-block caused by "ball peptides" attached to the inner part of each K channel. We have examined the question of how many functional inactivating balls are on each channel, and how this number affects inactivation and recovery from inactivation. To that purpose we expressed ShakerB in Sf9 cells, and gradually removed the fast inactivation by perfusing the cell interior with papain, under whole cell patch clamp. Inactivation slows down as the balls are removed, in a way consistent with the presence of four equivalent balls which are independent in their statistical behavior. The stability of the N-type inactivation do not depends on the number of balls. Reinactivation is not significant during recovery from inactivation.

**M-Pos479**

**MOLECULAR AND BIOPHYSICAL CHARACTERIZATION OF A NOVEL SHAKER-RELATED ISLET CELL $K^+$ CHANNEL GENE, KV1.7, LOCATED ON HUMAN CHROMOSOME 19Q13.3.** (( K. Kalman, J. Tseng-Crank*, G. Chandy, H Mohrenweizer+, B Brandriff+, J. Aiyar, G.A. Gutman, K.G. Chandy)). Dept. Physiol. & Biophys. UCI, CA 92717, *Glaxo Res. Labs. Res. Triangle Park, NC, +Lawrence Livermore Labs. CA.

Six mammalian *Shaker*-subfamily $K^+$ channel genes, Kv1.1-Kv1.6, have intronless coding regions. We report the isolation of a 7th member of this family, mouse Kv1.7, with a unique genomic structure. At least two exons, separated by a 1.9 kb intron, encode the coding region of this channel; the upstream exon encodes the amino terminus and the S1 segment, while the remainder of the coding region is contained in the second exon. Kv1.7 mRNAs were detected in the rat and hamster insulinoma cell lines RIN and HIT, and are only ~2 kb in size, unlike the much larger transcripts known for Kv1.1-Kv1.6. PCR primers corresponding to sequences flanking the intron were used to amplify and sequence a 588 bp fragment from RNA from HIT cells and mouse brain. *In-situ* hybridization methods demonstrated the presence of Kv1.7 mRNA in mouse pancreatic islet cells, while the *Shaw*-related Kv3.4 gene was primarily found in acinar cells surrounding the islet. The Kv1.7 gene maps to mouse chromosome 7 in close proximity to the *Shaw*-related Kv3.3 gene. The two genes occupy a homologous position on human chromosome 19q13.2-13.3, a region linked to type 2-diabetes mellitus and late onset Alzheimer's disease. In view of the expression Kv1.7 in the brain and in islet cells, it would be interesting to determine whether alterations in this gene might contribute to the development of these diseases. We are currently generating an expression construct of Kv1.7 for analysis of its biophysical properties.

**M-Pos480**

CLONING AND EXPRESSION OF A NOVEL INWARD RECTIFIER $K^+$ CHANNEL HRK1 FROM HUMAN HIPPOCAMPUS ((A. Kelly, E.N. Makhina, A.N.Lopatin, R.W. Mercer and C.G.Nichols)). Dept. Cell Biol. and Physiol. Washington U. Sch. Med., 660 So. Euclid, St. Louis, MO 63110.

Using an expression sequence tagged cDNA (GenBank M78731, Adams et al., 1992, Nature **355**, 632-4) with homology to the recently cloned mildly inwardly rectifying channel ROMK1 (Ho et al., 1993, Nature **362**, 127-33) as a probe, we have isolated a novel cDNA from human hippocampus (HRK1) encoding a 423 amino acid protein, with ~ 40 % identity to ROMK1 and ~ 55 % identity to the strongly inwardly rectifying IRK1 (Kubo et al., 1993, Nature **362**, 31-8). When in vitro transcribed HRK1 cRNA is injected into *Xenopus* oocytes, it expresses aclassic inward rectifier current similar to IRK1, with similar external $Ba^{2+}$- and $Cs^{2+}$-sensitivity, but the single channel conductance (10 pS) is lower than in IRK1 channels (20 pS). Neurons do not appear to express strong inward rectifier channels, but in glial cells, inward rectifier channels may play a role in buffering extracellular $[K^+]$ (Newman, 1993, J. Neurosci. **13**, 3333-45). Preliminary experiments suggest that inward rectification is not due to internal cation block since rectification was not abolished when patches were isolated into zero $[Mg^{2+}]$.

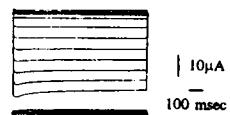


Whole cell HRK1 currents in response to voltage steps between -160 mV and +160 mV

**M-Pos481**

CYTOCHALASIN B AFFECTS KINETICS AND SENSITIVITY TO INTERNAL TEA IN DRK1 (KV2.1) POTASSIUM CHANNELS EXPRESSED IN OOCYTES.
((A.N. Lopatin and C.G. Nichols)) Dep. of Cell Biology and Physiology, Washington University School of Medicine, 660 South Euclid Avenue, St. Louis, MO 63110.

In an attempt to gain insight into the role of the cytoskeleton in regulation of ion channel function we have investigated the effects of the actin binding agent Cytochalasin B (Cyt B) on DRK1 $K^+$ channels expressed in Xenopus oocytes. After incubation of oocytes with Cyt B (50-100 μM) DRK1 currents display an apparent fast inactivation (τ ~ 40-50 ms). Internal injection of TEA reveals that the inactivating component is more sensitive to TEA block than the steady-state current. Open channel probability is significantly reduced but single channel conductance is unaffected in Cyt B treated channels. In inside-out membrane patches the apparent fast inactivation is a reversible and dose-dependent effect of bath applied Cyt B. At +50 mV 10-20 μM Cyt B reduces peak current by 10-30% while current at the end of the pulse is reduced by 40-80%. The results are consistent with cytoskeleton having an effect on channel function.

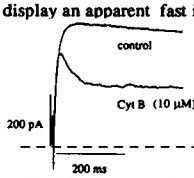


**M-Pos482**

SCREENING OF A RAT BRAIN cDNA LIBRARY FOR $K^+$ CHANNEL GENES BY COMPLEMENTATION IN YEAST ((E.N. Makhina and C.G.Nichols)). Dept. Cell Biol. and Physiol. Washington U. Sch. Med., 660 So. Euclid, St. Louis, MO 63110 (Spon. by R.S. Wilkinson)

$K^+$ transport in yeast *S. cerevisiae* is performed by high and low affinity transporters (TRK1 and TRK2 respectively). Transport deficiency caused by mutations in TRK1 is suppressed by $K^+$ channel genes (KAT1, AKT1) from *Arabidopsis thaliana* (Anderson et al., 1992, P.N.A.S. **89**, 3736-3740; Sentenac et al., 1992, Science, **256**, 663-665). We have attempted to use heterologous expression in yeast to isolate mammalian $K^+$ channel genes. Standard chemical mutagenesis techniques were used to isolate a yeast strain (J570a trkX) that was unable to grow on low $[K^+]$ medium. J570a trkX yeast were transformed by a rat brain cDNA library in the yeast vector pVT102. Colonies with restored growth on low $[K^+]$ media were selected. cDNAs encoding rat homologs of human T-cell leukemia virus enhancer factor (HTLF), and mouse erythroblastosis virus oncogene homolog 2 (ETS-2), were present in multiple independent isolates. We are investigating the possibility that these fork-head transcription activators restore growth on low $[K^+]$ by upregulating trk2 or deficient trk1 gene expression. A multiply isolated 890 bp cDNA showed ~80% nucleotide homology to mouse SNAP-25, a protein implicated in vesicle targeting and fusion. Four other cDNAs conferring $[K^+]$ independence in J570a trkX have no homology to known sequences. Preliminary electrophysiological analysis of oocytes injected with cRNA transcribed from these clones has not demonstrated $K^+$ channel activity.

**M-Pos483**

KINETIC PROPERTIES OF THE VOLTAGE DEPENDENT HUMAN DELAYED RECTIFIER CHANNEL h-DRK1

((R. Koopmann[1], K. Benndorf[1]*, C. Lorra[2] and O. Pongs[2])) [1]Institut für Vegetative Physiologie, Universität zu Köln, 50924 Köln. [2]Zentrum für molekulare Neurobiologie, Martinistr. 52, 20251 Hamburg. *Heisenberg-fellow of the Deutsche Forschungsgemeinschaft.(Spon. by P. Honerjäger)

The gene of the human delayed rectifier $K^+$ channel h-DRK1 was cloned and the channels were expressed in *Xenopus* oocytes. Whole cell currents at various potassium concentrations were measured with the two electrode voltage clamp technique. The currents activate at potentials positive to -20 mV and are shown to be highly selective for $K^+$ ions. Using the patch clamp technique macroscopic currents (macropatches or giant patches) and single channel currents (micropatches) were measured (5.4 mmol $[K^+]_o$). In giant patches, ionic and putative on- and off-gating currents were recorded simultaneously. It is estimated that less than 1% of the gating channels actually opened. In tail currents the putative off-gating current was separated from the ionic current by different kinetics. The instantaneous current-voltage relationship rectified outwardly to a higher degree than predicted by the Goldman-Hodgkin-Katz equation. Using a sequential Markovian model with four independent voltage controlled transitions, voltage dependence of the open probability could only be explained by assuming at least two components of activation. In the single channel activity, sublevel openings could be observed regularly but a main level with a unitary conductance of 9.4 pS (0 to +80 mV) was present. The open time was distributed biexponentially with voltage independent time constants in the range of 1 and 10 ms (filter 1 kHz). The time courses of cumulative first latency and ensemble averaged currents in single channel patches suggested that even a single channel may operate with two different components of activation.

**M-Pos484**

FUNCTIONAL DOMAINS IN THE AMINO-TERMINAL REGION OF MAMMALIAN NEURONAL $I_K$(A) CHANNELS.

((H. Ehmke, M. Koenen, J. Siara, J.P. Ruppersberg)). Max-Planck-Institut für Medizinische Forschung, Jahnstraße 29, 69120 Heidelberg, Germany (Spon. by L. Wollmuth).

Sudies on *Shaker B* $K^+$ channels have implicated two major functional domains located in the amino-terminal region: a sequence comprising the first 20 amino acids which mediates fast inactivation (Hoshi et al., Science 250:533-38, 1990), and a hydrophilic sequence of 114 amino acids which appears to be essential for subunit assembly (Li et al., Science 257:1225-30, 1992). We have examined whether these structure-function relationships also exist in a homologous mammalian voltage-dependent $K^+$ channel. Mouse Kv1.4 channels were expressed in *Xenopus* oocytes and macroscopic currents were obtained in the cell-attached and inside-out configuration. Surprisingly, deletion of the first 37 amino acids (ball-region) did not slow but even accelerated inactivation. Larger amino-terminal deletions, however, resulted in a loss of fast inactivation, while it was preserved in channels with internal deletions leaving the ball-region intact. Cytoplasmic application of the pore blocker TEA slowed inactivation in the wild type but not in the amino-terminal mutations. Expression of functional channels was still obtained when the amino-terminal deletion included most of the hydrophilic assembly site. These data 1) demonstrate the presence of a ball-and-chain inactivation gate in mammalian neuronal $K^+$ channels, but 2) argue against a functionally important assembly domain in the amino-terminal region.

## ENERGY TRANSDUCTION

**M-Pos485**

THYROID HORMONES INDUCE $Mg^{2+}$ RELEASE FROM ISOLATED RAT CARDIAC AND LIVER MITOCHONDRIA THROUGH THE ACTIVATION OF THE PERMEABILITY TRANSITION PORE.

A. Romani, C. Marfella and M. Lakshmanan*- Dept.s Physiology & Biophysics and *Medicine, Case Western Reserve University, Cleveland, OH, 44106, USA. (Spon. by T. Hoshiko).

Recently we provided evidence that the activation of mitochondrial adenine nucleotide translocase (AdNT) by cAMP induced the extrusion of a sizeable amount of $Mg^{2+}$ from cardiac or liver mitochondria. Since it has been proposed that AdNT may represent a target for $T_3$ as well, the possibility that thyroid hormones may also induce a similar $Mg^{2+}$ efflux from mitochondria was investigated. The addition of 5 pM $T_3$ or 10 pM $T_4$ to isolated cardiac or liver mitochondria prompted a release of approx. 2-3 nmol $Mg^{2+}$/mg protein from both mitochondria preparations. This efflux, which was quantitatively similar to that induced by cAMP stimulation, could also be induced by other thyroid hormone analogs, such as TRIAC, r-$T_3$, 3,3'-$T_2$, L94901 and 3,5-$T_2$. When these experiments were performed in the presence of 100 μM atractyloside, a specific inhibitor of AdNT, only the efflux induced by cAMP was prevented while the thyroid hormone mediated $Mg^{2+}$ extrusion was unaffected. HPLC measurements of mitochondrial ATP content showed a decrease in ATP content following the stimulation by cAMP. This decrease correlated well with the amount of $Mg^{2+}$ extruded under the same experimental conditions. In contrast, an increase in ATP content was observed following the stimulation by $T_3$. When these experiments were repeated in the presence of 1 μM cyclosporine-A, a specific inhibitor of the mitochondrial permeability transition pore (PTP), the $Mg^{2+}$ efflux induced by $T_3$ was completely blocked. These data indicate that the stimulation of cardiac and liver mitochondria by thyroid hormone induces a major efflux of $Mg^{2+}$ from mitochondria, which may have regulatory effects on mitochondria metabolism. This efflux appears to occur through the opening of PTP. (Grants N.I.H. 1K08DK01870 & N.I.H. HL 18708).

**M-Pos486**

**ATPase ACTIVITY, IF1 CONTENT AND PROTON CONDUCTIVITY OF ESMP FROM CONTROL AND ISCHEMIC SLOW AND FAST HEART-RATE HEARTS.**

**((W. Rouslin, C.W. Broge, F. Guerrieri and G. Capozza)) Department of Pharmacology and Cell Biophysics, Univ. of Cincinnati Col. of Medicine, Cincinnati, Ohio, USA and Inst. of Medical Biochemistry and Chemistry, Univ. of Bari, Bari, Italy.**

**Slow heart-rate hearts have heart rates of approx. 200 beats/min or less and contain predominantly the slow myosin ATPase isoform. Fast heart-rate hearts are capable of heart rates of approx. 300 beats/min or more and contain predominantly the fast myosin ATPase isoform. Earlier studies by us showed that slow heart-rate hearts exhibit a marked IF1-mediated inhibition of the mitochondrial ATPase during ischemia whereas fast heart-rate hearts do not. In the present study we used rabbit as the slow heart-rate species and rat as the fast heart-rate species. Rat is a fast heart-rate species that contains a low level of IF1. When sonicated at pH 8.0 with 2 mM EDTA, control rat heart ESMP exhibited approx. the same oligomycin-sensitive ATPase activity as control rabbit heart ESMP, but somewhat less than half the IF1 content and approx. twice the oligomycin-sensitive proton conductivity of control rabbit heart ESMP. In the same experiments, ischemic rabbit heart ESMP exhibited approx. 27% lower oligomycin-sensitive ATPase activity, approx. 1.5 IU/mg more IF1 and approx. 23% lower oligomycin-sensitive proton conductivity than control rabbit heart ESMP whereas ischemic rat heart ESMP exhibited only nominally lower ATPase activity, approx. 0.02 IU/mg more IF1 and unchanged oligomycin-sensitive proton conductivity compared to control rat heart ESMP. (This work was supported by NIH grant HL30926).**

**M-Pos487**

EFFECT OF SUBSTRATE ON NADH LEVELS OF OXYGENATED, ISOLATED VENTRICULAR MYOCYTES DURING ELECTRICAL PACING

((RL White† & BA Wittenberg‡)) †Temple University Medical School, Philadelphia, PA 19140 & ‡Albert Einstein College of Medicine, Bronx, NY 10461.

Mitochondrial NAD(P)H levels were measured using endogenous microfluorescence of single cells freshly isolated from rat heart. The NAD(P)H level was determined from the emitted fluorescence at 415 nm and 455 nm during brief epi-illumination at 365 nm. Cells were electrically paced by Pt-Ir field electrodes and superfused with MEM containing glucose and equilibrated with 95% $O_2$ and 5% $CO_2$ for the duration of the experiment. The fraction of reduced NAD[P], (NADH) was 0.41±0.04 (n=5) in myocytes contracting at 0.5 Hz for 20 min. When pacing was increased to 5 Hz for 10 minutes NADH decreased reversibly to 0.29±0.04 (n=5), and oxygen uptake increased 5-fold. At this stimulation rate, measured $pH_i$ remained constant and $[Ca^{++}]_i$ is known to increase. NADH recovered to control values after 20 min. at 0.5 Hz. Similar results were obtained when MEM containing glucose was supplemented with palmitate, octanoate, or ß-OH butyrate. In contrast, NADH remained essentially unchanged during stimulation when cells were superfused with MEM containing glucose supplemented with lactate, pyruvate, or α-ketoglutarate. Pyruvate enhances the activity of the mitochondrial pyruvate dehydrogenase and maintains high NADH during pacing. This suggests that increased $[Ca^{++}]_i$ does not maximally stimulate the rates of mitochondrial α-ketoglutarate or pyruvate dehydrogenases during increased pacing. Under these conditions, substrate supply to the dehydrogenases may be limiting. We conclude that during electrical pacing sufficient to increase oxygen consumption 5-fold, the reduction in NADH levels may reflect a drop in mitochondrial protonmotive force when dehydrogenase reaction rates are submaximal.

**M-Pos488**

EFFECTS OF THE CREATINE ANALOGUE β-GUANIDINOPROPIONIC ACID ON PORCINE CAROTID ARTERIES USING $^{31}$P NMR.

((E. A. Boehm, J. F. Clark and G. K. Radda)) Department of Biochemistry, University of Oxford, Oxford, OX1 3QU.

The responses of phosphocreatine and ATP as energy intermediates in vascular smooth muscle have been investigated by studying the acute energetic effects of the creatine analogue β-guanidinopropionic acid (β-GPA) on porcine carotid arteries using $^{31}$P NMR. β-GPA enters the smooth muscle cells, where it is phosphorylated by creatine kinase to produce β-GPA-P.

Fresh porcine carotid arteries were collected at the abattoire and kept cold till the experiments began. The tissue was superperfused for 12 hours with Krebs-Henseleit buffer at 22°C, containing NaCl substituted β-GPA (50 mM), and either glucose (10 mM) or pyruvate (5 mM) as substrate. Perfusion without β-GPA was used as a control system. Tissues were subsequently frozen in liquid nitrogen, for [metabolite] analysis.

Perfusion with β-GPA led to the formation of observable β-GPA-P after an initial lag period of about 2 hours with a concommitant decrease in [PCr]. The rate of β-GPA phosphorylation was significantly greater when glucose was used as substrate. Accumulation of β-GPA-P was accompanied by significant decreases in both tissue [lactate] and [ATP]. We hypothesise that increased ATP utilisation due to the presence of an additional phosphorylatable compound leads to a lower [ATP] which may stimulate oxidative metabolism (via increased [ADP]), with a concommitant decrease in tissue [lactate].

We conclude that the rate of β-GPA phosphorylation is greater with glucose as substrate as compared with pyruvate.Vascular smooth muscle (a glycolytic tissue) has a greater [ATP] when perfused with glucose. We believe that the greater [ATP] may enable a more rapid phosphorylation of β-GPA.